Synthesis of phosphonates and organofluorine compounds for bio-organic studies

Knight, Lee

Synthesis of Phosphonates and Organofluorine Compounds for Bio-Organic Studies

Lee Knight, BSc (Hons)

PhD Thesis

Department of Chemistry
University of Durham
1999

COPYRIGHT

DECLARATION

The work contained in this thesis was carried out in the Department of Chemistry at the University of Durham between October 1996 and September 1999. All the work was carried out by the author, unless otherwise indicated. It has not been previously submitted for a degree at this or any other university.

To Helen, my family and friends

Acknowledgements

I would like to thank Prof David O'Hagan, for not only being a good and amiable supervisor to work with but for giving me the opportunity to study for a PhD during three enjoyable and challenging years.

Of the many people that have helped me during my PhD, I particularly wish to thank Dr Jens Nieschalk who gave me invaluable help and advice, the crystallographers Clare Bilton, Dr Dimitri Yufit, Charlie Broder and Dr Mike Leech and the technical support staff in Durham, specifically the excellent service provided by the NMR staff. Finally I would to thank Hannah Sore for her hardworking and enthusiastic efforts whilst working with me as part of her 4^{th} year MSci project.

Abstract

This thesis focuses on two main areas: the synthesis of novel anti-metabolites of 1-deoxy-D-xyulose-5-phosphate (DXP) and the stereoelectronics which influence the conformation of fluoromethyl groups in organic compounds.

DXP, a sugar phosphate, has recently been established as a key biosynthetic intermediate to a number of plant and bacterial co-enzymes and vitamins. Chapter 1 describes the role of DXP in three biosynthetic pathways; in the formation of the isoprenoid building block isopentenyl pyrophosphate, and the vitamins B_1 and B_6. A new strategy to novel antibiotics and / or herbicides is proposed by the inhibition of DXP metabolism. A description of phosphonates as hydrolytically stable phosphate mimics is presented, including fluorine phosphonates that enable fine tuning of these mimics. Synthetic targets are designed as inhibitors of the DXP reductoisomerase catalysed reaction from DXP to 2-*C*-methyl-D-erythritol-4-phosphate (MEP). In Chapter 2 the successful synthesis of the CH_2 phosphonate analogues of DXP and MEP is described. The DXP analogue was initially approached *via* the diethyl phosphonate ester, however it proved necessary in the end to prepare the dibenzyl ester followed by hydrogenation. Synthesis towards the CF_2, and the α-fluorinated ketone, phosphonate analogues of DXP were incomplete due to low yields. Further syntheses is described towards the reduced form of the CH_2 phosphonate analogue of DXP, and to a compound related to fosmidomycin.

Chapter 3 describes fluorine's stereoelectronic influence in determining the conformations of fluoromethyl containing organic compounds through n/π-σ^* conjugation and *gauche* effects. Solid state evidence for the influence of these effects is presented through the first X-ray crystallographic data of fluoromethylaromatics and β-fluoroethylamides respectively. Structures of bis-2,6-(fluoromethyl)pyridine and its *N*-oxide displayed fluoromethyl conformations with the C-F bond co-planar to the aromatic ring whereas benzyl fluoride and 4-bromobenzyl fluoride displayed conformations with the C-F bond orthogonal to the aromatic ring. Structures of *N*-(2-fluoroethyl)-3,5-dinitrobenzamide and *N*-(2-fluoroethyl)-4-nitrobenzamide reveal a fluorine / amide *gauche* effect.

Contents

Chapter 2 - Synthesis of potential DXP anti-metabolites

Chapter 3 - Stereoelectronic effects of fluorine

Chapter 4 - Experimental

Abbreviations

18C6	18-Crown-6 ≡ 1,4,7,10,13,16-hexaoxacyclooctadecane
Ac	Acetyl
AD	Asymmetric dihydroxylation
aq	Aqueous
Bu	Butyl
Bn	Benzyl
BTSE	1,2-bis[(trimethylsilyl)oxy]ethane
calcd.	Calculated
CI	Chemical ionisation
CSD	Cambridge structural database
d	Doublet
DAST	Diethylaminosulphur trifluoride
DET	Diethyl tartrate
DHP	Dihydropyran
DMF	Dimethylformamide
DNA	Deoxyribonucleic acid
DTBP	2,6-Di*tert*butylpyridine
DX	1-Deoxy-D-xylulose
DXP	1-Deoxy-D-xylulose-5-phosphate
E. coli	*Escherichia coli*
EDTA	Ethylenediaminetetraacetic acid
ee	Enantiomeric excess
EI	Electron impact
EPSRC	Engineering and Physical Sciences Research Council
equiv.	Equivalent
Et	Ethyl
$Eu(hfc)_3$	tris[3-(heptafluoropropylhydroxymethylene)-(+)-camphoratol] europium (III) derivative
FAB	Fast atom bombardment
FAD	Flavin adenine dinucleotide, oxidised form

FMN	Flavin mononucleotide, oxidised form
GAP	Glyceraldehyde-3-phosphate
GC	Gas chromatography
GCMS	Gas chromatography-mass spectrometry
Gly	Glycine
GTP	Guanine triphosphate
HMG-CoA	Hydroxymethylglutaryl-Coenzyme A
HMPA	Hexamethylphosphoramide
HRMS	High resolution mass spectrometry
HT	4-Hydroxy-L-threonine
IC_{50}	Inhibitory concentration (for 50 % inhibition)
ID_{50}	Inhibitory dose (for 50 % inhibition)
IPA	*iso*propyl alcohol
IPP	Isopentenyl pyrophosphate
IR	Infra-red
LDA	Lithium di*iso*propylamide
Leu	Leucine
Lit.	Literature
M	Molar concentration (mol dm^{-3})
m	Multiplet
m/z	Mass-to-charge ratio
Me	Methyl
MEP	2-*C*-Methyl-D-erythritol-4-phosphate
Met	Methionine
MVA	Mevalonic acid
NAD^+	Nicotinamide adenine dinucleotide, oxidised form
NADH	Nicotinamide adenine dinucleotide, reduced form
NADPH	Nicotinamide adenine dinucleotide phosphate, reduced form
NMO	*N*-Methylmorpholine-*N*-oxide monohydrate
NMR	Nuclear magnetic resonance
OTf	Trifluoromethanesulphonate
p	Pentet
Ph	Phenyl
PHT	4-Phosphohydroxy-L-threonine

PLP	Pyridoxal 5'-phosphate
PMA	Phosphomolybdic acid
PNP	Pyridoxol 5'-phosphate
^{i}Pr	*iso*-Propyl
Pro	Proline
PTSA	*para*-Toluenesulphonic acid
Ptyr	Phosphotyrosine
q	Quartet
quant	quantitative
R_f	Retardation factor
RNA	Ribonucleic acid
s	Singlet
sat.	Saturated
SH-2	*src*-Homology region 2
sn	Stereospecific numbering
sp.	Species
t	Triplet
TBAB	Tetrabutylammonium bromide
TBHP	*tert*-Butyl hydroperoxide
THF	Tetrahydrofuran
tlc	Thin layer chromatography
TMS	Trimethylsilyl
Tos	Tosyl
TPP	Thiamin pyrophosphate
U	Uniform
UV	Ultra-violet
Val	Valine
w/w	Weight/weight

Chapter 1

Biosynthesis of DXP and its inhibition

1.1 Introduction

The discovery of chemicals to combat the growth of microbial and plant organisms remains a central pursuit of contemporary science. Study of the biosynthetic pathways to the essential metabolites of these organisms often provides insights into designing novel antibiotics and herbicides. The role of 1-deoxy-D-xylulose-5-phosphate, produced by both bacteria and plants, is highlighted in this thesis. This compound has recently been found to occupy a pivotal role in the biosynthesis of a number of metabolites including several vitamins. An excellent opportunity is therefore presented to synthesise rationally designed novel anti-metabolites based on the metabolism of 1-deoxy-D-xylulose-5-phosphate.

1.2 Biological role of 1-deoxy-D-xylulose-5-phosphate

Recent biosynthetic investigations have revealed that 1-deoxy-D-xylulose-5-phosphate (DXP) is an intermediate in three biosynthetic pathways (**Figure 1**) in bacteria and plants. Two of these pathways are involved in the biosynthesis of the vitamins B_1 and B_6. The other involves the production of isopentenyl pyrophosphate (IPP), an essential building block to compounds such as co-enzyme Q and cholesterol, collectively known as the isoprenoids. The involvement of this metabolite in these three pathways is discussed in greater detail in sections **1.3-1.5**.

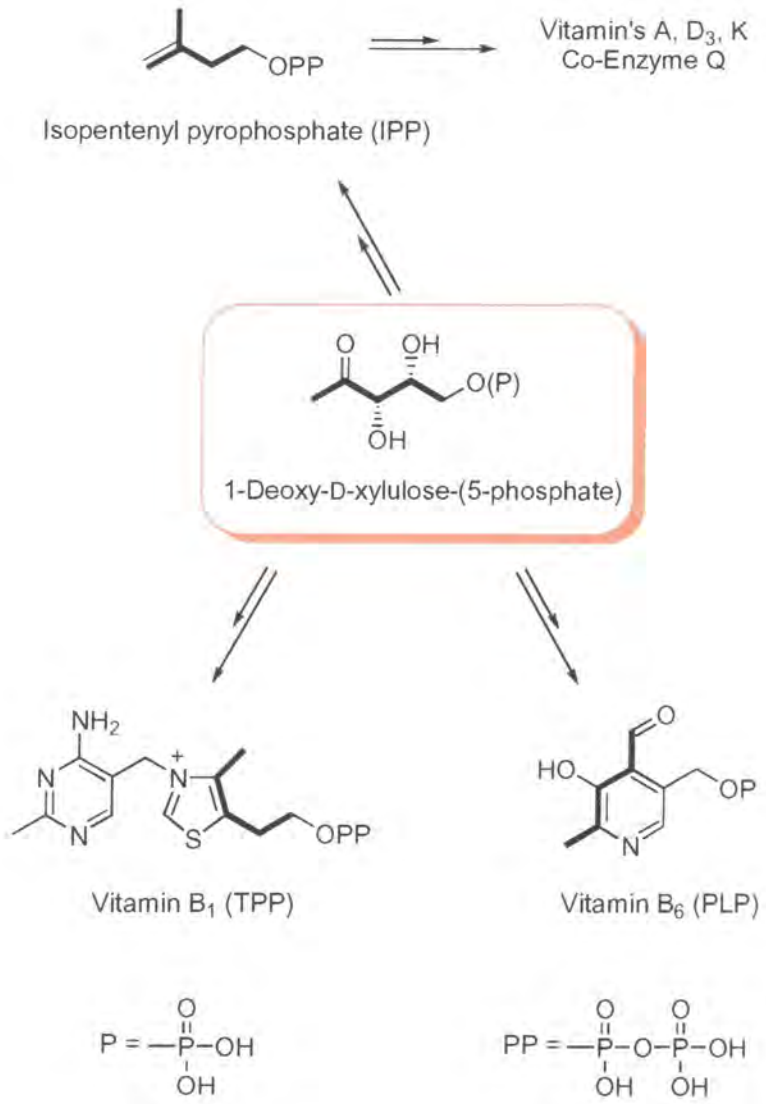

Figure 1 The intermediacy of 1-deoxy-D-xylulose-5-phosphate in three biosynthetic pathways to vitamins and IPP.

1.3 The 1-deoxy-D-xylulose-5-phosphate pathway

Isoprenoids are secondary metabolites of plants and micro-organisms, and representatives of them are well are known as flavours and fragrances. Examples of some isoprenoids are shown below. This large (greater than twenty thousand) family of ubiquitous natural compounds vary hugely in their structure, function and source organism, their unifying characteristic being that they are partly, or wholly derived from IPP. The unique importance of the isoprenoids in the pharmaceutical, agrochemical, and flavour and

fragances industries has therefore made studying the biosynthetic pathways to, and from IPP, of intrinsic value.

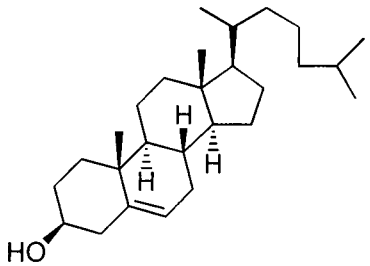

Cholesterol

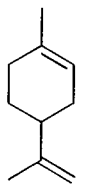

Limonene

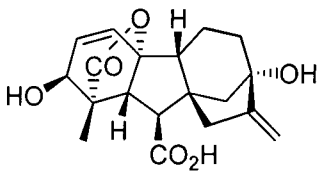

Gibberellin A_3

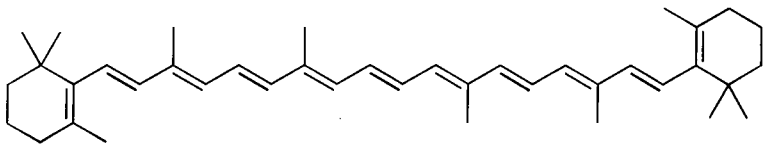

β-Carotene

Since the elucidation of IPP biosynthesis in the late 1950's,[1] by the pioneering studies of Bloch, Cornforth and coworkers, it was generally assumed that there was only one route (known as the mevalonic acid (MVA) pathway due to the intermediacy of MVA) operating to produce IPP. When [1-^{13}C]-glucose was fed to eubacteria (also known as true bacteria; this class encompases the enteric (gut) bacteria and the photosynthetic organisms formerly known as blue-green algae, but now better known as cyanobacteria), the MVA pathway results in an indicative labelling pattern in IPP, as shown in **Scheme 1**. This route was increasingly being called into doubt in bacterial systems by the late 1980's when a number of feeding experiments could not readily be rationalised by the intermediacy of MVA. In 1988 Flesch and Rohmer reported an unexpected labelling pattern in recovered hopanoids after feeding of [1-^{13}C]-acetate.[2] Although conflicting results had been reported before, they had not been so conclusive as to suggest that an alternative pathway was operating to form IPP. More conflicting results followed, after feeding of isotopically labelled glucose, pyruvate and erythrose to eubacteria revealed that the isoprenoid units of hopanoids, and the prenyl side chains of ubiquinones were *not* formed *via* the MVA pathway.[3]

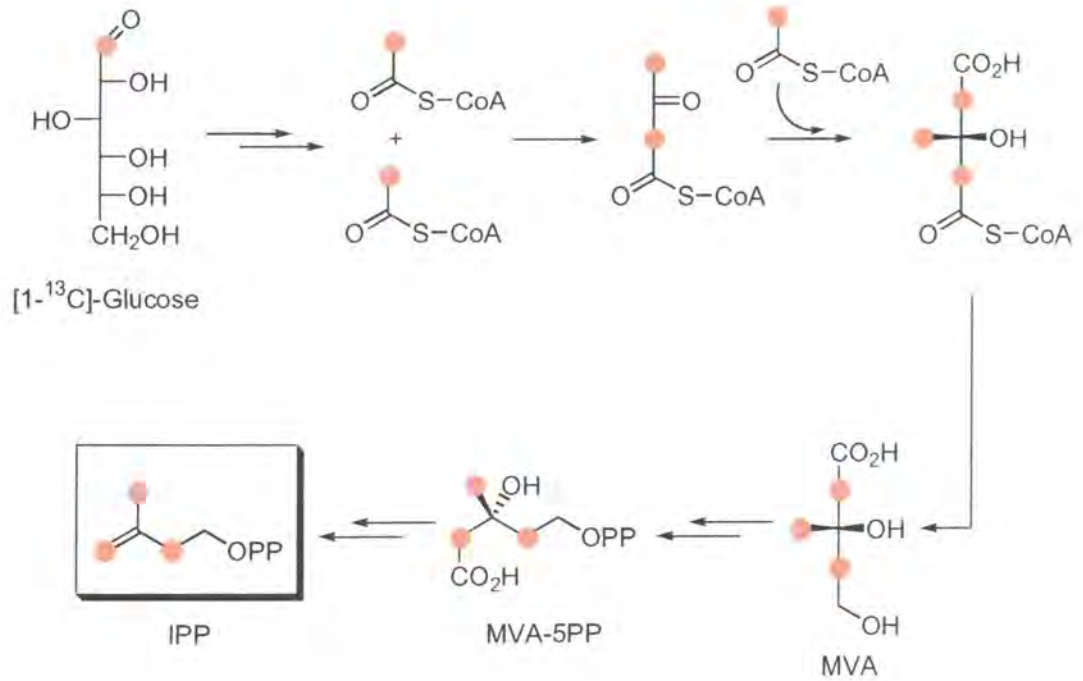

Scheme 1 The MVA pathway, showing the expected ^{13}C labelling pattern in IPP after feeding of [1-^{13}C]-glucose. ● = ^{13}C.

Initial forays to unmask this non-MVA pathway were carried out by Rohmer *et al*,[4,5] who established in bacteria that the novel route is initiated by the addition of a C_2 acyloin unit (derived from pyruvate in a TPP mediated decarboxylation) to a C_3 unit (a sugar phosphate) affording a C_5 phosphate sugar. The C_3 unit was later identified as glyceraldehyde-3-phosphate (GAP), after a series of experiments using different *E. coli* mutants.[6] Deuterium incorporation into the isoprenoids of *E. coli* after feeding experiments with deuterium-labelled 1-deoxy-D-xylulose showed[7] that condensation of GAP and the C_2 acyloin unit affords 1-deoxy-D-xylulose-5-phosphate (DXP). The TPP dependent enzyme that mediates this reaction, DXP synthase, has been isolated and overexpressed in *E.coli*.[8,9] The next enzyme on the pathway catalyses the first committed step to IPP formation, and was isolated in 1998 in Japan.[10,11] This enzyme was shown to produce 2-*C*-methyl-D-erythritol-4-phosphate (MEP) on incubation with DXP and NADPH and has been named DXP reductoisomerase by Seto and co-workers.[10,11] **Scheme 2** illustrates the progress made so far in elucidating the DXP (non-MVA) pathway.

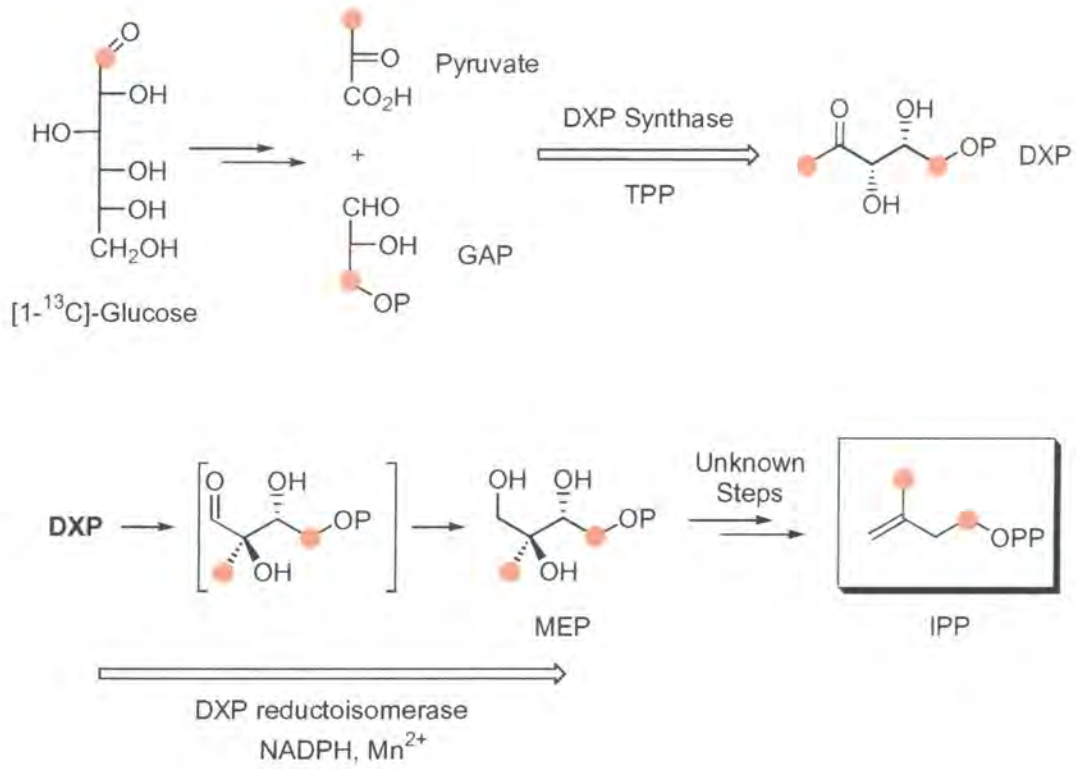

Scheme 2 The DXP pathway and the expected ^{13}C labelling pattern in IPP after feeding of [1-^{13}C]-glucose. ● = ^{13}C.

The subsequent steps required to convert MEP to IPP in bacteria are not known at present, although a number of recent reports[12,13,14] have placed significant restrictions on the possible intermediates. Apart from eubacteria, green algae[15] and higher plants[3,16,17,18,19,20,21,22] have also been shown to produce isoprenoids *via* DXP. The DXP reductoisomerase enzyme has recently been characterised in the green plant *Mentha* x *piperita*.[23] In higher plants however, both the DXP and MVA pathways operate to deliver different classes of terpene metabolite. The DXP pathway operates in subcellular organelles called the plastids, DXP reductoisomerase in *Mentha* x *piperita* being found to contain an additional preprotein that directs the enzyme to the plastids. The MVA pathway operates in the cytoplasm of the cells and in general is responsible for higher order terpenes, > C_{15}. Such findings appear to support endosymbiosis theory, where plant organelles evolved from bacteria.[3]

1.4 Biosynthesis of vitamin B_1

The elucidation of vitamin B_1 biosynthesis has been and continues to present a challenge.[24] Lack of vitamin B_1 (also known as thiamin) is the nutritional factor associated with the disease beriberi. Thiamin pyrophosphate (abbreviated to TPP, but also known as cocarboxylase), is the active co-enzyme which takes part in decarboxylation reactions,[25] an essential process required in channelling pyruvate and hydroxypyruvate into carbohydrate metabolism. TPP is also required in C-C bond forming reactions catalysed by transketolase enzymes. Thiamin biosynthesis occurs in most micro-organisms and higher plants, and different pathways exist for different classes of organisms. This is the case both for formation of pyrimidine and thiazole units (**Figure 2**) and also after coupling, in the final stages of co-enzyme biosynthesis.[24]

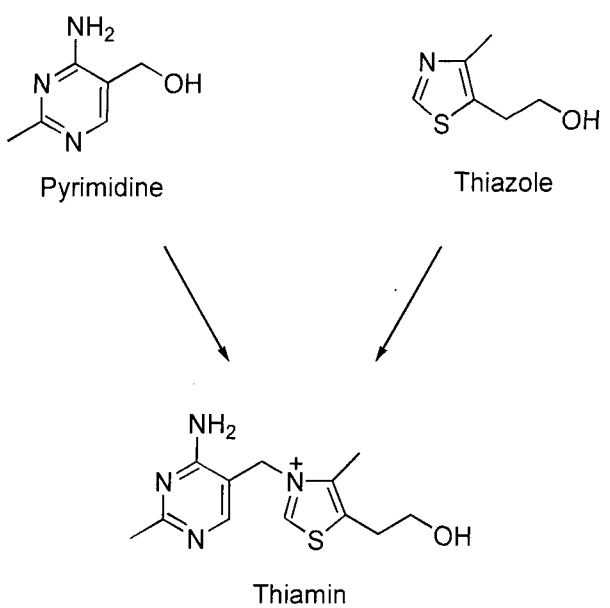

Figure 2 Thiamin and its subunits pyrimidine and thiazole.

1.4.1 Biosynthesis of the pyrimidine subunit

Full details of the biosynthetic pathways to pyrimidine formation have yet to be revealed. Formate supplies one carbon atom to the subunit in both entericbacteria[26] and yeast,[27] but in different positions. For prokaryotes, glycine[28] and ribose[29,30,31] have been found to

supply the remaining atoms, as delineated in **Scheme 3**, whilst in eukaryotes, glycine is not utilised at all and the remaining carbon atoms appear to be derived from glucose.

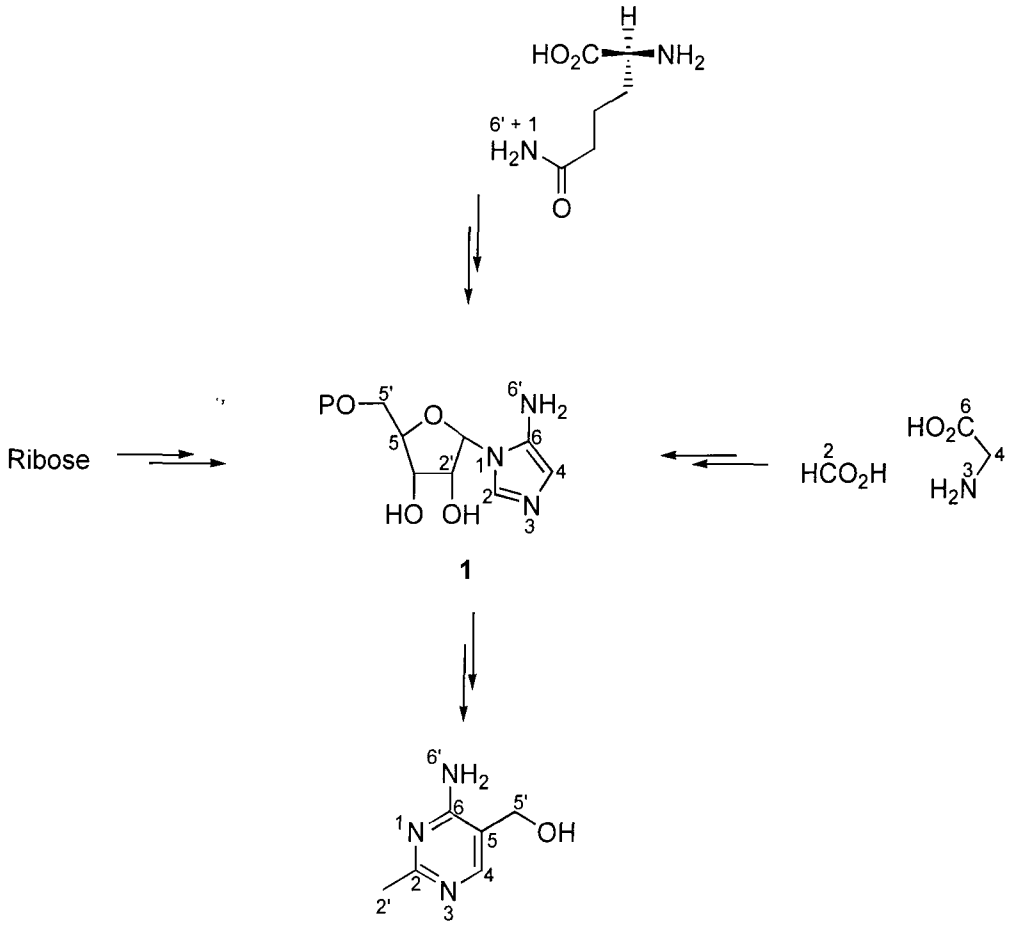

Scheme 3 Biosynthesis of the pyrimidine unit in entericbacteria.

(5-Aminoimidazolyl)ribotide **1** appears to be an advanced precursor to the pyrimidine ring system in entericbacteria. Isotopic labelling experiments carried out on bacteria with [5-^{14}C]-**1**, [3-^{15}N]-**1** and [$^{15}NH_2$]-**1** afforded incorporation of ^{14}C into the carbon skeleton and ^{15}N in positions N1 and NH_2 respectively of the pyrimidine ring system.[29,30] A key result demonstrated incorporation of label from [U-^{13}C]-**1** into pyrimidine in the presence of glucose, but no incorporation when unlabelled **1** was fed in the presence of [U-^{13}C]-glucose.[31] The conversion of the key intermediate **1** into pyrimidine has been rationalised through a series of hypothetical intramolecular rearrangements. In eukaryotes, such as yeast, **1** has not been found to be an advanced precursor.[24] Instead histidine[32] and pyridoxol[33] are implicated as the precursors to the pyrimidine ring in yeast. Further work

is needed however, to confirm if and how histidine and pyridoxol are incorporated into pyrimidine.

1.4.2 Biosynthesis of the thiazole subunit

From isotopic labelling experiments, yeast and entericbacteria have been found to possess different biosynthetic routes to the thiazole subunit (**Scheme 4**).[24] Preliminary results indicate that green plants utilise the same pathway as entericbacteria, whereas aerobic bacteria employ the yeast pathway.[24] In entericbacteria, tyrosine and DXP (or its unphosphorylated species, DX) have been found to provide the nitrogen and carbon atoms to the thiazole ring, whereas glycine and an unknown pentulose are the precursors to this ring system in yeast. The sulphur atom appears to derive from cystine in both micro-organisms.

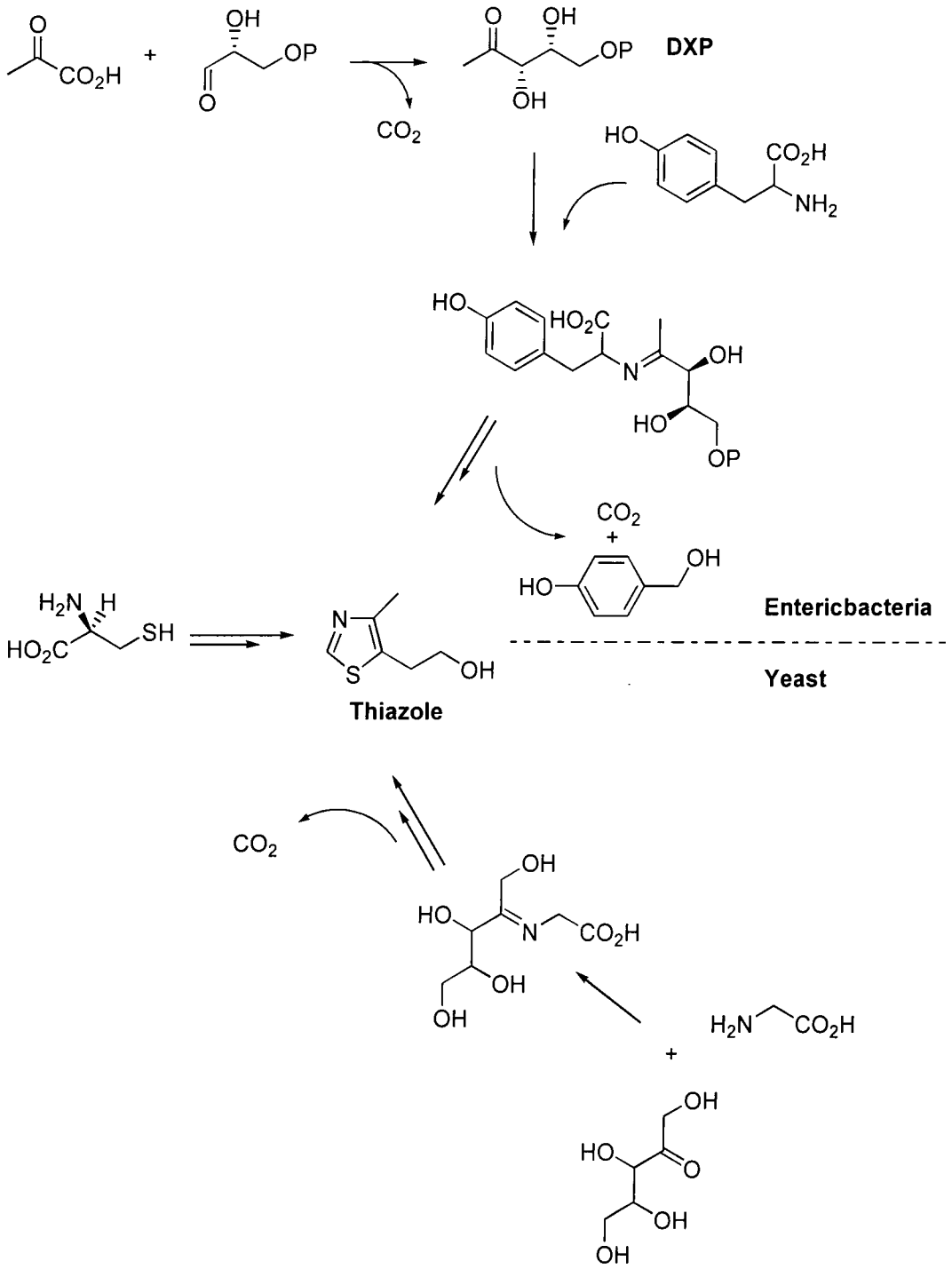

Scheme 4 A summary of the biosynthesis of the thiazole ring of thiamin in entericbacteria and yeast.

For entericbacteria tyrosine has been found to supply one carbon atom and the nitrogen atom of the thiazole ring. Feeding experiments with [α-^{14}C]-tyrosine and [U-^{14}C]-tyrosine have resulted in incorporation at C2 of the thiazole ring,[34] and a feeding experiment with [^{15}N]-tyrosine to a bacterium resulted in the incorporation of ^{15}N into the thiazole ring

system.[35] Incorporation of label into an unestablished position of thiamin after feeding of [α-^{14}C]-tyrosine to a green plant has also demonstrated the intermediacy of tyrosine in thiazole ring biosynthesis.[36] For yeast and aerobic bacteria intact incorporation of the C-N fragment, derived from glycine, serves as the precusor for the C2-N bond of the thiazole ring.[37]

In entericbacteria, the remaining carbon atoms in the thiazole ring have been shown to arise from a carbohydrate source by the incorporation of intact C_2 (C4',C4) and C_3 (C5-C7) units from [U-^{13}C]-glucose into the thiazole ring of thiamin.[37] Conclusive evidence that these two units combine to form the C_5 unit that is then incorporated into the ring has been obtained from the intact incorporation of [2,3-$^{13}C_2$]-1-deoxy-D-xylulose into C4-C5 of the thiazole ring.[38] **Scheme 5** shows the steps required for the conversion of tyrosine, DXP and cystine to form the thiazole ring of thiamin.

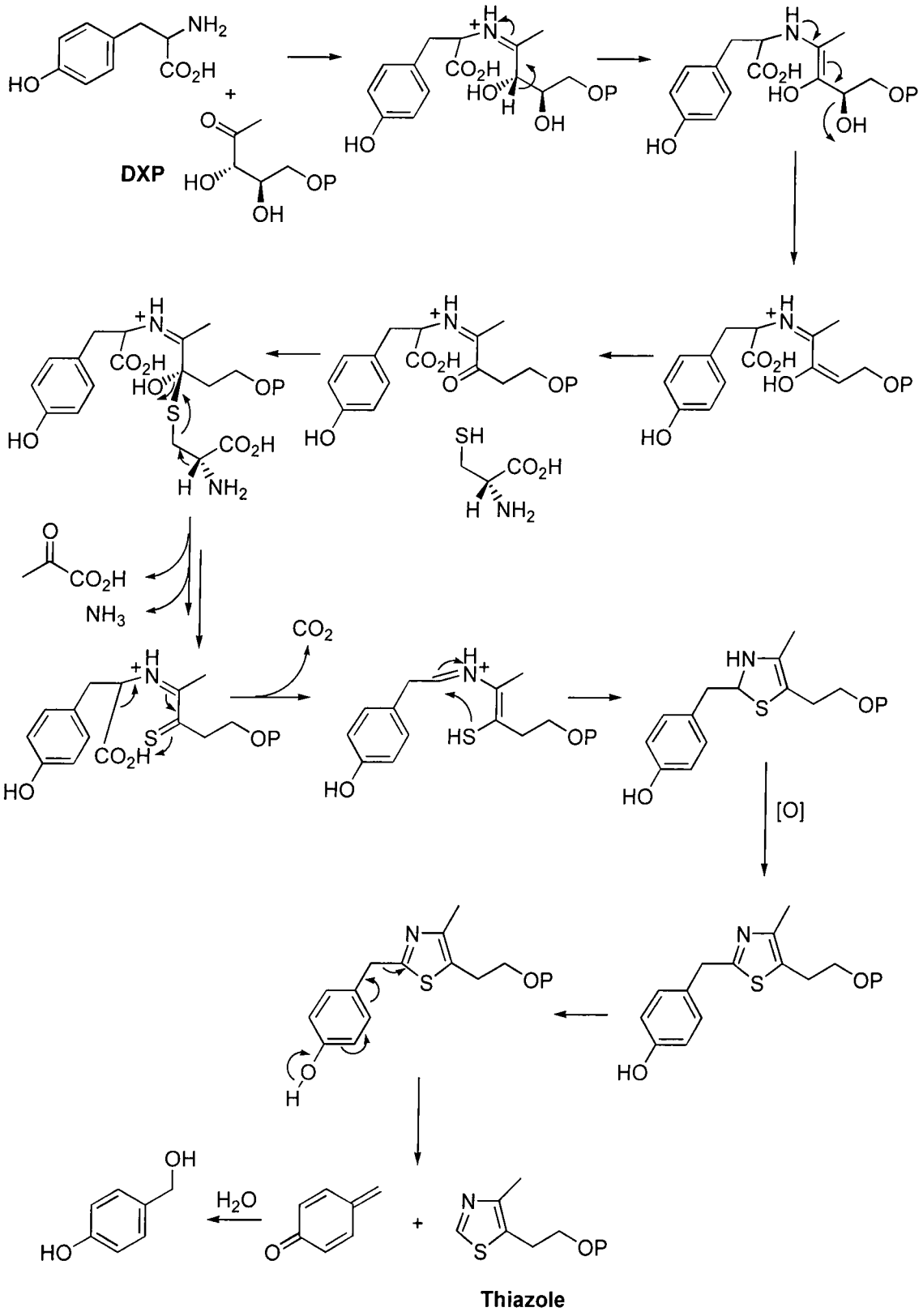

Scheme 5 Putative mechanism for the biosynthesis of the thiazole unit in entericbacteria from tyrosine and DXP.[24]

In yeast the five-carbon chain of the thiazole ring arises from a pentulose that is not derived from the combination of a C_2 and C_3 unit. Instead, the biosynthetic experiments indicate that either a xylulose or a ribulose (or their 5-phosphates) is utilised in the formation of the thiazole ring in a manner similar to entericbacteria, except that the pentulose combines with glycine (not tyrosine) and an oxidative step is not required, since the yeast's carbohydrate source is at a higher oxidation level.

1.4.3 Coupling of the subunits

Again both yeast and entericbacteria display different biosynthetic pathways. The biosynthetic steps (**Scheme 6**) that lead to TPP were mostly characterised by 1975. Separate enzymatic steps are required in entericbacteria for phosphorylation of the thiazole subunit and its coupling to the pyrimidine subunit, whereas a single enzyme catalyses this biotransformation in yeast and aerobic bacteria. Thiamin pyrophosphate is formed directly from thiamin monophosphate in entericbacteria, but by diphosphorylation of thiamin in yeast and aerobic bacteria.

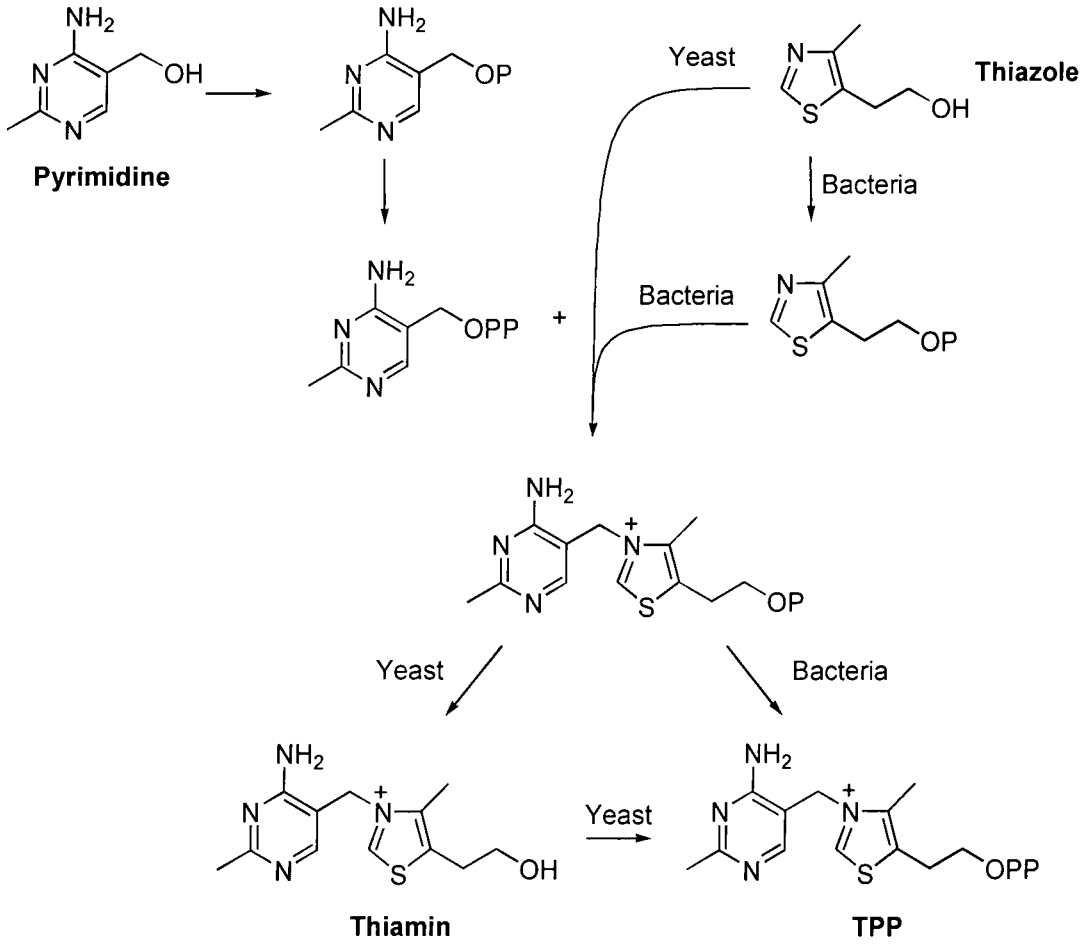

Scheme 6 Final biosynthetic steps to thiamin pyrophosphate for entericbacteria and for yeast and aerobic bacteria.[24]

1.5 Biosynthesis of vitamin B_6

Pyridoxal phosphate (PLP) which derives from vitamin B_6 is a necessary co-factor for the many enzymes that enable cellular transformations of amino acids, such as decarboxylation, transamination, β-elimination and racemisation. Deficiency of vitamin

B_6 leads to retarded growth, dermatitis, convulsions and other symptoms in humans.[25] The terms vitamin B_6 and pyridoxine are used interchangeably to denote the six compounds that all have some vitamin activity. These are pyridoxol, the corresponding 4'-amine, pyridoxamine, the corresponding 4-aldehyde, pyridoxal, and their 5'-O-phosphate esters.[39] Elucidation of pyridoxine biosynthesis has predominantly been studied with *E. coli*, although some evidence does suggest that a similar process takes place in plant chloroplasts.[40]

1.5.1 Biosynthesis of the immediate precursors to vitamin B_6

As with vitamin B_1 and terpene biosynthesis it has been found that GAP and pyruvate are condensed in a TPP mediated process to yield DXP. This sugar delivers the C_5 fragment C2', C2-C4 and C4' of pyridoxine (**Scheme 7**), GAP contributing C3, C4, and C4' of pyridoxine and pyruvate C2' and C2.[39] A feeding experiment with [2,3-$^{13}C_2$]-1-deoxy-D-xylulose showed the intact incorporation of the C2-C3 bond into pyridoxine.[38] Experiments with labelled glycolaldehyde[41,42] and glycine[43] have also shown that these metabolites provide the remaining atoms, N1, C6, C5 and C5' of pyridoxine in certain mutants of *E. coli*. However, the main pathway in *E. coli* has been found to utilise 4-phospho-D-erythrose[44,45] (**Scheme 7**) and interestingly this pathway requires the co-factor PLP. Intriguingly therefore PLP is involved in its own biosynthesis.[46] An experiment with 4-hydroxy-L-threonine (HT), contiguously labelled with ^{13}C at C2-C3, was shown to definitively supply these atoms as an intact unit, by bond-labelling C5-C6 of pyridoxine.[47] Additionally, unlabelled HT has been found to suppress incorporation of label from [U-^{13}C]-glucose into C6, C5 and C5', but not into the other carbon atoms of pyridoxine.[48] It has also been found that in *E. coli* one of the enzymes that converts 4-phospho-D-erythrose to pyridoxine is able to utilise only the phosphorylated form of HT, 4-phosphohydroxy-L-threonine (PHT), indicating that PHT, not HT is involved in pyridoxine biosynthesis, **Scheme 7**.

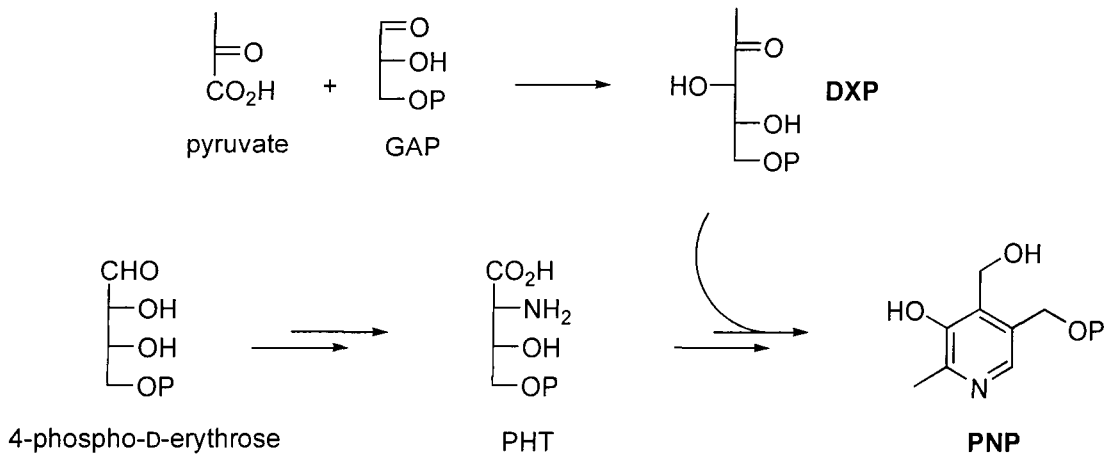

Scheme 7 Summary of the putative pathway to pyridoxol 5'-phosphate (PNP) biosynthesis in *E. coli*.

1.5.2 Final steps of vitamin B_6 biosynthesis

Studies have shown that the first B_6 vitamer produced is pyridoxol 5'-phosphate (PNP), and that it derives its phosphate from PHT, not DXP.[49,50,51] In *E. coli* two enzymes are now known to be required for the formation of PNP from PHT and DXP. The first catalyses the oxidation and decarboxylation of PHT (**Scheme 8**), to generate 1-amino-3-(phosphohydroxy)propan-2-one **2**.[52] The second enzyme pyridoxol phosphate synthase catalyses the condensation of **2** and DXP to generate PNP. The mechanistic details here remain to be resolved, however it is noteworthy that loss of DXP's phosphate group occurs during the ring closure reaction (**Scheme 8**).[50,51]

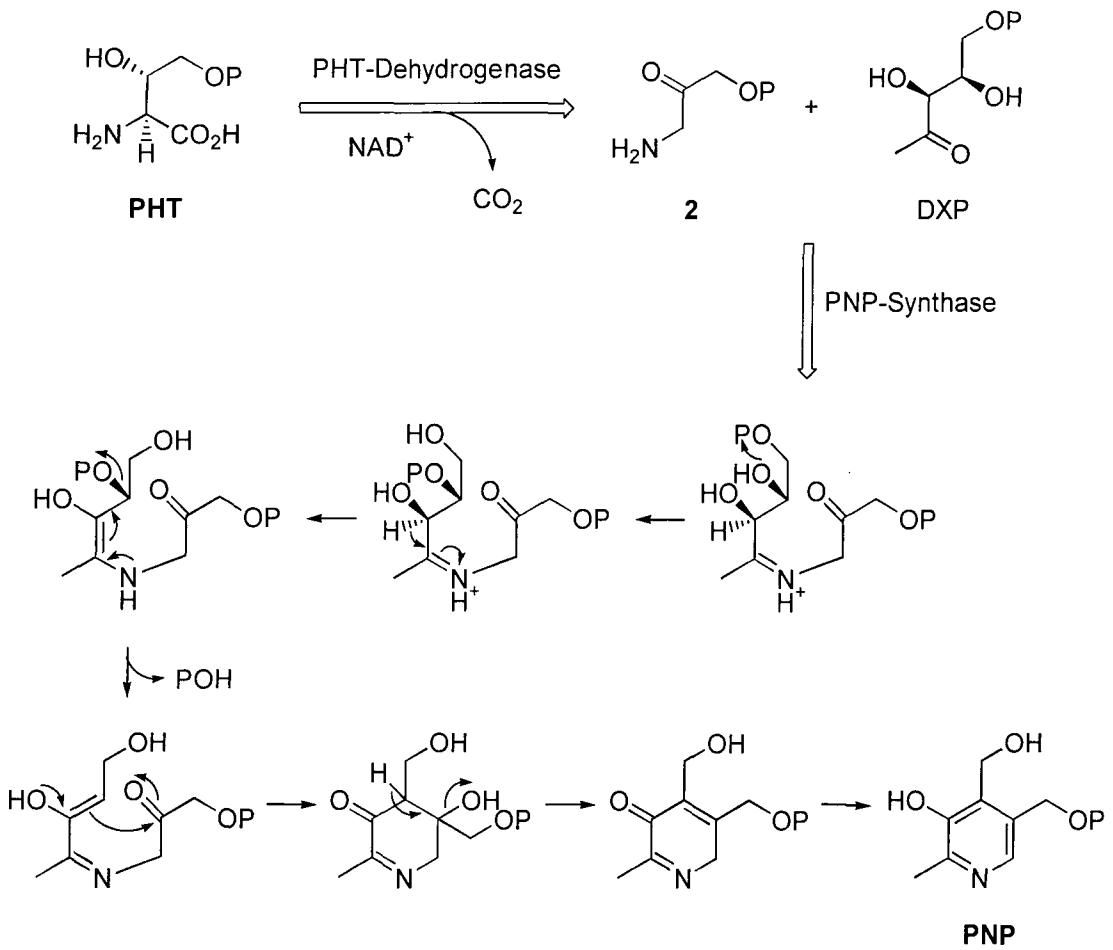

Scheme 8 Current hypothesis for the final steps to PNP from PHT and DXP.[51]

1.6 Summary of biosynthetic reactions utilising DXP

It emerges from this biosynthetic survey that DXP is a substrate for three enzymes in different pathways. Inhibition of DXP metabolism therefore emerges as an attractive target for the repression of the biosynthesis of certain vitamins and other essential metabolites in bacteria and green plants.

In the DXP biosynthetic route to IPP, DXP undergoes enzymatic isomerisation then reduction to yield 2-*C*-methyl-D-erythritol-4-phosphate (MEP). DXP reductoisomerase has been characterised from *E.coli* and a green plant, and requires NADPH and Mn^{2+} ions (**Scheme 9**, i). IPP biosynthesis *via* DXP is known to operate in bacteria, green algae and green plants.

Vitamin B_1 biosynthesis in entericbacteria (and potentially green plants)[24] is thought to involve reaction of DXP with tyrosine to form a Schiff base intermediate. This then undergoes a sequence of reactions to generate the thiazole subunit of vitamin B_1 (**Scheme 9**, ii).

In the final step to vitamin B_6, PNP synthase (characterised from *E.coli*) catalyses Schiff base formation between 1-amino-3-(phosphohydroxy)propan-2-one **2** and DXP. Loss of DXP's phosphate group is subsequently required in the final steps leading to PNP (**Scheme 9**, iii).

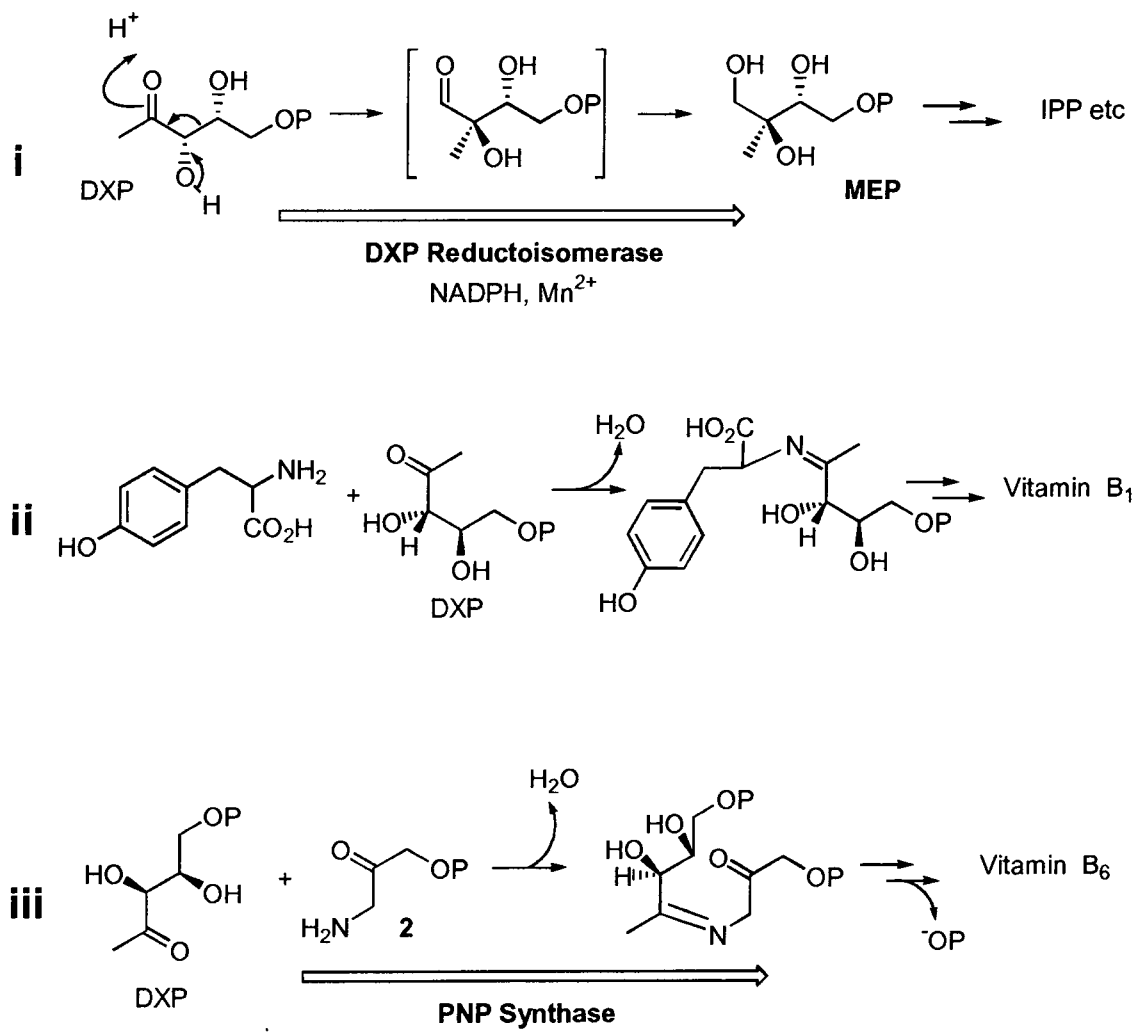

Scheme 9 Reactions of DXP in vitamin biosynthesis.

1.7 Precedence for inhibition of DXP metabolism

Specific inhibition of DXP reductoisomerase has recently been reported.[53] The inhibitor, fosmidomycin **3** was found from a database search of compounds that inhibited known DXP dependent bacteria, but not mevalonate dependent bacteria.

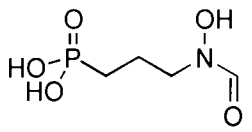

Fosmidomycin **3**

Kinetic studies with **3** indicate that it inhibits DXP reductoisomerase in a dose dependent manner with an IC_{50} value of 8.2 nM.[53] Inhibition was found to occur through a mixed (competitive and noncompetitive) manner, with a K_i value of 38 nM. Fosmidomycin **3** also specifically inhibits the conversion of DXP to MEP in chromoplasts of higher plants, being found to hinder production of β-carotene from DXP, again in a dose dependent manner with an IC_{50} value of 2.5 μM.[20] DXP reductoisomerase thereby provides an example of a novel target for both herbicidal as well as antibacterial action.

1.7.1 Structural-activity relationship of fosmidomycin 3

Fosmidomycin and the putative aldehydic intermediate in the DXP reductoisomerase reaction have close structural similarities with each other, with the *N*-formyl group mimicking the aldehyde and the phosphonate mimicking the phosphate (**Figure 3**). As **3** is an effective inhibitor of DXP reductoisomerase, then a good strategy to developing novel antibiotics and / or herbicides would appear to be the design of fosmidomycin type inhibitors.

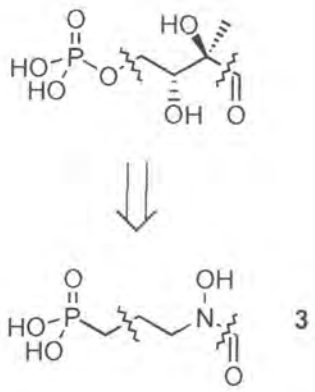

3

Figure 3 Structural relationship between the putative aldehydic intermediate in the DXP reductoisomerase reaction and fosmidomycin **3**.

1.8 Phosphonates as phosphate analogues

Phosphates are ubiquitous in biological systems, the monoesters found as alkyl phosphates, sugar phosphates and phosphoproteins. The phosphodiester linkage comprises the backbone of the nucleic acids RNA and DNA, and is also found in the phospholipid component of biological membranes.[54] Some examples of biologically important phosphates are shown below.

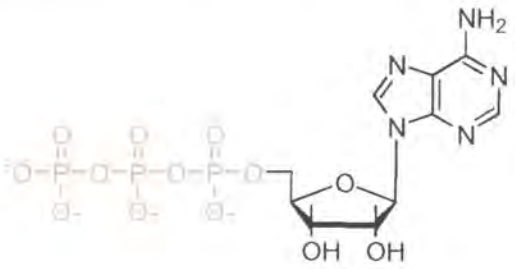

adenosine 5'-triphosphate

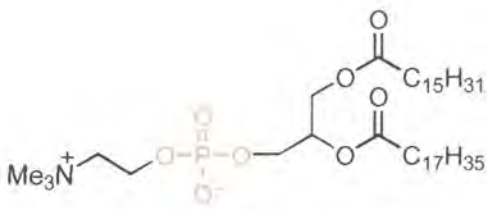

phosphatidylcholine
component of membranes

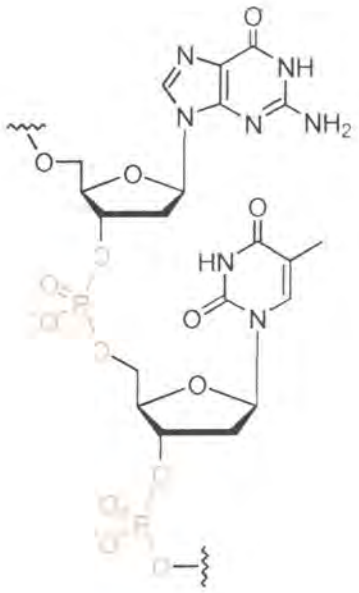

phosphodiester backbone of DNA

In biological systems phosphates are hydrolysed to inorganic phosphate and alcohols by phosphatases, a widely distributed class of enzymes that have a broad substrate specificity. However, the change from a P-O-C to a P-C-C linkage (**Figure 4**) greatly enhances the metabolic stability of the phosphonate, the new linkage being unable to be hydrolysed by phosphatase enzymes.

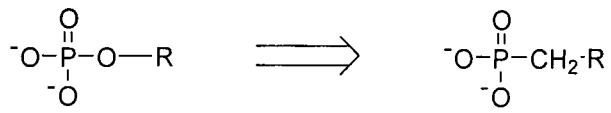

Figure 4 Phosphonates as phosphate mimics.

The use of phosphonates as phosphate analogues thus provides a method of metabolic regulation or perturbation. It has been said that, 'if phosphate esters represent the currency of metabolism, then the analogous phosphonates can be viewed as exquisite counterfeits: perhaps passible in many transactions but ultimately forgeries nonetheless.[55] However, phosphonate analogues do have significantly different characteristics to their parent phosphates. These include a change in the second pK_a of the acids, the first pK_a for both phosphonic and phosphoric acids indicating complete ionisation at physiological pH. Geometric changes also result on replacing O for methylene. These factors are discussed below.

1.8.1 Optimisation of phosphonates as phosphate mimics

The second pK_a and geometry of the phosphonate can be altered through fluorine substitution of the methylene hydrogens. **Figure 5** shows the average second pK_a of a phosphate and various phosphonates.[56] Both the dihydro and difluoro phosphonates have a pK_a about one unit higher and lower respectively than the phosphate group, and the CHF phosphonate has a pK_a that most closely approximates the phosphate group. Analysis of the X-ray structures of the amino phosphate / phosphonates **4**, **5**, **6** and **7** has revealed the C-X-P angles, depicted in **Figure 5**. The difluoro analogue now approximates the geometry of the phosphate most closely in this respect, with increasing disparity shown for the monofluoro and dihydro analogues. Another aspect to consider when using

phosphonates as phosphate analogues is the electrostatic profile of the bridging unit. For example, the replacement of oxygen for a difluoromethylene group in a biological system, may have a significant impact on the analogues ability to bind in the close confines of an enzymes active site. A combination of ionic, geometric, steric and electrostatic factors determines which of the analogues emerge as the most effective at binding to a given enzyme system.

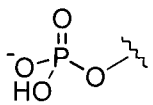

pK_a ca. 6.45

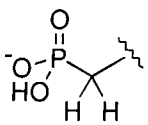

pK_a ca. 7.65

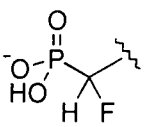

pK_a ca. 6.2

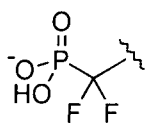

pK_a ca. 5.64

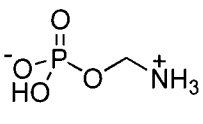

4

C-X-P angle 118.7°

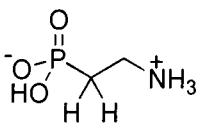

5

112.1°

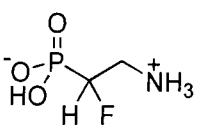

6

113.2°

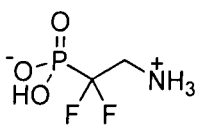

7

116.5°

Figure 5 pK_a values of phosphates and phosphonate and C-X-P angles of the compounds **4** to **7**.

1.9 Examples of phosphonate mimics

A number of systems have been evaluated that have shown either the CF_2 or CH_2 phosphonate to be the most effective analogue in replacing a phosphonate for a phosphate group in an enzymatic reaction. For example, in the enzyme catalysed condensation for addition of IPP to geranyl pyrophosphate **8**, the CH_2 and CF_2 phosphonate analogues have been studied, **Figure 6**.[57] It emerged that the first-order rate constant for the reaction is higher for the CF_2 than the CH_2 substrate, indicating that here, the CF_2 phosphonate is the better mimic of the phosphate group.

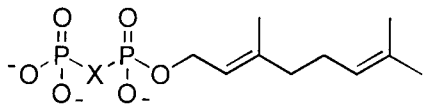

X	K / s^{-1}
O, **8**	3.0×10^{-4}
CH_2, **9**	1.1×10^{-6}
CF_2, **10**	3.9×10^{-4}

Figure 6 First-order rate constants for condensation of IPP onto substrates **8**, **9** and **10**.[57]

The CH_2, CHF and CF_2 phosphonate analogues of phosphotyrosine (pTyr) (**Figure 7**) were assayed for their binding ability when part of a pentapeptide acting as an inhibitor of a tyrosine phosphatase signalling protein.[58] The results indicate that the CF_2 phosphonate mimic is most effective at promoting binding, with an efficacy similar to the phosphate, pTyr. The excellent performance of the CF_2 analogues in such cases has been rationalised mainly in terms of the low pK_a imparted by the presence of the fluorine atoms.

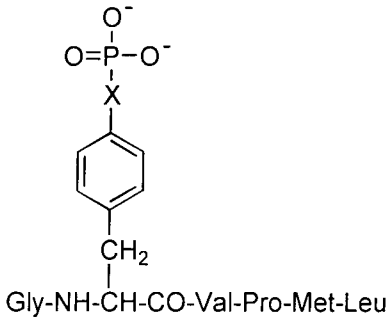

X	ID_{50} / μM
O, pTyr	0.17
CH_2, **11**	1.0
CHF, **12**	0.50
CF_2, **13**	0.17

Figure 7 Competitive bindings of peptides incorporating pTyr or the phosphonates **11**, **12**, or **13** with the C-terminal SH-2 domain of phosphatidylinositol 3-kinase.[58]

A system that has been used to compare all of the phosphonate congeners against the parent phosphate group is the NADH linked oxidation by glycerol-3-phosphate dehydrogenase (**Figure 8**).[59] Here the affinity of the *sn*-glycerol-3-phosphate / 3-phosphonate substrate for the enzyme was analysed in terms of K_m and V_{rel} values for the oxidation reaction, these results are summarised in **Figure 8**. The CF_2 analogue now emerged as the least effective mimic of the phosphate, with the CHF and CH_2 analogues performing *significantly better* than the parent phosphate. This result has been rationalised in terms of the enzyme preferring a substrate that can best minimise the electrostatic interaction in the active site, an interaction that has apparently not been optimised by the evolutionary process (ie. K_m for CH_2 and CHF < O, the natural phosphate).

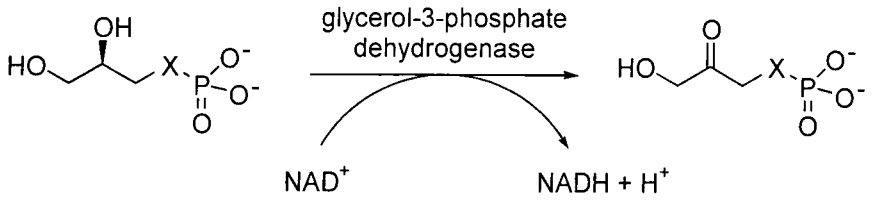

X	K_m / mM	V_{rel}
O, **14**	0.29	1.0
CH_2, **15**	0.18	0.8
CHF, **16**	0.17	0.9
CF_2, **17**	0.73	0.8

Figure 8 Kinetic data for the enzyme catalysed oxidation of **14**, **15**, **16** and **17**.[59]

As is evident from the above experiments different biological systems can respond differently to the phosphonate congeners. Therefore each phosphonate analogue in turn must be tested in a particular system.

1.10 Natural products containing a C-P bond

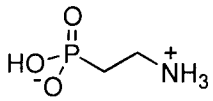

18

The first naturally occurring compound to be isolated containing a C-P bond was 2-aminoethylphosphonic acid **18**, in 1959.[60] Since then over 25 C-P containing compounds have been described. Some of these compounds are found to have antibacterial, antiviral, antibiotic, pesticidal, herbicidal and anti-cancer properties.[60] This wide range of activity has prompted extensive interest in the synthesis of these molecules to enable evaluation of their biological activity and examination of their structural-activity relationships. Two of these compounds, fosmidomycin **3** and phosphonothrixin **19** are particularly notable.

1.10.1 Fosmidomycin 3

Fosmidomycin **3** which has already been discussed as a potent inhibitor of DXP reductoisomerase in bacteria and higher plants (**1.7**), was isolated from a culture broth of *Streptomyces lavendulae* in 1980 as a co-metabolite of other *N*-hydroxyamino phosphonic acids.[61] Synthesis of the C-P bond in **3** was achieved *via* the Michaelis-Becker reaction of sodium diethyl phosphonate with 3-(*N*-tosyl-*N*-benzyloxyamino)propyl bromide **20**. Hydrolysis of the tosylate then afforded **21**, **Scheme 10**. *N*-Formylation of **21** with acetic-formic anhydride, followed by hydrolysis of the phosphonate ester finally afforded **3**.[61]

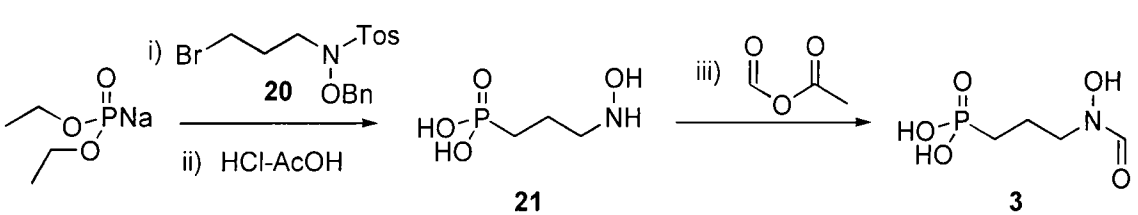

Scheme 10 i. PhH, 5 h, reflux; ii. 50 h, reflux, 63 %; iii. 30 min, RT, 70 %.

1.10.2 Phosphonothrixin 19

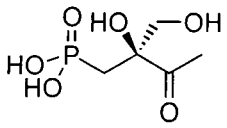

(*S*)-(-)-Phosphonothrixin **19**

Phosphonothrixin **19** is a novel herbicidal antibiotic that inhibits germination of grass and broadleaf weeds as well as inhibiting chlorophyll production upon foliar application on weeds.[60] It was first isolated in 1995 from a fermentation broth of *Saccharothrix sp.* ST-888.[60] Its structure was elucidated in the same year[62] and an enantioselective synthesis described in 1997 securing the absolute stereochemistry of **19**.[63] A sample of (*S*)-**19** had been synthesised in 92 % ee (**Scheme 11**) by exploiting a Sharpless asymmetric epoxidation to generate the chiral epoxy alcohol **22** in 92 % ee.[63] Attack on the epoxide with the chloromagnesium salt of dibenzyl phosphite followed by ozonolysis, yielded the phosphonate diester **23**, hydrogenation of which afforded (*S*)-**19**. The origin of the biological activity of **19** is not known, however it must be noted that it is a close structural isomer of **24**, the CH_2 phosphonate analogue of DXP (**Figure 9**), and this may underlie its wide ranging potency. Phosphonothrixin **19** also has close structural similarities to a proposed intermediate in the biosynthesis of riboflavin.

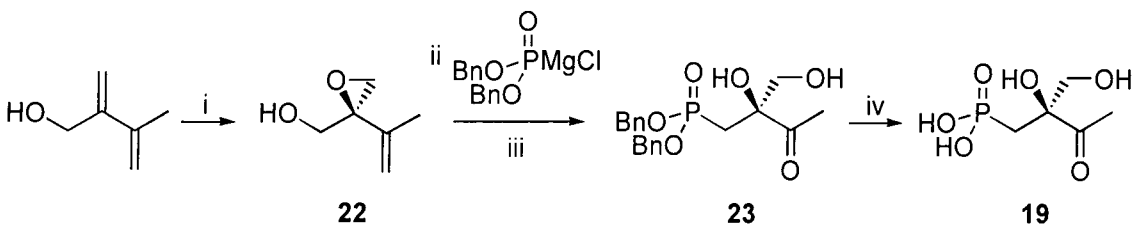

22 **23** **19**

Scheme 11 i. D-DET, $Ti(O^iPr)_4$, TBHP, CH_2Cl_2, 1 d, -20 °C, 57 %; ii. Et_2O, 2.5 h, -50 to 0 °C, 40 %; iii. O_3, CH_2Cl_2, 3 min, -78 °C then Me_2S, 1 h, RT, 79 %; iv. H_2-Pd(C), MeOH / H_2O, quant.

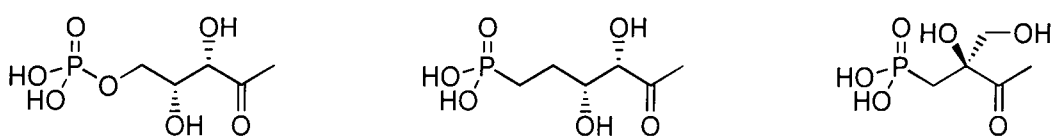

DXP **24** **19**

Figure 9 Structural analogies between DXP, **24** and **19**.

1.10.2.1 Biosynthesis of riboflavin

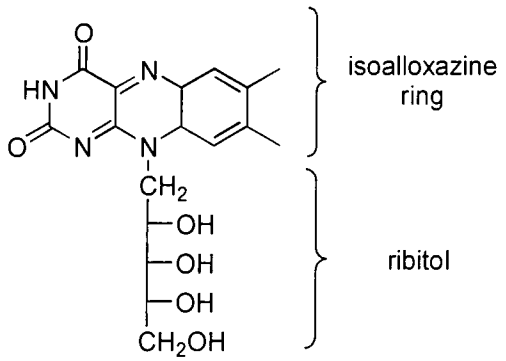

Riboflavin

Riboflavin (Vitamin B_2) provides the functional isoalloxazine ring of two co-enzymes, flavin adenine dinucleotide (FAD) and flavin mononucleotide (FMN). Flavoproteins bind to one of the above co-enzymes to provide an essential enzymatic system that mediates two-electron oxidation and reduction reactions, including hydride and oxygen transfer. These are reactions essential to all cells, but only plants and certain micro-organisms can synthesise riboflavin, the deficiency of this vitamin being known to cause skin lesions and dermatitis in man.[64] A variety of pathogenic bacteria however, such as the *Escherichia* and *Salmonella* species are absolutely dependent on their ability to synthesise riboflavin because they lack an uptake system of this vitamin.[65] Inhibition of the pathway to riboflavin is therefore a potential target for chemotherapy of bacterial infections.

Biosynthetic studies on riboflavin have mainly been carried out on bacteria and yeast.[65] Their pathways have been characterised to a high level and are found to be similar, both involving seven distinct enzyme-catalysed reactions.[66] The convergent biosynthesis requiring one molecule of guanine triphosphate (GTP) and two molecules of ribulose-5-phosphate **25** as substrates, is shown in **Scheme 12**.[65,66]

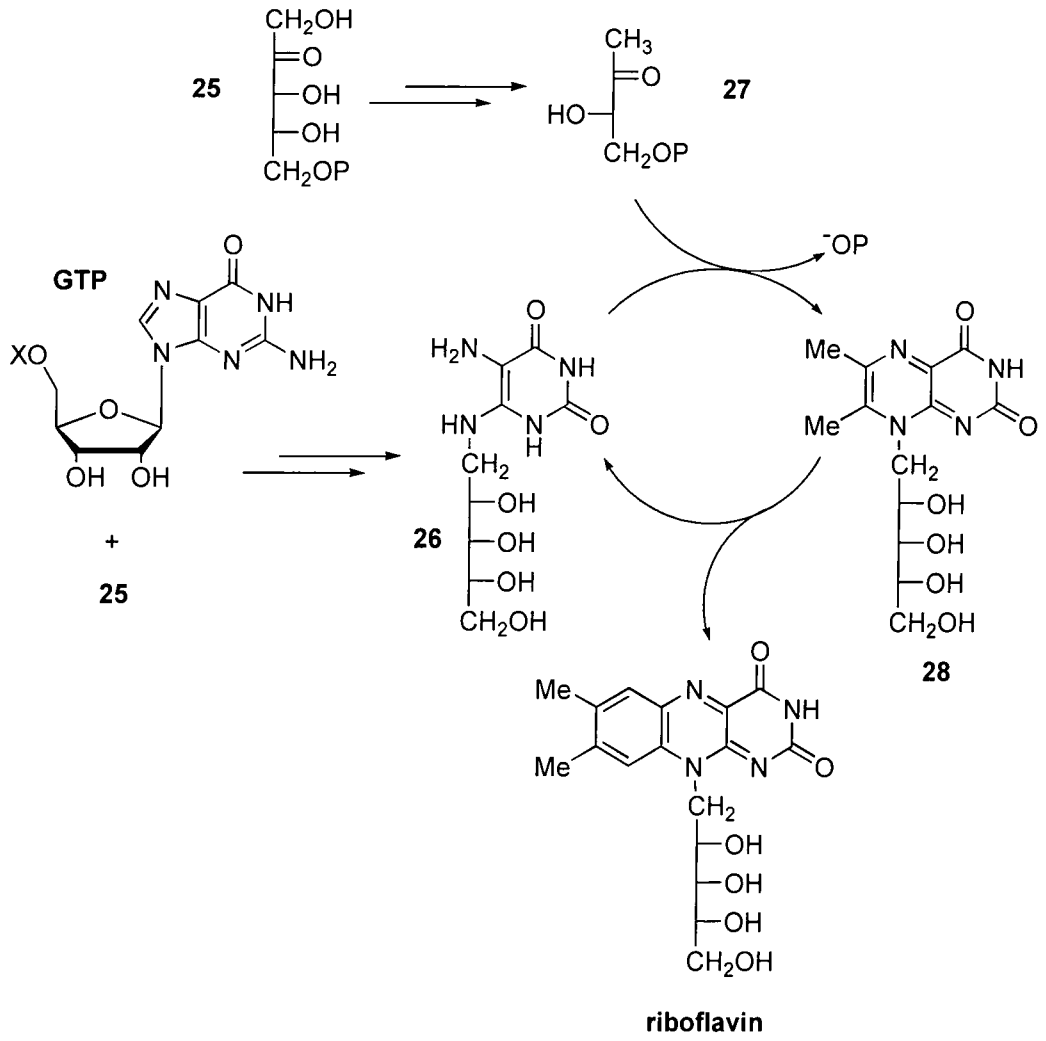

Scheme 12 Biosynthesis of riboflavin.

During the biosynthesis of riboflavin, GTP combines with **25** to form the intermediate **26**. Reaction of **26** with L-3,4-dihydroxy-2-butanone-4-phosphate **27** then affords the riboflavin precursor **28**, which after dismutation yields riboflavin and the intermediate **26** the latter then being reutilised in the pathway. The biosynthesis of **27** from **25** is catalysed by 3,4-dihydroxy-2-butanone-4-phosphate synthase, a Mg^{2+} requiring enzyme, which has been characterised from bacteria and plants. This small enzyme of only about 200 amino acids catalyses a highly complex reaction that involves the rearrangment between C3 and C5 of **27**, followed by the elimination of C4 as formate, **Scheme 13**.[67,68]

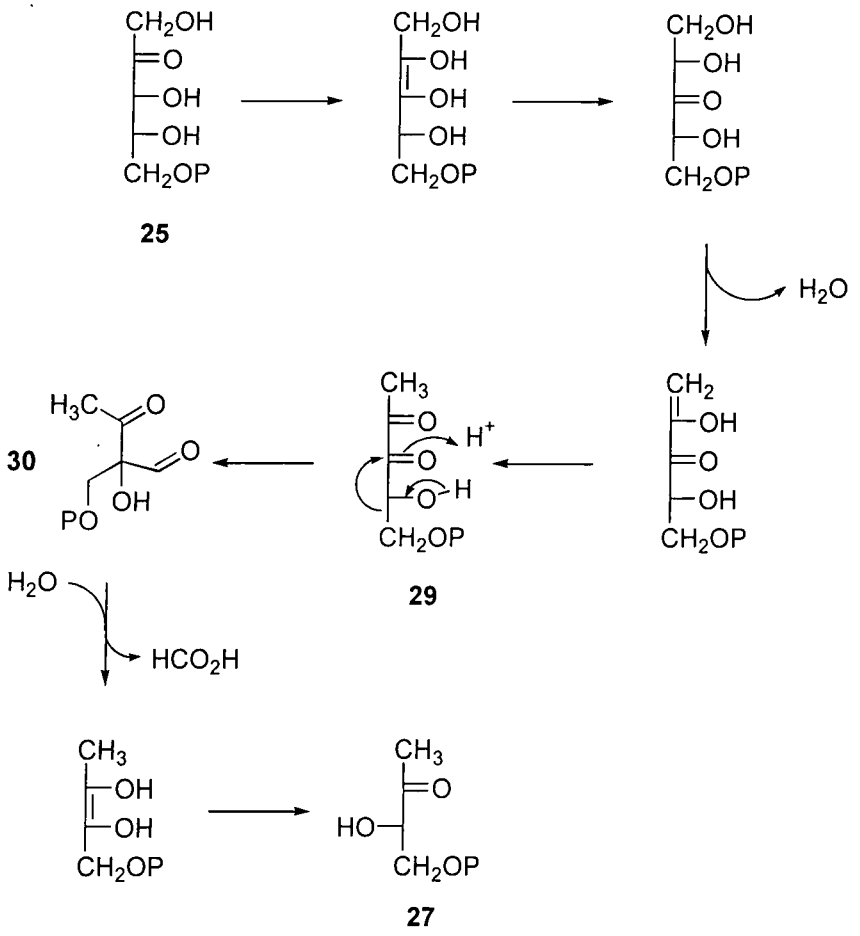

Scheme 13 Putative reaction mechanism for the formation of L-3,4-dihydroxy-2-butanone-4-phosphate **27**.[68]

Of particular interest in the above mechanism is the rearrangement of **29** to **30**. Structure **29** bears a close resemblance to DXP (**Figure 10**), the only difference is that the C3 hydroxy of DXP is oxidised to the ketone in **29**.

Figure 10 Structural analogies between DXP and **29**.

The rearranged product **30** has a very similar structure to phosphothrixin **19** (**Figure 11**). If **19** does inhibit this enzyme, as described below, then this could also account for the observed herbicidal and antibiotic activity of **19**.

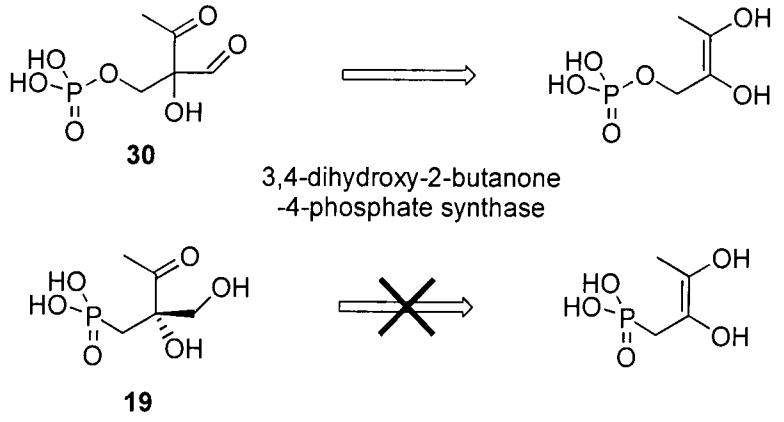

Figure 11 Structural analogies between **30** and **19**.

1.11 α-Fluorinated ketone inhibitors

α-Fluorocarbonyls are more readily hydrated than their non-fluorinated counterparts (**Figure 12**) due to stability incurred by the high electronegativity of the fluorine atom. This inductive effect of fluorine has been employed in the design of inhibitors of enzymes that progress through tetrahedral transition-state complexes.[69,70,71] A striking example of how effective this can be is the inhibition of acetylcholinesterase, a serine mediated hydrolase (**Figure 12**). In the enzyme active site, the first step of the hydrolysis reaction requires the serine's alkoxide nucleophile to attack the substrate's carbonyl to form a tetrahedral intermediate. However, the hemiketal adduct of the trifluoroketone analogue **31** of acetylcholine **32** is so stable that its dissociation equilibrium is remarkably low, with a first-order half-life of 30 h at 25 °C, this affords **31** a K_i value of 6×10^{-11} M for acetylcholinesterase.[72] Comparison of the dissociation rates (**Figure 12**) from the acetylcholinesterase enzyme for the analogues **33** to **35** exemplifies the inductive effect of fluorine.[69]

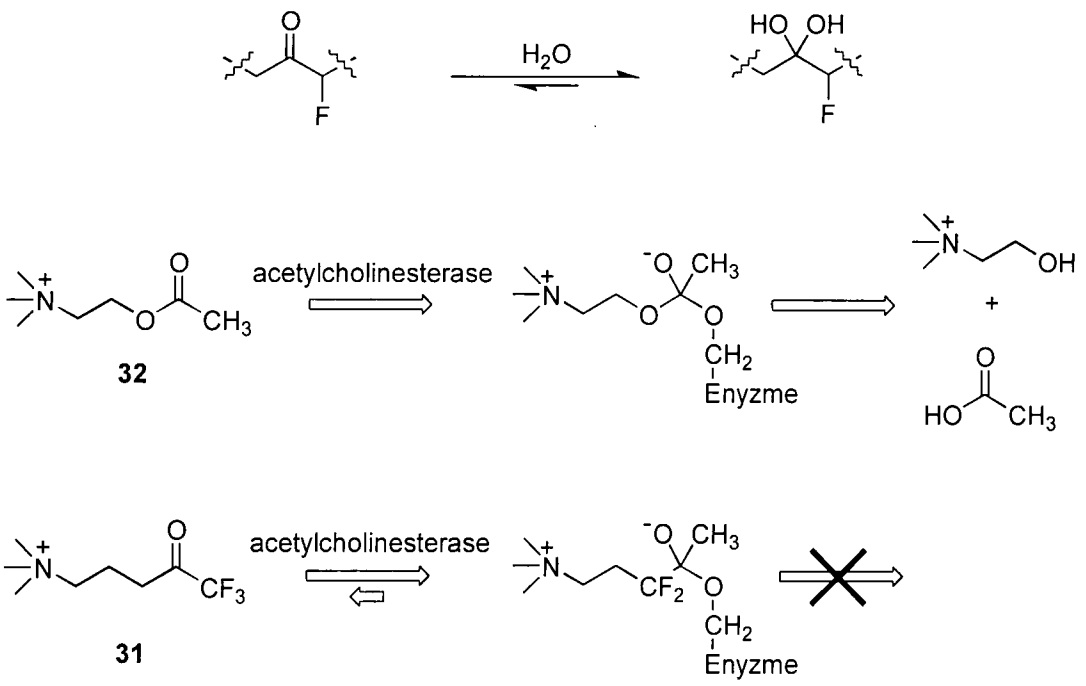

Analogues of 32	$K_{dissociation}$
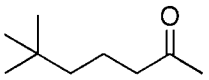 **33**	310000
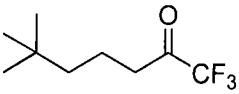 **34**	16
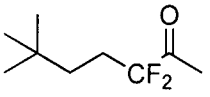 **35**	1.6

Figure 12 Acetylcholinerase inhibition with compounds **31**, **33**, **34** and **35**.

The 1-fluoro- **36** and 1,1-difluoro-1-deoxy-D-xylulose **37** analogues of DX had been synthesised recently to assess their potency as antibiotics.[73] However, these fluorinated sugars showed no antibacterial activity. This was most probably due to **36** and **37** existing predominantly in their cyclic form in solution (as determined by ^{19}F NMR), and thereby preventing *in vivo* phosphorylation of the terminal hydroxymethyl group to generate the corresponding DXP analogues (**Figure 13**).

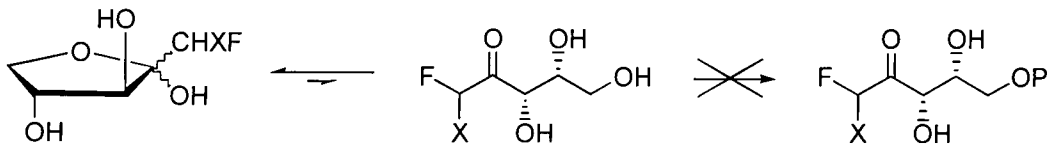

36 X = H
37 X = F

Figure 13

1.12 Synthetic targets

In this thesis work is described towards the synthesis of a number of potential DXP anti-metabolites. A description of these target compounds follows below, with a more detailed retrosynthetic analysis described in section **1.4**.

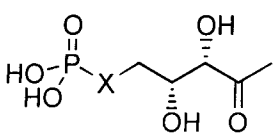

24 X = CH_2
38 X = CHF
39 X = CF_2

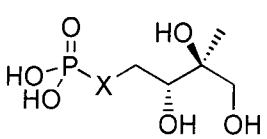

40 X = CH_2
41 X = CHF
42 X = CF_2

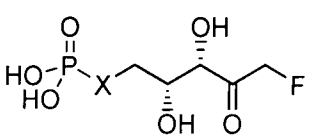

43 X = CH_2
44 X = CHF
45 X = CF_2

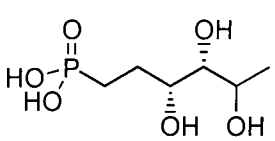

46

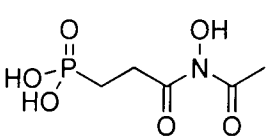

47

The synthetic targets shown above have been selected as potential inhibitors of the reaction catalysed by DXP reductoisomerase. Compounds **24**, **38**, **39** and **40**, **41**, **42** are the phosphonate analogues of DXP and MEP respectively. Targets **43**, **44**, **45** are also phosphonate analogues of DXP, but they contain a fluorine atom in place of a hydrogen alpha to the carbonyl group. Another target, **46**, the reduced form of **24**, was selected as it may act as an inhibitor of DXP metabolism, unable to undergo rearrangement mediated by the reductoisomerase enzyme, **Scheme 9** (page 18), or imine formation as illustrated in the reactions in **ii** and **iii** of **Scheme 9**. The remaining target compound, **47**, was selected as an analogue of fosmidomycin.

1.13 Synthetic methods for C-P bond formation

The above phosphonate targets require the formation of C-P bonds. Three main strategies for forming a C-P bond are applicable to the syntheses of the target compounds in section **1.12**, and are described below.

1. The Michaelis-Arbuzov reaction of a trialkylphosphite with an alkylhalide:

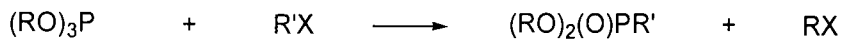

2. The Michaelis-Becker reaction of an alkali salt of a dialkylphosphite with an alkylhalide:

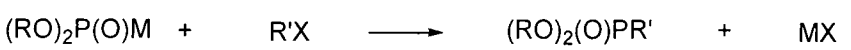

3. A Michael type reaction of either a trialkylphosphite or alkali salt of dialkylphosphite with an α, β-unsaturated C=C double bond:

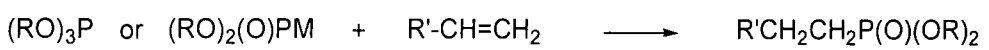

1.14 Proposed routes to synthetic targets

1.14.1 DXP analogues 24, 38, 39 and 43 to 45

The retrosynthetic analysis for the DXP analogues is illustrated in **Figure 14**. The major synthetic problems posed by these targets are the construction of the C-P bond and the selective preparation of single diastereoisomers. The chosen retrosynthetic route requires hydrolysis of the alkyl (ethyl) esters to afford the phosphonic acid. Such hydrolytic reactions are generally mediated by TMSBr.[74] Direct access to diols with the *threo* relative configuration will be addressed by utilising the Sharpless AD-mix asymmetric dihydroxylation reaction.[75] This reaction utilises OsO_4 and a chiral auxiliary and has been shown to work with high selectivity for mainly unconjugated alkenes, however there is precedence for this reaction in enones,[76] and 1-alkenylphosphonates.[77]

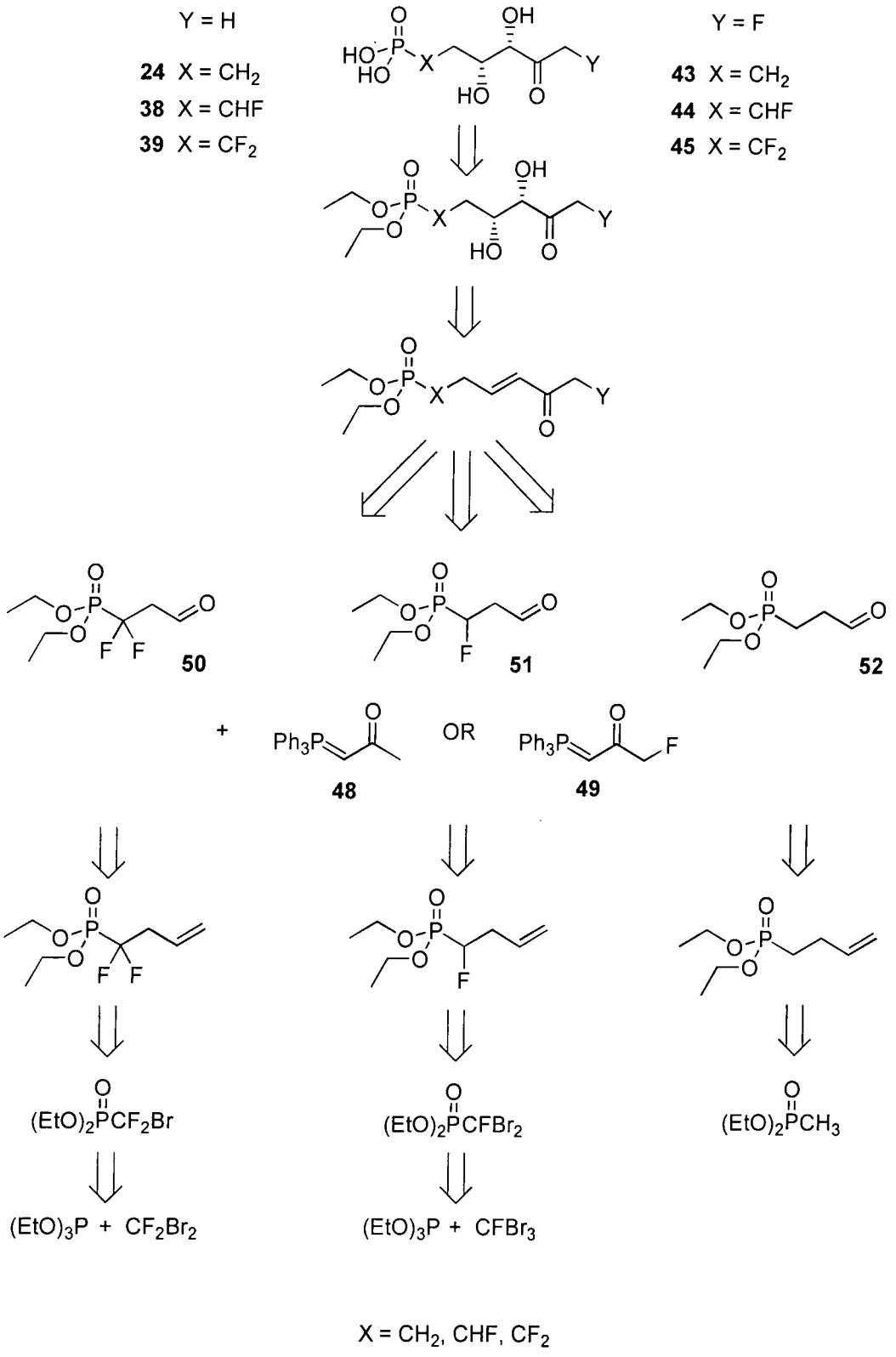

Figure 14 Retrosynthetic analysis for the formation of **24**, **38**, **39** and **43** to **45**.

Facile installation of the enone functionality is envisaged *via* Wittig methodology, through reaction of the ylids **48** or **49** with the phosphono aldehydes, **50**, **51** and **52**. Aldehydes **50** to **52** are conceived to be accessible through reductive ozonolysis of the corresponding alkenes.[78] The synthesis of the phosphono alkenes will be approached through allylation of the respective starting phosphonates.[79] For the CH_2 analogue **24**, the commercially available diethyl methylphosphonate will be utilised, whereas the fluorinated phosphonates will be synthesised *via* a Michaelis-Arbuzov reaction between triethylphosphite and dibromodifluoromethane or tribromofluoromethane.[80]

1.14.2 MEP analogues 40 to 42

A retrosynthetic analysis for the synthesis of **40** to **42** will also employ the phosphono aldehydes **50** to **52**, **Figure 15**. A Grignard reaction using these aldehydes with isopropenylmagnesium bromide should provide access to the racemic allylic alcohol. Introduction of the vicinal diol group will also be explored by Sharpless AD-mix dihydroxylation to generate the protected phosphono triol. Deprotection using a TMSBr mediated hydrolysis reaction should yield the target molecules **40** to **42**.

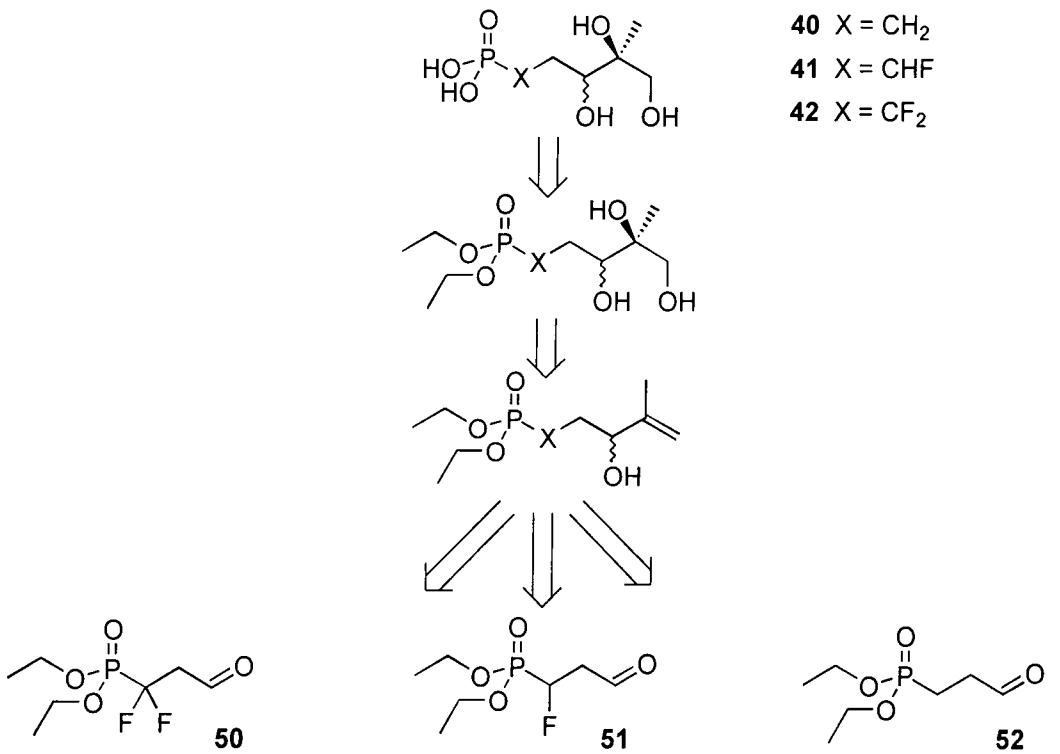

Figure 15 Retrosynthetic analysis for the formation of **40** to **42**.

1.14.3 3(*R*),4(*S*),5(*R*,*S*)-3,4,5-Trihydroxyhexylphosphonic acid 46

Triol **46** is the reduced form of **24**. A standard $NaBH_4$ reduction of suitably protected **24** should afford the triol as a mixture of diastereoisomers. Removal of the phosphonate esters with TMSBr offers a straightforward route to this compound (**Figure 16**).

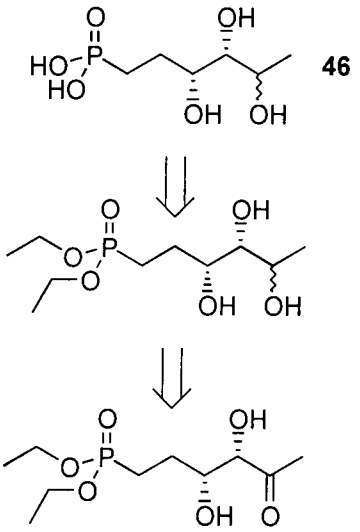

Figure 16 Retrosynthetic analysis for the formation of **46**.

1.14.4 Fosmidomycin analogue 47

The synthesis of the fosmidomycin type structure **47** (**Figure 17**), is again envisaged to utilise a TMSBr mediated hydrolysis to afford **47**. The diethyl *N*-hydroxyimide precusor **53** could be accessible through oxidation of the imide **54** following a literature method.[81] The imide **54** itself may be formed through reaction of the acid chloride with acetamide.[82] Finally, conversion of the commercially available ester **55** to the acid chloride under previously described literature conditions will allow generation of the C-P bond.[83]

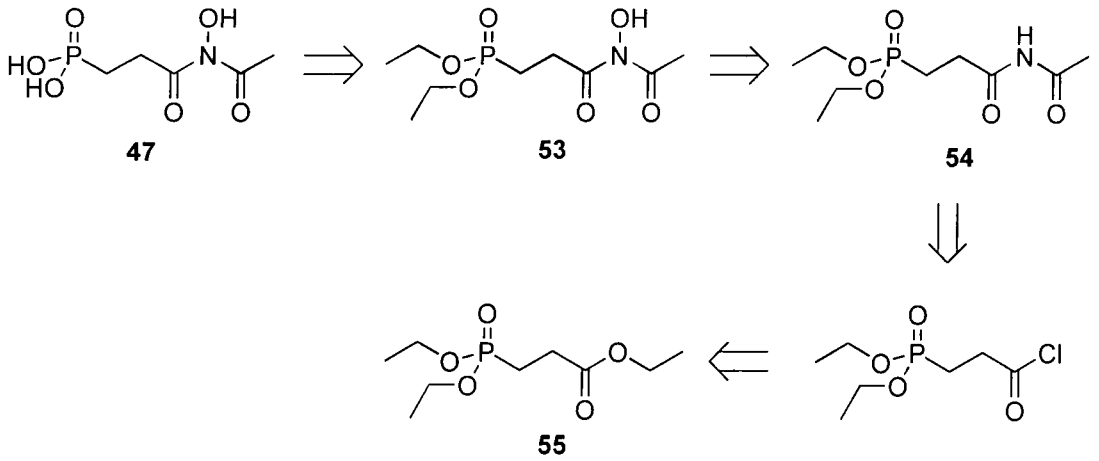

Figure 17 Retrosynthetic analysis for the formation of **47**.

Chapter 2

Synthesis of potential DXP anti-metabolites

2.1 Introduction

Chapter 2 discusses in detail the synthesis of the novel target compounds highlighted in section **1.13**. The DXP analogues are described first; the CH_2 analogue **24** in sections **2.2** and **2.3**, and the CF_2 analogue **39** in section **2.4**. Synthesis of the CH_2 analogue **40** of MEP, and the triol **46** are outlined next in sections **2.5** and **2.6** respectively. Finally, work carried out by Hannah F. Sore towards the fosmidomycin analogue **47** is described in section **2.7**.

2.2 Synthesis of DXP analogue 24 *via* diethyl phosphonate

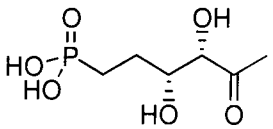

Threo-3(*R*),4(*S*)-3,4-dihydroxy-5-oxohexylphosphonic acid **24**

2.2.1 Syntheses of phosphono aldehydes 50 to 52

Initially syntheses were devised towards the aldehydic compounds diethyl 1,1-difluoro-3-oxopropylphosphonate **50**, diethyl 1-fluoro-3-oxopropylphosphonate **51** and diethyl 3-oxopropylphosphonate **52**. These compounds were identified as key intermediates for the preparation of the required 1-deoxy-D-xylulose-5-phosphate (DXP) analogues.

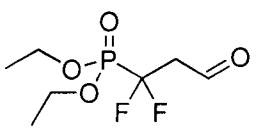

50

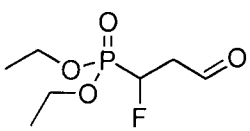

51

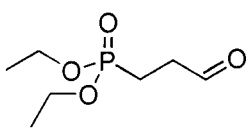

52

2.2.1.1 Preparation of diethyl 1,1-difluoro-3-oxopropylphosphonate **50**

Chambers and co-workers first reported[78] the preparation of the difluorinated aldehyde **50** (**Scheme 14**), *via* a reductive ozonolysis of diethyl 1,1-difluorobut-3-enylphosphonate **56**, the reaction proceeding in a yield of 75 %. Their synthesis of the olefinic precursor **56** to this aldehyde followed that reported[79] by Burton and co-workers by the reaction of the cadmium reagent **57** with allyl bromide. Burton found that a change in solvent from dioxane[79] to THF[78] proved expedient in increasing the yield of this reaction from 31 to 62 %. The organo-cadium reagent **57** itself had been prepared from cadium metal and diethyl bromodifluoromethylphosphonate **58**, and was found to be stable in solution. The phosphonate **58** had been formed *via* an apparent Michaelis-Arbuzov reaction between triethyl phosphite and dibromodifluoromethane in 95 % yield, as described by Burton and Flynn.[80]

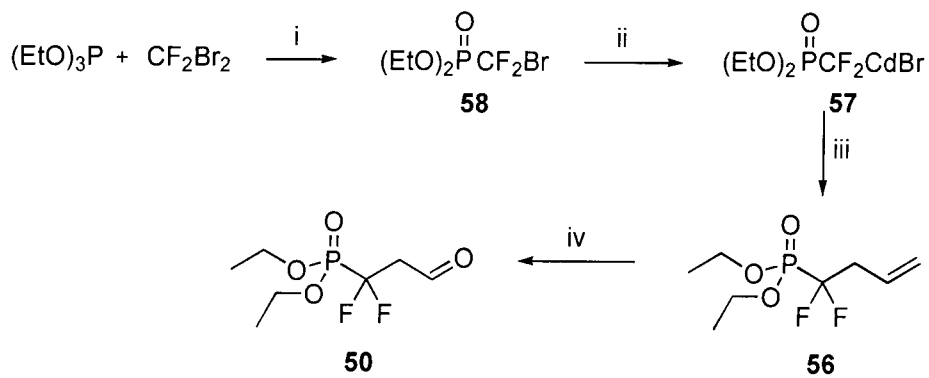

Scheme 14 i. Et_2O, 12 h, reflux, 95 %; ii. Cd, THF, 3h, 65 °C; iii. C_3H_5Br, NaI, THF, 20 h, 25 °C reflux; 62 %; iv. O_3, CH_2Cl_2 / MeOH, -78 °C, then Me_2S, 75 %.

Burton and Sprague subsequently described[84] an alternative organozinc reagent that facilitates alkylation of **58** to afford 1,1-difluoro-3-alkenephosphonates (**Scheme 15**). Allylation had been achieved by addition of allyl bromide to the organozinc reagent **59**, in the presence of a catalytic amount of CuBr, to afford **56** in a moderate yield of 47 %. Synthesis of the organozinc reagent **59** itself is achieved by addition of **58** to acid-washed zinc in a monoglyme solution.[84]

Preparation of **56** was chosen to be carried out *via* the organozinc reagent **59** (**Scheme 15**), utilising the above methods.[80,84,78] In our hands carrying out the allylation of the organozinc reagent as described afforded an improved yield of 77 %, *cf* 47 % reported in the literature. Otherwise reproducible yields and high purity of products were obtained as previously described.

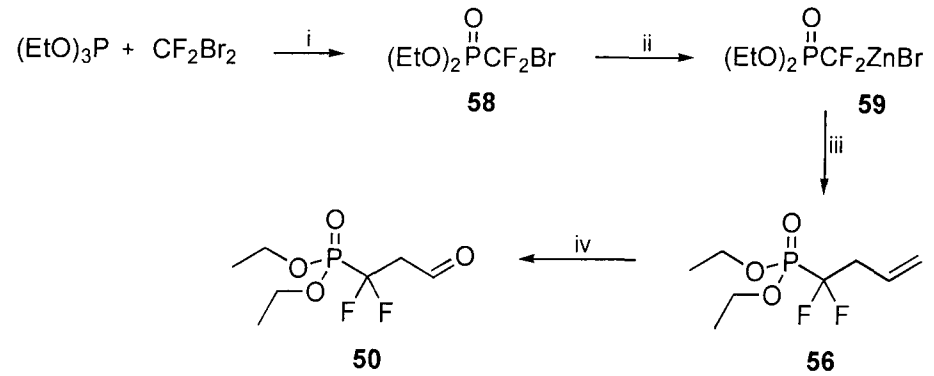

Scheme 15 i. Et_2O, 12 h, reflux, 95 %; ii. Zn, monoglyme, 95 %; iii. C_3H_5Br, CuBr, monoglyme, 12 h reflux; 77 %; iv. O_3, CH_2Cl_2 / MeOH, -78 °C, then Me_2S, 75 %.

2.2.1.2 Preparation of diethyl 1-fluoro-3-oxopropylphosphonate **51**

The monofluorinated aldehyde diethyl 1-fluoro-3-oxopropylphosphonate **51** had not previously been reported, however the synthesis of the olefinic precursor diethyl 1-fluorobut-3-enylphosphonate **60** (**Scheme 16**) had been described[85] by Savignac and Patois. This involved a reaction between diethyl dibromofluoromethylphosphonate **61** and allyl iodide, *via* the double halogen exchanged intermediate α-lithiated-α-fluorophosphonate **62**, obtained by addition of *n*-BuLi and TMSCl (2:1) to **61**. Alkylation of **62** with allyl iodide followed by ethanolysis to remove the TMS group afforded the desired material **60**. The formation of the starting phosphonate **61** had been investigated[80] by Burton and Flynn, who obtained a 78 % yield of this phosphonate by reaction of triethyl phosphite and tribromofluoromethane. A brief overview of this reaction is given by Savignac and co-workers,[86] describing optimised conditions that afford **60** in 97 % yield.

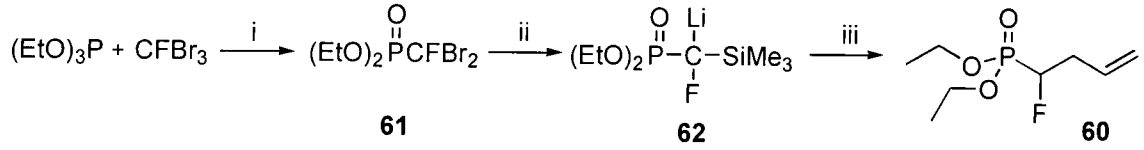

Scheme 16 i. Et_2O, 12 h, reflux, 78 %; ii. *n*-BuLi (2.2 equiv.), TMSCl, THF, -78 °C; iii. C_3H_5I, -78 °C, then LiOEt / EtOH, 0 °C, $NH_4Cl_{(aq)}$, 91 %.

It was envisaged that after following the above reactions, the aldehyde could be accessed through reductive ozonolysis of the alkene as described above (**2.2.1.1**). Accordingly **61** was obtained in 85 % yield and **60** in 80 %. However, initial attempts to obtain the aldehyde *via* ozonolysis of the alkene were unsuccessful.

Performing the ozonlysis reaction under the same conditions as the difluoro analogue **56** yielded a mixture of products. From NMR analysis at least two aldehydic products were apparent and by comparison of integral values, it was evident that aldehydic products comprised the majority of the sample. ^{19}F NMR revealed that there were two fluorine containing species, whereas the ^{31}P NMR spectrum indicated that less than half of the total phosphorus containing species showed any heteronuclear coupling. The most intense peak in the ^{31}P NMR spectrum, comprising over half of the sample, was a singlet. After addition of Et_3N to the sample the relative size of this peak increased, and the ^{19}F resonances disappeared. From the above results it is proposed that the predominant product from the ozonolysis reaction was the aldehyde **63**, derived by HF elimination of the desired product **51**. Further work on this reaction was postponed due to the lack of success with this methodology.

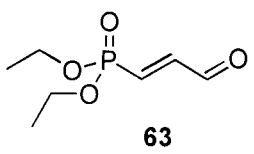

63

2.2.1.3 Preparation of diethyl 3-oxopropylphosphonate **52**.

Diethyl 3-oxopropylphosphonate **52** has been prepared previously by several routes. One method utilised a $PdCl_2$ catalysed oxidation of the alkenic phosphonate **64**.[87] This gave an equal mixture of aldehyde and ketone **65** products (**Scheme 17**).

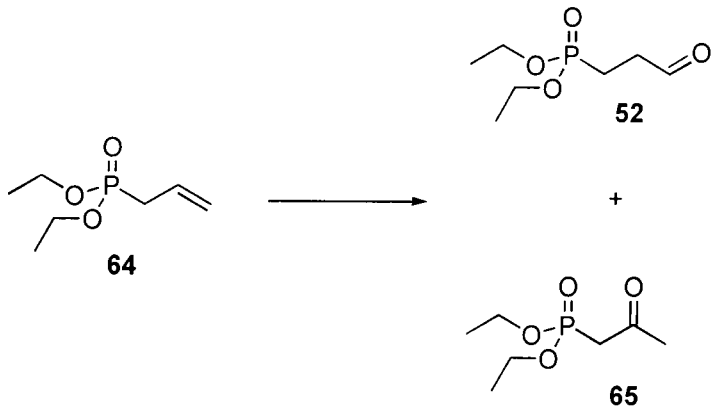

Scheme 17 $PdCl_2$, $CuCl_2$, O_2, H_2O, 6 h, 85 °C, 40 % for **52** and 40 % for **65**.[87]

A more general route to phosphorylated aldehydes has been described.[88] A Michaelis-Arbuzov reaction between a triakyl phosphite and a dihaloalkene affords haloalkenic phosphonate **66**. Halide substitution of these products with alcoholate anions afforded enol ethers, which after hydrolysis gave the corresponding aldehydes (**Scheme 18**) such as **52**.

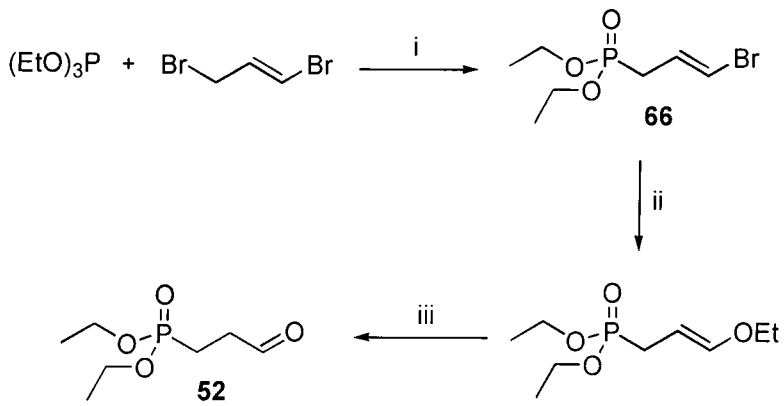

Scheme 18 i. 120-140 °C, 90 %; ii. NaOEt / EtOH, 1 h, reflux, 66 %; iii. $HCl_{(aq)}$ (no yield given).[88]

Another strategy to the required aldehyde **52** and other phosphorylated aldehydes has utilised acetal protection,[89,90,91,92] *via* a Michaelis-Arbuzov reaction with a haloalkylacetal followed by acid hydrolysis to give the aldehyde. In the event a novel approach to **52** was proposed. It was envisaged that coupling of diethyl methylphosphonate with allyl bromide, utilising *n*-BuLi as the base, would give diethyl but-3-enylphosphonate **67**. Reductive ozonolysis of the alkene **67** should then afford the aldehyde **52**.

Initial attempts at alkene synthesis in this manner afforded **67** in low (~ 25 %) yield. A change of electrophile to allyl iodide or allyl mesolate did little to improve this yield (27 % and < 20 % respectively), **Scheme 19**. Using a five-fold excess of allyl bromide increased the yield of **67** to 52 %, and a product could be isolated after distillation in > 97 % purity (**Scheme 19**). In order to access the aldehyde, ozonolysis was initially performed using the conditions described above (**2.2.1.1**). These conditions yielded the desired product, but only as the minor component of the crude product mixture. The unidentifiable component that made up the majority of the sample remained inseparable from **52** by either distillation or column chromatography. Ozonolysis using CH_2Cl_2 as the only solvent (*cf* previous CH_2Cl_2 / MeOH mix), curtailed the production of side-products affording pure aldehyde **52** after distillation, albeit in low (40 %) yield (**Scheme 19**).

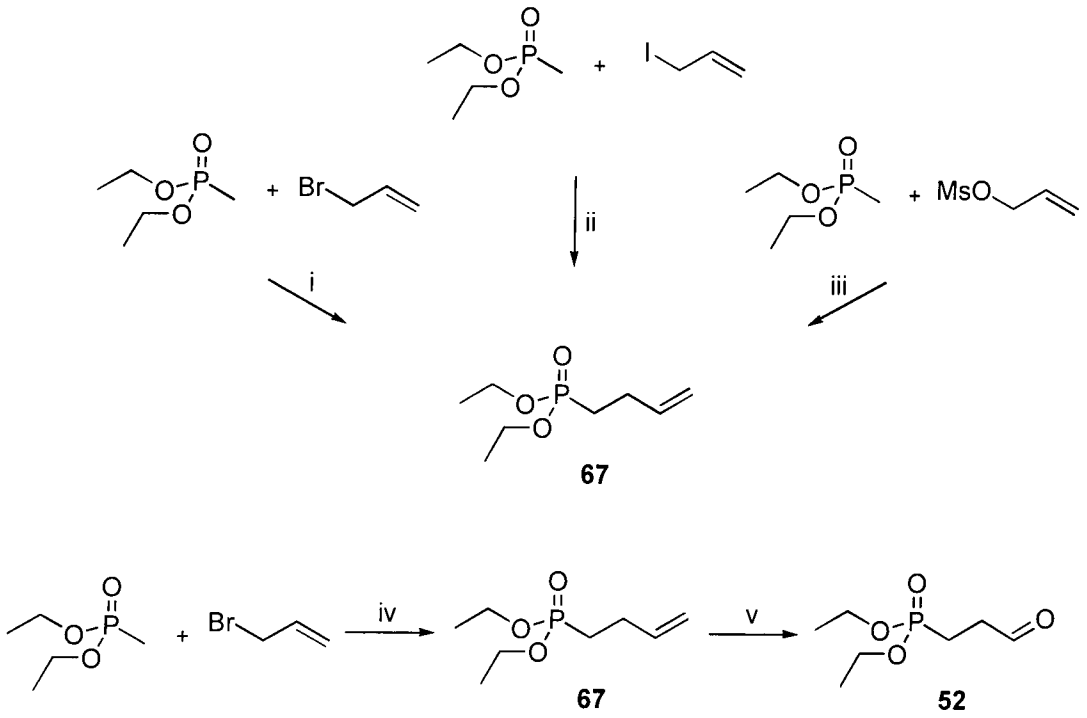

Scheme 19 i. *n*-BuLi, THF, -78 °C, then C_3H_5Br (1 equiv.), then $NH_4Cl_{(aq)}$, 0 °C, ~25 %; ii. *n*-BuLi, THF, -78 °C, then $NH_4Cl_{(aq)}$, 0 °C, 27 %; iii. *n*-BuLi, THF, -78 °C, then $NH_4Cl_{(aq)}$, 0 °C, < 20 %; iv. *n*-BuLi, THF, -78 °C, then C_3H_5Br (5 equiv.), then $NH_4Cl_{(aq)}$, 0 °C, 52 %; v. O_3, CH_2Cl_2 / MeOH, -78 °C, then Me_2S, 40 %.

Further material was brought forward utilising dimethyl methylphosphonate **68** as the starting phosphonate because of its relatively low cost. Using an excess of allyl bromide as before yielded the desired material dimethyl but-3-enylphosphonate **69** in 43 % yield after distillation. Reductive ozonolysis of **69** using CH_2Cl_2 as the only solvent afforded the aldehyde dimethyl 3-oxopropylphosphonate **70** in 35 % yield (**Scheme 20**). The poor yields prompted another survey of the literature and this resulted in an investigation into the allylation reaction above (**Scheme 20**).[93] It had been found that by converting a lithiomethylphosphonate to a copper (I) methylphosphonate and using this as the nucleophilic species, considerably higher allylation yields were obtained.[93] Dimethyl copper (I) methylphosphonate **71** was duly prepared as described[93] and subsequently reacted with one equivalent of allyl bromide to generate **69** after distillation, in an excellent yield of 95 % and with > 99 % purity (**Scheme 20**). This product was then subjected to ozonolysis and quenched with DMS. Attempted distillation of the crude ozonised product after quenching, resulted in a violent explosion. The reaction was

carefully repeated, ensuring that DMS was used in excess to quench any ozonide formed. After obtaining a negative test for peroxides, the mixture still exploded shortly after distillation had begun. It was judged imprudent to pursue this method and a different approach to aldehyde **70** was pursued.

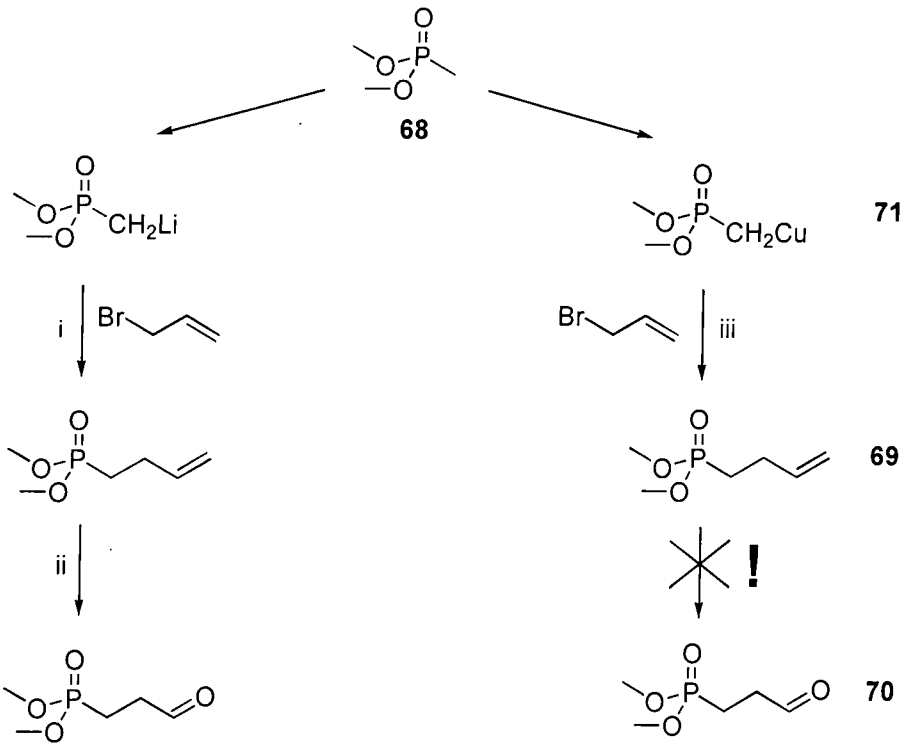

Scheme 20 i. *n*-BuLi, THF, -78 °C, then C_3H_5Br (5 equiv.), then $NH_4Cl_{(aq)}$, 0 °C, 43 %; ii. O_3, CH_2Cl_2, -78 °C, then Me_2S, 35 %; iii. *n*-BuLi, THF, -78 °C, then Cu(1)I, -35 °C, then C_3H_5Br, -35 °C, 95 %.

An alternative route to the phosphorylated aldehyde was now sought. Formation of the aldehyde by deprotection of its acetal protecting group had previously been successful, the acetal phosphonate being accessible from a Michaelis-Arbuzov reaction. However, because the allylation of **71** had proved a high yielding coupling strategy, reaction of **71** with a haloalkylacetal was now attempted. Reaction of the protected aldehyde 2-bromomethyl-1,3-dioxolane **72** with **71** was duly carried out (**Scheme 21**), however all attempts to couple the two reactants were unsuccessful. Dimethyl methylphosphonate was first deprotonated with LDA at -78 °C, but neither the resultant lithiomethylphosphonate or the organocopper reagent **71** reacted in either a THF or DMF solvent, the crude reaction mixture always yielding a moderate recovery of starting

material. Another route to the aldehyde was again sought, and to this end the Michaelis-Becker reaction between 2-(2-bromoethyl)-1,3-dioxane **73** and dibenzyl phosphite was attempted. Use of NaH as the base to produce the desired acetal phosphonate (**Scheme 21**), again resulted in only recovery of the starting material.

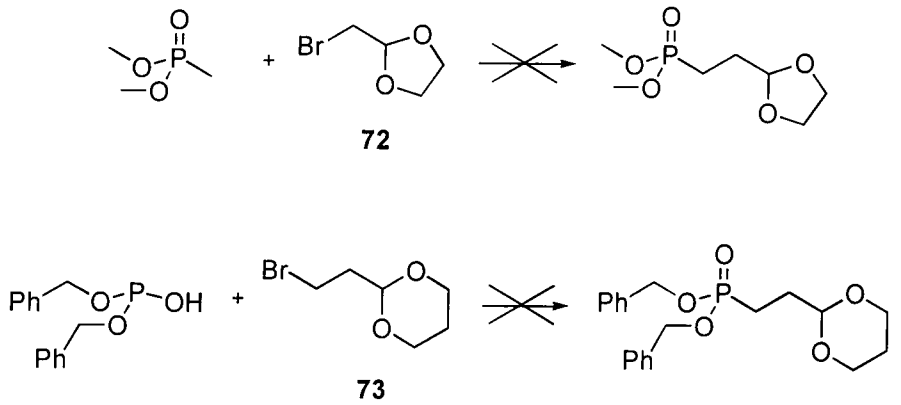

Scheme 21 Proposed routes to protected phosphono acetals.

Martin and co-workers[94] had found that they could not induce efficient coupling between **68** and a halo or tosyl alkylacetonide. However, by utilising the Michaelis-Arbuzov methodology they successfully overcame the problematic coupling reaction. It therefore seemed prudent to follow this strategy for the synthesis of the target acetal phosphonate.[95,96,97,98]

Accordingly, the reaction of triethyl phosphite with **73** did indeed generate the acetal phosphonate, 2-(2-diethoxyphosphonylethyl)-1,3-dioxane **74** in good (70 %) yield (**Scheme 22**). However, attempts to obtain the aldehyde **52** by selective removal of the acetal protecting group with aqueous HCl or PTSA, resulted in low mass recovery of a crude organic mixture (**Scheme 22**), which still contained acetal. Concurrent hydrolysis of the phosphonate ester could perhaps account for the low yield, since ^{31}P NMR did reveal phosphorus containing species in the aqueous phase, even after continuous extraction.

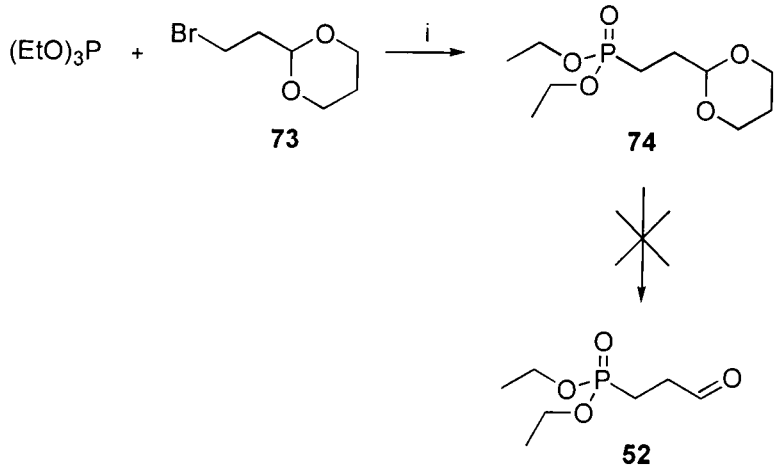

Scheme 22 i. 4 h, 145 °C, 30 min, 165 °C, 68.5 %.

It was clear that the present acetal moiety was incompatible with the phosphonate group. An aldehydic protecting group that would hydrolyse at a faster rate was required. The relative rate of acid-catalysed hydrolysis of cyclic acetals (**Figure 18**) has been studied and the results indicate that hydrolysis of a dioxolane (5 membered ring) acetal proceeds at a greater rate than a dioxane (6 membered ring) acetal.

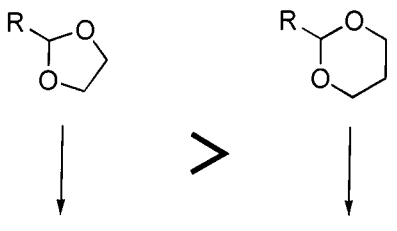

Figure 18 Relative rate of acid-catalysed hydrolysis of cyclic acetals.

In the light of these observations it appeared prudent to undertake the synthesis of 2-(diethoxyphosphonylethyl)-1,3-dioxolane **75**. Accordingly the Michaelis-Arbuzov reaction again afforded the acetal **75** in high (85 %) yield (**Scheme 23**), and its hydrolysis to **52** was now investigated. Firstly a series of preliminary reactions with HCl, PTSA and PPTS were carried out to ascertain the best proton source for the hydrolysis. HCl was found to be the most promising and further reactions were assayed for the yield and purity of **52**, in an effort to establish the optimum hydrolysis conditions, **Table 1**. The optimised

conditions (**Entry 6**, **Table 1**) afforded **52** in near quantitative (> 98 %) yield with > 97.5 % purity, as illustrated in **Scheme 23**.

	$[HCl_{(aq)}]$ / mol dm^{-3}	$[75_{(aq)}]$ / mol dm^{-3}	Duration of reflux / h	Purity by ^{31}P NMR / %	Yield of reaction / %
1	0.5	0.42	3	73	82
2	0.5	0.42	4	68	88
3	0.25	0.14	3.25	82	96
4	0.1	0.125	3.5	94	97
5	0.1	0.085	3	95	97
6	0.1	0.085	3	98	97

Table 1 Reaction conditions utilised during optimisation of the hydrolysis reaction of **75**.

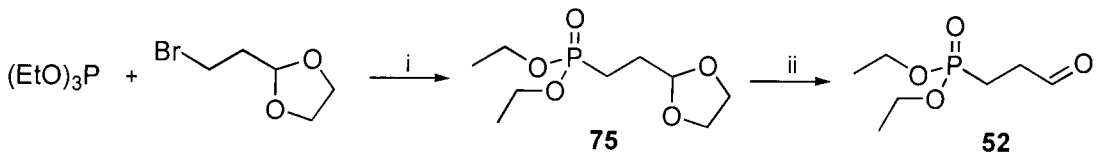

Scheme 23 i. 4 h, 145 °C, 1 h, 165 °C, 85 %; ii. 0.1 M $HCl_{(aq)}$, 3 h, reflux, 98 %.

The synthetic route in **Scheme 23** was reproducible and was used to generate **52** in high yield and purity. The crude product could be processed further without the need for purification. After this work had been completed a comprehensive review on phosphorylated aldehydes was published.[99] This review also detailed the preparation of **52** *via* the general methodology of a Michaelis-Arbuzov reaction to afford a phosphono acetal (in this case, a diethyl acetal), followed by acid hydrolysis to form **52**.

2.2.2. Synthesis of DXP analogue 24 from aldehyde 52

Now that the key aldehyde intermediate **52** was available, the synthesis of the CH_2 analogue of DXP could progress. A retrosynthetic analysis to the CH_2 analogue **24** of DXP from the aldehyde **52** is shown in **Figure 19**. The next step towards **24** required the Wittig reaction to afford the enone **76**. Preparation of the fluorinated ylid **49** would afford access to the DXP analogue **43**.

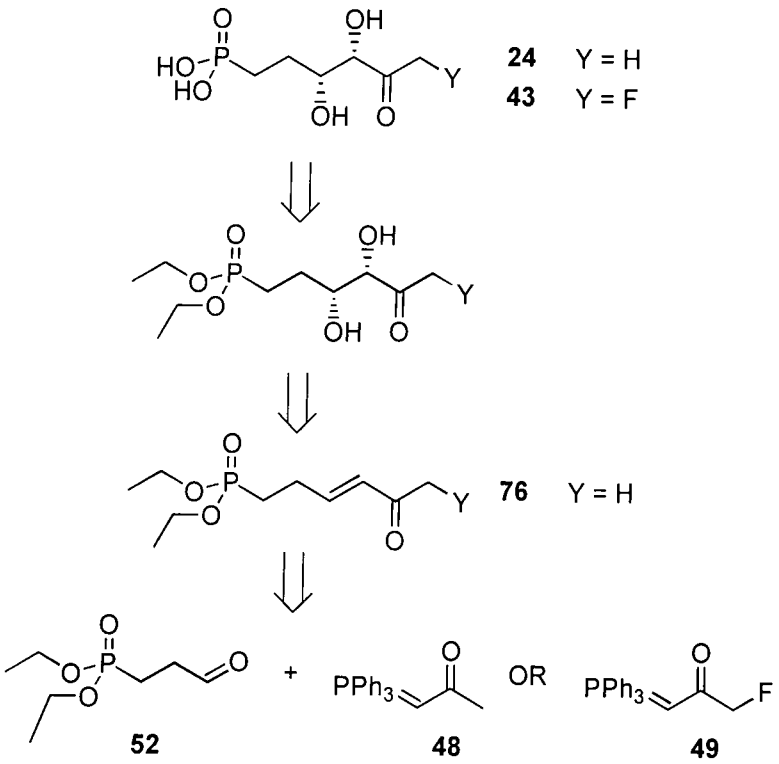

Figure 19 Retrosynthetic analysis to **24** and **43**.

2.2.2 Synthesis of enone 76

Reaction of the commercially available ylid **48**, with the previously prepared aldehyde **52** (**2.2.1.3**) generated a mixture of diethyl (*E*)-5-oxohex-3-enylphosphonate **76** and triphenylphosphine oxide. The progress of the reaction could be monitored conveniently by tlc or more straightforwardly by ^{31}P NMR. A variety of purification methods were utilised to optimise the yield of **76**, with column chromatography resulting in clean

product (> 99 % purity) and in a 70 % yield, **Scheme 24**. The success of this reaction now prompted the synthesis of the fluoro ylid **49**.

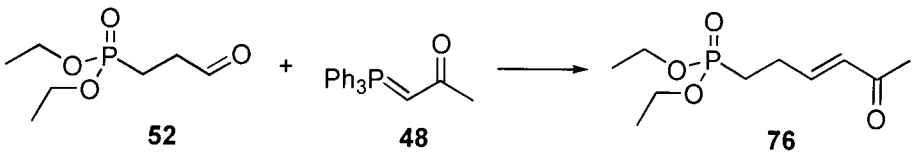

52 **48** **76**

Scheme 24 THF, 16 h, reflux, 70 %.

2.2.2.2 Synthesis of fluoro ylid **49**

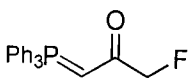

3-Fluoro-2-oxopropylidenetriphenylphosphorane **49**

DXP analogues (**43** to **45**) with fluorine substituted alpha to the carbonyl were identified as key target compounds as discussed in **1.13**. The synthesis of the fluorinated ylid **49** was undertaken to enable access to the 6-fluorinated enones using the above methodology (**2.2.2.1**). Conversion of the 6-fluorinated enones to DXP analogues could clearly follow an analogous route to that for the non-fluorinated analogue, as discussed above.

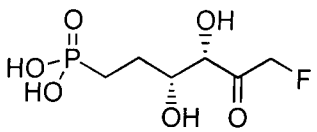

43

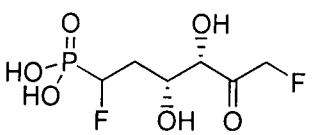

44

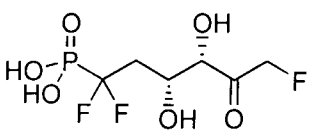

45

Preparation of the fluorinated ylid **49** has been reported *via* the ketone chloro-3-fluoropropan-2-one 77.[100] Ketone 77 itself had been prepared *via* nucleophilic attack of fluoride on epichlorohydrin at the least hindered site,[101,102,103,104] followed by oxidation[104,105] of the intermediate alcohol **78** to afford 77, **Scheme 25**.

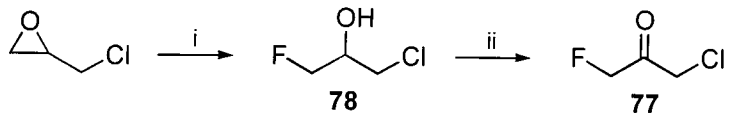

Scheme 25 i. $Et_3N.3HF$, 4 h, 100 °C, 55 %; ii. $Na_2Cr_2O_7$, TBAB, CH_2Cl_2 / H_2O, RT, then 50 % $H_2SO_{4(aq)}$, then 1 d, RT, 55 %.

The availability of 1,3-dichloropropanone **79** however, prompted an investigation into preparing **49** *via* halogen exchange of the ylid 3-chloro-2-oxopropylidenetriphenylphosphorane **80**. In the event dichloroketone **79** was converted in a straightforward manner to the chloro ylid **80** in approximately 70 % overall yield, via **79b**, following a literature preparation (**Scheme 26**).[106] However, attempts to achieve halogen exchange were unsuccessful using the fluorinating agents KF or KHF_2, **Scheme 27**.

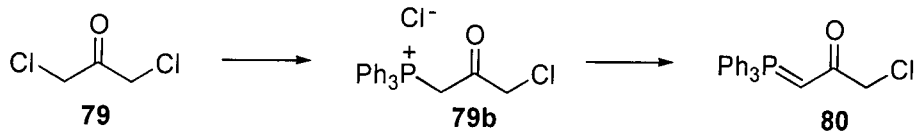

Scheme 26 i. Ph_3P, THF, 4 h, reflux, 84 %; iv. Na_2CO_3, MeOH / H_2O, 80 %.

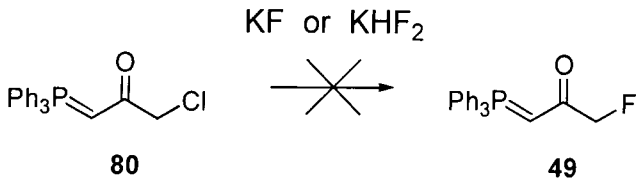

Scheme 27 Attempted synthesis of **49**, *via* halogen exchange.

Due to the failure of this approach, the synthesis of **49** (**Scheme 28**) from epichlorohydrin was resumed. Inconsistant yields (30-52 %) were obtained in the epoxide opening reaction with $Et_3N.3HF$. In general the yields were lower than that described (55 %),[101] none-the-less after distillation chloro-3-fluoropropan-2-ol **78** was attainable. Oxidation of ketone **77** was sluggish and only about a 65 % conversion could be achieved, even with

extended reaction times. Separation of the alcohol from the ketone by treatment with sodium bisulphite worked well, however a poor recovery of the ketone, even after continuous extraction, resulted in a low isolated yield (14 %). However, conversion of chloro-3-fluoropropan-2-one **77** to the ylid **49**, via **77b**, as previously described,[100] proved straightforward and afforded **49** in an overall yield of 65 % from ketone **77**, **Scheme 28**.

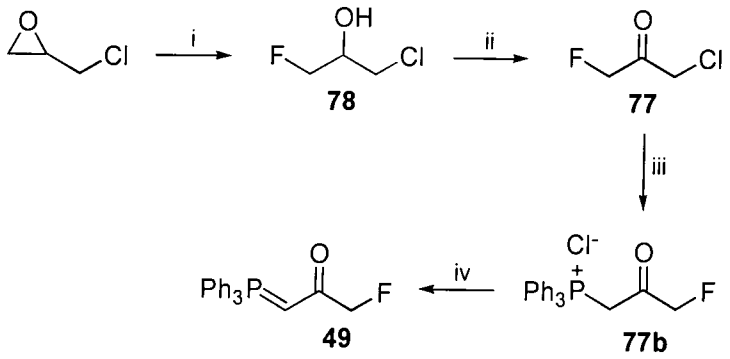

Scheme 28 i. $Et_3N.3HF$, 4 h, 100 °C, 52 %; ii. $K_2Cr_2O_7$, TBAB, CH_2Cl_2 / H_2O, RT, then 50 % $H_2SO_{4(aq)}$, then 5 d, RT, 14 %; iii. Ph_3P, THF, 5 h, reflux, 70 %; iv. Na_2CO_3, MeOH / H_2O, 92 %.

The Wittig reaction between aldehyde **52** and the ylid **49** was carried out in refluxing THF (**Scheme 29**) and progressed at a very slow rate. After five days reaction the ^{19}F NMR and ^{31}P NMR of the reaction mixture indicated that the conversion to the desired product, diethyl (*E*)-6-fluoro-5-oxohex-3-enylphosphonate **81**, was low (< 10 %). As a result further work on this reaction was postponed and the synthesis of **82** became the focus of attention.

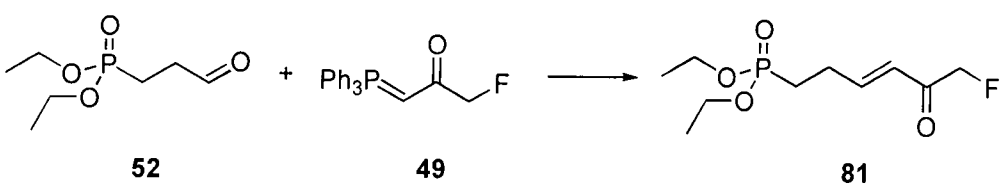

Scheme 29 THF, 5 d, reflux, < 10 % conversion.

2.2.2.3 Dihydroxylation of enone **76**

DXP has the *threo* relative configuration between the stereogenic centres carrying the 3,4-hydroxy groups. As discussed in **1.14.1** during the synthesis of DXP analogues this stereochemistry should be accessible from a Sharpless asymmetric dihydroxylation (AD) reaction on the *trans* olefin. However, standard Sharpless conditions on **76** (**Scheme 30**) using the appropriate AD-mix reagent, did not result in any *threo* diol **82** product, even after an extended reaction time. Repeating the reaction with 1 mol % of OsO_4, and then a stoichiometric amount of OsO_4 reagent in the presence of the chiral ligand, was still unsuccessful. This lack of reactivity was deduced to be due to the conjugated double bond deactivating the system towards electrophilic attack.

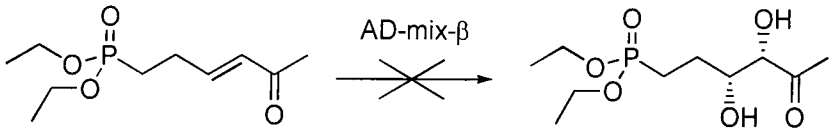

76 **82**

Scheme 30 Failed AD-mix reaction to form **82**.

In order to remove the conjugation, methods to protect the carbonyl group of **76** by forming a ketal, were investigated. Standard ketone protection conditions with triethyl orthoformate in EtOH gave the Michael addition product, diethyl 3-ethoxy-5-oxohexylphosphonate **83**, **Scheme 31**, in an efficient but frustrating 70 % yield. Attempted formation of the dioxolane **84** by reaction of ethylene glycol with oxalic acid[107] afforded a mixture of starting material and products, but no **84**.

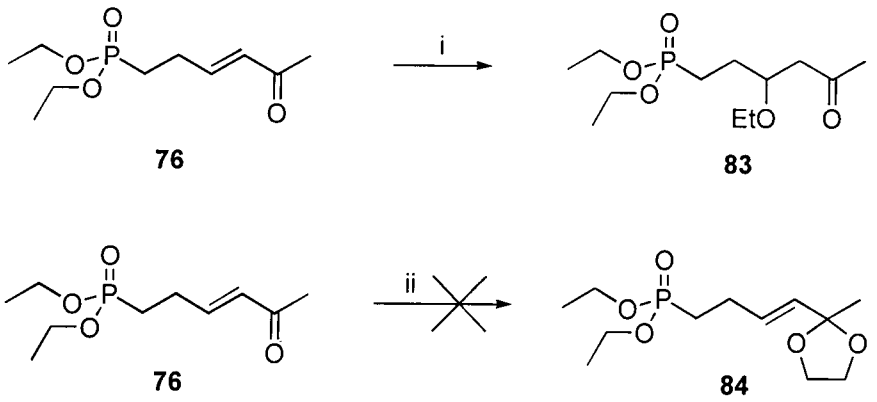

76 83

76 84

Scheme 31 i. $(EtO)_3CH$, EtOH, PTSA, 30 min, 72 %; ii. $(HOCH_2)_2$, $(HCO_2)_2$, CH_3CN, 90 min.

Next, a low temperature aprotic method of carbonyl protection, pioneered by Noyori,[108,109,110] was attempted. This methodology utilises the organosilicon compounds, trimethylsilyl trifluoromethanesulphonate (TMSOTf) and 1,2-bis[(trimethylsilyl)oxy]ethane (BTSE) as catalyst and acetalisation agent respectively. It has been shown to afford the dioxolanes **85**, **86** and **87** of α,β-unsaturated ketones **88**, **89** and **90** (**Scheme 32**) in high yield and without concomitant double bond migration. The formation of hexamethylsiloxane (TMS_2O) was proposed as a major factor in shifting the equilibrium towards the products. The initial results were encouraging and after optimisation this reaction afforded the ketal (*E*)-2-(4-diethoxyphosphonylbut-1-enyl)-2-methyl-1,3-dioxolane **84** in moderate (55 %) yield with > 90 % purity, **Scheme 33**.

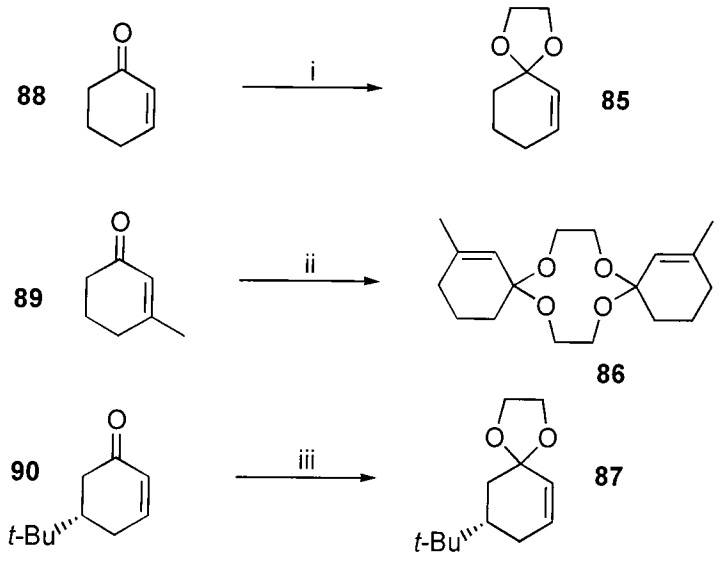

Scheme 32 Reported aprotic acetalisations of α, β-unsaturated ketones. $(TMSOCH_2)_2$, TMSOTf, CH_2Cl_2; i. 20 h, -78 °C, 92 %;[108] ii. 30 min, -78 °C, 48 h, 20 °C, 57 %;[110] iii. 44 %.[111]

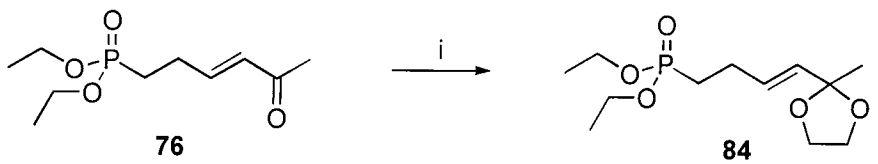

Scheme 33 i. $(TMSOCH_2)_2$, TMSOTf, CH_2Cl_2, 28 h, -60 °C, 55 %.

Now an AD-mix dihydroxylation reaction of the protected enone **84** did afford the *threo*-diol **91**, albeit inconsistantly and in low (20 %) yield (**Scheme 34**). This material showed a positive optical rotation of $[\alpha]_D^{20}$ +10.5 ° (c. 1.0, $CHCl_3$). However, assessment of the diol's enantiomeric excess through ^1H NMR and by using the $Eu(hfc)_3$ chiral shift reagent proved inconclusive. Further analysis such as preparing a suitable derivative (eg with Mosher's acid), was not pursued due to lack of sufficient material.

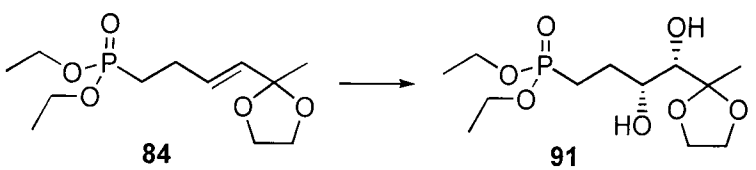

Scheme 34 AD-mix-β, $(CH_3)_3COH$ / H_2O, 22 h, 20 %.

In an effort towards finding improved methods for *syn* dihydroxylation of **76**, alternative strategies were investigated. Use of $KMnO_4$ under alkaline conditions rarely affords diols in high yield,[112] primarily due to oxidative cleavage. However, Woodward's[113] method of *syn* dihydroxylation, using iodine and silver acetate in wet acetic acid, followed by alkaline hydrolysis, has been shown to yield *syn* diols in good yield. The reaction proceeds through an iodo acetate intermediate and has been modified by use of KIO_3, instead of silver acetate, to provide a less expensive means of dihydroxylation.[114] Utilisation of the modified Woodward's method afforded a mixture of products alongside the starting material, but failed to yield appreciable amounts of the desired diol.

Apart from OsO_4, another group VIII metal oxide, RuO_4, has been shown to mediate *syn* dihydroxylation in moderate to excellent yield (**Scheme 35**).[115] The use of catalytic RuO_4 with the co-oxidant $NaIO_4$, enables a very rapid reaction (~ 3 min) which has been termed 'flash' dihydroxylation.[115] Higher yields are shown for those substrates that contain one or more electron withdrawing groups in conjugation with, or adjacent to, the alkene moiety.

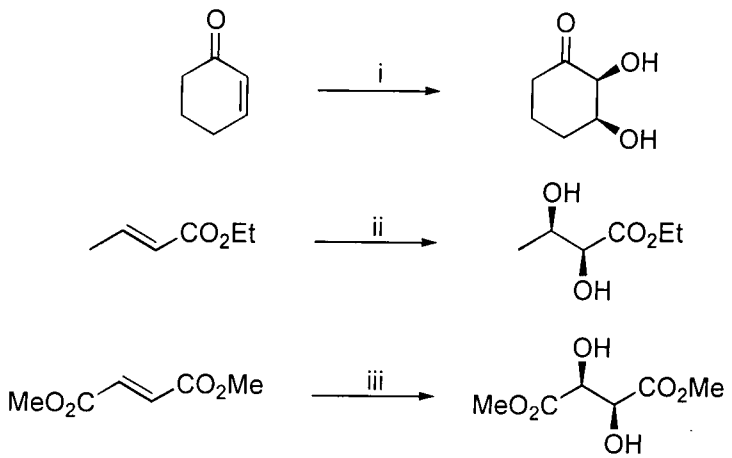

Scheme 35 Literature reactions. Cat. RuO_4, $NaIO_4$; i. CH_3CN, 0.5 min, 51 %;[115] ii. CH_3CN, 3 min, 69 %;[115] iii. EtOAc / CH_3CN / H_2O, 3 min, 90 %.[115]

The ruthenium catalysed dihydroxylation of **76** was duly carried out and did afford racemic *threo*-diol **82**, but again in a low (13 %) yield, **Scheme 36**. Attempts to improve the reaction by deviating from the reported conditions were unsuccessful, being hampered by over oxidation and glycol cleavage of **82**.

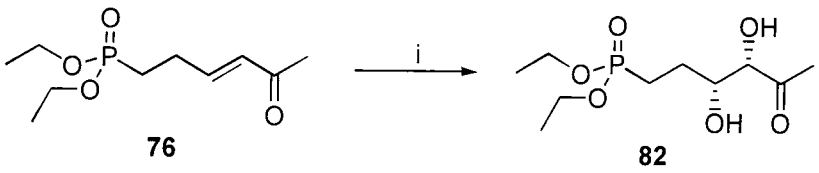

Scheme 36 i. Cat. RuO_4, $NaIO_4$, EtOAc / CH_3CN / H_2O, 3 min, 13 %.

During efforts towards finding alternative *syn* dihydroxylation strategies, a number of relevant OsO_4 dihydroxylation reactions on phosphonates were noted. In particular a previously reported[116] reaction on **92** (**Scheme 37**, ii) had similarities to the current dihydroxylation reaction. Another report[117] described the efficient dihydroxylation of the alkenic phosphonate **67**, using reaction conditions developed by Sharpless and co-workers.[118] In an effort towards finding improved methods for the dihydroxylation of **76**, these conditions were investigated further.

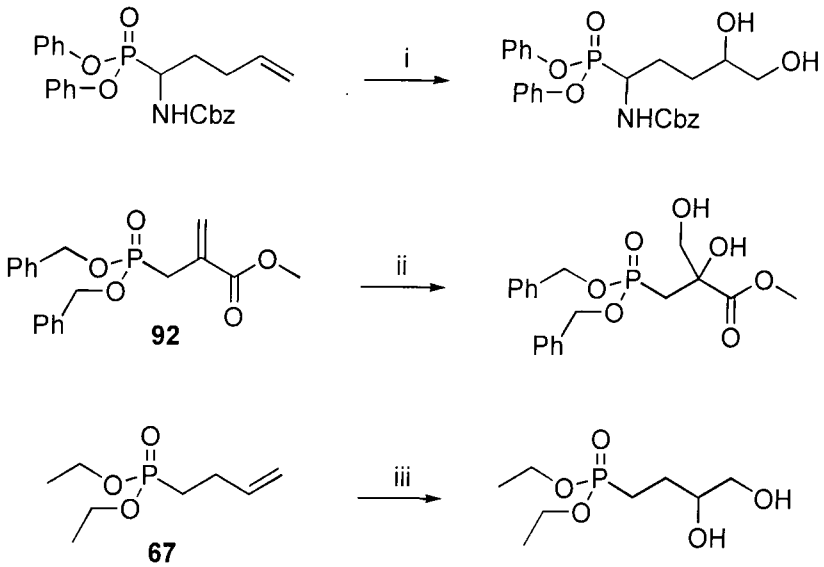

Scheme 37 i. OsO_4, NMO, THF, H_2O, 12 h, 22 °C, 94 %;[119] ii. OsO_4, NMO, dioxane, 19 h, RT, 92 %;[116] iii. OsO_4, *t*-BuOOH, Et_4NOAc, $(CH_3)_2CO$, 1 d, RT, 85 %.[117]

The reactions depicted in **Scheme 37** focused attention on performing a standard OsO_4 mediated dihydroxylation reaction on **76**, without addition of any chiral chelating agent. Accordingly **76** was treated with OsO_4 as described[117] and within 24 h all of the starting material had been consumed. Purification afforded racemic *threo* diol **82** in 50 % yield and with > 99 % purity. This result clearly suggests that the dihydroxylation of **76** was inhibited by the chiral chelating agent and not the lack of reactivity of OsO_4.

2.2.2.4 Hydrolysis of *threo* diol **82**

The final step in the route to **24** involved phosphonate hydrolysis. TMSBr reactions have been repeatedly successful for such reactions under comparatively mild conditions. The TMSBr reaction on **82** however, afforded only decomposition products (**Scheme 38**). Deviations from the standard procedure by performing the reaction at low (-20 °C) temperature[120] or in the presence of mild base to neutralise traces of HBr, also failed to afford **82**. The use of TMSI, as a more reactive substitute for TMSBr, also resulted in decomposition, and final attempts to dealkylate the phosphonate *via* traditional acid or base mediated hydrolysis protocols again afforded only decomposition products.

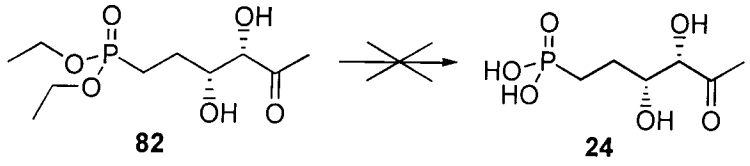

Scheme 38 Failed dealkylation of diethyl *threo*-3,4-dihydroxy-5-oxohexylphosphonate **82** to afford *threo*-3,4-dihydroxy-5-oxohexylphosphonic acid **24**.

All attempts at hydrolysing the phosphonate had failed to afford **24**, resulting in only decompositon products. Although the synthesis to the diethyl precusor **82** had been successful, it was apparent that a different dialkyl phosphonate ester was required that would release **24** under neutral conditions. Such a dialkyl phosphonate is a dibenzyl phosphonate.

2.3 Synthesis of DXP analogue 24 *via* dibenzyl phosphonate

Hydrogenation of benzyl phosphonates has been shown to provide facile access to phosphonic acids,[121,122,123,124] and it was envisaged that this would provide a more suitable method of deprotection for the synthesis of **24**. Preparation of the required penultimate compound dibenzyl *threo*-3,4-dihydroxy-5-oxohexylphosphonate **93** was to follow the same route as that mapped out for diethyl phosphonate **82**, with hydrogenation affording the desired compound **24** (**Figure 20**). Synthesis of the phosphono aldehyde **94**, was the first objective towards preparing the target compound **24**.

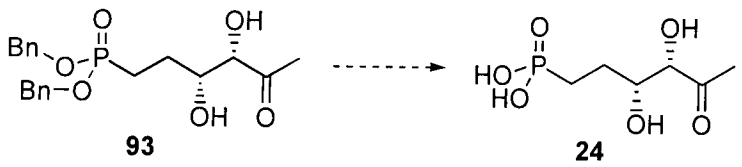

Figure 20 Hydrogenation of the dibenzyl phosphonate **93** to afford **24**.

2.3.1 Preparation of dibenzyl 3-oxopropylphosphonate 94

Following the preparation (**Scheme 23**) of the aldehydic intermediate **52** for the diethyl phosphonate, the corresponding reaction to generate 2-(dibenzoxyphosphonylpropyl)-1,3-dioxolane **95** was now undertaken. However, tribenzyl phosphite **96** had to be prepared as it is not commercially available. This compound has been prepared from benzyl alcohol and PCl_3 in 90 % yield,[122,125,126] however in our hands this reaction proved problematic. A low yield of 20 % was obtained using what appeared to be a straightforward procedure (**Scheme 39**).[122] Isolated **96** was found to be stable under nitrogen at ambient temperature but in the crude product mixture it decomposed to dibenzyl phosphite and tribenzyl phosphate. ^{31}P NMR indicated that **96** initially comprised 80 % of the phosphorus containing species in the crude mixture. After leaving this mixture for 12 h in the freezer, **96** comprised only 50 % of the product. This afforded an isolated yield of 20 % after dry column chromatography.

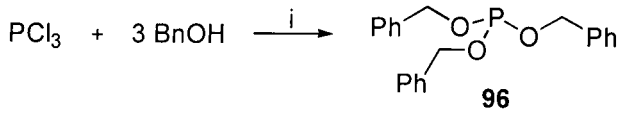

Scheme 39 i. Et_3N, Et_2O, 2 h, -78 °C, then 8 h, RT, 20 %.

With **96** in hand it was treated with 2-(2-bromoethyl)-1,3-dioxolane **97** under the same conditions as previously described for other Michaelis-Arbuzov reactions with tribenzyl phosphite **96**.[125,127] This afforded **95**, but only in low (< 20 %) yield (**Scheme 40**). A key sideproduct was the isomer dibenzyl benzylphosphonate **98** (> 30 % yield) which indicated that an efficient Michaelis-Arbuzov reaction with the *in situ* generated benzyl bromide, was competing with the intended reaction. The initial reaction conditions had utilised a ten-fold excess of **97**, and lowering the proportion of **97** was found to consequently lower the yield of **95**.

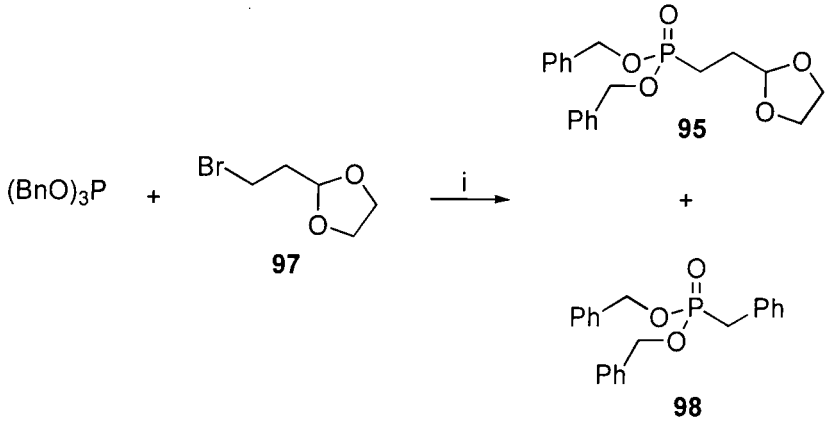

Scheme 40 i. 5 h, 120 °C, 18 % for **95** and 31 % for **98**.

An alternative strategy was required that would afford the acetal **95**. The Michaelis-Becker reaction between dibenzyl phosphite and 2-(2-bromoethyl)-1,3-dioxane **73** (**Scheme 21**) had been attempted before (**2.2.1.3**), but without success. Performing the reaction with the corresponding iodo dioxane offered a possibility of achieving a more efficient coupling reaction. Accordingly **73** was converted to 2-(2-iodoethyl)-1,3-dioxane **99** under standard Finkelstein reaction conditions with NaI.[128] This reaction proved straightforward and generated the desired (**Scheme 41**) iodide in 80 % yield. However, the subsequent reaction of 2-(2-iodoethyl)-1,3-dioxane **99** with dibenzyl phosphite in either a THF or DMF solvent at low (-15 °C) temperature, with NaH as a base, resulted in a maximum yield of 10 % for the coupled product **100**.

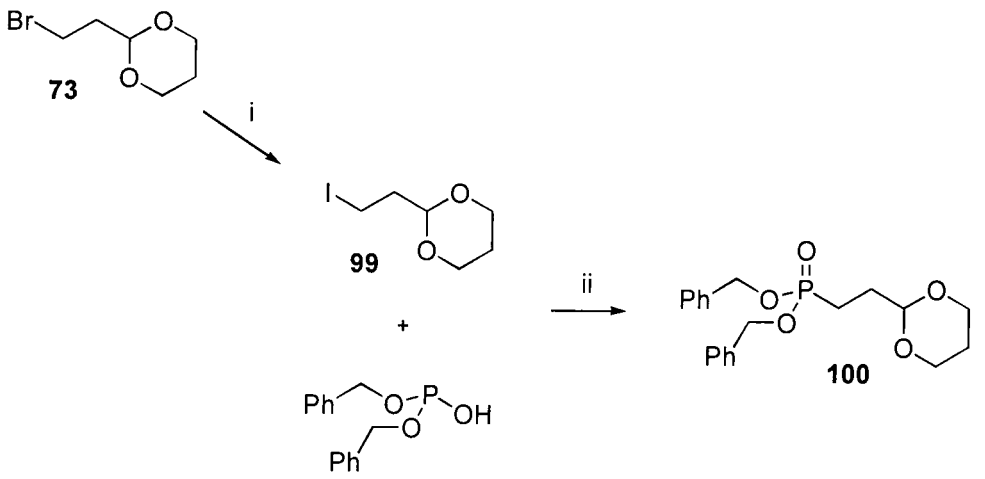

Scheme 41 i. NaI, $(CH_3)_2CO$, 16 h, reflux, 80 %; ii. NaH, THF, 4 h, -15 °C, 10 %.

In view of the unsatisfactory coupling reactions with the bromo and iodo acetals, use of a triflate group was then explored. It was important to identify a triflate which possessed a latent aldehyde three carbon atoms from the leaving group. A compound that satisfied this was 3,3-diethoxypropyl trifluoromethanesulphonate **101**. An attempt to prepare this electrophile from commercially available 3,3-diethoxypropan-1-ol **102** and triflic anhydride was pursued, **Figure 21**.

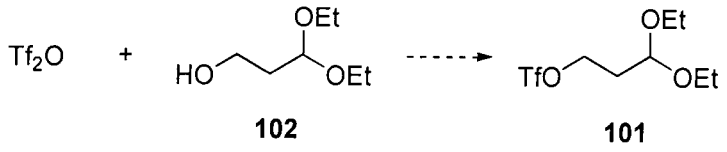

Figure 21 Proposed preparation of **101**

Attempts to isolate the triflate **101** utilising 2,6-di-*tert*-butylpyridine as the base were unsuccessful due to the instability of **101** at ambient temperature. *In situ* formation of the triflate followed by addition of sodium dibenzyl phosphonate did not afford any detectable product. The triflic pyridinium salt **103** was isolated after attempted formation of the triflate from triflic anhydride and **102**, using pyridine as the base. However, Michaelis-Becker reaction with **103** and sodium dibenzylphosphonate was also unsuccessful.

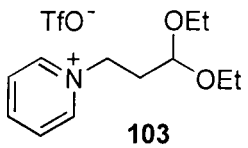

Formation of dibenzyl 3,3-diethoxypropylphosphonate **104** *via* a Michaelis-Arbuzov type reaction (**Scheme 42**) between the triflate **101** and tribenzylphosphite was also attempted. However, due to the weak nucleophilicity of the triflate anion, only the first step of the Michaelis-Arbuzov reaction takes place. These triflate phosphonuim ions have been noted before,[129,130,131] and in one case were used to form an organophosphonate.[129] After formation of the phosphonium salt, addition of a nucleophile such as water is sufficient to induce formation of the phosphonate (**Scheme 42**).[129] The reaction was performed a number of times, but there was only a very low conversion to the desired product, with a number of side-products, most notably dibenzyl phosphite, produced in larger quantities.

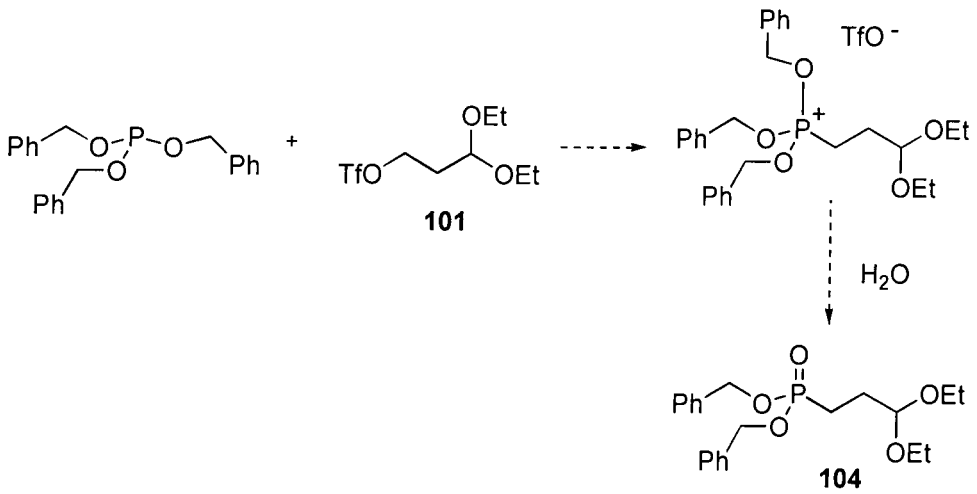

Scheme 42 Proposed route to form dibenzyl 3,3-diethoxypropylphosphonate **104**.

An alternative synthetic route to generate the key aldehydic intermediate dibenzyl 3-oxopropylphosphonate **94** was explored, **Scheme 43**. This route utilised the reaction between dibenzyl phosphite and methyl iodide to generate dibenzyl methylphosphonate **105**.[124] The reaction was reported to proceed in a yield of 85 %, and was found after purification by dry column chromatography, to afford **105** in about 70 % yield. The next step required allylation of the methyl group to afford dibenzyl but-3-enylphosphonate **106**. This transformation, which is analogous to that performed in **2.2.1.3**, was successfully carried out under the conditions developed by Savignac and co-workers,[93] to afford **106** in approximately 70 % yield.

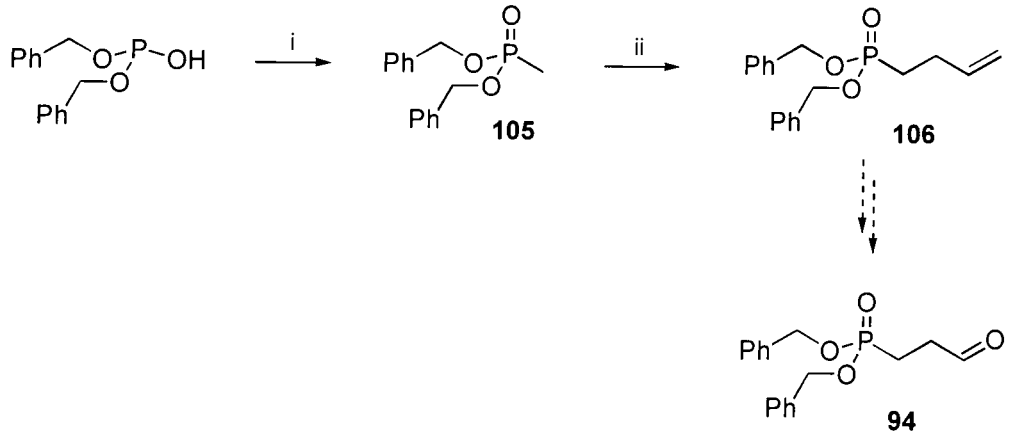

Scheme 43 i. NaH, THF, -15 °C, MeI, then 2 h, 0 °C, then 20 h, RT, 68 %; ii. *n*-BuLi, THF, -60 °C, then Cu(1)I, 1 h, -35 °C, then C_3H_5Br, 4 h, -35 °C, 68 %;

The remaining steps now focused on obtaining aldehyde **94** from the alkene **106**. This had previously (**2.2.1.3**) been attempted by performing a one step reductive ozonolysis reaction. However, a new approach which utilised a two step process was investigated. Firstly dihydroxylation of the alkene moiety with OsO_4, followed by a $NaIO_4$ glycol cleavage to yield the desired aldehyde **94**. The dihydroxylation conditions that had been developed for the same reaction on diethyl but-3-enylphosphonate **67** (**Scheme 37**, iii) were explored. Performing the OsO_4 reaction under these conditions[117] did indeed afford the desired dihydroxylated material dibenzyl 3,4-dihydroxybutylphosphonate **107** in high (85 %) yield (**Scheme 44**). The second step required cleavage of the diol **107** with $NaIO_4$, to afford the aldehyde **94**. This reaction was found to proceed very cleanly and in an excellent yield of 99 % (**Scheme 44**). In the event the crude product, dibenzyl 3-oxopropylphosphonate **94**, was reacted immediately as it gradually decomposed on storage.

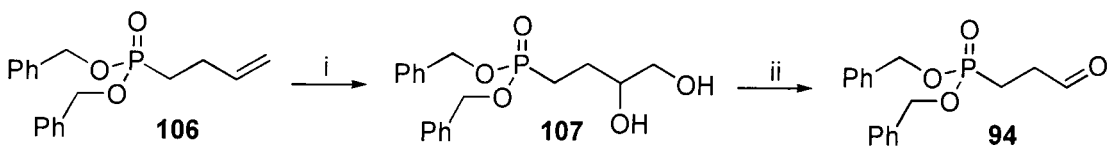

Scheme 44 i. OsO_4, TBHP, Et_4NOAc, $(CH_3)_2CO$, 3 d, RT, 85 %; ii. $NaIO_4$, THF / H_2O, 1 h, RT, 99 %.

2.3.2 Preparation of *threo*-3,4-dihydroxy-5-oxohexylphosphonic acid 24

2.3.2.1 Synthesis of dibenzyl enone **108**

The successful preparation of dibenzyl 3-oxopropylphosphonate **94** now enabled the Wittig reaction with **48** to be carried out as described previously (**2.2.2.1**) for the analogous diethyl ester **76** (**Scheme 24**). As before the reaction proceeded cleanly generating the resultant enone, dibenzyl (*E*)-5-oxohex-3-enylphosphonate **108**, however purification was not so straightforward. Changing the phosphonate ester from ethyl to benzyl significantly increased the phosphonate's boiling point. As a consequence distillation was not viable, and chromatography was explored. After optimisation a solvent system was developed that afforded sufficient R_f separation on tlc to warrant purification by column chromatography. This method resulted in the recovery of **108** (~ 93 % purity) in a 94 % yield, the main impurity (5 %) being triphenylphosphine oxide (**Scheme 45**).

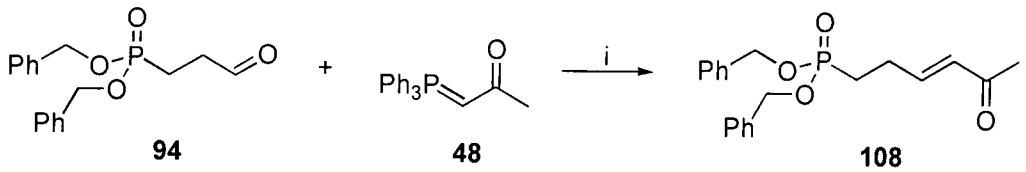

94 **48** **108**

Scheme 45 i. THF, 18 h, reflux, 94 %.

2.3.2.2 Synthesis of dibenzyl *threo* diol **109**

The next step required the dihydroxylation of **108** to afford the penultimate compound on the synthetic route to *threo*-3,4-dihydroxy-5-oxohexylphosphonate **24**. Performing the reaction under the same OsO_4 dihydroxylation conditions that had been successful for the diethyl analogue (**2.2.2.3**) afforded **109** in 66 % yield, with > 99 % purity (**Scheme 46**), as a stable creamy coloured solid.

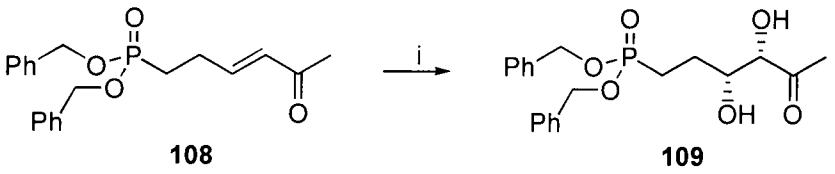

108 109

Scheme 46 i. OsO_4, *t*-BuOOH, Et_4NOAc, $(CH_3)_2CO$, 27 h, RT, 66 %.

2.3.2.3 Hydrogenation of dibenzyl *threo* diol **109**

The final step in the synthesis of the target **24**, required debenzylation by hydrogenation to release the phosphonic acid. The hydrogenation was initially carried out in MeOH mediated by 10 % palladium on carbon catalyst. Analysis of the reaction mixture showed only decomposition products. However, fortuitously changing the reaction solvent to a THF / water mix and repeating the reaction, otherwise under the same conditions, proved successful and did deliver the desired material **24** in about 80 % yield, with > 99 % purity (**Scheme 47**). After isolation, **24** was found to gradually decompose on standing over several days by visual inspection and NMR analysis. Formation of the disodium phosphonate salt was achieved by neutralising the filtered reaction product mixture with dilute $NaOH_{(aq)}$ to generate the more stable salt **110**. This compound was also found to decompose within two weeks at ambient temperature.

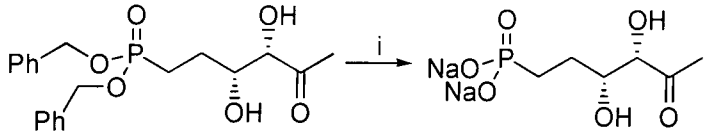

109 110

Scheme 47 i. H_2 (2-3 atm), 10 % Pd on C, THF, H_2O, 45 min, RT, then $NaOH_{(aq)}$, 77 %.

2.4 Synthesis towards the CF_2 analogue 39 of DXP

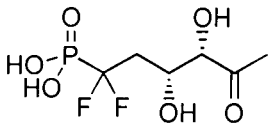

Threo-3(*R*),4(*S*)-1,1-difluoro-3,4-dihydroxy-5-oxohexylphosphonic acid **39**

In light of the experience for deprotection of **82** preparation of the diethyl ester of the CF_2 analogue of DXP was not pursued. Instead a synthesis was initiated towards the benzyl ester as this offered the more satisfactory protecting group. At the outset the preparation of dibenzyl 1,1-difluoro-3-oxopropylphosphonate **111** was approached in an analogous manner to that of **94**, the first step in the synthesis to **94** being a Michaelis-Arbuzov type reaction between triethyl phosphite and dibromodifluoromethane (**2.2.1.1**, **Scheme 15**). Accordingly tribenzyl phosphite (previously prepared in **2.2.2.3**) was mixed with dibromodifluoromethane but a number of attempts at this reaction failed to afford the coupled phosphonate **112**. The reaction is known to work for the ethyl and butyl phosphites,[132] but only starting material was recovered from the tribenzyl phosphite reaction (**Scheme 48**). The failure of such reactions has been noted before,[133] however no explanation for this was proposed. A Michaelis-Becker type reaction between dibromodifluoromethane and dibenzylphosphite also failed, again with only reactants being recovered.

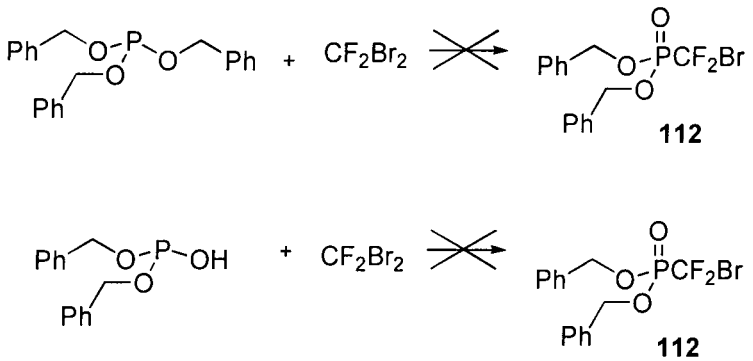

Scheme 48 Failed Michaelis-Arbuzov and Michaelis-Becker reactions to form **112**.

An alternative Michaelis-Becker reaction was then undertaken, designed to produce dibenzyl difluoromethylphosphonate **113**. This involved treatment of the sodium salt of dibenzylphosphite with chlorodifluoromethane, a reaction which had been reported to afford **113** in 75 % yield.[134] Deprotonation of this phosphonate generates a rather unstable and weak nucleophile, which has however been shown to react with alkyl triflates in moderate yield.[135] Reaction details for the preparation of **113** are not provided in the literature but after some experimentation the formation of **113** was achievable in reproducible yields of about 60 %, with > 99 % purity (**Scheme 49**).

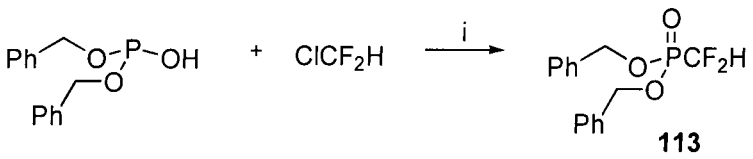

Scheme 49 i. NaH, THF, -15 °C, then 12 h, RT, 61 %.

The successful generation of dibenzyl difluoromethylphosphonate provided access towards the synthesis of the target, **39**. Successful allylation of **113** was now required for the synthesis of the benzyl CF_2 aldehyde **111**. Initial attempts used an excess of allyl bromide in a reaction with **113** as this had proven expedient during the synthesis of the diethyl analogue **56** (**2.2.1.3**, **Scheme 19**). On the first few attempts the reaction worked, producing dibenzyl 1,1-difluorobut-3-enylphosphonate **114** in about a 20 % yield, however all attempts to improve on the initial successes failed. With the olefin **114** in hand, a trial OsO_4 reaction using the previous conditions (**2.3.2.2**) was undertaken (the two step process of dihydroxylation followed by gylcol cleavage being preferred over the one step ozonolysis reaction), however this reaction yielded only decomposition products, **Scheme 50**. Because of the problems encountered in making the aldehydic precursor **111** by this route, an altenative was sought.

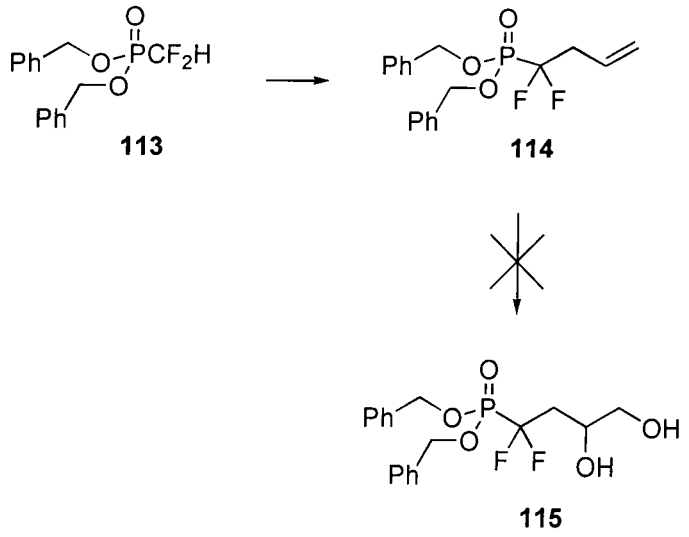

Scheme 50 Attempted synthesis of dibenzyl 1,1-difluoro-3,4-dihydroxybutylphosphonate **115**.

The alternative route towards the difluoro aldehyde **111**, utilised an acetal protecting group. This general method of forming an phosphonoacetal had been previously attempted (**2.2.1.3**), using 2-bromomethyl-1,3-dioxolane **72** in a coupling reaction with dimethyl methylphosphonate **68** (**Scheme 21**). However, use of an acetal with a better leaving group, such as the triflate **116** was considered more promising. Hydrolysis of the acetal **117** would clearly afford the desired aldehyde **111** (**Scheme 51**).

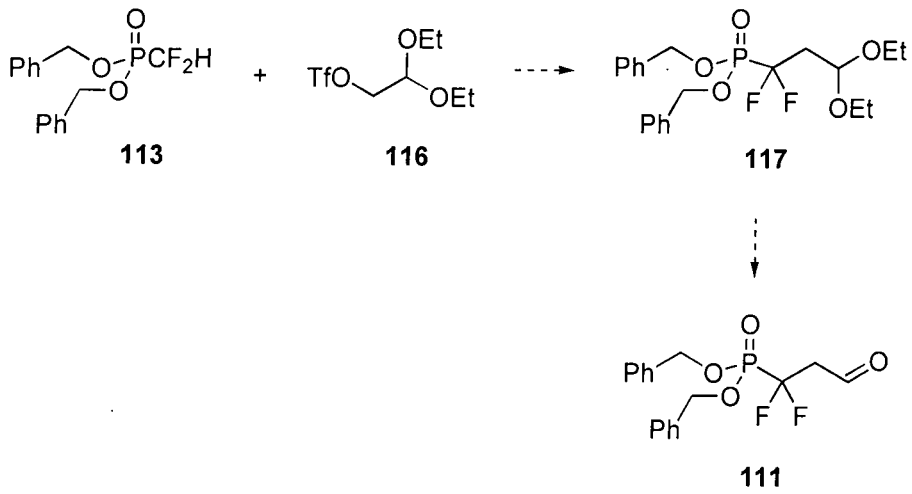

Scheme 51 Proposed route to dibenzyl 1,1-difluoro-3-oxopropylphosphonate **111**.

The formation of **116** from glycoladehyde diethylacetal **118** and triflic anhydride has been reported before, but no synthetic details were supplied.[136] Initial attempts to form **116** using pyridine as the base afforded the pyridinium triflate **119**. It was envisaged that reaction of this salt **119** with dibenzyl lithiodifluoromethylphosphonate would deliver **117**, displacing pyridine as the leaving group. However, attempted coupling of these two reagents did not afford any product as determined by ^{19}F and ^{31}P NMR analysis. In the end, the generation of **116** was achieved by use of the non-nucleophilic base 2,6-di-*tert*-butylpyridine,[137] the triflate being isolated after column chromatography in ~ 65 % yield. The product was contaminated with some of the base (**Scheme 52**). The coupling reaction with **113** was carried out as described for other triflate reactions with **113**,[135,138] and after workup ^{19}F and ^{31}P NMR analysis of the crude product mixture indicated that the required dibenzyl 3,3-diethoxy-1,1-difluoropropylphosphonate **117** had been generated, but in < 10 % yield, **Scheme 52**. Further work on this reaction was postponed due to the inefficiency of this process.

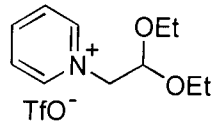

119

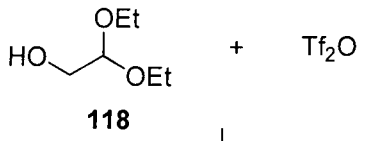

118

i

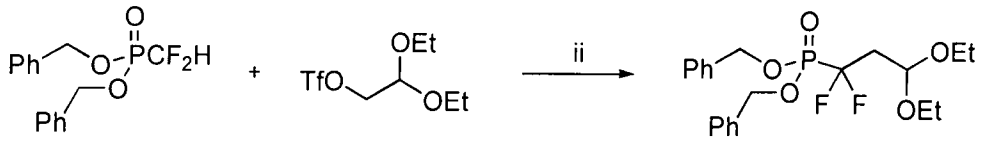

113 **116** **117**

Scheme 52 i. DTBP, CH_2Cl_2, 25 min, -20 °C, ~ 65 %; ii. LDA, THF / HMPA, 2 h, -78 °C, < 10 %.

2.5 Synthesis of CH_2 analogue 40 of MEP

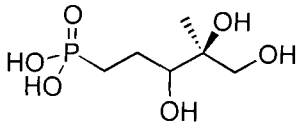

3(*R,S*),4(*S*)-3,4,5-trihydroxy-4-methylpentylphosphonic acid **40**

Synthesis of the methylene analogue of 2-*C*-methyl-D-erythritol-4-phosphate (MEP) **40**, as a diastereomeric mixture, epimeric at the C-3 centre was envisaged to be accessible through diethyl 3-oxopropylphosphonate **52**. Utilisation of the aldehyde **52** (prepared previously, **2.2.1.3**, **Scheme 23**) in a Grignard reaction with isopropenylmagnesium bromide **120** should afford the racemic allylic alcohol **121**. Asymmetric dihydroxylation mediated by OsO_4 of **121** should yield the triol **122** with a diastereomeric excess. Finally it was envisaged that TMSBr deprotection would then provide access to the target compound **40**, **Scheme 53**.

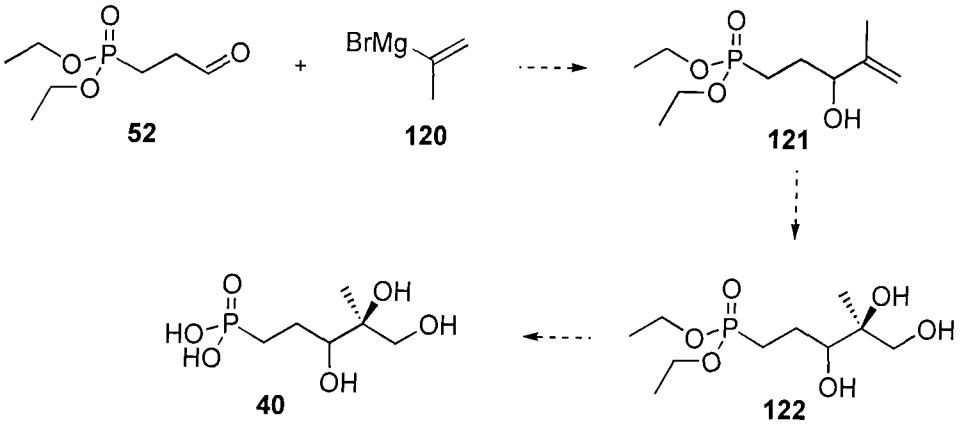

Scheme 53 Proposed route to **40**.

2.5.1 Synthesis of allylic alcohol 121

Preparation of the Grignard reagent **120** was achieved most consistently using an iodine initiator in THF at ambient temperature. Grignard reactions with **120** were first performed at 0 °C and yielded a mixture of products. Analysis by ^{1}H, ^{13}C and ^{31}P NMR suggested that Grignard attack took place at both the phosphonate and aldehydic centres, generating a number of products, including the desired allylic alcohol **121** (**Scheme 54**).

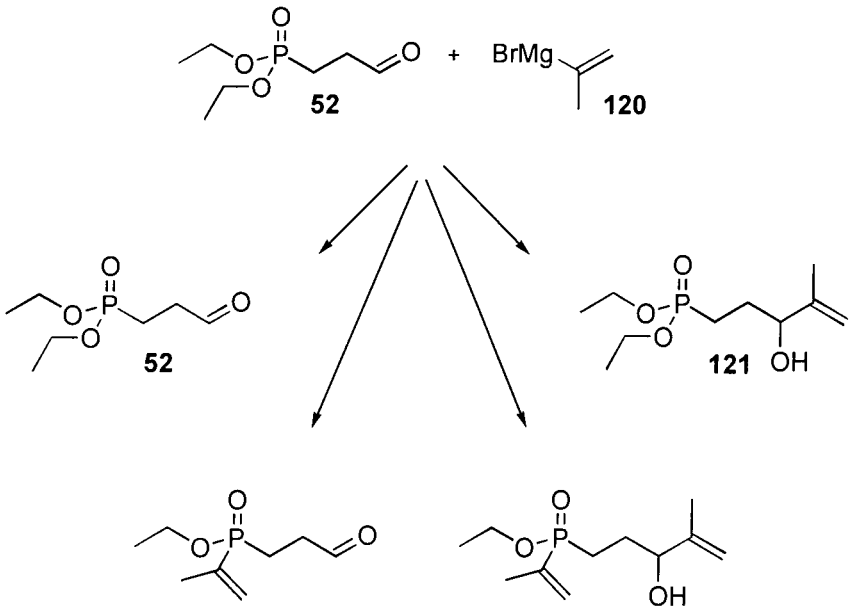

Scheme 54 Reaction products of diethyl 3-oxopropylphosphonate **52** with isopropenylmagnesium bromide **120** at 0 °C.

The selectivity of this reaction was improved by conducting the reaction at the lower temperature of -78 °C. Reaction at this temperature afforded no detectable phosphonate addition product. However, only a low conversion of the aldehyde to the desired alcohol **121** was achieved, even with the use of a large excess of Grignard reagent. This initially presented problems with purification of the product mixture, but after careful choice, a solvent system for column chromatography was found that separated **121** from the aldehyde **52**, affording diethyl 3-hydroxy-4-methylpent-4-enylphosphonate **121** in approximately 45 % yield, with > 99 % purity, **Scheme 55**.

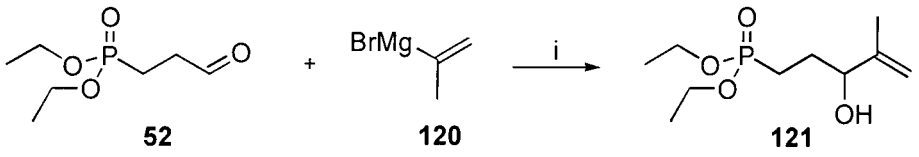

Scheme 55 i. THF, 40 min, -78 °C, 44 %.

2.5.2 Synthesis of triol 122

The next step towards formation of **40** required dihydroxylation of the allylic alcohol **121** in a stereoselective manner. An OsO_4 AD-mix reaction could afford the triol **122**, containing the desired stereochemistry at the C-4 centre, however a previous AD-mix reaction on the related diethyl (*E*)-5-oxohex-3-enylphosphonate **76** (**2.2.2.3**) had not yielded product. After prolonged reaction of **121** under Sharpless AD-mix-β conditions, again no detectable product was formed (**Scheme 56**), thus prompting an investigation into standard racemic OsO_4 mediated dihydroxylation reactions of allylic alcohols.

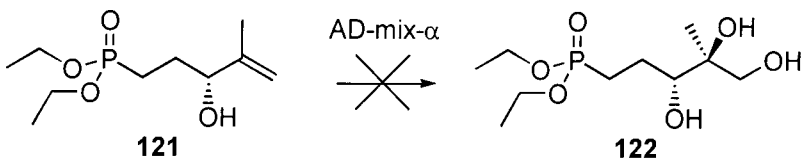

Scheme 56 Failed AD-mix reaction to form **122**.

Studies[139] have shown that OsO_4 oxidation of allylic alcohols and ethers has a moderate to high stereoselectivity with 'the relative stereochemistry between the pre-existing hydroxyl or alkoxyl group and the adjacent newly introduced group of the major product, in all cases being *erythro*.'[139] This relative stereochemistry was fortuitously that of the desired product **40**. From the literature there are a few comparable examples of dihydroxylation reactions relevant to the system of interest (**Scheme 56**). Two of the osmylation reactions (**Scheme 57**, i and iii) have been reported as highly stereoselective. In the case of (i) this is due to the stereoelectronic effect of the carbomethoxyl substituent,[140] and in the case of (iii) it is most probably due to the steric influence of the pendent R group.[141] Although the hydroxyl or alkoxyl group can have strong directing influences in osmylation reactions on its own, reaction (ii) 'showed considerably less stereoselectivity'[140] highlighting a potential weakness of this methodology.

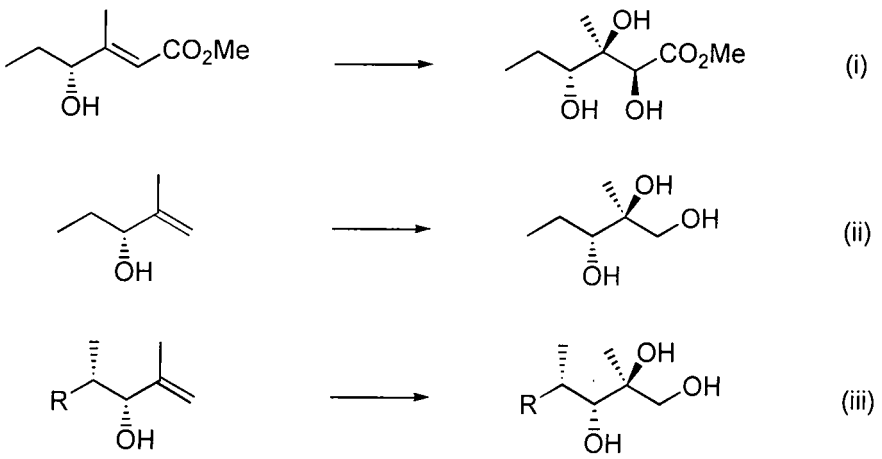

Scheme 57 Reported OsO_4 reactions. (i),[140] (ii)[140] and (iii).[141]

The dihydroxylation reaction of **121** may then generate the required triol **122** at best as a racemic mixture and at worst as a mixture of four diastereoisomers. The allylic alcohol **121** was duly reacted with OsO_4 utilising the previous conditions that had been successful (**2.2.2.3**), and the progress of the reaction was monitored by ^{31}P NMR. After **121** had been consumed the reaction was quenched. Analysis of the isolated material showed that ketone **123** was the predominant product (**Scheme 58**), with pure (> 99 %) material isolated in 30 % yield after column chromatography. Formation of **123** is postulated to arise by oxidation of allylic alcohol **121** or the desired triol **122** by either TBHP or OsO_4, **Scheme 58**.

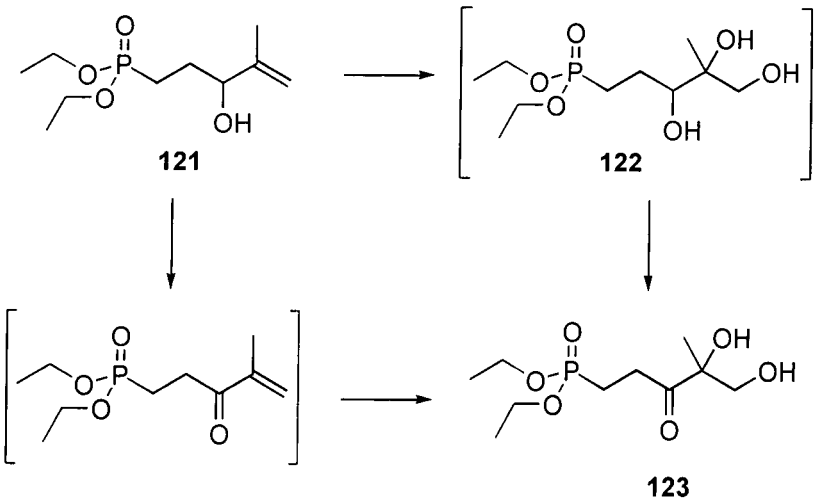

Scheme 58 Possible routes for synthesis of **123**. OsO_4, TBHP, Et_4NOAc, $(CH_3)_2CO$, 28 h, RT, 28 %.

Although the production of this ketone **123** had not been envisaged, it offered an intermediate for either generating **124**, an isomer of the CH_2 analogue of DXP or after reduction, the triol **122**. However, ester hydrolysis under standard TMSBr conditions caused immediate decomposition of starting material. Conducting the $NaBH_4$ reaction of **123** was also found to generate only decomposition products from NMR analysis, **Scheme 59**.

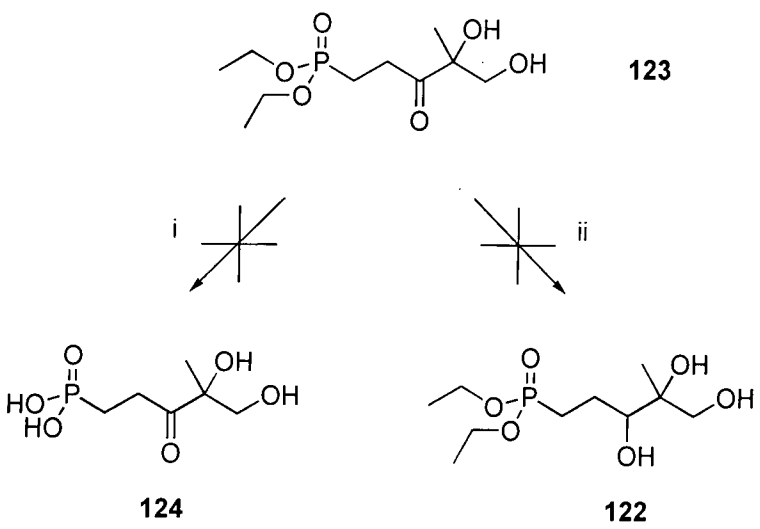

Scheme 59 i. TMSBr, 2 h, RT, then H_2O, 12 h, RT; ii. $NaBH_4$, MeOH, 15 min, -20 °C.

It was envisaged that the generation of ketone **123** may be suppressed if the allylic alcohol **121** was converted to an allylic ether prior to osmylation. To investigate this the THP protecting group was chosen due to its ease of introduction and removal. Formation of the THP protected alcohol **125**, proceeded in a straightforward manner, the product being isolated in a yield of about 70 % after column chromatography (**Scheme 60**). A much higher crude yield was obtained but it was found that some of the THP protected alcohol **125** decomposed on the column presumably due to its instability over mildly acidic silica.

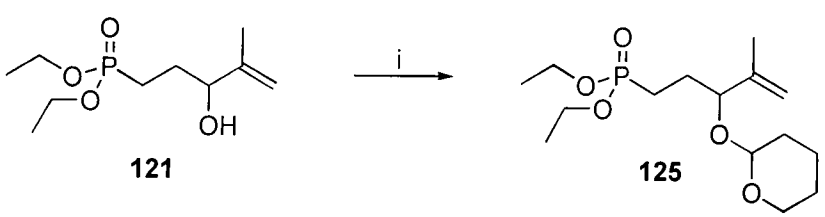

Scheme 60 i. DHP, PTSA, CH_2Cl_2, 25 min, RT, 66 %.

A preliminary OsO_4 mediated dihydroxylation of **125** was followed by ^{31}P NMR. Once the majority of the starting material had been consumed, the reaction mixture was quenched and extracted into CH_2Cl_2. Partial purification of the crude sample from the organic phase *via* column chromatography did afford an impure sample of the intended dihydroxy ether **126** in about 30 % yield (**Scheme 61**), but also an impure sample of triol **122** in about 5 % yield, most probably again due to the instability of the THP group over silica.

Comparison of the main peaks in the ^{31}P NMR spectra of the triol **122** and the aqueous fraction from the OsO_4 mediated dihydroxylation of **121** indicated that they had comparable chemical shifts. This prompted a continuous extraction of the aqueous phase from the reaction of **121**, however the ^{31}P species could not be extracted from the water even under continuous extraction with EtOAc or CH_2Cl_2. Freeze drying the aqueous solution enabled confirmation by ^{1}H NMR that the species in the aqueous phase was the desired triol **122**. The approximate amount of material isolated from freeze drying amounted to a yield of ~ 2 %.

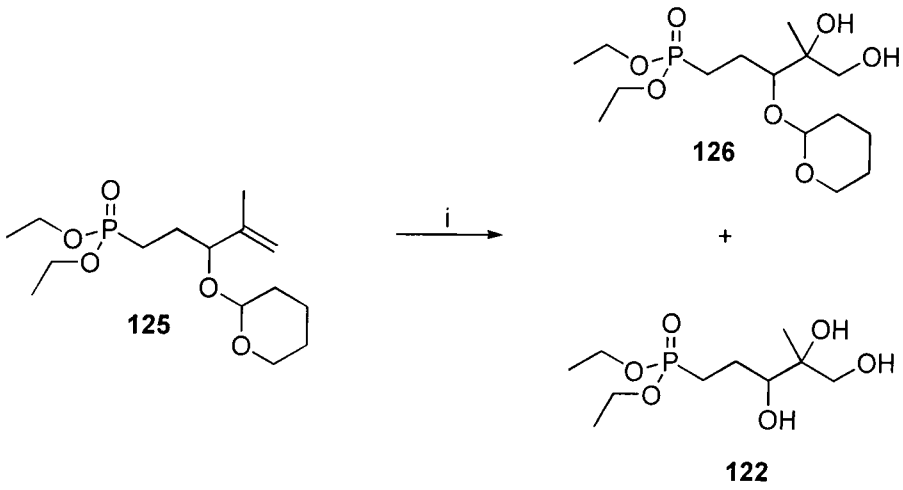

Scheme 61 i. OsO_4, TBHP, Et_4NOAc, $(CH_3)_2CO$, 20 h, RT, ~ 30 % for **126** and ~ 5 % for **122**.

The low yields encountered for the dihydroxylation of the THP ether **125**, prompted a re-analysis of the previous OsO_4 dihydroxylation of the allylic acohol **121**, and in particular an accurate assessment of how much product had been lost to the aqueous phase. After performing the reaction again, the mixture was quenched and solvent

removed using $CHCl_3$ to azeotrope the majority of the water. Freeze drying to remove the remaining water, and then purification by column chromatography gave **123** in about 20 % yield, followed by the desired product **122**, also in about 20 % yield, with > 99 % purity, **Scheme 62**.

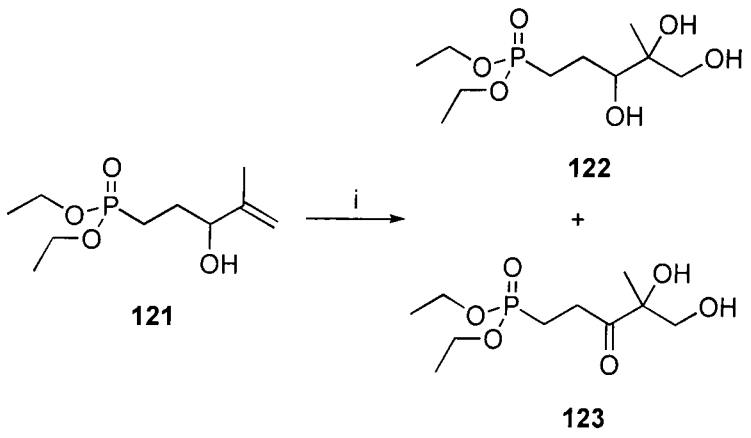

Scheme 62 i. OsO_4, TBHP, Et_4NOAc, $(CH_3)_2CO$, 5 h, RT, 18 % for **122** and ~ 20 % for **123**.

2.5.3 Deprotection of 122

The final step in the preparation of the CH_2 analogue of MEP required hydrolysis of the diethyl phosphonate ester to yield the corresponding phosphonic acid **40**. The first attempt at hydrolysis utilised TMSBr methodolgy. However, as had been found previously (**2.2.2.4** and **2.6.2**) addition of TMSBr to **122** caused decomposition. Due to the small amount of **122** remaining the reaction was not repeated, and an alternative, non acidic, deprotection strategy was sought. In the event, reaction of **122** with 0.1 M $NaOH_{(aq)}$ for 1 h under reflux, cleanly afforded the monosodium salt **127**, **Scheme 63**. A further 5 h reflux with 2 M $NaOH_{(aq)}$ was then required to complete the hydrolysis and generate the target compound **40**, as its disodium salt **128**, > 99 % pure by ^{31}P NMR analysis, **Scheme 63**. An accurate yield was not attainable for the hydrolysis reaction due to contamination by NaCl, produced from neutralisation of the reaction mixture.

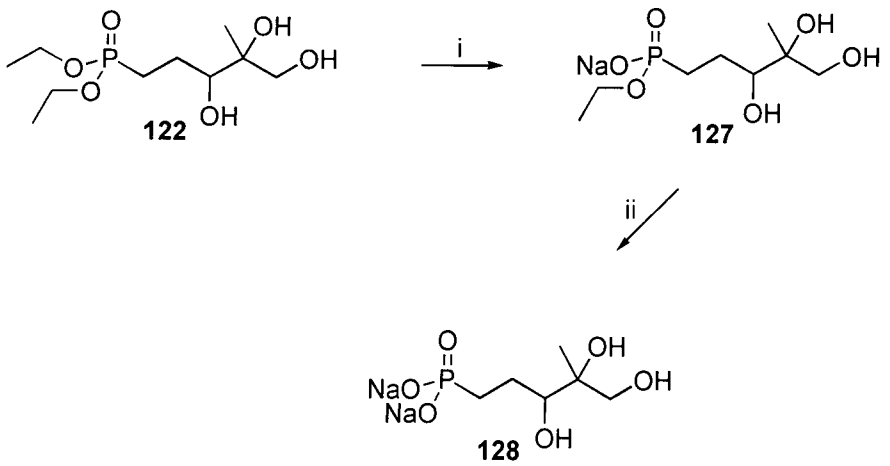

Scheme 63 i. 0.1 N $NaOH_{(aq)}$, 1 h, reflux; ii. 2 N $NaOH_{(aq)}$, 5 h, reflux.

2.6 Synthesis of reduced DXP analogue 46

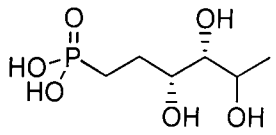

Threo-5(*R*,*S*)-3,4,5-trihydroxyhexylphosphonic acid **46**

Target compound **46** was next addressed. It was envisaged that **46** could be prepared by $NaBH_4$ reduction of diethyl *threo*-3,4-dihydroxy-5-oxohexylphosphonate **82** (**2.2.2.3**), to afford the triol diethyl 3,4,5-trihydroxyhexylphosphonate **129**. Phosphonate deprotection with TMSBr should generate the desired phosphonic acid **46** (**Scheme 64**) as a mixture of diastereoisomers.

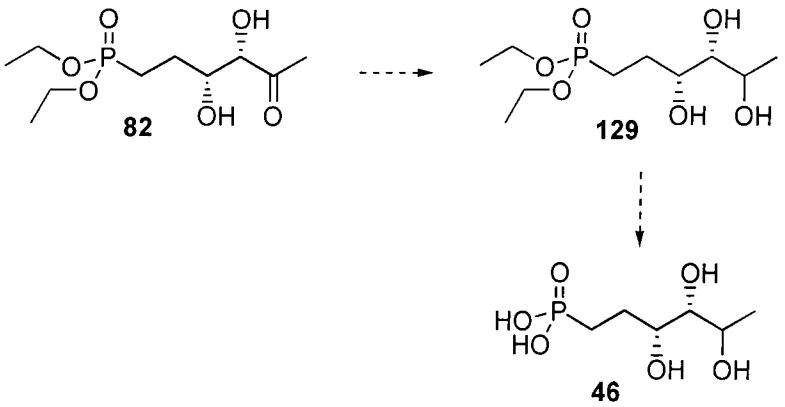

Scheme 64

In the event, treatment of **82** with $NaBH_4$ in MeOH at 0 °C for 1 h generated two unforseen products. These were diethyl (*E*)-5-hydroxyhex-3-enylphosphonate **130** and diethyl 5-hydroxyhexylphosphonate **131** as the major and minor products respectively. Although these compounds were not isolated, ^{31}P NMR analysis indicated that they had been formed in near quantitative conversion and in an approximate ratio of 3 : 1, **Scheme 65**. Changing the reaction temperature to -78 °C also failed to afford the desired material, the reaction yielding a low mass recovery from the organic phase of a mixture of products. ^{31}P NMR Analysis also indicated a mixture of products in the aqueous phase.

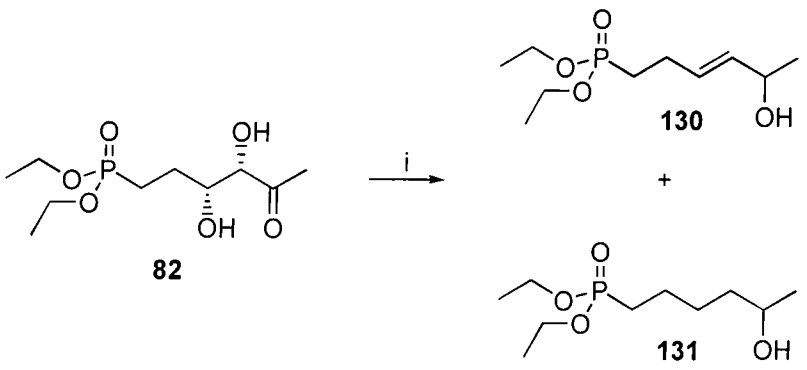

Scheme 65 i. $NaBH_4$, MeOH, 0 °C, 1 h, ~ 75 % for **130** and ~25 % for **131**.

Formation of the α, β-unsaturated alcohol **130** from $NaBH_4$ reduction of **82** suggested an alternative route to triol **129** *via* reduction of the enone diethyl (*E*)-5-oxohex-3-enylphosphonate **76** to generate **130**, followed by dihydroxylation to afford the triol **129**. Subsequent $NaBH_4$ reactions with **76** did appear to have generated **130** by ^{31}P NMR analysis of the crude reaction mixture, however only a crude yield of ~ 50 % was obtained. A more efficient route to **46** could potentially be achieved by other means, **Scheme 66**. Acetonide protection of **82**, would afford *threo*-5-acetyl-4-(2-diethoxyphosphonylethyl)-2,2-dimethyl-1,3-dioxolane **132** which could undergo $NaBH_4$ reduction to the alcohol **133**. Finally, it was envisaged that deprotection with TMSBr would remove both the acetonide and phosphonate protecting groups in a single step.

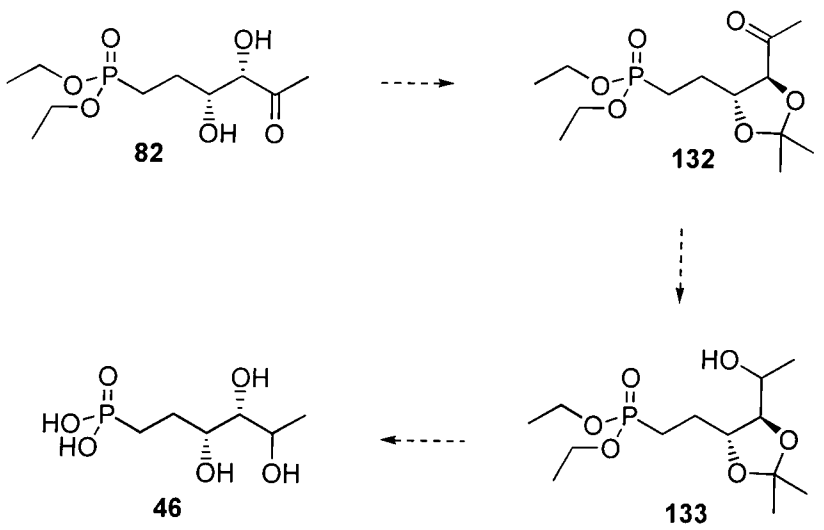

Scheme 66 Proposed alternative synthesis of **46**.

Efficient acetonide protection of **82** using 2,2-dimethoxypropane with PTSA as the acid catalyst was achieved affording **132** (**Scheme 67**) after purification in 80 % yield with > 99 % purity. Reduction then of **132** with $NaBH_4$ proceeded cleanly affording two diastereoisomers of **133** in a ratio of approximately 3 : 7 > 90 % yield, with a purity of > 99 %, **Scheme 67**. Deprotection of **133** with TMSBr followed a standard protocol and generated the target phosphonic acid **46** (**Scheme 67**), as its disodium salt **134**, in about 85 % purity. This was contaminated with the mono sodium salt **135**, ~ 12 %, with both species containing the previous diastereomeric ratio of 3 : 7 as determined by NMR analysis.

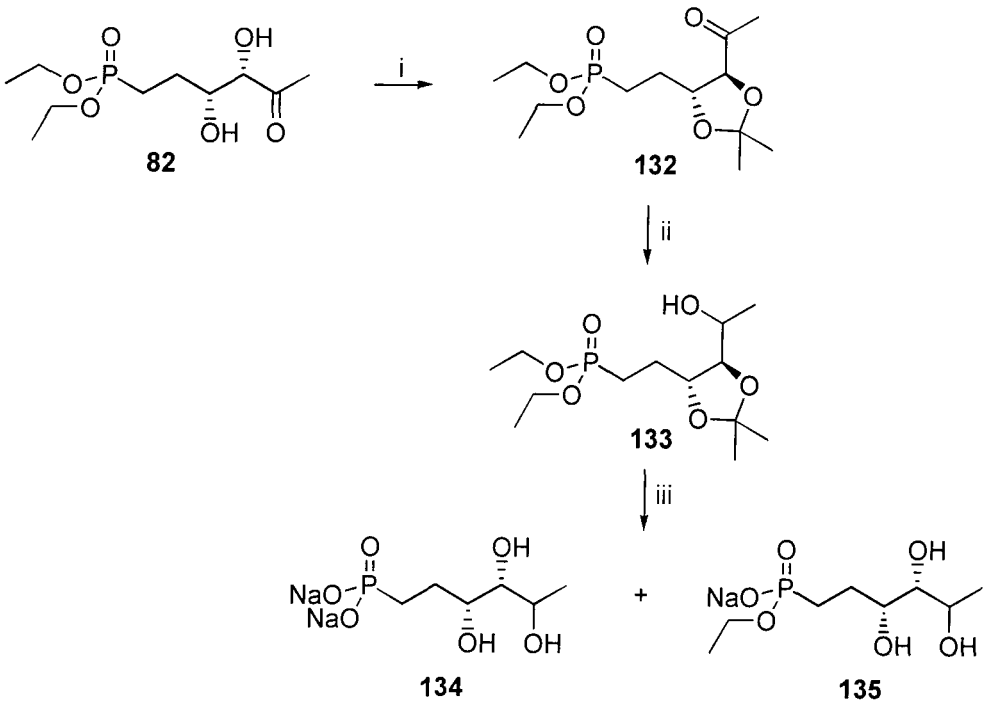

Scheme 67 i. $(CH_3)_2C(OMe)_2$, PTSA, 14 h, RT, 80 %; ii. $NaBH_4$, MeOH, 15 min, RT, 91 %; iii. TMSBr, 4 h, H_2O, 14 h, $NaOH_{(aq)}$.

2.7. Synthesis of fosmidomycin analogue 47

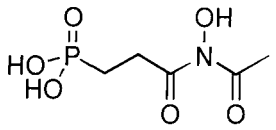

3-(*N*-Acetyl-*N*-hydroxyamino)-3-oxopropylphosphonic acid **47**

This work was carried out by Hannah F. Sore (4th year MSci project student) under my guidance. In developing a route towards **47**, formation of the *N*-hydroxyimide functional group presented the main synthetic challenge. A significant amount of literature precedent exists for the formation of imides, but little work has been directed towards preparation of an *N*-hydroxyimide from an imide, and none for coupling either an imide or *N*-hydroxyimide group to a phosphonate group. The methodologies that have been developed for the formation of imides are generally through the *N*-acylation of amides, one *N*-acyl group being in most cases an acetyl group, as is the case for **47**. These methodologies have included the use of ketene,[142] but are normally achieved by acylation

of an amide through use of an acid chloride in conjuction with pyridine[143] or NaH.[82] A more general method for *N*-acetylating amides has also been developed that utilises H_2SO_4 and acetic anhydride.[144]

Of the above imide formation methods the most promising and straightforward method appeared to utilise an acyl chloride in conjuction with NaH. This method could be incorporated into a synthetic route towards **47** as delineated in **Scheme 68**. Synthesis of the acid chloride **136** from the commercially available triethyl 3-phosphonopropionate **55** has been described,[83] generating a reactive intermediate that could react with acetamide. Coupling would afford the imide **54**, which could then be oxidised to the *N*-hydroxyimide **53**, following a literature method.[81] Finally, a TMSBr mediated hydrolysis reaction may afford the desired phosphonic acid **47**.

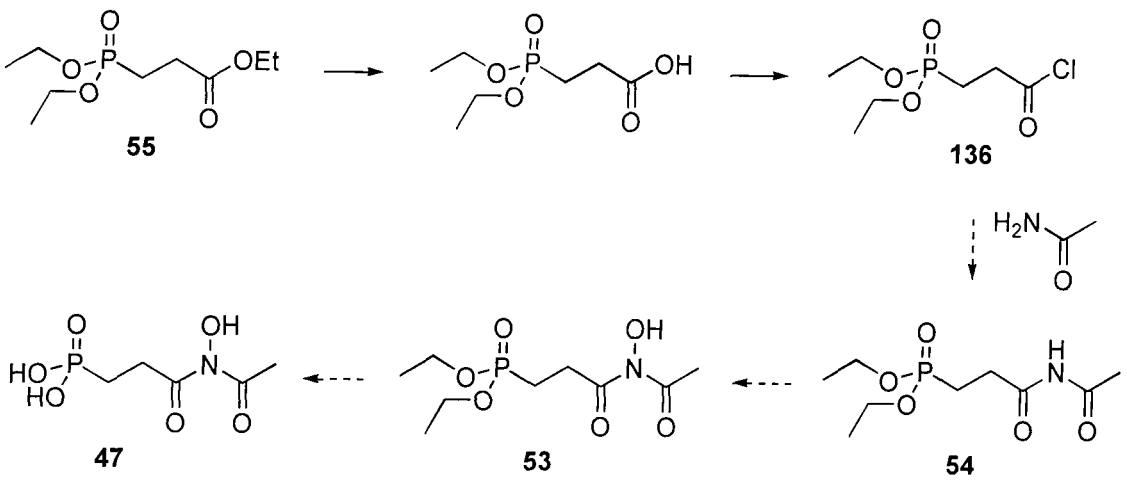

Scheme 68 Proposed synthetic route towards 3-(*N*-acetyl-*N*-hydroxyamino)-3-oxopropylphosphonic acid **47**. i. $NaHCO_{3(aq)}$, 30 min, reflux, 66 % for methyl ester;[83] ii. $(COCl)_2$, CH_2Cl_2, 2 h, 35 °C, ~ 100 %.[83]

Synthesis of the acid chloride **136** was readily achieved[83] in about 60 % yield from **55**. Attempted acylation of the acetamide was not so straightforward. Neither pyridine or NaH as base at low (-60 °C) or ambient temperature respectively were able to mediate a coupling reaction to form *N*-(3-diethoxyphosphonyl)propionyl-acetamide **54**. Lack of success here prompted an investigation into an alternative coupling strategy using a phosphonoamide with a ketene or, as had been successful for other workers, with acetic anhydride and a H_2SO_4 catalyst.

2.7.1 Revised synthetic strategy towards 47

The phosphono amide 2-(diethoxyphosphonyl)propanamide **137** required for the modified strategy towards **47** had been reported in an 85 % yield from triethylphosphite and acrylamide in a Michael / Michaelis-Arbuzov type reaction.[145] The reaction had been found to proceed most cleanly with phenol as the protic source, thereby producing phenetole (PhOEt) as side-product. The amide **137** was synthesised as described and after purification over silica was isolated in > 99 % purity with a yield of about 60 % (**Scheme 69**). Preliminary attempts to afford *N*-acetylimide **54** by reaction with ketene, were not successful. The starting material **137** was recovered from the reaction, suggesting that ketene had not throughly mixed with **137**.

Reaction with acetic anhydride and H_2SO_4 catalyst, at 85 °C for 2 h however did afford **54** in 33 % yield after distillation. During optimisation of this reaction, it was found that increasing the temperature or amount of sulphuric acid decreased the yield of **54**. However, decreasing the duration of the reaction to 1 h maintained a yield of 33 %, but increasing the stochiometry of acetic anhydride to 5 equivalents was found to afford the most significant change, the yield of **54** improving to about 45 %, although the product was contaminated with ~ 5 % of an unidentified material, **Scheme 69**.

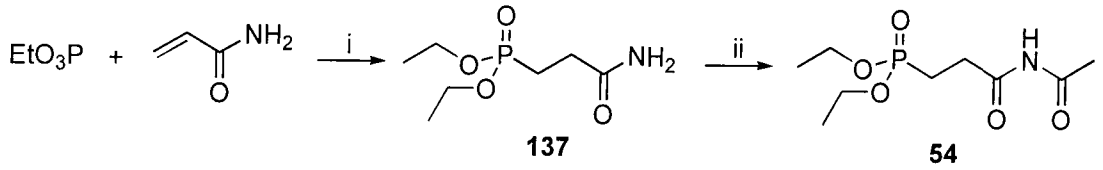

Scheme 69 i. PhOH, 1 d, 100 °C, 58 %; ii. $(CH_3CO)_2O$, H_2SO_4, 2 h, 84 °C, ~ 44 %.

The next step towards formation of the *N*-hydroxyimide **53** was now attempted using methodology that had been successful for formation of *N*-hydroxyamides from secondary amides.[146] This utilised a peroxy-molybdenum complex, MoO_5.DMF as the oxidant, requiring first the trimethylsilylation of the imide to activate it towards oxidation. Reaction of **54** was carried out under the conditions described, but analysis of the crude product mixture showed only decomposition products (**Scheme 70**). Further work on this reaction was postponed due to the failure of this methodology.

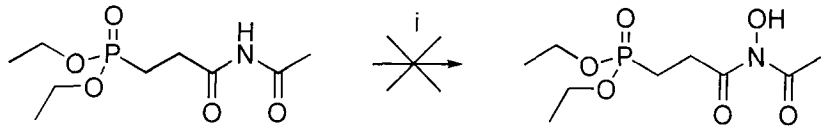

54 53

Scheme 70 i. NaH, THF, 15 min, RT, then TMSCl, 1 h, RT, then MoO_5.DMF, CH_2Cl_2, 18 h, RT, then 1 M $Na_4(EDTA)_{(aq)}$.

In order to hydrolyse the esters of **54**, a standard TMSBr reaction was duly performed. Care had to be taken in neutralising the reaction mixture immediately after addition of water to minimise hydrolysis of the imide, but otherwise the reaction proceeded cleanly generating the desired compound 3-(*N*-acetyl)-3-oxopropylphosphonic acid, as its disodium salt **138** in ~ 80 % purity, **Scheme 71**. An accurate yield for the reaction could not be obtained due to contamination by NaBr.

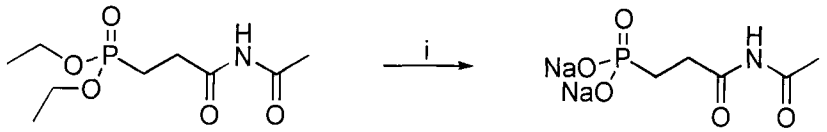

54 138

Scheme 71 i. TMSBr, 2 h, RT, then $NaOH_{(aq)}$, 1 h, RT.

2.8 Biological Testing

The disodium salts **110** and **138** were tested (Biological Department, University of Durham) to assay their antibiotic activity against *E. coli* and *S. aureus*. The results indicated that these compounds did not elicit any antibacterial response. Compound **110** was also assayed against DXP reductoisomerase by Prof H. Seto's group at the University of Tokyo, but was found not to display inhibitory activity or act as a substrate for the enzyme. However, **110** did act as a weak competitive inhibitor of DXP synthase. Assaying of **110** against the PNP synthase enzyme is currently being carried out by Prof D. Cane's group at Brown University, Rhode Island, USA.

Chapter 3

Stereoelectronic effects of fluorine

3.1 Introduction

This chapter is divided into two parts. Both are concerned with the stereoelectronic influence of the fluorine atom in determining the conformation of organofluorine compounds. Part A focuses on the conformation of fluoromethyl aromatics, and Part B describes the fluorine amide *gauche* effect in peptides. The X-ray crystal structures described in this chapter were obtained by Clare Bilton (and Dr D. S. Yufit, for benzyl fluoride) in a collaboration with Prof Judith Howard's research group.

Incorporation of a fluorine atom into an organic compound as a hydrogen or hydroxy mimic is acknowledged as having a profound and sometimes unexpected effect on the biological activity of the fluorinated analogue. The success of the strategy can be attributed to the small size of the fluorine atom which generally does not distort the shape of the analogue relative to the parent substrate. However, the high electronegativity of the fluorine atom can dramatically alter the outcome of an enzymatic process. The van der Waals radius for fluorine is approximately 1.47 Å, and is intermediate between that of hydrogen (1.2 Å) and oxygen (1.57 Å).[147] The electronegativities differ more however with values based on the Pauling scale, of 4 for F, 2.2 for H and 3.5 for O.[148] Comparison of these values alone may suggest that fluorine will act as a better oxygen mimic. However, fluorine is a poor hydrogen bond acceptor relative to oxygen, and this significantly weakens fluorine's ability to replace a hydroxy group.[149] Amongst the subtle effects of replacing hydrogen for fluorine are the stereoelectronic implications of such a change.[56] Organofluorine compounds are known to participate in the anomeric, Anh-Eisenstein, and *cis* and *gauche* effects.[56] The Anh-Eisenstein and *gauche* effects are discussed in detail in Parts A and B respectively.

3.2 Part A

3.2.1 The Anh-Eisenstein effect

Various models have been put forward to rationalise observed facial attack at a carbonyl centre. The Felkin model is perhaps the most successful in rationalising experimental results.[150] This model describes a preferred transition state based on a conformation in which the sterically most bulky (L) of the carbonyl's α-ligands takes up a position opposite and perpendicular to the incoming nucleophile, and the next largest (M) α-ligand is *gauche* to the carbonyl (**Figure 22**). The remaining small (S) α-ligand is then *gauche* to the group (R) attached to the carbonyl carbon.

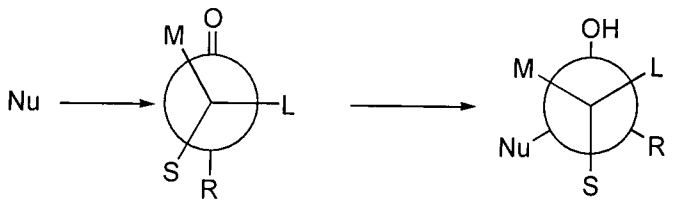

Figure 22 Felkin transition state model of nucleophile attack to a carbonyl.

Ambiguity can arise in assigning the order of ligands according to their size. Anh and Eisenstein have refined the Felkin model and have argued that electronic effects must also be considered when determining the order of ligands. This was exemplified by the outcome of a theoretical study of hydride attack on 2-chloropropionaldehyde **139** (**Figure 23**).[151] For **139** the Felkin order of ligands for L > M > S would be Me > Cl > H, however the study suggested that the most stable transition state will have the HOMO of the hydride nucleophile attacking the LUMO of the carbonyl in an *anti*-parallel approach to the C-Cl bond. It was rationalised that this approach will relax the electrostatic repulsion between chlorine and hydride and also allow for mixing of the developing σ-bond electrons with the σ*-orbital of the C-Cl bond. An analogous study was made for cyanide attack to 2-fluoropropionaldehyde **140** (**Figure 23**) by Paddon-Row and Wong.[152] Here, the Felkin model has Me as the bulkiest ligand and thus *anti* to the incoming nucleophile, whereas the Anh-Eisenstein model requires that the best acceptor ligand, the C-F bond, be *anti* to the nucleophile. This study found that the lowest energy transition

state had the C-F bond *anti*, thereby affording strong support for the Anh-Eisenstein model of nucleophilic attack in such systems.[152]

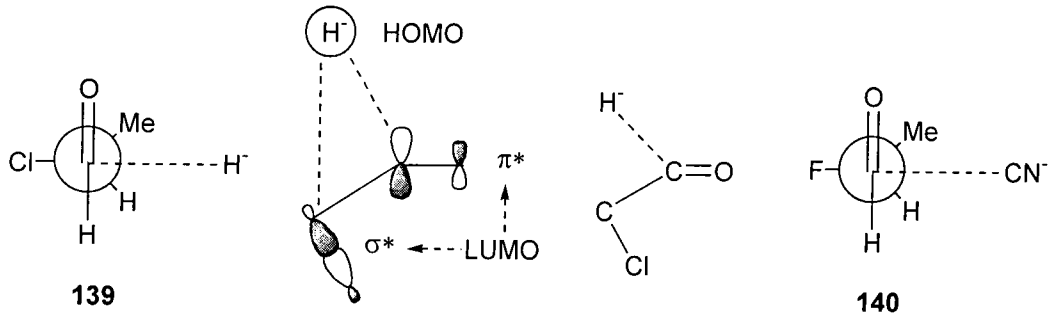

Figure 23 Anh-Eisenstein stabilisation, rationalised through a molecular orbital approach for nucleophilic attack to 2-chloropropionaldehyde **139** and 2-fluoropropionaldehyde **140**.

3.2.2 Anh-Eisenstein effect in enzymatic reactions

The enzymatic hydrolysis[153,154] of racemic or *meso* α-fluorinated esters (**Figure 24**) has been rationalised by considering Anh-Eisenstein type transition states. Classically lipase enzyme resolutions have been interpreted to arise by steric interactions of S, M and L groups with the surface of the protein. For the fluorinated substrates however, it is difficult to rationalise selectivity in terms of a size difference between fluorine and hydrogen. This deficiency, and the theoretical analysis of diastereoisomeric transition states for nucleophilic attack by lipases, suggests that the resolution is due to Anh-Eisenstein type stabilisation and is essentially controlled stereo-electronically.[155] This would occur in the lipase active site as the serine alkoxide nucleophile of the enzyme attacks the ester carbonyl (**Figure 24**). This stabilisation (estimated to be about 10 kJ mol^{-1}) is sufficient to account for the observed enantioselectivity of 99 % ee.[155]

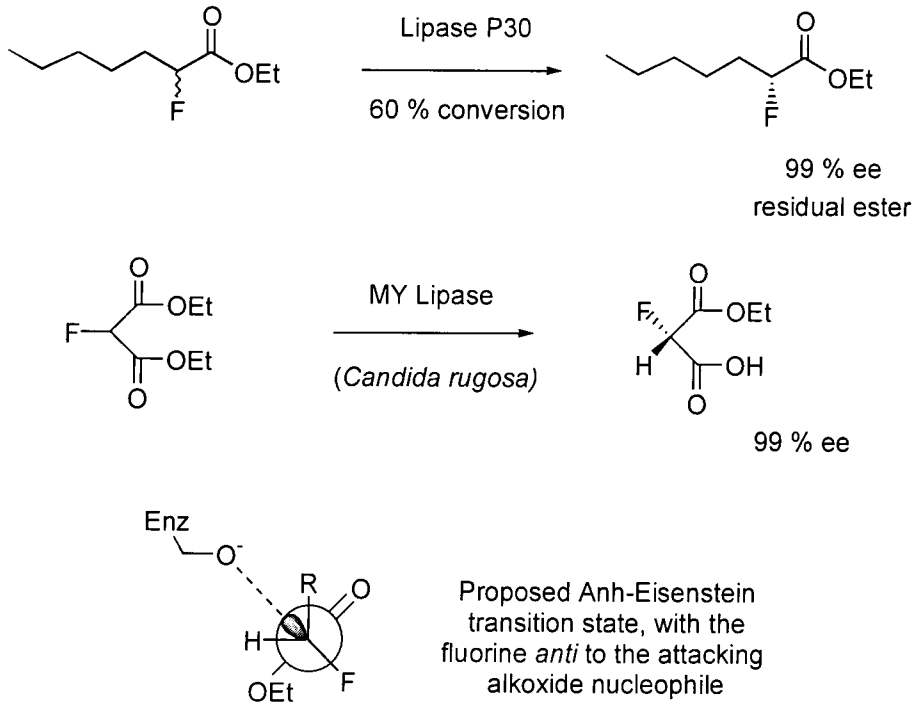

Figure 24 Enzymatic lipase reactions with α-fluoro esters, with proposed Anh-Eisenstein diastereomeric transition state.

3.2.3 Intramolecular stabilisation through n-σ* hyperconjugation

The Anh-Eisenstein effect has been used to rationalise the results of enzymatic reactions on fluorinated substrates, but there is little experimental evidence, beyond theoretical studies, which support these conclusions. Experimental evidence to demonstrate the n-σ* interaction for fluorinated compounds has arisen from *ab initio* and microwave studies on the conformational preference of 2-(fluoromethyl)pyridine **141**.[156] Previous work[156] on the related 2-(alkoxymethyl)pyridines **142** had shown from crystal structures that there is a strong preference for an *anti*-periplanar conformation, with an N-C-C-O dihedral angle close to 180° (**Figure 25**). The observed *anti* conformation was rationalised to be largely due to orbital overlap between the ring nitrogen's lone pair and the C-O antibonding (σ*) orbital. This type of orbital overlap, between an incoming HOMO and an anti-bonding LUMO parallels the interaction in the Anh-Eisenstein transition states for π-facial selectivity. A gas phase analysis of **142** was now required to remove interactions arising from crystal packing forces. 2-(Alkoxymethyl)pyridines **142** however, were found not to

be suitable for gas phase studies owing to their large number of degrees of freedom and their low vapour pressure. 2-(Fluoromethyl)pyridine **141** however, was found to be a good model with *ab initio* calculations finding the same conformational preference as that calculated for **142**. Microwave spectroscopic studies were found to be in strong agreement with the *ab initio* predictions, revealing a preferred *anti*-periplanar conformation as shown in **Figure 25** predominanting in the gas phase.[156] This conformation arises by n-σ* hyperconjugation and has an origin similar to the Anh-Eisenstein model.

142 **141**

Figure 25 The preferred conformation of 2-(alkoxymethyl)pyridines **142** and 2-(fluoromethyl)pyridine **141**.

Seven different conformations of **141** can be envisaged (**Figure 26**). *Ab initio* calculations predict a theoretical energy difference between conformers A and G of 20.2 kJ mol^{-1}, with C-F bond lengths of 1.396 Å and 1.382 Å for A and G respectively.[156] Conformers A and G have the C-F bond co-planar with the ring, B, C, E and F have C-F *gauche* to the ring, whereas for D the C-F is perpendicular. Conformation G is not an energy minimum due to electrostatic replusion between fluorine and nitrogen. Conformations A and D can both accommodate hyperconjugation between the σ* orbital of the C-F bond and the lone pair on N in the former case, and with the π-orbitals of the aromatic ring in the latter case (**Figure 26**). As a consequence the most stable conformations should be either A or D. In the event A emerged as the most stable conformer of **141** suggesting that N lone pair donation into the C-F σ* orbital is more stabilising than π-orbital donation. However, it must be noted that electrostatic repulsion between N and F will have an important part to play in determining the most stable conformation of **141**, and N and F are maximally separated in A.

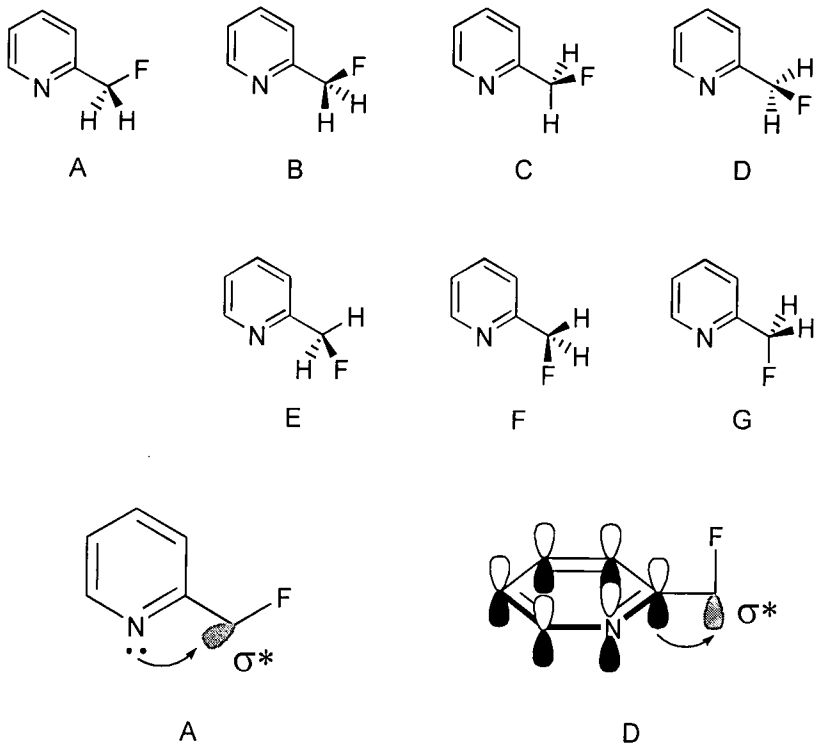

Figure 26 Seven different conformations of 2-(fluoromethyl)pyridine **141**.

3.2.4 Objectives

In an effort to obtain further evidence to reinforce this conjugative hypothesis, crystallographic data to support the above conclusions was sought. Synthesis of 2-(fluoromethyl)pyridine **141** and the 2-(fluoromethyl)pyridine derivatives **143-146** (following page) were undertaken in anticipation of generating compounds for X-ray analysis. The N-C-C-F dihedral angles were clearly of interest. A dihedral angle of 180° would suggest n-σ* stabilisation, with the C-F bond parallel and *anti* to the N-C bond. Also if significant donation was occurring from the N lone pair into the σ* orbital of the C-F bond, then the length of the C-F bond might become extended as the antibonding orbital is populated. However, secondary intermolecular interactions may well also perturb the length of the C-F bond and / or the conformation of the fluoromethyl group in the solid state relative to the gaseous state. For this reason analysis of the intermolecular interactions will also be undertaken.

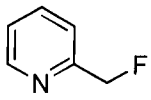

141

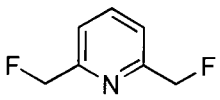

143

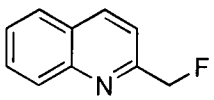

144

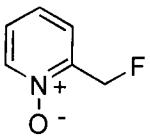

145

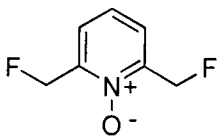

146

3.2.5 Synthesis

In general fluoromethylpyridines can be prepared from the corresponding chlorinated compounds by halogen exchange. 2-(Fluoromethyl)pyridine **141** was prepared *via* halide exchange of 2-(chloromethyl)pyridines as previously described[156] using KF in conjunction with 18-crown-6 in CH_3CN (**Scheme 72**).[157] After 8 days the reaction was worked up and the product purified by distillation. In the event **141** was isolated in 14 % yield. Bis-2,6-(fluoromethyl)pyridine **143** was prepared in a similar manner after a 10 day reaction. Distillation afforded **143** as a low melting solid in 50 % yield, and recrystallisation from an acetone / petrol mix at -20 °C gave crystals of **143** suitable for X-ray analysis. Reaction of 2-(chloromethyl)quinoline with KF also afforded the corresponding fluorinated compound 2-(fluoromethyl)quinoline **144**. This reaction was sluggish, and after 14 days reaction distillation afforded a fraction of **144** as a clear colourless oil, in about a 50 % yield, **Scheme 72**.

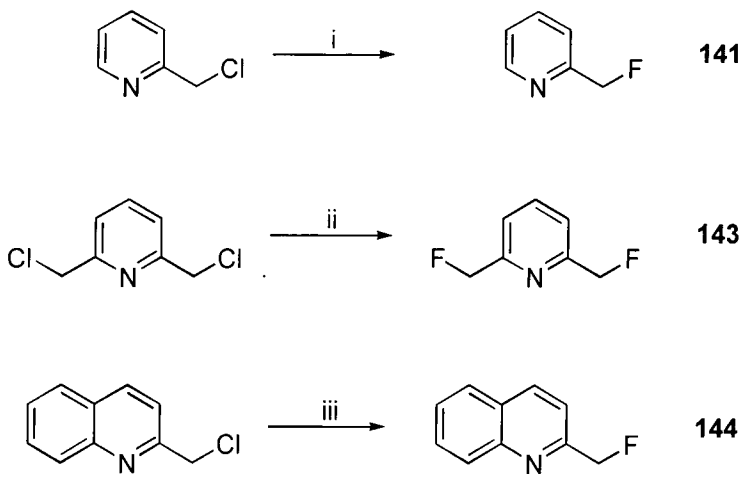

Scheme 72 All reactions, KF, 18C6, MeCN, reflux; for i. 8 d, 14 %; for ii. 10 d, 50 %; for iii. 14 d, ~ 50 %.

The *N*-oxide of the pyridines **141** and **143** were prepared following conditions developed by Ochiai (**Scheme 73**).[158] Accordingly, treament of **141** in an acetic acid / hydrogen peroxide mixture, followed by distillation, afforded 2-(fluoromethyl)pyridine-*N*-oxide **145** as an oil, in 46 % yield. Likewise, the formation of bis-2,6-(fluoromethyl)pyridine-*N*-oxide **146**, was achieved in 61 % yield, affording a white solid. Recrystallisation of **146** gave crystals which were suitable for X-ray analysis.

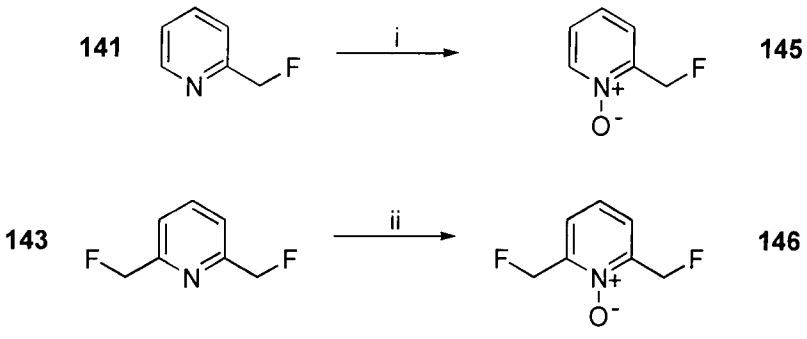

Scheme 73 i. AcOH, H_2O_2, 2 h, 70 °C, 46 %; ii. AcOH, H_2O_2, 3 h, 70 °C, 61 %;

3.2.6 X-ray crystal structures

3.2.6.1 2-(Fluoromethyl)pyridine **141**

At the outset obtaining an X-ray structure of 2-(fluoromethyl)pyridine **141** was a priority, as this parent structure could be compared directly to the structure obtained from *ab initio* and microwave studies.[156] However, **141** is an oil at ambient temperature and attempts at low temperature crystallisation on the diffractometer failed, generating an amorphous glass rather than a crystalline material. In view of this, other structures were sought that were analogous to **141**.

3.2.6.2 Bis-2,6-(fluoromethyl)pyridine **143**

Bis-2,6-(fluoromethyl)pyridine **143** was found to be a low melting solid (~ 35 °C) at ambient temperature. Crystallisation in the fridge only generated a waxy solid. Fortunately however, low temperature (-20 °C) recrystallisation did afford a sample suitable for X-ray crystal structure analysis and the X-ray diffraction data was solved with a R-factor < 7 %. The structural data are presented in **Appendix 1**. **Figure 27** clearly shows that both of the fluoromethyl groups adopt *anti*-planar conformations, relative to nitrogen. The dihedral angles and C-F bond lengths differ for the two fluoromethyl groups, with one having a N-C-C-F dihedral angle of 175.9° and a C-F bond length of 1.401 Å, whereas the other has values of 174.3° and 1.385 Å respectively.

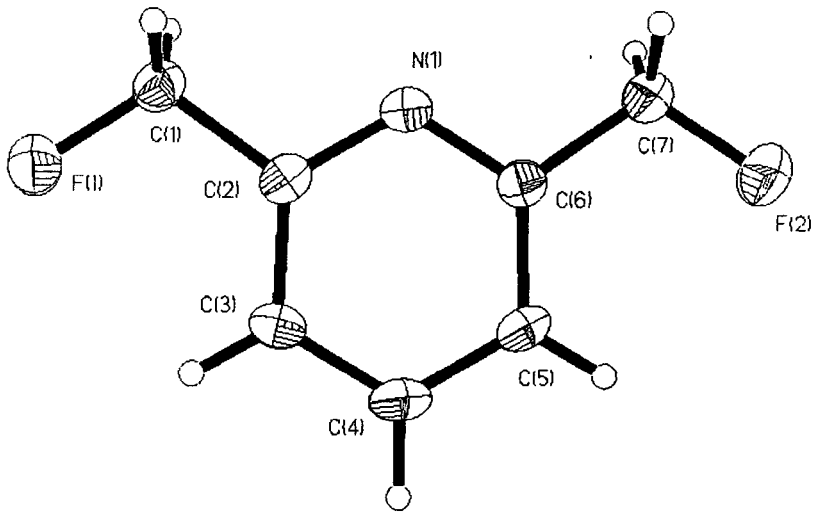

C(1)-F(1) = 1.401 Å C(7)-F(2) = 1.385 Å
N-C(2)-C(1)-F(1) = 175.9° N-C(6)-C(7)-F(2) = 174.3°

Figure 27 50 % Probability ellipsoid plot of bis-2,6-(fluoromethyl)pyridine **143**.

The crystal packing shows a potential intermolecular H-F bond between H(5) and F(1) (**Figure 28** and **Figure 29**). However, the distance of 2.56 Å between these H and F atoms suggests that this is at best a weak H-F bond. Possibly, this interaction may contribute to the difference in the N-C-C-F dihedral angles and C-F bond lengths.

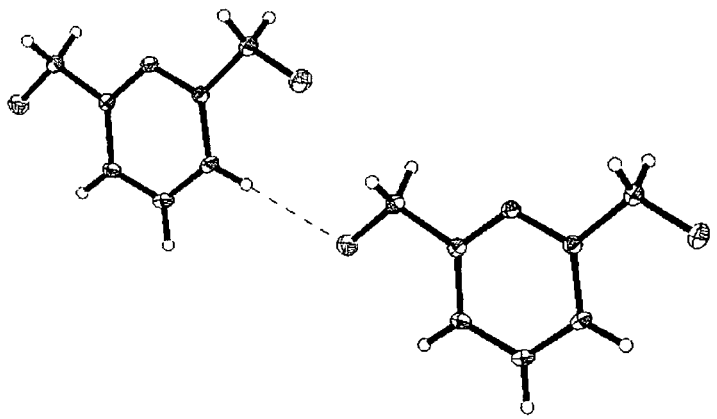

H-F = 2.560 Å

Figure 28 50 % Probability ellipsoid plot of bis-2,6-(fluoromethyl)pyridine **143**, indicating potential H-F intermolecular interaction.

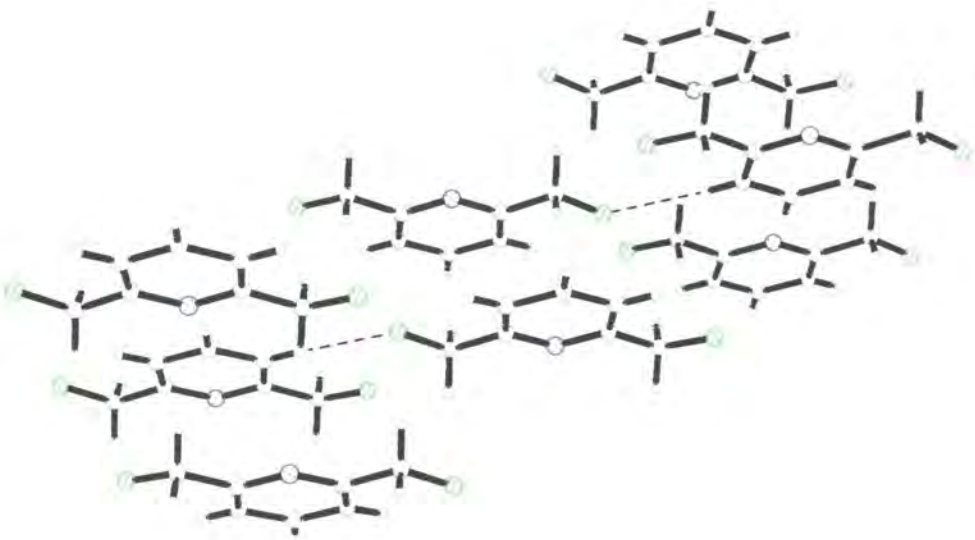

Figure 29 50 % Probability ellipsoid plot of bis-2,6-(fluoromethyl)pyridine **143**, indicating stacking in crystal.

3.2.6.3 Bis-2,6-(fluoromethyl)pyridine-*N*-oxide **146**

The *N*-oxide of **143** has a higher mp (81 °C vs 35 °C) than the parent pyridine **143** most probably due to the highly ionic nature of the *N*-oxide bond. **Figure 30** clearly shows that again, both of the fluoromethyl groups adopt an *anti*-planar conformation, with respect to the nitrogen. The dihedral angles of the fluoromethyl groups being 176.0° and 176.1°, with the C-F bond lengths both being at 1.412 Å. The structural data for **146** are presented in **Appendix 2**.

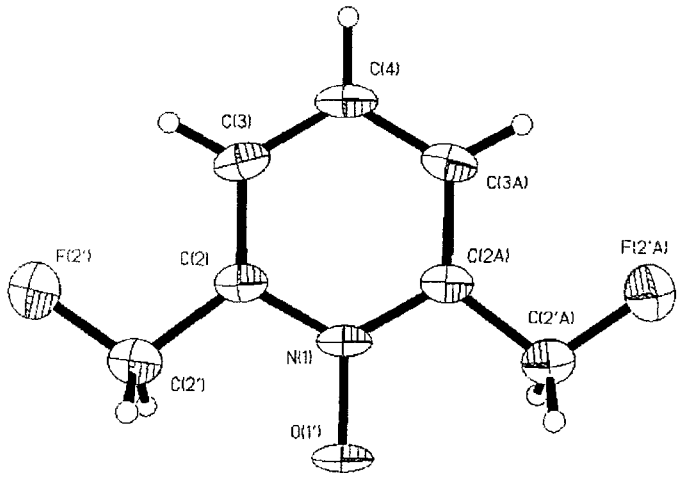

C-F = 1.412 Å

N-C(2)-C(2')-F(2') = 176.0° N-C(2A)-C(2'A)-F(2'A) = 176.1°

Figure 30 50 % Probability ellipsoid plot of bis-2,6-(fluoromethyl)pyridine-*N*-oxide **146**.

The crystal packing depicted in **Figure 31** shows head to tail intermolecular hydrogen bonding (2.191 Å) from H(4) to O, with a C-H-O-N dihedral angle of 180°. Further analysis of the molecular packing shows that there are symmetrical interactions around the fluoromethyl groups with all methylene hydrogens having a H bond to O. This symmetry affords a C_2 axis for bis-2,6-(fluoromethyl)pyridine-*N*-oxide **146**, consistent with the identical C-F bond lengths.

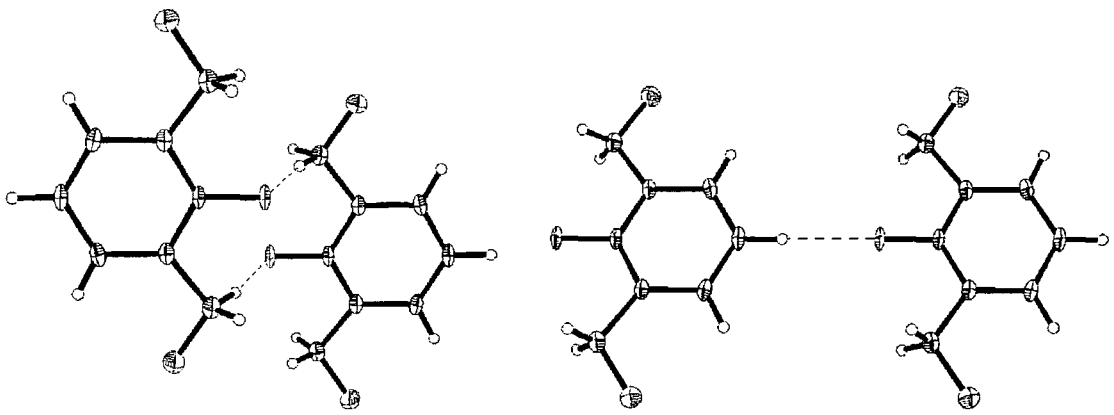

H-O = 2.490 Å H-O = 2.191 Å

Figure 31 50 % Probability ellipsoid plots of bis-2,6-(fluoromethyl)pyridine-*N*-oxide **146**, indicating potential intermolecular interactions.

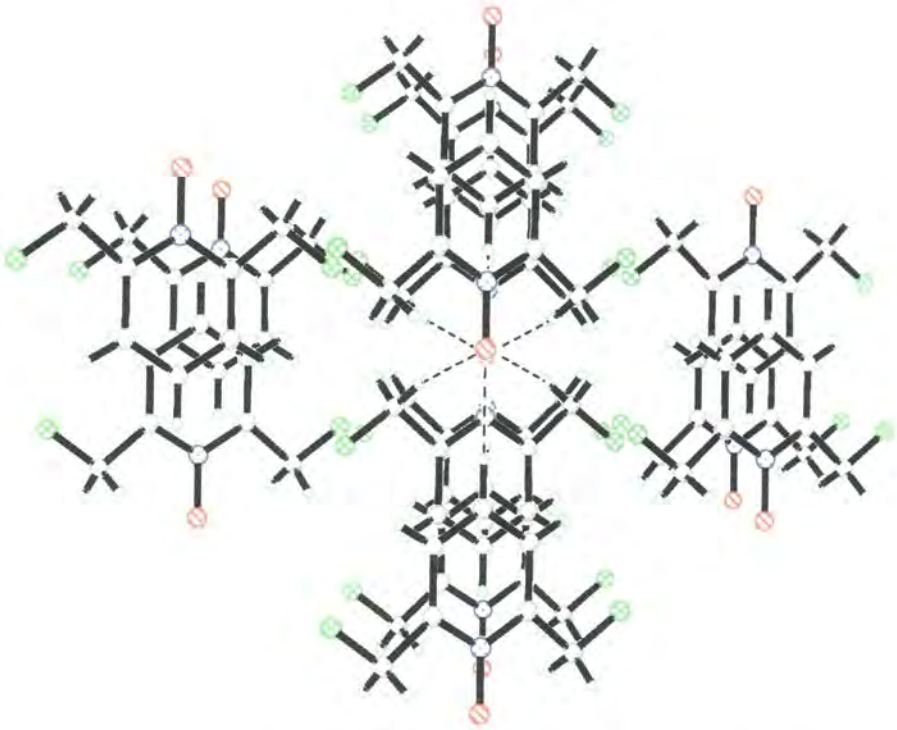

Figure 32 Stacking plot of bis-2,6-(fluoromethyl)pyridine-*N*-oxide **146**.

3.2.6.4 2-(Fluoromethyl)quinoline **144**

2-(Fluoromethyl)quinoline **144** is an oil at ambient temperature, therefore attempts were made at obtaining *in situ* crystal growth on the diffractometer at low temperature. This however failed, but crystallisation from a MeOH / H_2O mix at -10 °C afforded a sample of the monohydrate **147** from which a X-ray structure could be solved (**Figure 33**). The hydrate **147** structure had a fluoromethyl conformation with a N-C-C-F dihedral angle of 172.0° and a C-F bond length of 1.392 Å. The structural data for **147** are presented in **Appendix 3**.

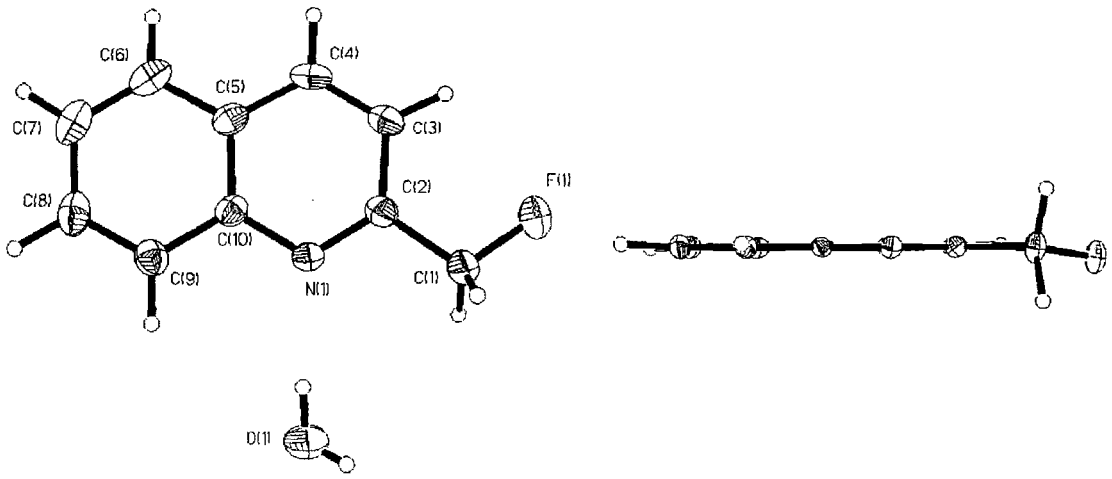

C(1)-F(1) = 1.392 Å N-C(2)-C(1)-F(1) = 172.0°

Figure 33 50 % Probability ellipsoid plot of 2-(fluoromethyl)quinoline monohydrate **147**.

Analysis of the intermolecular interactions for **147** reveals the presence of a short (2.026 Å) and presumably strong hydrogen bond between nitrogen and the hydrogen of a water molecule, **Figure 34**. The water molecule is also H-bonded to another molecule of water which then in turn H-bonds to another molecule of **144**, **Figure 35**. The water molecules in the structure of **147** in **Figure 35** have one hydrogen disordered, giving rise to the appearance of water as H_3O molecules. There is also a potential intermolecular interaction between fluorine and H(3), of 2.498 Å, but again due to the distance between the atoms this must be considered a weak interaction.

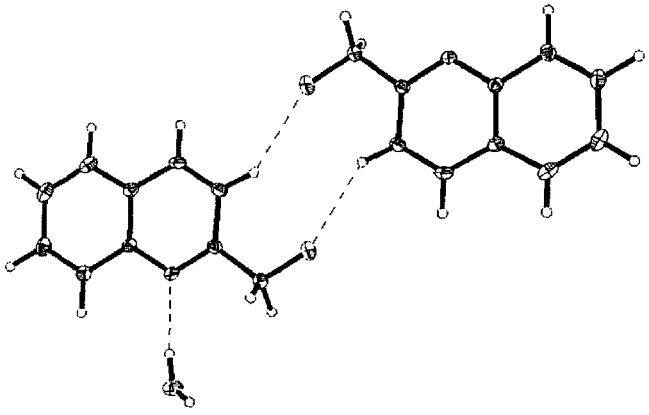

N-H = 2.026 Å H-F = 2.498 Å

Figure 34 50 % Probability ellipsoid plot of 2-(fluoromethyl)quinoline monohydrate **147**, indicating potential intermolecular interactions.

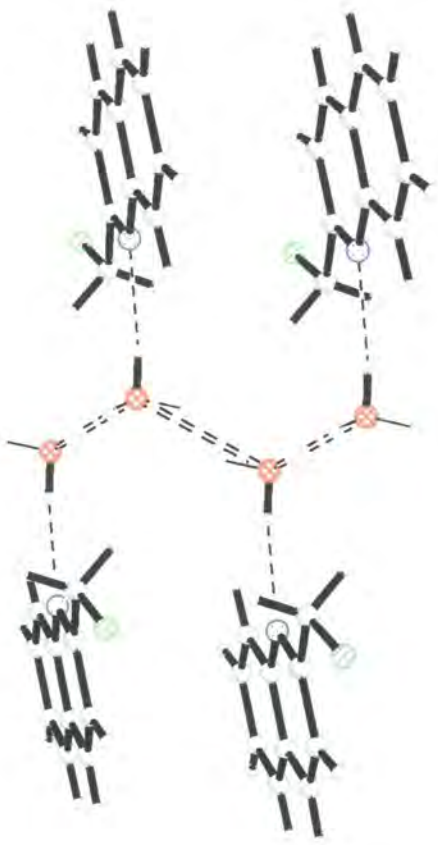

Figure 35 Stacking plot of 2-(fluoromethyl)quinoline monohydrate **147**. The broader dotted lines depict water molecules that are hydrogen bonded to each other.

3.2.7 Discussion of crystal structures

The structures of the bis-(fluoromethyl) systems of **143** and **146**, were solved. Despite some effort, the structure of 2-(fluoromethyl)pyridine **141** remained elusive. In order to investigate an analogous system, a crystal structure of 2-(fluoromethyl)quinoline **144** was sought. Attempts at crystallisation of **144** on the diffractometer at low temperature were unsuccessful, however a suitable crystal of **144** as its monohydrate **147** was obtained for X-ray analysis. The C-F bond lengths and dihedral angles obtained from the crystal structures of compounds **143**, **146** and **147** are tabulated below in **Table 2**. All of the dihedral angles are within 10° of the ideal angle (180°) calculated from *ab initio* and microwave studies for 2-(fluoromethyl)pyridine **141**. The C-F bond lengths are also found to be close to that predicted for **141**, within 0.016 Å of the predicted bond length.

Compound	N-C-C-F angles / °	C-F Bond lengths / Å
143	F(1) = 175.9 F(2) = 174.3	F(1) = 1.401 F(2) = 1.385
146	F(2') = 176.0 F(2'A) = 176.1	F(2') = 1.412 F(2'A) = 1.412
147	172.0	1.392

Table 2 C-F bond lengths and the dihedral angles in the N-C-C-F crystal structures **143**, **146** and **147**.

From the above data for structures **143** and **146** there appears to be a correlation between the N-C-C-F dihedral angle and the C-F bond length. An explanation for this could be that a higher degree of planarity enables an increased level of hyperconjugation into the C-F σ* orbital. However, this analysis does not extend to **147** which has the lowest dihedral angle and would be anticipated to have the shortest C-F bond.

In order to place the length of these C-F bonds in a broader context, a comparison of C-F bond lengths was made with other X-ray structures. The Cambridge Structural Database (CSD) provides an excellent archive for doing this. A selective search of all CH_2F groups yielded 68 hits (**Figure 36**), although none of these were fluoromethyl aromatics. It is interesting, and perhaps surprising to note therefore that **143**, **146** and **147** are the first fluoromethyl aromatic X-ray structures yet recorded.

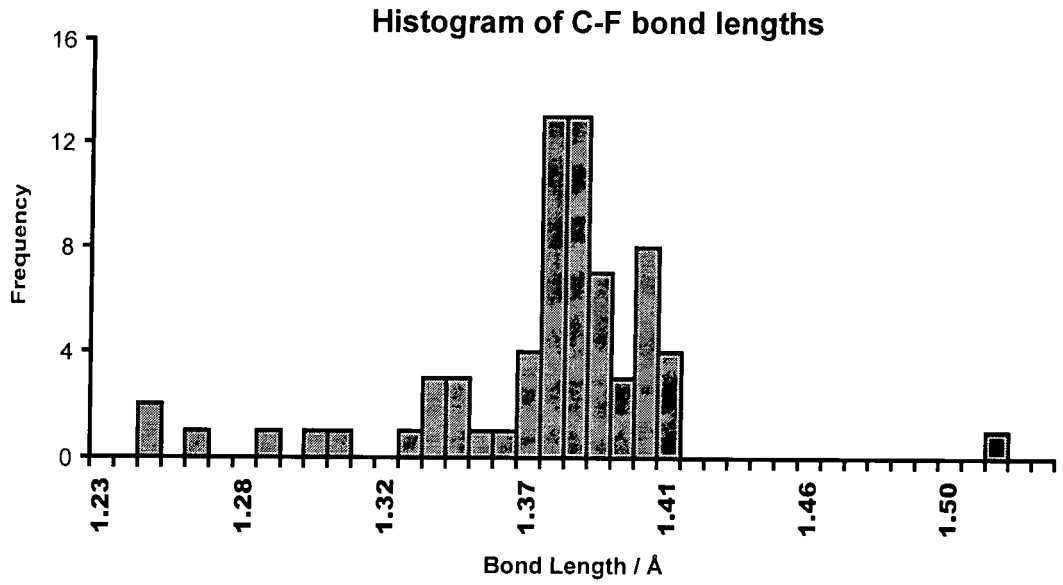

Figure 36 Histogram of all fluoromethyl C-F bond lengths in the CSD.

Refining the dataset in **Figure 36** by removing all those structures that were inorganic, showed disorder or had a R-factor ≥ 10 %, reduced the dataset to 37 separate C-F bond lengths. These are correlated in the histogram in **Figure 37**.

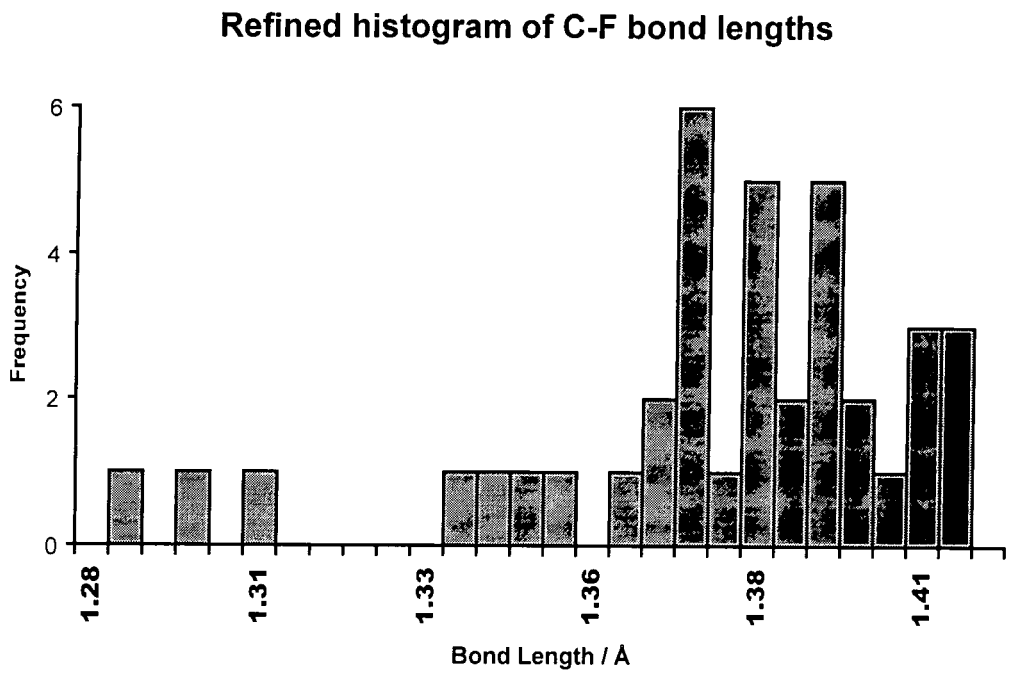

Figure 37 Refined histogram of fluoromethyl C-F bond lengths in the CDS.

Comparison of the C-F bond lengths for **143**, **146** and **147** to the mean C-F bond length of 1.381 Å in the histogram of **Figure 37** shows all of the fluoromethyl aromatics have longer than average C-F bond lengths. Perhaps n-σ^* hyperconjugation and N-F repulsion contributes to this phenomenon. In the next section fluoromethyl aromatics, such as benzyl fluoride **148**, which do not have N-F replusion are shown to adopt an orthogonal conformation.

3.2.8 The conformation of benzyl fluoride

The minimum energy conformation of the C-F bond in benzyl fluoride **148** has been discussed extensively in the literature and contrary conclusions have emerged. Brownlee and Craik[159] has reported that there is a significant temperature dependence of the ^{19}F NMR chemical shift for **148** and a series of 4-substituted benzyl fluorides. It was concluded that this is due to a temperature dependence on the different populations of planar and perpendicular conformations. A spectroscopic study afforded very similar results for **148** and benzyl alcohol, suggesting that **148** would have the same orthogonal conformation as that determined for benzyl alcohol.[160] A microwave spectroscopic study has recently reported a preferred orthogonal conformation (by 0.7 kJ mol^{-1}) for benzyl fluoride.[161] This contradicts early *ab initio* calculations, which indicated that the perpendicular conformation is preferred by 1.7 kJ mol^{-1}.[159] However, more recent theoretical studies[162,163] concluded that for **148** the perpendicular conformation is lower in energy in solution, yet the calculations arriving at this conclusion suggested that the planar form was preferred in the gas phase. Until very recently the discrepancy between theoretical and experimental studies remained. This has now been resolved by Dr. D. Tozer (Durham University) using a higher level of basis sets in the computational analysis. It emerged that the orthogonal conformer had the lower energy, with a calculated rotational energy barrier of 2.1 kJ mol^{-1} and a C-F bond length of 1.412 Å, **Figure 38**.[164] It remained an objective of this research programme to obtain the first X-ray structure showing this conformation in such a system.

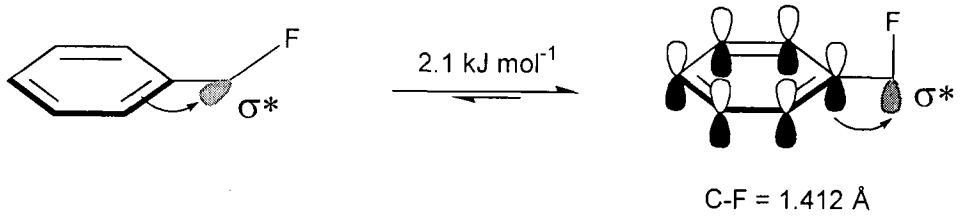

Figure 38 Conformation of benzyl fluoride **148**, as predicted by recent computational data.[164]

3.2.9 The preparation of fluoromethyl benzyl aromatics

Benzyl fluoride **148**, 4-bromobenzyl fluoride **149** and *trans*-4-fluoromethylstilbene **150**, were selected as target molecules (**Scheme 74**) for X-ray structure analysis. Benzyl fluoride **148** has been synthesised *via* halogen exchange of benzyl bromide by treatment with CsF and NBu_4F.[165] Fluorination of the alcohols **151** and **152** with DAST was judged to offer an appropriate preparation of 4-bromobenzyl fluoride **149** and *trans*-4-fluoromethylstilbene **150**.[166]

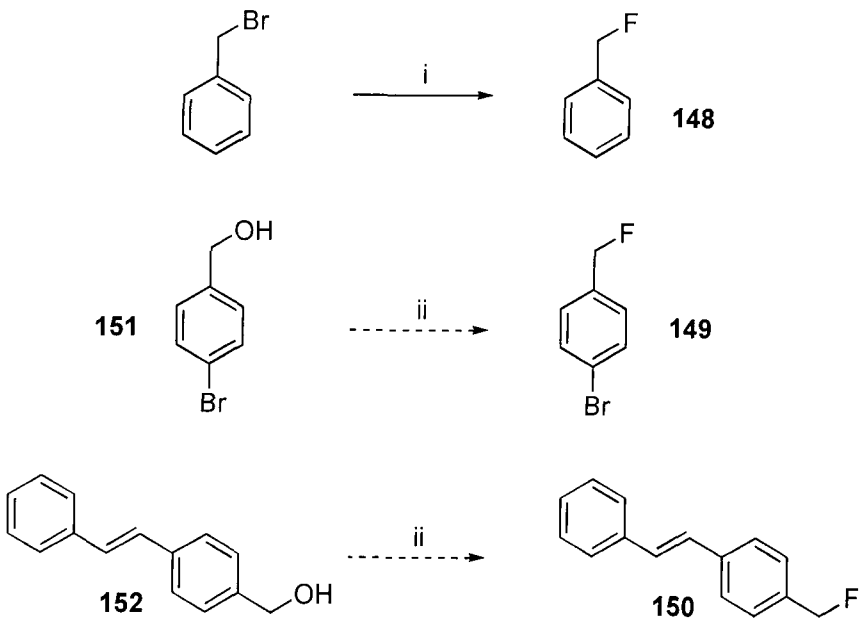

Scheme 74 Synthesis of benzyl fluoride **148**, 4-bromobenzyl fluoride **149** and *trans*-4-fluoromethylstilbene **150**. i. CsF, TBAB, 3 h, 85 °C, 94 %; ii. DAST, CH_2Cl_2, -78 °C.

Benzyl fluoride was indeed prepared in 64 % yield following the literature method.[165] Redistillation afforded a sample which was > 99.9 % pure as judged by GCMS analysis. 4-Bromobenzyl fluoride **149** was successfully prepared from **151** by reaction with DAST at -78 °C in CH_2Cl_2 to afford the fluoromethyl product in 30 % yield, as a low melting solid. Recrystallisation from CH_2Cl_2 gave crystals of **149** suitable for X-ray analysis. Formation of **150** proved problematical. Treatment with DAST at -78 °C in CH_2Cl_2 resulted in an inseparable mixture of products. A change of solvent to THF proved expedient in affording the desired material, however it was contaminated, mainly with starting material. Purification by column chromatography did afford **150** in 24 % yield, as a solid, contaminated with **152** (~ 10 %). Recrystallisation from $CHCl_3$ gave suitable crystals from which X-ray diffraction data was collected.

3.2.10 Crystal structures of benzyl fluorides

3.2.10.1 4-Bromobenzyl fluoride **149**

Analysis of the diffraction pattern from a suitable crystal of **149** indicated that the crystal was twinned affording poor data, from which only a poorly determined structure could be obtained. The structure that was solved was disordered with the C-F bond of the fluoromethyl group in two conformations in approximately equal proportions (**Figure 39**). The conformers present in the crystal structure however clearly show that the C-F bond does not lie planar with the aromatic ring. One conformer is nearly orthogonal (83.5°), and the other occupies a more *gauche* conformation (56.7°). Both C-F bonds seem very short, however this is due to the computed values being an average of a C-F and a much shorter C-H bond length.

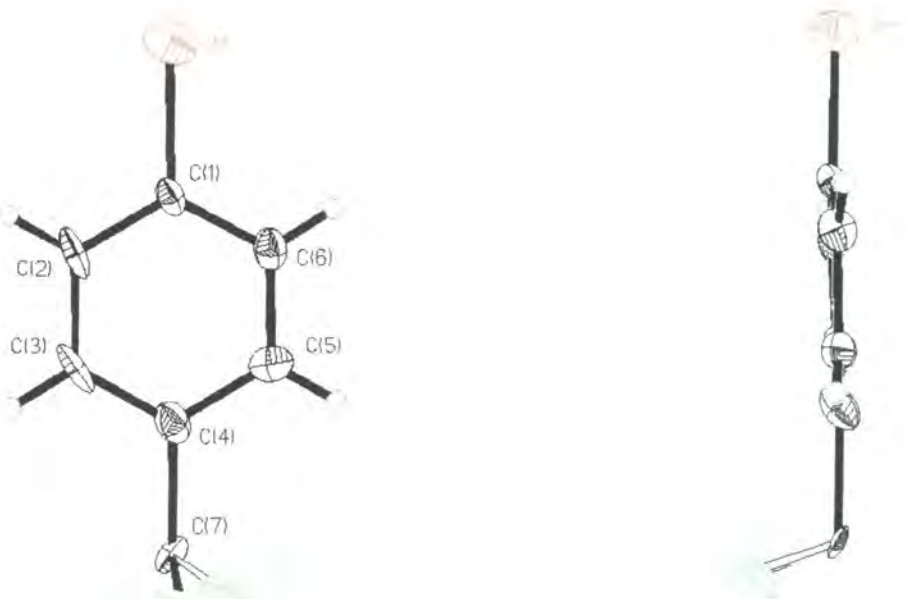

C(5)-C(4)-C(7)-F(1A) = 83.5° C(5)-C(5)-C(7)-F(1B) = 56.7°
C(7)-F(1A) = 1.23 Å C(7)-F(1B) = 1.32 Å

Figure 39 50 % Probability ellipsoid plot of 4-bromobenzyl fluoride **149**.

The crystal packing diagram of **149** shows a potential intermolecular H-F bond between H(2) and F(B) of 2.547 Å. A fluorine to hydrogen bond of this length is anticipated to be a weak interaction.[149]

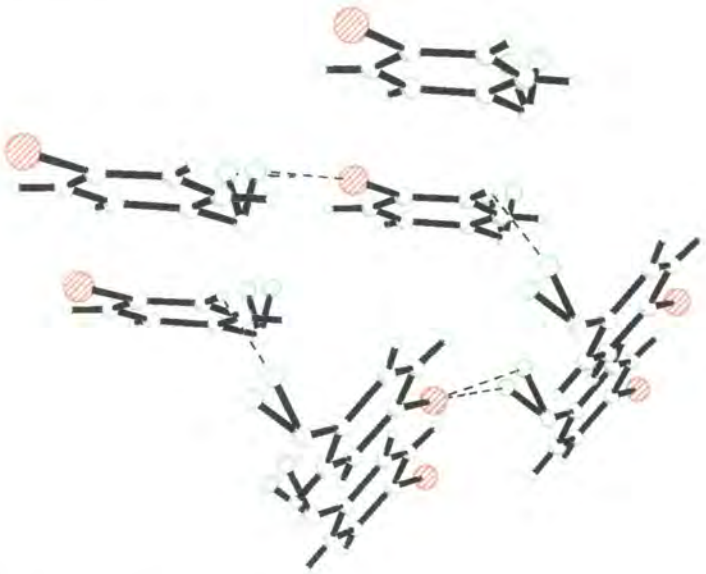

Figure 40 50 % Probability ellipsoid plot of 4-bromobenzyl fluoride **149**, indicating stacking in crystal.

3.2.10.2 *Trans*-4-fluoromethylstilbene **150**

Diffraction data was collected for *trans*-4-fluoromethylstilbene **150**, but all attempts to obtain a sufficiently resolved structure failed. Thus the conformation of the fluoromethyl group could not be accurately assessed in this case.

3.2.10.3 Benzyl fluoride **148**

Numerous attempts at obtaining a X-ray diffraction pattern from low temperature crystallisation of 2-(fluoromethyl)quinoline **144** and 2-(fluoromethyl)pyridine **141** were unsuccessful. However, the first attempt at obtaining *in situ* crystal growth on the diffractometer at about 230 K succeeded for benzyl fluoride, yielding a crystal which defracted well at 150 K in the X-ray beam. The resultant highly solved structure (**Figure 41**) shows benzyl fluoride with a C(3)-C(2)-C(1)-F dihedral angle of 76.6° and a C-F bond length of 1.419 Å. The crystal packing in **Figure 42** does not show an apprecible intermolecular contact to suggest that this conformation is perturbed by such interactions.

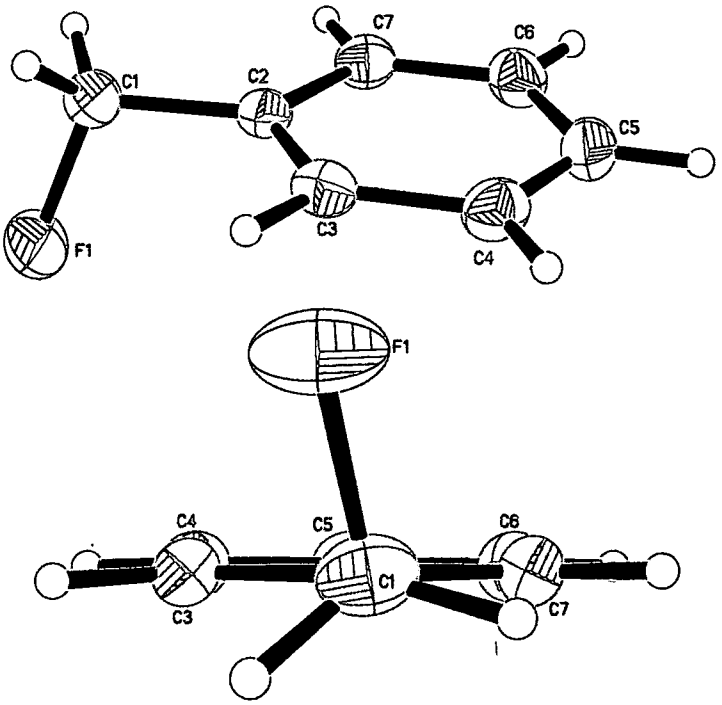

C(1)-F(1) = 1.419 Å C(3)-C(2)-C(1)-F(1) = 76.6°

Figure 41 50 % Probability ellipsoid plot of benzyl fluoride **148**.

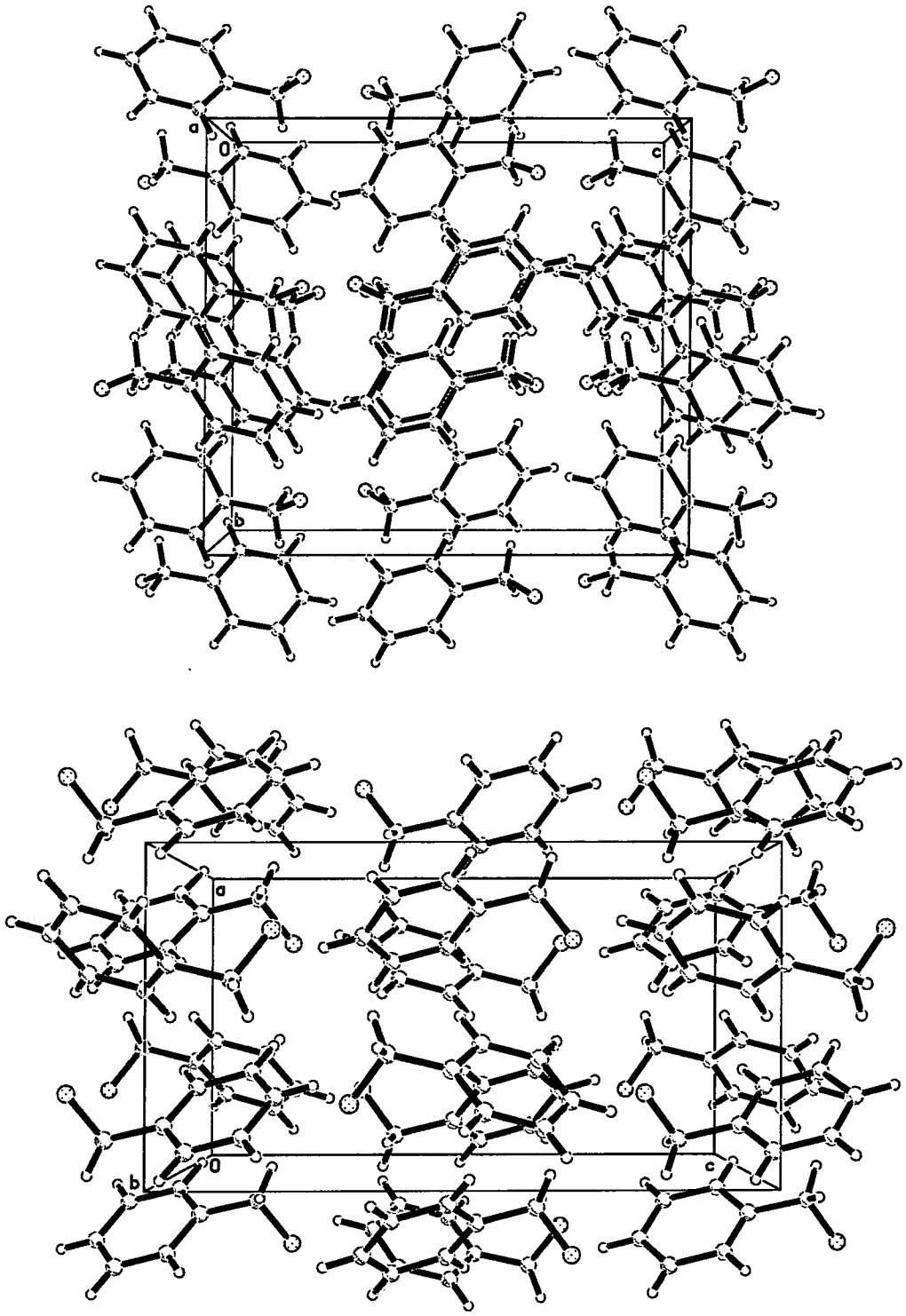

Figure 42 50 % Probability ellipsoid plots of benzyl fluoride **148**, in the stacking diagram.

3.2.11 Discussion of crystal structures of benzyl fluorides

The solid state structures of benzyl fluoride **148**, and 4-bromobenzyl fluoride **149** have shown a strong correlation with the spectroscopic and theoretical experiments revealing the predicted lower energy perpendicular conformation of the C-F bond. This conformation can again be rationalised through electron donation into the σ* orbital of the C-F bond, but now from the π orbitals. This conjugation could perhaps have contributed to the relatively long C-F bond of 1.419 Å found for **148**.

3.2.12 Summary

Solid state X-ray structures have been determined for the first time for several fluoromethyl aromatics. Comparison of the C-F bond lengths in benzyl fluoride **148** and bis-2,6-(fluoromethyl)pyridine-*N*-oxide **146** to those found in the CSD suggest that they have relatively long C-F bonds. This is consistent with electron donation into the C-F σ* orbital from either the π electrons of **148** or the O lone pair of **146**. The fluoromethyl group in the benzyl systems has been found to adopt an orthogonal conformation whereas the fluoromethylpyridine systems adopt a planar conformation with the fluorine *anti* to the ring nitrogen. The different conformations in the two systems can be rationalised in at least two ways: donation from the N lone pair into the C-F σ* orbital will be more efficient than from the π orbitals of the aromatic, and secondly, electrostatic replusion between F and N will also favour an *anti* conformation to minimise this interaction.

3.3 Part B

3.3.1 Introduction to the *gauche* effect

The term *gauche* effect describes the 'tendency (of a molecule) to adopt that structure (conformation) which has the maximium number of *gauche* interactions between the adjacent electron pairs and / or polar bonds'.[167] This effect, which seems to contradict the basic principles of steric interactions has been shown to exist for a number of structures that contain electronegative atoms vicinal to each other.[168,169] It is well known for example that 1,2-difluoroethane **153** prefers a *gauche* rather than *anti* conformation by approximately 3 kJ mol^{-1} (**Figure 43**).[170]

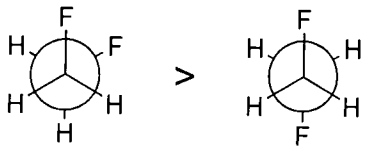

Figure 43 The gauche effect in 1,2-difluoroethane **153**.

The origin of the *gauche* effect has been rationalised in two different ways. One explanation suggests that the energy difference between the conformers lies to some extent in bent bonding in the C-C bond between adjacent electronegative groups.[171] Comparison of this bent-bond contribution (**Figure 44**) has shown that the *anti* conformation has the C-C bond paths lying in opposite directions, whereas the *gauche* conformation has the bond paths bent towards the same direction. For the *gauche* conformation this leads to greater orbital overlap and a stronger C-C bond.

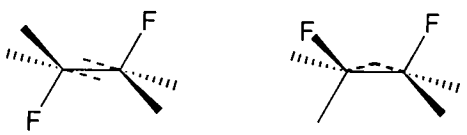

Figure 44 Comparsion of the sp^3 orbital overlap (dashed lines) for the *anti* and *gauche* conformers of 1,2-difluoroethane **153**.

An alternative and widely promulgated explanation for the *gauche* effect considers again electron donation into the C-F σ* orbitals. The preference for conformations in which the best donor bond (eg C-H) is antiperiplanar to the best acceptor bond (eg C-F) being now invoked to rationalise the *gauche* effect.[172] This holds true for a range of 1,3-interactions.[169] For example, crystal structures of X-CH_2-CH_2-OY for a variety of Y in which X=F or SiR_3 have all shown the X=F structures to have *gauche* conformations, whereas for X=SiR_3 the structures display *anti* conformations, **Figure 45**. This preferred *gauche* conformation most probably arises due to the C-SiR_3 bond being a better donor than the C-H bond, ie. the best electron donating bond is still *anti* to the best electron acceptor bond.

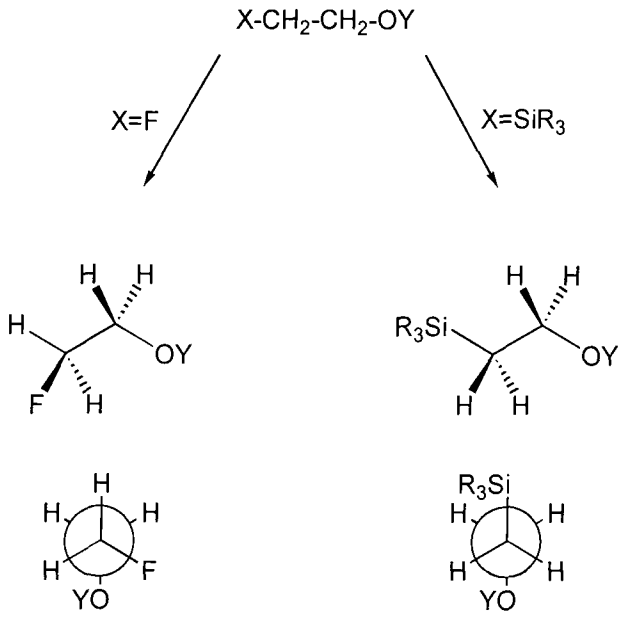

Figure 45 1,3-Interactions in determining the conformation of a molecule.

The *gauche* effect has generally been demonstrated in a few small, well defined compounds such as difluoroethane **153**. Recently however, the *gauche* effect has been cited as a potential origin from which one of the strongest protein chains, collagen, partly derives its stability.[173] Collagen, the most abundant protein in animals, is present as chains wound in tight triple helices which are organised into fibrils of great tensile strength and thermal stability. Collagen is composed of the repeat amino acid sequence of X-Y-Gly, where X and Y are often L-proline (Pro) and L-4(*R*)-hydroxyproline residues respectively. The collagen triple helix mimics, $(ProProGly)_{10}$, $(ProHypGly)_{10}$ and

$(ProFlpGly)_{10}$ (Flp = L-4(*R*)-fluoroproline) were prepared by Holmgren and co-workers, and their midpoint thermal transitions evaluated as, 41±1, 69±1 and 91±1 °C respectively.[173] The results indicated that increasing the electronegativity of the Y residue's 4(*R*) substituent, from H to OH to F, dramatically increased the thermal stability of the collagen mimic. Holmgren identified the strong inductive effect of the electronegative element O and more so F, to be responsible for this increased stability. It was proposed that the inductive effect increased collagens stability in at least three separate ways, one being the *gauche* effect, which controls the conformation of the pyrrolidine ring. This had not been invoked before to explain any aspect of protein structure. In an effort to provide additional evidence for this effect, crystal structures of a more conformationally felixible mimic of 4(*R*)-fluoroproline residues, ie. β-fluoroethylamides, were sought (**Figure 46**).

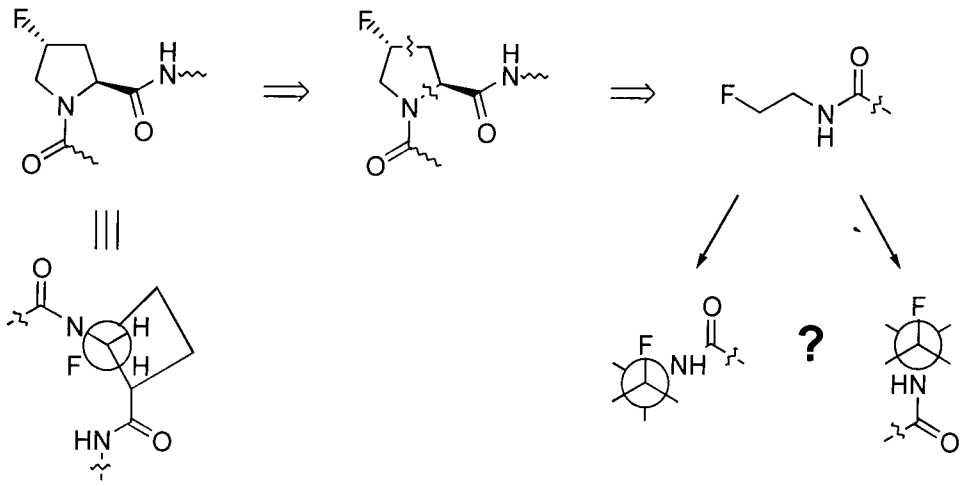

Figure 46 β-Fluoroethylamides as 4(*R*)-fluoroproline residue mimics.

3.3.2 β-Fluoroethylamides and synthesis

Conformationally felixible β-fluoroethylamides were required that would afford crystals suitable for X-ray analysis. The nitrobenzamides, *N*-(2-fluoroethyl)-3,5-dinitrobenzamide **154** and *N*-(2-fluoroethyl)-4-nitrobenzamide **155** were selected as suitable compounds, as they contain polar functionality that should afford a crystalline material. *N*-(2-Fluoroethyl)acetamide **156** was also selected as a substrate. Although anticipated to

be a liquid, if low temperature X-ray analysis was successful for this compound, information could be obtained for the core β-fluoroethylamide structural motif.

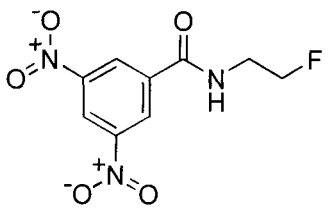

154

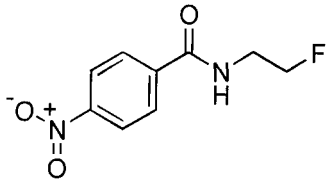

155

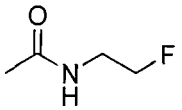

156

The amides were synthesised by reaction of their respective acid chlorides with 2-fluoroethylamine hydrochloride in the presence of base.[174] The benzamides were formed in low but unoptimised yields of about 4 and 6 % for **154** and **155** respectively. Recrystallisation of **154** from CH_2Cl_2 / $CHCl_3$ afforded a crystal which defracted well in the X-ray beam. A crystal of **155** was also found to be suitable for X-ray defraction after recrystallisation from THF. *N*-(2-Fluoroethyl)acetamide **156** was prepared from acetyl chloride and pyridine in about 20 % yield, with ~ 90 % purity.

3.3.3 Crystal structures and *ab initio* studies of β-fluoroethylamides

3.3.3.1 *N*-(2-Fluoroethyl)-3,5-dinitrobenzamide **154**

The X-ray structure of **154** clearly shows a *gauche* (63.9°) relationship between the C-F and the C-N (of the amide) bonds, **Figure 47**. The stacking plot of **154** (**Figure 48**) reveals an intermolecular H-bond of 2.346 Å, between amide groups in adjacent molecules.

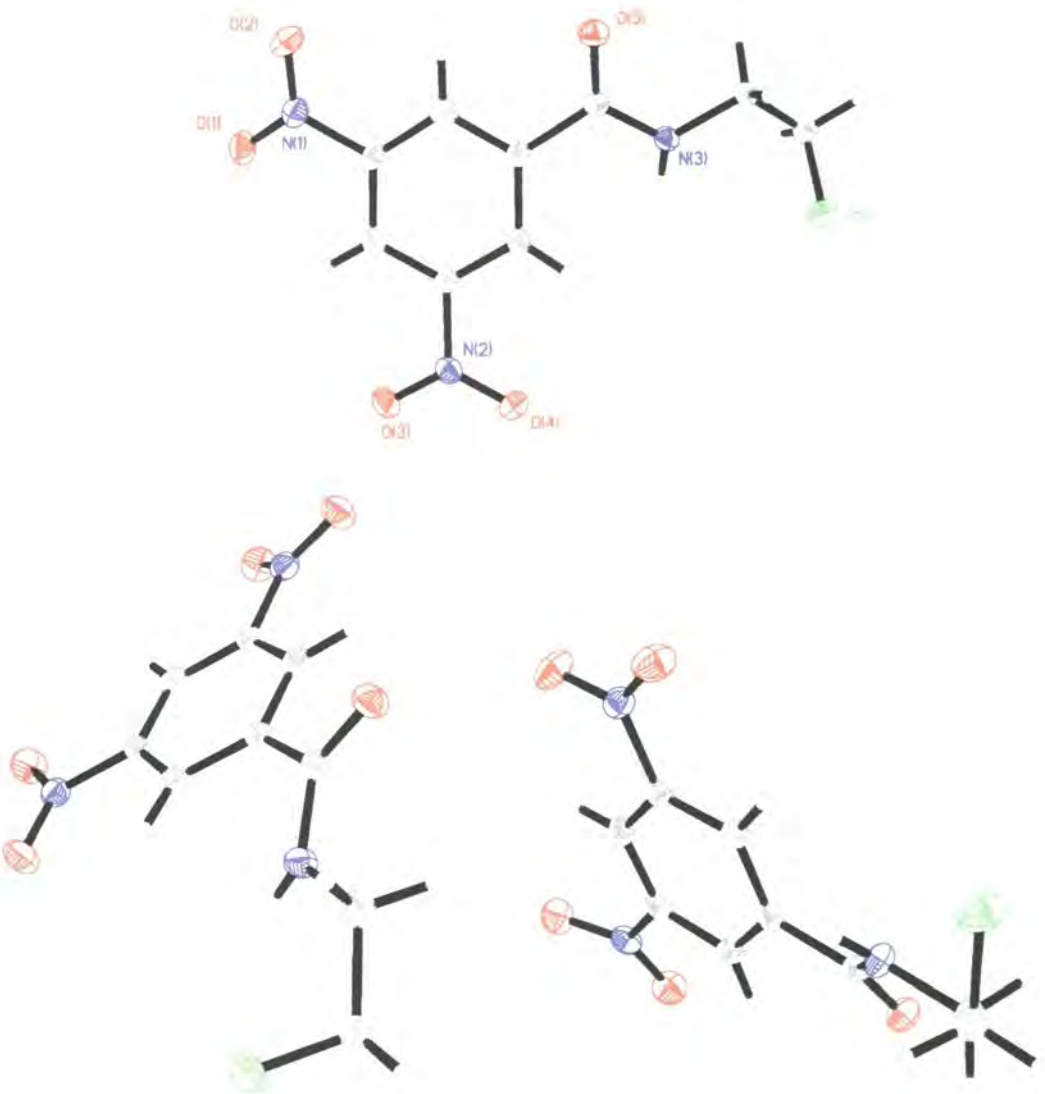

N(3)-C(8)-C(9)-F(1) = 63.9°
C(7)-F(1B) = 1.415 Å

Figure 47 50 % Probability ellipsoid plots of *N*-(2-fluoroethyl)-3,5-dinitrobenzamide **154**.

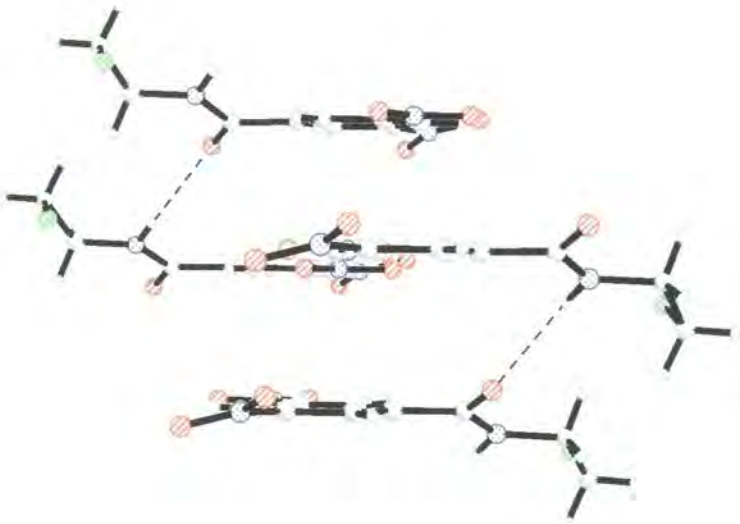

Figure 48 50 % Probability ellipsoid plot of *N*-(2-fluoroethyl)-3,5-dinitrobenzamide **154**, indicating stacking in crystal.

3.3.3.2 *N*-(2-Fluoroethyl)-4-nitrobenzamide **155**

Analysis of the diffraction data afforded a structure of **155** which indicated disorder in the fluoromethyl group (**Figure 49**). However, both of the conformers retain the *gauche* relationship between C-N and C-F bonds with dihedral angles of 57.2° and 50.6°. One of the C-F bonds has an *anti*-parallel relationship to the amide C=O bond, whilst the other C-F bond is orthogonal to this bond. Again the C-F bond lengths appear short as a consequence of this disorder.

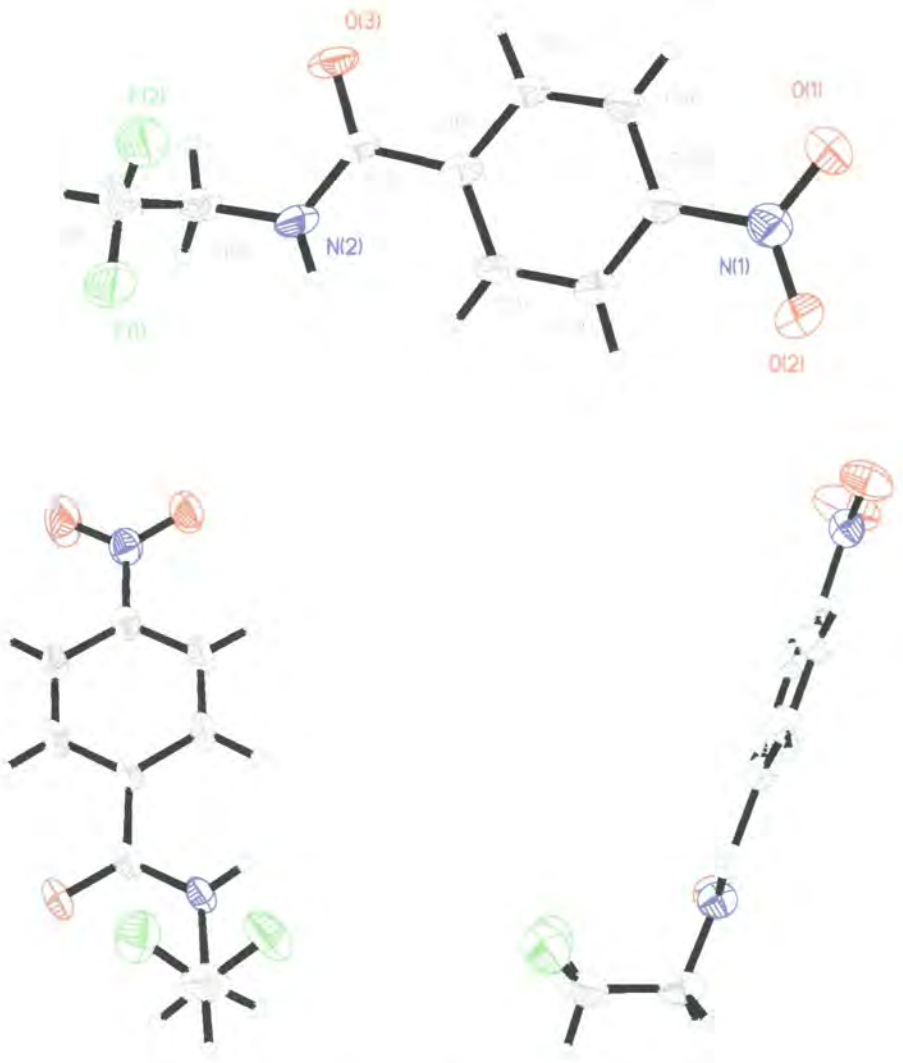

C(1)-F(1) = 1.305 Å C(7)-F(2) = 1.270 Å
N(2)-C(8)-C(9)-F(1) = 57.2° N(2)-C(9)-C(8)-F(2) = 50.6°

Figure 49 50 % Probability ellipsoid plots of *N*-(2-fluoroethyl)-4-nitrobenzamide **155**.

The stack plot of **155** shows a H-bond (2.056 Å) linking the amides of adjacent molecules. There is also a potential intermolecular bond (2.560 Å) between F(2) and H(1).

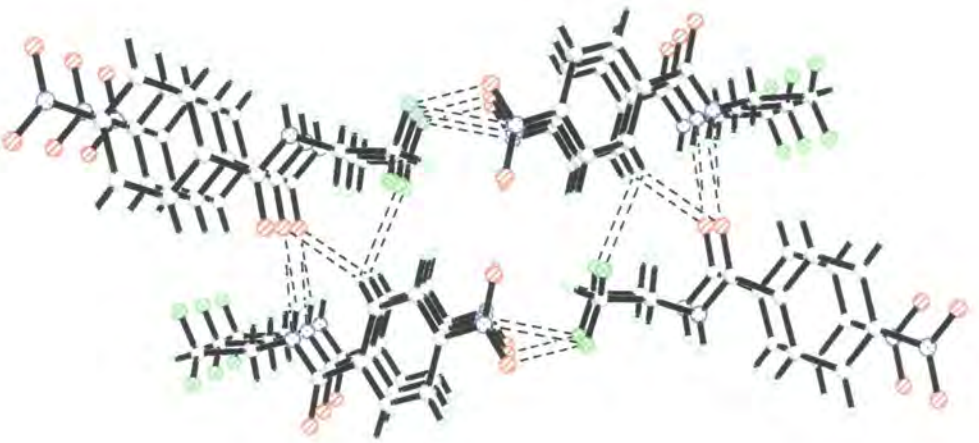

Figure 50 50 % Probability ellipsoid plot of *N*-(2-fluoroethyl)-3,5-dinitrobenzamide **153** indicating molecular stacking.

3.3.3.3 *N*-(2-Fluoroethyl)acetamide **156**

A number of attempts were made at obtaining *in situ* growth of a crystal of **156** on the diffractometer at low temperature, but none succeeded in providing a crystal of sufficient quality for X-ray analysis. Although crystallographic data was not available for this compound, *ab initio* calculations were carried out by Dr. D. Tozer on **156** as a model system for β-fluoroethylamides.[175] A high level of theory for the *ab initio* calculations yielded a *gauche* minimum conformation for **156** (**Figure 51**, a) that was 7.5 kJ mol^{-1} lower in energy than the analogous *anti* minimum conformation (**Figure 51**, b). This value is over twice that found in the classical system of 1,2-difluoroethane **153**.

Figure 51 Calculated energy difference between *gauche* (a) and *anti* conformations (b) for *N*-(2-fluoroethyl)acetamide **156**.

A complication arose when comparing the two conformers in **156** due to the orientation of the amide carbonyl. To assess the influence of the carbonyl orientation on the energy of the different conformers, additional calculations were performed on **156**, that allowed only the *gauche* to *anti* interconversion (**Figure 52**). These calculations again showed the *gauche* conformation to be lower in energy, by 9.2 kJ mol^{-1}.

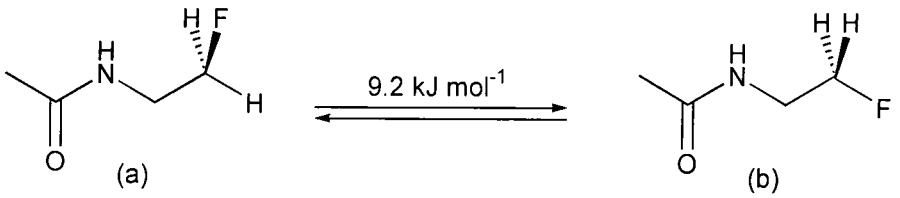

Figure 52 Calculated energy difference for the *gauche* (a) and *anti* conformations (b) of *N*-(2-fluoroethyl)acetamide **156** with the CCNH, CNCO and CCNC dihedral angles constrained at 0, 0 and 180° respectively.

3.3.4 Discussion of crystal structures

The X-ray determined solid state structures of both **154** and **155** exhibit a *gauche* relationship between the C-F and C-N bonds, with all of the N-C-C-F dihedral angles being close to 60° (±10). Structure **155** has the C-F bonds of the fluoromethyl group disordered, thereby affording two conformers. *Ab initio* calculations suggested that the conformation with the C-F bond *anti*-parallel to the C=O bond was the lower in energy.

3.3.5 Summary

Crystal structures of *N*-(2-fluoroethyl)-3,5-dinitrobenzamide **154**, and *N*-(2-fluoroethyl)-4-nitrobenzamide **155** have, for the first time, shown the fluorine amide *gauche* effect in the solid state for β-fluoroethylamides. *Ab initio* studies performed on *N*-(2-fluoroethyl)acetamide **156** have revealed a preference for the *gauche* over the *anti* conformation by 7.5 kJ mol^{-1}. It is anticipated that the *gauche* effect in β-fluoroethylamides could clearly influence the conformation of appropriate peptides, although this remains to be fully evaluated.

Chapter 4

Experimental

4.1 General Section

Optical rotations were measured on an Optical Activity Ltd AA-10 Automatic Polarimeter and are recorded in units of 10^{-1} deg cm^2 g^{-1}. Melting points were measured on a Gallenkamp variable heater and are uncorrected. NMR spectra were recorded on Bruker AC-250 (250.133 MHz) and Varian Inova (499.779 MHz), VXR-400S (399.958 MHz), Unity (299.908 MHz) and Mercury (199.991 MHz) spectrometers in deuterochloroform solution unless stated otherwise, using the deuterated solvent as a lock and residual solvent as an internal reference. IR spectra were recorded with absorption values in cm^{-1} on a Perkin-Elmer 257 Spectrometer as a neat film between NaCl plates or as a KBr disc. GCMS analysis was performed on a VG TRIO 1000 spectrometer (under EI or ammonia gas CI conditions) equipped with a HP1 capillary column (25 m long, 0.22 mm i.d., 0.2 μm film thickness) connected to a H.P. 5890 series II oven. Mass spectra were also recorded with a Micromass Autospec spectrometer (at low and high resolution, under EI or ammonia gas (or where stated methane gas) CI conditions) or with a VG ZAB spectrometer (at low resolution, under FAB conditions) or by the EPSRC National Mass Spectrometry Service Centre at Swansea, with a Finnigan MAT 900 XLT (at high resolution, under EI or ammonia gas CI) or with a Micromass Autospec spectrometer (at high resolution, under FAB conditions).

Reaction glassware was dried in an oven at 120 °C and cooled in a dry atmosphere of nitrogen immediately prior to use or heated by a hot air gun to about 200 °C under high (< 0.1 mbar) vacuum. Reaction solvents were dried and freshly distilled prior to use. Petrol refers to the fraction of petroleum ether boiling at 40-60 °C. Unless stated otherwise reactions were carried out at ambient temperature under a nitrogen atmosphere with stirring. Thin layer chromatography (tlc) was carried out on Merck, Kieselgel 60, F_{254} aluminium and glass backed plates. Visualisation of plates was achieved by use of a UV lamp at wavelengths of 254 or 366 nm or by use of permanganate, phosphomolybdic acid or iodine stains. Column chromatography was carried out over silica gel Merck, Kieselgel 60, 230-400 mesh.

4.2 Experimental Procedures

4.2.1 Experimental section for Chapter 2

4.2.1.1 Diethyl bromodifluoromethylphosphonate[80] 58

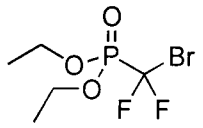

Triethyl phosphite (12.82 g, 77.2 mmol) was added to an ice cold solution of dibromodifluoromethane (17.00 g, 81.0 mmol) in Et_2O (40 ml). After 45 min the mixture was warmed to ambient temperature and 1 h later was heated under reflux for 20 h. After cooling, solvent was removed under reduced pressure and distillation (43-45 °C / 0.01 mbar, Lit.[80] 99-102 °C / 21 mbar) afforded **58** (20.05 g, 97.3 %) as a clear colourless oil. GCMS analysis indicated ≥ 99 % purity.

^{1}H NMR (400.0 MHz) δ 1.37 (6H, dt, $^3J_{H\text{-}H}$ = 7.1 Hz, $^4J_{H\text{-}P}$ = 0.5Hz, C**H**$_3$) 4.25-4.38 (4H, m, C**H**$_2$).

^{13}C NMR (100.6 MHz) δ 16.2 (2C, d, $^3J_{C\text{-}P}$ = 5.7 Hz, **C**H$_3$), 66.2 (2C, d, $^2J_{C\text{-}P}$ = 6.5 Hz, **C**H$_2$), 116.6 (1C, dt, $^1J_{C\text{-}F}$ = 328.6 Hz, $^1J_{C\text{-}P}$ = 238.0 Hz, **C**F$_2$Br).

^{19}F NMR (376.3 MHz) δ -61.5 (2F, d, $^2J_{F\text{-}P}$ = 93.4 Hz, (EtO)$_2$P(O)C**F**$_2$Br).

^{31}P NMR (161.9 MHz) δ 2.3 (1P, t, $^2J_{F\text{-}P}$ = 93.4 Hz, (EtO)$_2$**P**(O)CF$_2$Br).

IR: 2986, 1280, 1016, 877, 626.

m/z (CI): 286 ([M+NH$_4$]$^+$ 97.2 %), 284 ([M+NH$_4$]$^+$ 100 %).

4.2.1.2 [(Diethoxyphosphonyl)difluoromethyl]zinc bromide[84] 59

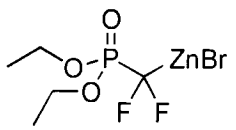

Diethyl bromodifluoromethylphosphonate **58** (25.98 g, 97.3 mmol) was added dropwise to a solution of activated zinc powder (6.50 g, 99.4 mmol) (zinc washed with 1M $HCl_{(aq)}$, distilled water then acetone and dried overnight at 120 °C) in monoglyme (50 ml) at 0 °C. After warming to ambient temperature and leaving for 20 h the solution was filtered

through a medium frit Schlenk filter to afford a monoglyme solution of **59** in 95 % yield from ^{19}F and ^{31}P NMR analysis.

^{19}F NMR (Monoglyme, 235.3 MHz) δ -128.5 (2F, d, $^{2}J_{F\text{-}P}$ = 93.0 Hz, PCF_2ZnBr).

^{31}P NMR (Monoglyme, 101.3 MHz) δ 13.4 (1P, t, $^{2}J_{F\text{-}P}$ = 93.0 Hz, PCF_2ZnBr).

4.2.1.3 Diethyl 1,1-difluorobut-3-enylphosphonate[84] 56

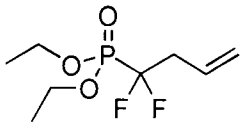

Allyl bromide (11.78 g, 96.6 mmol) was added in two equal portions to a solution of copper (I) bromide (60 mg, 0.43 mmol) and [(diethoxyphosphonyl)difluoromethyl]zinc bromide **59** (freshly prepared from **4.2.1.2**) in monoglyme. After leaving for 14 h, approximately half of the solvent was removed under reduced pressure. The remainder was washed with water (50 ml), and extracted into CH_2Cl_2 (3 × 50 ml), the organic extracts combined, dried over $MgSO_4$ and solvent removed under removed pressure. Distillation (55-57 °C / 0.08 mbar, Lit.[84] 34 °C / 0.03 mbar) with a 10 cm Vigreux column afforded **56** (17.03 g, 76.7 %) as a clear colourless oil. GCMS analysis indicated a purity ≥ 93 % with the main impurities being diethyl difluoromethylphosphonate, ~ 5.5 % and triethyl phosphate, ~ 1.5 %.

^{1}H NMR (400.0 MHz) δ 1.34 (6H, t, $^{3}J_{H\text{-}H}$ = 7.3 Hz, CH_3), 2.79 (2H, tt, $^{3}J_{H\text{-}F}$ = 19.4 Hz, $^{3}J_{H\text{-}P}$ = 6.6 Hz, $^{3}J_{H\text{-}H}$ = 6.6 Hz, CF_2CH_2CH), 4.23 (4H, p, $^{3}J_{H\text{-}P}$ = 7.3 Hz, $^{3}J_{H\text{-}H}$ = 7.3 Hz, OCH_2), 5.21-5.26 (2H, m, $CHCH_2$), 5.75-5.86 (1H, m, $CHCH_2$).

^{13}C NMR (100.6 MHz) δ 16.3 (2C, d, $^{3}J_{C\text{-}P}$ = 5.3 Hz, CH_3), 38.6 (1C, dt, $^{2}J_{C\text{-}F}$ = 21.4 Hz, $^{2}J_{C\text{-}P}$ = 15.3 Hz, CF_2CH_2), 64.3 (2C, d, $^{2}J_{C\text{-}P}$ = 6.8 Hz, OCH_2), 119.5 (1C, dt, $^{1}J_{C\text{-}F}$ = 260.4 Hz, $^{1}J_{C\text{-}P}$ = 215.4 Hz, PCF_2), 121.7 (1C, s, $CHCH_2$), 126.8 (1C, q, $^{4}J_{C\text{-}F/P}$ = 5.5 Hz, CH).

^{19}F NMR (376.3 MHz) δ -111.3 (2F, dt, $^{2}J_{F\text{-}P}$ = 107.5 Hz, $^{3}J_{H\text{-}F}$ = 19.4 Hz, $P(O)CF_2CH_2$).

^{31}P NMR (161.9 MHz) δ 10.0 (1P, t, $^{2}J_{F\text{-}P}$ = 107.5 Hz, $(EtO)_2P(O)CF_2CH_2CHCH_2$).

IR: 2988, 1646, 1261, 1014, 793.

m/z (EI): 229 ($[M+H]^+$ 5.5 %), 228 ($[M]^+$ 2.3 %), 109 ($[(EtO)(HO)P(O)]^+$ 100 %).

4.2.1.4 Diethyl 1,1-difluoro-3-oxopropylphosphonate[78] 50

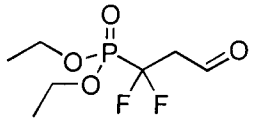

Ozone was bubbled through (at a flow rate of ~ 60 l / h) a solution of diethyl 1,1-difluoro-3-butenephosphonate **56** (8.02 g, 35.2 mmol) in CH_2Cl_2 (140 ml) and MeOH (30 ml) at -78 °C until the solution turned blue (after ~ 45 min). Nitrogen was then bubbled through at a steady rate, for 5 min after the blue colour had disappeared. Dimethyl sulphide (5.00 g, 76.8 mmol) was added, then the solution was left to warm to ambient temperature over 12 h. Solvent was removed under reduced pressure and the product distilled (75-76 °C / 0.03 mbar, Lit.[78] 80-83 °C / 0.08 mbar) to afford **50** (6.19 g, 26.9 mmol, 76.5 %, > 99 % purity from ^{31}P NMR analysis) as a clear colourless oil. This compound gradually decomposed to a dark red viscous oil on storage.

^1H NMR (400.0 MHz) δ 1.38 (6H, t, $^3J_{H-H}$ = 7.3 Hz, C**H**$_3$), 3.08 (2H, ddt, $^3J_{H-F}$ = 19.1 Hz, $^3J_{H-P}$ = 7.1 Hz, $^3J_{H-H}$ = 2.5 Hz, $CF_2C\mathbf{H}_2CHO$), 4.29 (4H, p, $^3J_{H-P}$ = 7.3 Hz, $^3J_{H-H}$ = 7.3 Hz, O**CH**$_2$), 9.79 (1H, s, $CH_2C\mathbf{H}O$).

^{13}C NMR (100.6 MHz) δ 16.3 (2C, d, $^3J_{C-P}$ = 5.3 Hz, **C**H$_3$), 47.5 (1C, dt, $^2J_{C-F}$ = 20.2 Hz, $^2J_{C-P}$ = 14.1 Hz, $CF_2\mathbf{C}H_2$), 65.0 (2C, d, $^2J_{C-P}$ = 6.8 Hz, O**C**H$_2$), 118.2 (1C, dt, $^1J_{C-F}$ = 261.8 Hz, $^1J_{C-P}$ = 218.5 Hz, P**C**F$_2$), 194.1 (1C, s, **C**HO).

^{19}F NMR (376.3 MHz) δ -118.9 (2F, dt, $^2J_{F-P}$ = 103.2 Hz, $^3J_{H-F}$ = 19.1 Hz, P(O)C**F**$_2$CH$_2$).

^{31}P NMR (161.9 MHz) δ 8.3 (1P, t, $^2J_{F-P}$ = 103.2 Hz, (EtO)$_2$**P**(O)CF$_2$CH$_2$CHO).

IR: 2988, 1733, 1253, 1011, 794.

m/z (CI): 248 ([M+NH$_4$]$^+$ 65.7 %), 231 ([M+H]$^+$ 26.9 %), 228 ([M–H$_2$]$^+$ 100 %).

4.2.1.5 Diethyl dibromofluoromethylphosphonate[86] 61

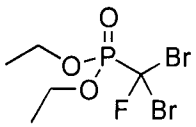

Tribromofluoromethane (6.13 g, 22.6 mmol) in THF (5 ml) was added to a THF (5 ml) solution of triethyl phosphite (3.60 g, 21.7 mmol) and the mixture was then heated under

reflux for 12 h. After cooling the solvent was removed under reduced pressure and the product distilled (58-60 °C / 0.01 mbar, Lit.[86] 170-175 °C / 27 mbar) to afford **61** (6.01 g, 84.6 %, ≥ 99 % pure from NMR analysis) as a clear colourless oil.

^{1}H NMR (400.0 MHz) δ 1.37 (6H, dt, $^3J_{H\text{-}H}$ = 7.1 Hz, $^4J_{H\text{-}P}$ = 0.9Hz, C**H**$_3$), 4.30-4.40 (4H, m, C**H**$_2$).

^{13}C NMR (62.9 MHz) δ 16.3 (2C, s, **C**H$_3$), 66.7 (2C, d, $^2J_{C\text{-}P}$ = 6.3 Hz, **C**H$_2$), 88.2 (1C, dd, $^1J_{C\text{-}F}$ = 333.9 Hz, $^1J_{C\text{-}P}$ = 202.1 Hz, P**C**FBr$_2$).

19F NMR (235.3 MHz) δ -76.7 (1F, d, $^2J_{F\text{-}P}$ = 77.4 Hz, (EtO)$_2$P(O)C**F**Br$_2$).

^{31}P NMR (161.9 MHz) δ 4.6 (1P, d, $^2J_{F\text{-}P}$ = 77.1 Hz, (EtO)$_2$(O)**P**CFBr$_2$), Lit.[86] δ 1.6.

m/z (EI): 331 ([M+H]$^+$ 10.4 %), 329 ([M+H]$^+$ 19.5 %), 327 ([M+H]$^+$ 10.4 %), 137 ([(EtO)$_2$P(O)]$^+$ 47.4 %), 109 ([(EtO)(HO)P(O)]$^+$ 54.9 %), 81 ([(HO)$_2$P(O)]$^+$ 30.5 %), 29 ([Et]$^+$ 100%).

4.2.1.6 Diethyl 1-fluorobut-3-enylphosphonate[85] 60

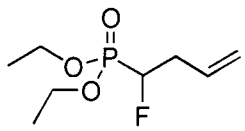

1.6 M Butyllithium in n-hexane (16 ml, 25.6 mmol) was added dropwise to a solution of diethyl dibromofluoromethylphosphonate **60** (3.67 g, 11.2 mmol) and TMSCl (1.22 g, 11.2 mmol) in THF (16 ml) at -78 °C. After 10 min at -78 °C, allyl iodide (1.90 g, 11.3 mmol) was added, then 2 h later EtOH (4.7 ml, 80.1 mmol) then 1.6 M butyl lithium in n-hexane (7.7 ml, 12.3 mmol) were added. After a further 2 h at -78 °C the reaction was allowed to warm up to 0 °C and was then quenched with sat. $NH_4Cl_{(aq)}$ (2 ml), washed with water (10 ml), and extracted into Et_2O (3 × 50 ml). The organic extracts were combined, washed with sat. $NaHCO_{3(aq)}$, dried over $MgSO_4$ and solvent removed under reduced pressure followed by kugelrohr bulb to bulb distillation (65-75 °C / 0.02 mbar, Lit.[85] 165-170 °C / 21 mbar) to afford **60** (1.87 g, 79.3 %) as a clear colourless oil. GCMS analysis gave purity as ≥ 94 % with the main impurities being diethyl fluoromethylphosphonate, ~ 2 % and triethyl phosphate, ~ 1 %.

^{1}H NMR (400.0 MHz) δ 1.33 (6H, t, $^{3}J_{H\text{-}H}$ = 7.0 Hz, C**H**$_3$), 2.55-2.70 (2H, m, CHFC**H**$_2$), 4.13-4.03 (4H, m, OC**H**$_2$), 4.63-4.80 (1H, m, C**H**F), 5.11-5.21 (2H, m, CHC**H**$_2$), 5.78-5.89 (1H, m, C**H**CH$_2$).

^{13}C NMR (100.6 MHz) δ 16.35, 16.39 (2C, d, $^{3}J_{C\text{-}P}$ = 5.5 Hz, **C**H$_3$), 34.5 (1C, d, $^{2}J_{C\text{-}F}$ = 20.6 Hz, CHF**C**H$_2$), 62.8, 63.1 (2C, d, $^{2}J_{C\text{-}P}$ = 6.6 Hz, O**C**H$_2$), 87.9 (1C, dd, $^{1}J_{C\text{-}P}$ = 182.2 Hz, $^{1}J_{C\text{-}F}$ = 169.9 Hz, P**C**HF), 118.6 (1C, s, CH**C**H$_2$), 131.9 (1C, dd, $^{4}J_{C\text{-}P}$ = 13.8 Hz, $^{4}J_{C\text{-}F}$ = 3.8 Hz, **C**HCH$_2$).

^{19}F NMR (376.3 MHz) δ -(208.2-208.7) (1F, m, (EtO)$_2$P(O)CH**F**CH$_2$CHCH$_2$).

^{31}P NMR (161.9 MHz) δ 20.6 (1P, d, $^{2}J_{F\text{-}P}$ = 75.0 Hz, (EtO)$_2$**P**(O)CHFCH$_2$CHCH$_2$), Lit.[85] δ 18.0, $^{2}J_{F\text{-}P}$ = 74.2 Hz).

m/z (CI): 228 ([M+NH$_4$]$^+$ 100 %), 211 ([M+H]$^+$ 100 %).

4.2.1.7 Diethyl but-3-enylphosphonate[176] 67

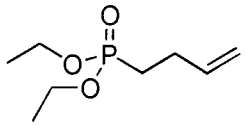

Diethyl methylphosphonate (2.21 g, 14.5 mmol) was added dropwise to a solution of lithium diisopropyl amide (prepared by addition of 1.6 M butyl lithium in n-hexane (10 ml, 16.0 mmol) to diisopropyl amine (2.35 ml, 16.8 mmol) at ambient temperature) in THF (10 ml) at -78 °C. After 15 min a solution of allyl bromide (6.3 ml, 72.2 mmol) in THF (14 ml) was added dropwise and after 5 h at -78 °C the reaction was allowed to warm to ambient temperature. The reaction was quenched with EtOH (10 drops) and sat. NH$_4$Cl$_{(aq)}$ (10 ml) and extracted into Et$_2$O (3 × 100 ml). The organic extracts were combined, dried over MgSO$_4$ and the solvent removed under reduced pressure. Distillation (62-64 °C / 0.13 mbar, Lit.[176] 70 °C / 1.3 mbar) afforded **67** as a clear colourless oil (1.45 g, 52.0 %). GCMS analysis indicated > 97 % purity, with an unknown impurity, ~ 2 %.

^{1}H NMR (250.1 MHz) δ 1.46 (6H, t, $^{3}J_{H\text{-}H}$ = 7.1 Hz, C**H**$_3$), 1.94-2.04 (2H, m, PC**H**$_2$), 2.52-2.56 (2H, m, PCH$_2$C**H**$_2$), 4.16-4.32 (4H, m, OC**H**$_2$), 5.10-5.25 (2H, m, CHC**H**$_2$), 5.90-6.06 (1H, m, C**H**CH$_2$).

^{13}C NMR (100.6 MHz) δ 16.3 (2C, d, $^{3}J_{C\text{-}P}$ = 6.0 Hz, **C**H_3), 24.9 (1C, d, $^{1}J_{C\text{-}P}$ = 140.8 Hz, P**C**H_2), 26.4 (1C, d, $^{2}J_{C\text{-}P}$ = 4.5 Hz, PCH_2**C**H_2), 61.4 (2C, d, $^{2}J_{C\text{-}P}$ = 6.5 Hz, O**C**H_2), 115.0 (1C, s, CH**C**H_2), 137.2 (1C, d, $^{3}J_{C\text{-}P}$ = 141.0 Hz, **C**H).

^{31}P NMR (161.9 MHz) δ 34.6 (1P, s, $(EtO)_2$**P**(O)$CH_2CH_2CHCH_2$).

IR: 3078, 2982, 2931, 2910, 1641, 1444, 1392, 1243, 1218, 1163, 1098, 1056, 1029, 965, 821, 791.

m/z (EI): 193 ($[M+H]^+$ 16.6 %), 192 ($[M]^+$ 14.9 %), 177 ($[M\text{-}CH_3]^+$ 2.5 %), 165 ($[M\text{-}C_2H_3]^+$ 8.9 %), 164 ($[M\text{-}C_2H_4]^+$ 10.0 %), 149 ($[M\text{-}C_2H_4,\text{-}CH_3]^+$ 8.7 %), 148 ($[M\text{-}EtO]^+$ 15.3 %), 138 ($[(EtO)_2POH]^+$ 17.4 %), 137 ($[(EtO)_2PO]^+$ 28.4 %), 136 ($[M\text{-}C_2H_4,\text{-}C_2H_4]^+$ 31.7 %), 135 ($[M\text{-}Et,\text{-}C_2H_4]^+$ 36.5 %), 111 ($[(EtO)P(OH)(OH_2)]^+$ 62.9 %), 110 ($[(EtO)P(OH)_2]^+$ 24.4 %), 109 ($[(EtO)PO(OH)]^+$ 25.6 %), 83 ($[(HO)_3PH]^+$ 33.7 %), 82 ($[(HO)_3P]^+$ 100 %), 81 ($[(HO)PO]^+$ 67.4 %), 65 ($[(HO)_2P]^+$ 44.4 %), 55 ($[CH_2CH_2CHCH_2]^+$ 92.1 %), 54 ($[CH_2CHCHCH_2]^+$ 70.5 %).

4.2.1.8 Diethyl 3-oxopropylphosphonate[91] 52

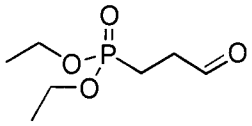

4.2.1.8.1 From diethyl but-3-enylphosphonate 67

O_3 was bubbled through (flow rate of 50 l/h) a solution of diethyl 3-butenephosphonate **67** (1.52 g, 7.9 mmol) in CH_2Cl_2 (35 ml) at -78 °C until the solution turned blue (after about 20 min). N_2 was then bubbled through till the blue colour disappeared, and dimethyl sulphide (1.17 g, 18.8 mmol) added, and the solution was left to warm to ambient temperature over 12 h. Solvent was then removed under reduced pressure and distillation (80-81.5 °C / 0.045 mbar, Lit.[91] 104-106 °C / 0.27 mbar) afforded **52** as a clear colourless oil (0.60 g, 3.1 mmol, 39.1 %, purity > 97 % from GCMS analysis).

^{1}H NMR (400.0 MHz) δ 1.27 (6H, t, $^{3}J_{H\text{-}H}$ = 7.0 Hz, C**H**$_3$), 1.99 (2H, dt, $^{2}J_{H\text{-}P}$ = 18.1 Hz, $^{3}J_{H\text{-}H}$ = 7.7 Hz, PC**H**$_2$), 2.73 (2H, dt, $^{3}J_{H\text{-}P}$ = 12.4 Hz, $^{3}J_{H\text{-}H}$ = 7.7 Hz, CH_2C**H**$_2$CHO), 3.99-4.14 (4H, m, OC**H**$_2$), 9.74 (1H, s, C**H**O).

^{13}C NMR (100.6 MHz) δ 16.2 (2C, d, $^{3}J_{C\text{-}P}$ = 6.1 Hz, **C**H_3), 17.7 (1C, d, $^{1}J_{C\text{-}P}$ = 146.0 Hz, P**C**H_2), 36.7 (1C, d, $^{2}J_{C\text{-}P}$ = 4.2 Hz, PCH_2**C**H_2), 61.7 (2C, d, $^{2}J_{C\text{-}P}$ = 6.4 Hz, O**C**H_2), 199.1 (1C, d, $^{3}J_{C\text{-}P}$ = 15.3 Hz, **C**HO).

^{31}P NMR (161.9 MHz) δ 33.8 (1P, s, $(EtO)_2$**P**(O)CH_2CH_2CHO).

IR : 2984, 2933, 2909, 2732, 2235, 1724 (C=O), 1443, 1393, 1237, 1163, 1098, 1058, 1029, 967, 828, 791, 733, 645.

m/z (CI): 195 ($[M+H]^+$ 100 %), 166 ($[M\text{-}C_2H_4]^+$ 24.4 %), 149 ($[M\text{-}EtO]^+$ 4.8 %), 139 ($[(EtO)_2POH_2]^+$ 6.8 %), %), 138 ($[(EtO)_2POH]^+$ 14.1 %), 121 ($[(EtO)_2P]^+$ 4.9 %), 111 ($[(EtO)P(OH)(OH_2)]^+$ 8.0 %).

4.2.1.8.2 From 2-(2-Diethoxyphosphonylethyl)-1,3-dioxolane 75

2-(2-Diethoxyphosphonylethyl)-1,3-dioxolane **75** (2.00 g, 8.40 mmol) was added to 0.1 M $HCl_{(aq)}$ (100 ml) and was then placed in a preheated oil bath set at 120 °C and heated under reflux for 3 h. After cooling, the organics were extracted into CH_2Cl_2 (3 × 200 ml), the organic fractions were combined, dried over $MgSO_4$ and solvent removed under reduced pressure to afford **52** (1.60 g, 8.25 mmol, 98.2 %) as a clear colourless oil. ^{31}P NMR analysis indicated > 97.5 % purity.

Analytical data was identical to that described in **4.2.1.8.1**.

4.2.1.9 Dimethyl but-3-enylphosphonate[177] 69

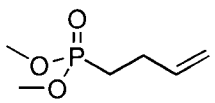

4.2.1.9.1 With Li counterion

Dimethyl methylphosphonate (1.79 g, 14.4 mmol) was added dropwise to a solution of lithium diisopropyl amide (prepared by addition of 1.6 M butyl lithium in n-hexane (10 ml, 16.0 mmol) to diisopropyl amine (2.35 ml, 16.8 mmol) at 0 °C) in THF (10 ml) at -78 °C, and after 1 h allyl bromide (3.50 g, 28.9 mmol) was added dropwise and the

reaction allowed to warm to ambient temperature after 100 min at -78 °C. The reaction was quenched with sat. $NaCl_{(aq)}$ (10 ml), then the aqueous phase was separated and extracted into Et_2O (3 × 70 ml). The organic extracts were combined, dried over $MgSO_4$ and solvent was removed under reduced pressure. Distillation (29-32 °C / 0.1 mbar) afforded **69** as a clear colourless oil (1.02 g, 43 %). GCMS analysis indicated > 98 % purity.

^{1}H NMR (400.0 MHz) δ 1.72-1.82 (2H, m, PC**H**$_2$), 2.22-2.33 (2H, m, PCH$_2$C**H**$_2$), 3.67 (6H, d, $^3J_{H\text{-}P}$ = 10.8 Hz, C**H**$_3$), 4.92-5.03 (2H, m, CHC**H**$_2$), 5.71-5.83 (1H, m, C**H**CH$_2$).
^{13}C NMR (100.6 MHz) δ 23.9 (1C, d, $^1J_{C\text{-}P}$ = 141.1 Hz, P**C**H$_2$), 26.2 (1C, d, $^2J_{C\text{-}P}$ = 4.6 Hz, PCH$_2$**C**H$_2$), 52.1 (2C, d, $^2J_{C\text{-}P}$ = 6.4 Hz, **C**H$_3$), 115.1 (1C, s, CH**C**H$_2$), 136.9 (1C, d, $^3J_{C\text{-}P}$ = 8.8 Hz, **C**H).
^{31}P NMR (161.9 MHz) δ 37.2 Lit.[177] 33.5 (1P, s, (MeO)$_2$**P**(O)CH$_2$CH$_2$CHCH$_2$).
IR: 3079, 2955, 2853, 1642, 1447, 1247, 1221, 1185, 1058, 1033, 918, 820.
m/z (EI): 164 ([M]$^+$ 21.4 %), 149 ([M-CH$_3$]$^+$ 4.0 %), 124 ([(MeO)$_3$P]$^+$ 8.5 %), 111 ([(MeO)$_2$POH$_2$]$^+$ 8.3 %), 110 ([(MeO)$_2$POH]$^+$ 100 %), 109 ([(MeO)$_2$PO]$^+$ 14.1 %), 95 ([(MeO)$_2$PH$_2$]$^+$ 12.8 %), 94 ([(MeO)$_2$PH]$^+$ 8.5 %), 93 ([(MeO)$_2$P]$^+$ 10.6 %), 80 ([(MeO)POH$_2$]$^+$ 19.3 %), 79 ([(MeO)POH]$^+$ 23.9 %).
HRMS: (EI) Calcd. for $C_6H_{13}O_3P$: 164.0602, found: 164.0603.

4.2.1.9.2 With Cu counterion

Dimethyl methylphosphonate (12.50 g, 0.10 mol) was added dropwise to a solution of 1.6 M butyl lithium in n-hexane (69 ml, 0.11 mol) in THF (70 ml) at -78 °C, and after 5 min at this temperature copper (I) iodide (21.1 g, 0.11 mol) was added. After 10 min at -78 °C the solution was allowed to warm to -35 °C, then after 1 h allyl bromide (3.50 g, 28.9 mmol) was added dropwise and the reaction allowed to warm to ambient temperature after 4 h at -35 °C. The reaction was quenched with H_2O (100 ml), the solution filtered through celite, and the cake washed with CH_2Cl_2 (3 × 100 ml). The organic washings were combined, dried over $MgSO_4$ and the solvent was removed under reduced pressure.

Distillation (42-44 °C / 0.3 mbar) afforded **69** as a clear colourless oil (15.63 g, 95.3 %). GCMS analysis indicated > 99 % purity.

Analytical data was identical to that described in **4.2.1.9.1**.

4.2.1.10 Dimethyl 3-oxopropylphosphonate[178] 70

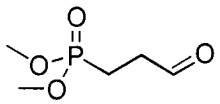

O_3 was bubbled through (flow rate of 50 l/h) a solution of dimethyl but-3-enylphosphonate **69** (0.93 g, 5.7 mmol) in CH_2Cl_2 (25 ml) at -78 °C until the solution turned blue (after about 10 min). N_2 was then bubbled through to remove ozone, and dimethyl sulphide (0.85 g, 13.7 mmol) added, then the solution was left to warm to ambient temperature over 12 h. The solvent was removed under reduced pressure and distillation (68-72 °C / 0.11 mbar, Lit.[178] 103-105 °C / 3.7 mbar) afforded **70** as a clear colourless oil (0.329 g, 2.0 mmol, 35 %). GCMS analysis indicated > 98 % purity.

^{1}H NMR (400.0 MHz) δ 2.05 (2H, dt, $^2J_{H\text{-}P}$ = 18.3 Hz, $^3J_{H\text{-}H}$ = 7.7 Hz, PC**H**$_2$), 2.76 (2H, ddt, $^3J_{H\text{-}P}$ = 14.5 Hz, $^3J_{H\text{-}H}$ = 7.7 Hz, $^3J_{H\text{-}H}$ = 0.6 Hz, CH_2C**H**$_2$CHO), 3.72 (6H, d, $^2J_{H\text{-}P}$ = 10.8 Hz, C**H**$_3$), 9.76 (1H, d, $^4J_{H\text{-}P}$ = 2.0 Hz, C**H**O).

^{13}C NMR (100.6 MHz) δ 16.2 (1C, d, $^1J_{C\text{-}P}$ = 146.1 Hz, P**C**H_2), 36.6 (1C, d, $^2J_{C\text{-}P}$ = 4.2 Hz, PCH_2**C**H_2), 52.5 (2C, d, $^2J_{C\text{-}P}$ = 6.4 Hz, **C**H_3), 198.9 (1C, d, $^3J_{C\text{-}P}$ = 14.9 Hz, **C**HO).

^{31}P NMR (161.9 MHz) δ 36.6 (1P, s, $(MeO)_2$**P**(O)CH_2CH_2CHO).

m/z (EI): 167 ($[M+H]^+$ 49.7 %), 138 ($[M\text{-}CO]^+$ 25.7 %), 135 ($[M\text{-}CH_3O]^+$ 12.8 %), 110 ($[(MeO)_2POH]^+$ 100 %), 109 ($[(MeO)_2PO]^+$ 45.1 %), 95 ($[(MeO)_2PH_2]^+$ 20.8 %), 93 ($[(MeO)_2P]^+$ 10.0 %), 80 ($[(MeO)POH_2]^+$ 24.7 %), 79 ($[(MeO)POH]^+$ 77.9 %).

4.2.1.11 2-(2-Diethoxyphosphonylethyl)-1,3-dioxane 73

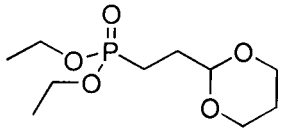

2-(2-Bromoethyl)-1,3-dioxane (0.50 g, 2.56 mmol) was added to triethyl phosphite (0.85 g, 5.12 mmol) in a flask attached to a distillation apparatus equipped with a 10 cm Vigreux column, and heated at 145 °C for 4 h, then at 165 °C for 30 min. After cooling, then stirring for 12 h at ambient temperature, distillation (96-99 °C / 0.02 mbar) afforded **73** (0.44 g, 1.76 mmol, 68.5 %) as a clear colourless oil. GCMS analysis indicated > 97 % purity, with the main impurity being diethyl ethylphosphonate, ~ 2 %.

^{1}H NMR (400.0 MHz) δ 1.29 (6H, t, $^{3}J_{H\text{-}H}$ = 7.0 Hz, C**H**$_3$), 1.31-1.34 (1H, m, OCH$_2$C**H**$_A$H$_B$), 1.77-1.89 (4H, m, PC**H**$_2$C**H**$_2$), 1.96-2.05 (1H, m, OCH$_2$CH$_A$**H**$_B$), 3.69-3.77 (2H, m, OC**H**$_A$H$_B$CH$_2$), 4.01-4.11 (6H, m, POC**H**$_2$, OCH$_A$**H**$_B$CH$_2$), 4.60 (1H, t, $^{3}J_{H\text{-}H}$ = 4.4 Hz, C**H**).

^{13}C NMR (100.6 MHz) δ 16.4 (2C, d, $^{3}J_{C\text{-}P}$ = 6.0 Hz, **C**H$_3$), 19.8 (1C, d, $^{1}J_{C\text{-}P}$ = 143.4 Hz, P**C**H$_2$), 25.6 (1C, s, CH$_2$**C**H$_2$CH$_2$), 28.1 (1C, d, $^{2}J_{C\text{-}P}$ = 4.5 Hz, PCH$_2$**C**H$_2$), 61.4 (2C, d, $^{3}J_{C\text{-}P}$ = 6.4 Hz, PO**C**H$_2$), 66.8 (2C, s, O**C**H$_2$CH$_2$**C**H$_2$O), 100.9 (1C, d, $^{3}J_{C\text{-}P}$ = 18.3 Hz, **C**H).

^{31}P NMR (161.9 MHz) δ 33.2 (1P, s, (EtO)$_2$**P**(O)CH$_2$CH$_2$CH(O(CH$_2$)$_3$O)).

IR: 2977, 2855, 1657, 1443, 1391, 1279, 1244, 1216, 1146, 1127, 1055, 1033, 964, 871.

m/z (CI): 253 ([M+1]$^+$ 100 %).

HRMS: (CI) Calcd. for (M+1) C$_{10}$H$_{22}$O$_5$P: 253.1205, found: 253.1203.

4.2.1.12 2-(2-Diethoxyphosphonylethyl)-1,3-dioxolane[179] 75

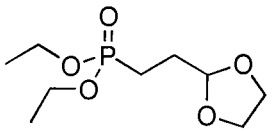

2-(2-Bromoethyl)-1,3-dioxolane (5.00 g, 27.6 mmol) was added to triethyl phosphite (9.17 g, 55.2 mmol) in a flask attached to a distillation apparatus equipped with a 10 cm Vigreux column, and heated at 145 °C for 3 h, then at 165 °C for 1 h. Distillation

(90.5-93.5 °C / 0.01 mbar) afforded **75** (5.61 g, 23.6 mmol, 85.4 %) as a clear colourless oil. GCMS analysis indicated > 99 % purity.

^{1}H NMR (400.0 MHz) δ 1.31 (6H, t, d, $^{3}J_{H\text{-}H}$ = 7.0 Hz, C**H**$_3$), 1.79-1.98 (4H, m, PC**H**$_2$C**H**$_2$), 3.83-3.97 (4H, m, OC**H**$_2$C**H**$_2$O), 4.03-4.13 (4H, m, POC**H**$_2$), 4.93 (1H, t, $^{3}J_{H\text{-}H}$ = 4.0 Hz, C**H**).

^{13}C NMR (100.6 MHz) δ 16.4 (2C, d, $^{3}J_{C\text{-}P}$ = 6.1 Hz, **C**H$_3$), 19.5 (1C, d, $^{1}J_{C\text{-}P}$ = 144.2 Hz, P**C**H$_2$), 26.9 (1C, d, $^{2}J_{C\text{-}P}$ = 4.2 Hz, PCH$_2$**C**H$_2$), 61.5 (2C, d, $^{2}J_{C\text{-}P}$ = 6.4 Hz, PO**C**H$_2$), 65.1 (2C, s, O**C**H$_2$**C**H$_2$O), 103.3 (1C, d, $^{3}J_{C\text{-}P}$ = 19.5 Hz, **C**H).

^{31}P NMR (161.9 MHz) δ 33.1 (1P, s, (EtO)$_2$**P**(O)CH$_2$CH$_2$CH(OCH$_2$)$_2$).

IR: 2983, 2938, 2898, 1641, 1443, 1393, 1244, 1140, 1031, 963, 867, 828, 789.

m/z (CI): 239 ([M+1]$^+$ 100 %), 193 ([M-EtO]$^+$ 4.2 %).

HRMS: (CI) Calcd. for (M+1) $C_9H_{20}O_5P$: 239.1048, found: 239.1059.

4.2.1.13 Diethyl (*E*)-5-oxohex-3-enylphosphonate 76

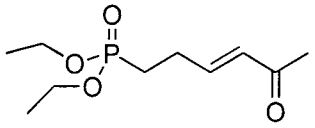

Diethyl 3-oxopropylphosphonate **52** (4.29 g, 22.1 mmol) was added to 1-triphenylphosphoranylidene-2-propanone (7.04 g, 22.1 mmol) in THF (130 ml) and the mixture heated under reflux for 16 h. After cooling, the solvent was removed under reduced pressure and the residue throughly mixed with petrol (4 × 100 ml). The petrol washings were combined, and then the solvent was removed under reduced pressure and kugelrohr bulb to bulb distillation (125-155 °C / 0.1 mbar) afforded **76** (3.66 g, 15.6 mmol, 71 %) as a clear colourless oil. GCMS analysis indicated > 99 % purity.

^{1}H NMR (400.0 MHz) δ 1.31 (6H, t, $^{3}J_{H\text{-}H}$ = 6.8 Hz, POCH$_2$C**H**$_3$), 1.82-1.92 (2H, m, PC**H**$_2$), 2.24 (3H, s, COC**H**$_3$), 2.46-2.56 (2H, m, PCH$_2$C**H**$_2$), 4.04-4.15 (4H, m, POC**H**$_2$), 6.09 (1H, d, $^{3}J_{H\text{-}H}$ = 16.0 Hz, C**H**COCH$_3$), 6.80 (1H, dt, $^{3}J_{H\text{-}H}$ = 16.0 Hz, $^{3}J_{H\text{-}H}$ = 6.6 Hz, CH$_2$C**H**).

^{13}C NMR (100.6 MHz) δ 16.4 (2C, d, $^{3}J_{C\text{-}P}$ = 5.7 Hz, $POCH_2\mathbf{C}H_3$), 24.2 (1C, d, $^{1}J_{C\text{-}P}$ = 142.6 Hz, $P\mathbf{C}H_2$), 25.4 (1C, d, $^{2}J_{C\text{-}P}$ = 4.2 Hz, $PCH_2\mathbf{C}H_2$), 27.0 (1C, s, $CO\mathbf{C}H_3$), 61.7 (2C, d, $^{2}J_{C\text{-}P}$ = 6.5 Hz, $PO\mathbf{C}H_2$), 131.4 (1C, s, $\mathbf{C}HCOCH_3$), 145.9 (1C, d, $^{3}J_{C\text{-}P}$ = 16.0 Hz, $CH_2\mathbf{C}H$), 198.3 (1C, s, $CH\mathbf{C}OCH_3$).

^{31}P NMR (161.9 MHz) δ 31.1 (1P, s, $(EtO)_2\mathbf{P}(O)CH_2CH_2CHCHCOCH_3$).

IR: 2983, 2931, 2909, 1697, 1675, 1629, 1364, 1243, 1163, 1097, 1055, 1029, 965, 732.

m/z (CI): 254 ($[M+NH_4+2H]^+$ 10.1 %), 253 ($[M+NH_4+H]^+$ 6.7 %), 252 ($[M+NH_4]^+$ 86.7 %), 238 ($[M+4H]^+$ 14.9 %), 237 ($[M+3H]^+$ 100 %), 236 ($[M+2H]^+$ 35.3 %), 235 ($[M+H]^+$ 100 %), 221 ($[M+2H-CH_3]^+$ 13.1 %), 219 ($[M-CH_3]^+$ 8.7 %), 193 ($[M+2H-COCH_3]^+$ 10.4 %), 191 ($[M-COCH_3]^+$ 17.2 %).

HRMS: (CI) Calcd. for (M+1) $C_{10}H_{20}O_4P$: 235.1099, found: 235.1102.

4.2.1.14 3-Chloro-2-oxopropyltriphenylphosphonium chloride[106] 79b

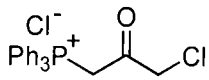

1,3-Dichloropropan-2-one (4.84 g, 38.1 mmol) was added dropwise to a solution of triphenylphosphine (10.0 g, 38.1 mmol) in THF (40 ml). After heating under reflux for 4 h (precipitation occuring after 15 min) the solvent was removed under reduced pressure. The solid was then precipated from a refluxing MeOH solution with addition of EtOAc. The product was filtered and dried under high vacuum to afford **79b** (12.44 g, 32.0 mmol, 84 %) as a cream white powder.

^{1}H NMR (299.9 MHz) (CD_3OD) δ 4.89 (2H, s, $PC\mathbf{H}_2$), 4.53 (2H, s, $C\mathbf{H}_2Cl$), 7.70-7.95 (15H, m, Ph).

^{31}P NMR (81.0 MHz) (CD_3OH) δ 21.4 (1P, s, $Ph_3\mathbf{P}^+CH_2COCH_2Cl$ Cl^-).

4.2.1.15 3-Chloro-2-oxopropylidenetriphenylphosphorane[106] 80

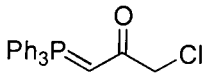

A solution of Na_2CO_3 (1.68 g, 15.8 mmol) in H_2O (10 ml) was added rapidly to a vigorously stirred solution of (1-chloroacetonyl)-triphenylphosphonium chloride **79b** (12.44 g, 32.0 mmol) in MeOH (20 ml). The reaction was then diluted with H_2O (25 ml) and stirred for 30 min. After filtering the mixture, the solid was washed with H_2O, then dried under high vacuum to afford **80** (9.01 g, 25.5 mmol, 80 %) as a white powder (mp dec. 170 °C, Lit.[106] mp 179 °C).

^{1}H NMR (400.0 MHz) δ 4.01 (2H, s, C**H**$_2$Cl), 4.28 (1H, d, $^2J_{H\text{-}P}$ = 24.0 Hz, PC**H**), 7.42-7.71 (15H, m, Ph).

^{13}C NMR (100.6 MHz) δ 8.3 (1C, d, $^3J_{C\text{-}P}$ = 16.1 Hz, **C**H$_2$Cl), 51.4 (1C, d, $^1J_{C\text{-}P}$ = 109.8 Hz, P**C**H), 126.1 (3C, d, $^1J_{C\text{-}P}$ = 91.6 Hz, αPh), 128.9 (6C, d, $^3J_{C\text{-}P}$ = 12.2 Hz, γPh), 132.3 (3C, d, $^4J_{C\text{-}P}$ = 3.0 Hz, δPh), 133.0 (6C, d, $^2J_{C\text{-}P}$ = 10.4 Hz, βPh), 185.1 (1C, d, $^2J_{C\text{-}P}$ = 4.6 Hz, **C**O).

^{31}P NMR (161.9 MHz) δ 17.3 (1P, d, $^4J_{F\text{-}P}$ = 7.1 Hz, Ph$_3$**P**CHCOCH$_2$Cl).

IR: (KBr) 3048, 3015, 2958, 2927, 2855, 1575, 1551, 1481, 1435, 1395, 1107, 953, 861, 751, 719, 692, 520, 509.

m/z (EI): 354 ([M]$^+$ 1.6 %), 352 ([M]$^+$ 4.5 %), 304 ([M-CHCl]$^+$ 2.7 %), 303 ([M-CH$_2$Cl]$^+$ 100 %), 278 ([Ph$_3$PO]$^+$ 1.8 %), 262 ([Ph$_3$P]$^+$ 4.1 %), 108 ([PhP]$^+$ 6.3 %), 77 ([Ph]$^+$ 10.6 %), 51 ([C$_4$H$_3$]$^+$ 6.7 %).

4.2.1.16 1-Chloro-3-fluoropropan-2-ol[101] 78

Epichlorohydrin (9.57 g, 0.103 mol) was added to triethylamine trihydrofluoride (24.9 g, 0.154 mol) and stirred at 100 °C for 4 h. After cooling, H_2O (50 ml) was added and the mixture washed with Et_2O (3 × 125 ml). The organic washings were combined, neutralised with $NaHCO_3$, washed with H_2O (40 ml) then dried over $MgSO_4$ and the solvent removed under reduced pressure. Distillation (49-56 °C / 15 mmHg,

Lit.[101] 62 °C / 15 mmHg) with a 10 cm Vigreux column afforded **78** (6.05 g, 0.054 mol, 52.0 %) as a clear colourless oil. GCMS analysis indicated > 99 % purity.

^{1}H NMR (400.0 MHz) δ 2.62 (1H, s, CHO**H**), 3.60-3.69 (2H, m, C**H**$_2$Cl), 4.02-4.12 (1H, m, C**H**OH), 4.51 (2H, dd, $^2J_{H\text{-}F}$ = 47.0, $^3J_{H\text{-}F}$ = 4.6 Hz, C**H**$_2$F).
^{13}C NMR (100.6 MHz) δ 44.7 (1C, d, $^3J_{C\text{-}F}$ = 6.4 Hz,**C**H$_2$Cl), 69.9 (1C, d, $^2J_{C\text{-}F}$ = 20.6 Hz, **C**HOH), 83.3 (1C, d, $^1J_{C\text{-}F}$ = 170.6 Hz, **C**H$_2$F).
^{19}F NMR (376.3 MHz) δ -232.5 (1F, dt, $^2J_{H\text{-}F}$ = 47.0, $^3J_{H\text{-}F}$ = 17.4 Hz, **C**H$_2$F).
IR: 3386 (br, OH), 2964, 2904, 1704, 1433, 1233, 1112, 1093, 1080, 1021, 944, 919, 753, 629.
m/z (EI): 115 ([M+H]$^+$ 1.2 %), 113 ([M+H]$^+$ 4.0 %), 81 ([HCOHCH$_2$Cl]$^+$ 13.3 %), 79 ([HCOHCH$_2$Cl]$^+$ 42.5 %), 63 ([HCOHCH$_2$F]$^+$ 100 %), 49 ([CH$_2$Cl]$^+$ 52.0 %), 43 ([HCOCH$_2$]$^+$ 89.9 %), 33 ([CH$_2$F]$^+$ 51.4 %).

4.2.1.17 1-Chloro-3-fluoropropan-2-one[105] 77

50 % $H_2SO_{4(aq)}$ (26 ml) was added dropwise over 1 h to a vigorously stirred solution of 1-chloro-3-fluoropropan-2-ol **78** (6.00 g, 53.3 mmol), $K_2Cr_2O_7$ (15.83 g, 53.8 mmol) and TBAB (0.867 g, 2.69 mmol) in CH_2Cl_2 (50 ml) and H_2O (50 ml). After 5 d $K_2Cr_2O_7$ (10.00 g, 34.0 mmol) was added and 1 d later ^{19}F NMR indicated that was present comprising ~ 25 % of the product. The organic layer was separated and 40 % $Na_2S_2O_{5(aq)}$ (50 ml) added. The aqueous layer was acidified with 1M $H_2SO_{4(aq)}$ until effervescence ceased, and it was then continuously extracted into Et_2O for 2 d. The organic layer was then separated, the solvent removed under reduced pressure and distillation (35-40 °C / 15 mmHg, Lit.[105] 52 °C / 20 mmHg) afforded **77** (0.80 g, 7.24 mmol, 13.6 %) as a clear colourless oil. ^{19}F NMR analysis indicated > 99 % purity.

^{1}H NMR (400.0 MHz) δ 4.34 (2H, d, $^4J_{H\text{-}F}$ = 2.0 Hz, C**H**$_2$Cl), 5.07 (2H, d, $^2J_{H\text{-}F}$ = 47.1 Hz, C**H**$_2$F).
^{13}C NMR (100.6 MHz) δ 45.8 (1C, s, **C**H$_2$Cl), 84.2 (1C, d, $^1J_{C\text{-}F}$ = 184.2 Hz, **C**H$_2$F), 198.1 (1C, d, $^2J_{C\text{-}F}$ = 20.6 Hz, **C**O).

^{19}F NMR (376.3 MHz) δ -232.0 (1F, tt, $^{2}J_{H\text{-}F}$ = 47.1, $^{4}J_{H\text{-}F}$ = 2.1 Hz, **C**H_2F).

m/z (EI): 112 ([M+2]$^+$ 4.60 %), 110 ([M]$^+$ 14.3 %), 79 ([$COCH_2Cl$]$^+$ 10.9 %), 77 ([$COCH_2Cl$]$^+$ 33.0 %), 61 ([$COCH_2F$]$^+$ 53.1 %), 51 ([CH_2Cl]$^+$ 25.2 %), 49 ([CH_2Cl]$^+$ 84.8 %), 42 ([$COCH_2$]$^+$ 100 %), 33 ([CH_2F]$^+$ 89.7 %).

4.2.1.18 3-Fluoro-2-oxopropyltriphenylphosphonium chloride[100] 77b

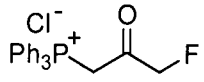

1-Chloro-3-fluoropropan-2-one (0.80 g, 7.24 mmol) was added dropwise to a solution of triphenylphosphine (1.90 g, 7.25 mmol) in THF (15 ml). After heating under reflux for 5 h (precipitation occuring after 15 min) the solvent was removed under reduced pressure. The solid was then washed with EtOAc and dried under high vacuum to afford **77b** (1.88 g, 5.04 mmol, 69.6 %) as a white powder.

^{1}H NMR (200.0 MHz) (CD_3OD) δ 4.88 (2H, s, PC**H**$_2$), 5.09 (2H, d, $^{2}J_{H\text{-}F}$ = 46.5 Hz, C**H**$_2$F), 7.65-7.95 (15H, m, Ph).

^{19}F NMR (188.2 MHz) (CD_3OD) δ -227.8 (1F, dt, $^{2}J_{H\text{-}F}$ = 46.5 Hz, $^{4}J_{F\text{-}P}$ = 6.7 Hz, CH_2**F**).

4.2.1.19 3-Fluoro-2-oxopropylidenetriphenylphosphorane[100] 49

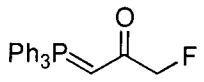

A solution of Na_2CO_3 (280 mg, 2.7 mmol) in H_2O (1.6 ml) was added rapidly to a vigorously stirred solution of (1-fluoroacetonyl)-triphenylphosphonium chloride **77b** (1.88 g, 5.04 mmol) in MeOH (2.5 ml). The reaction was then diluted with H_2O (12 ml) and stirred for 30 min. After filtering the mixture, the solid was washed with H_2O, then dried under high vacuum to afford **49** (1.56 g, 4.65 mmol, 92.3 %) as a white powder (dec.).

^{1}H NMR (400.0 MHz) δ 4.15 (1H, d, $^2J_{H\text{-}P}$ = 24.8 Hz, PC**H**), 4.75 (2H, d, $^2J_{H\text{-}F}$ = 48.4 Hz, C**H**$_2$F), 7.45-7.70 (15H, m, Ph).

^{13}C NMR (100.6 MHz) δ 49.4 (1C, d, $^1J_{C\text{-}P}$ = 110.3 Hz, P**C**H), 84.6 (1C, dd, $^1J_{C\text{-}F}$ = 185.2 Hz, $^3J_{C\text{-}P}$ = 13.5 Hz, **C**H$_2$F), 126.3 (3C, d, $^1J_{C\text{-}P}$ = 91.2 Hz, αPh), 128.9 (6C, d, $^3J_{C\text{-}P}$ = 12.6 Hz, γPh), 132.3 (3C, d, $^4J_{C\text{-}P}$ = 3.0 Hz, δPh), 133.1 (6C, d, $^2J_{C\text{-}P}$ = 10.4 Hz, βPh), 187.1 (1C, dd, $^2J_{C\text{-}F}$ = 17.4 Hz, $^2J_{C\text{-}P}$ = 3.6 Hz, **C**O).

^{19}F NMR (376.3 MHz) δ -216.5 (dt, $^2J_{H\text{-}F}$ = 48.4 Hz, $^4J_{F\text{-}P}$ = 6.3 Hz, CH$_2$**F**), Lit.[100] -216.7.

^{31}P NMR (161.9 MHz) δ 17.2 (1P, d, $^4J_{F\text{-}P}$ = 7.1 Hz, Ph$_3$**P**CHCOCH$_2$F).

m/z (CI): 337 ([M+H]$^+$ 31.8 %), 336 ([M]$^+$ 25.3 %), 304 ([M-CHF]$^+$ 45.0 %), 303 ([M-CH$_2$F]$^+$ 100 %), 278 ([Ph$_3$PO]$^+$ 12.4 %), 262 ([Ph$_3$P]$^+$ 12.6 %), 108 ([PhP]$^+$ 7.4 %), 77 ([Ph]$^+$ 14.2 %), 51 ([C$_4$H$_3$]$^+$ 4.1 %).

4.2.1.20 Diethyl 3-ethoxy-5-oxohexylphosphonate 83

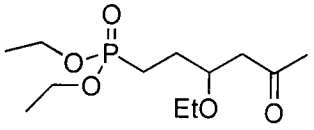

Diethyl (*E*)-5-oxohex-3-enylphosphonate **76** (106 mg, 0.45 mmol) was added to a solution of PTSA.H$_2$O (10 mg, 0.05 mmol) and triethylorthoformate (180 mg, 1.21 mmol) in EtOH (0.1 ml). After 30 min the solvent was removed under reduced pressure, H$_2$O (10 ml) was added and the mixture was extracted into CH$_2$Cl$_2$ (3 × 50 ml). The organic extracts were combined, dried over MgSO$_4$ and solvent was removed under reduced pressure. The residue was purified over silica gel (CH$_2$Cl$_2$ / EtOAc / IPA, 3:1:0.2, R$_f$= 0.28 for **83**, KMnO$_4$ stain as visualiser) affording **83** (91 mg, 0.32 mmol, 71.8 %) as a clear colourless oil. GC analysis indicated > 95 % purity.

^{1}H NMR (400.0 MHz) δ 1.11 (3H, t, $^3J_{H\text{-}H}$ = 7.0 Hz, CHOCH$_2$C**H**$_3$), 1.28 (6H, t, $^3J_{H\text{-}H}$ = 7.0 Hz, POCH$_2$C**H**$_3$), 1.63-1.89 (4H, m, PC**H**$_2$C**H**$_2$), 2.14 (3H, s, COC**H**$_3$), 2.40 (1H, dd, $^3J_{H\text{-}H}$ = 5.2 Hz, $^3J_{H\text{-}H}$ = 16.0 Hz, C**H**$_A$H$_B$COCH$_3$), 2.67 (1H, dd, $^3J_{H\text{-}H}$ = 7.2 Hz, $^3J_{H\text{-}H}$ = 16.0 Hz, CH$_A$**H**$_B$COCH$_3$), 3.44 (2H, q, $^3J_{H\text{-}H}$ = 7.1 Hz, CHOC**H**$_2$CH$_3$), 3.74-3.81 (1H, m, C**H**OCH$_2$CH$_3$), 4.00-4.11 (4H, m, POC**H**$_2$CH$_3$).

^{13}C NMR (100.6 MHz) δ 15.3 (1C, s, $CHOCH_2\mathbf{C}H_3$), 16.4 (2C, d, $^3J_{C\text{-}P}$ = 5.7 Hz, $POCH_2\mathbf{C}H_3$), 21.1 (1C, d, $^1J_{C\text{-}P}$ = 142.6 Hz, $P\mathbf{C}H_2$), 30.0 (1C, d, $^2J_{C\text{-}P}$ = 4.6 Hz, $PCH_2\mathbf{C}H_2$), 31.0 (1C, s, $CO\mathbf{C}H_3$), 47.9 (1C, s, $\mathbf{C}H_2COCH_3$), 61.4 (2C, d, $^2J_{C\text{-}P}$ = 6.4 Hz, $PO\mathbf{C}H_2$), 64.8 (1C, s, $CHO\mathbf{C}H_2CH_3$), 74.7 (1C, d, $^3J_{C\text{-}P}$ = 17.5 Hz, $\mathbf{C}HOCH_2CH_3$), 207.1 (1C, s, $CH_2\mathbf{C}OCH_3$).

^{31}P NMR (161.9 MHz) δ 33.3 (1P, s, $(EtO)_2\mathbf{P}(O)CH_2CH_2CH(OEt)CH_2COCH_3$).

IR: 2977, 2931, 2905, 2875, 1713, 1443, 1391, 1369, 1245, 1163, 1097, 1055, 1027, 963, 832, 787.

m/z (CI): 281 ($[M+H]^+$ 29.0 %), 252 ($[M\text{-}C_2H_4]^+$ 17.5 %), 237 ($[M\text{-}C_2H_3O]^+$ 30.4 %), 236 ($[M\text{-}C_2H_4O]^+$ 7.1 %), 235 ($[M\text{-}C_2H_5O]^+$ 100 %).

HRMS: (CI) Calcd. for (M+1) $C_{12}H_{26}O_5P$: 281.1518, found: 281.1515.

4.2.1.21 (*E*)-2-(4-Diethoxyphosphonylbut-1-enyl)-2-methyl-1,3-dioxolane 84

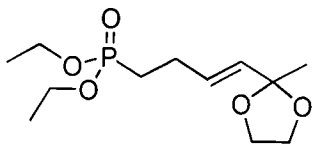

1,2-Bis[(trimethylsilyl)oxy]ethane (1.27 g, 6.15 mmol) was added to trimethylsilyl trifluoromethanesulphonate (~ 30 mg, ~ 0.13 mmol) in CH_2Cl_2 (5 ml) at -78 °C followed by diethyl (*E*)-5-oxohex-3-enylphosphonate **76** (1.06 g, 4.55 mmol). The solution was then stirred for 28 h at -60 °C. The reaction was quenched with dry pyridine (0.1 ml) and sat. $NaHCO_{3(aq)}$ (10 ml), and was then extracted into CH_2Cl_2 (3 × 20 ml). The organic extracts were combined, dried over $MgSO_4$ then solvent removed under reduced pressure. The residue was purified over silica gel (IPA / Et_2O, 1:12, $KMnO_4$ stain as visualiser) affording **84** (0.70 g, 2.51 mmol, 55 %) as a clear colourless oil. ^{31}P NMR analysis indicated ~ 90 % pure, with the major impurity being 2-(2-diethoxyphosphonylethyl)-1,3-dioxolane **75**, ~ 8 %.

^1H NMR (400.0 MHz) δ 1.29 (6H, t, $^3J_{H\text{-}H}$ = 7.2 Hz, $POCH_2C\mathbf{H}_3$), 1.41 (3H, s, $CO(OCH_2)_2C\mathbf{H}_3$), 1.73-1.83 (2H, m, $PC\mathbf{H}_2$), 2.26-2.35 (2H, m, $PCH_2C\mathbf{H}_2$), 3.82-3.94 (4H, m, $OC\mathbf{H}_2C\mathbf{H}_2O$), 4.01-4.11 (4H, m, $POC\mathbf{H}_2$), 5.44 (1H, d, $^3J_{H\text{-}H}$ = 15.6 Hz, $C\mathbf{H}C(OCH_2)_2CH_3$), 5.81 (1H, dt, $^3J_{H\text{-}H}$ = 15.6 Hz, $^3J_{H\text{-}H}$ = 6.6 Hz, $PCH_2CH_2C\mathbf{H}$).

^{13}C NMR (100.6 MHz) δ 16.4 (2C, d, $^{3}J_{C\text{-}P}$ = 6.1 Hz, $POCH_2\mathbf{C}H_3$), 24.7 (1C, d, $^{2}J_{C\text{-}P}$ = 4.6 Hz, $PCH_2\mathbf{C}H_2$), 24.8 (1C, s, $CO\mathbf{C}H_3$), 25.1 (1C, d, $^{1}J_{C\text{-}P}$ = 141.2 Hz, $P\mathbf{C}H_2$), 61.5 (2C, d, $^{2}J_{C\text{-}P}$ = 6.4 Hz, $PO\mathbf{C}H_2$), 64.4 (2C, s, $O\mathbf{C}H_2\mathbf{C}H_2O$), 107.1 (1C, s, $CH\mathbf{C}(OCH_2)_2CH_3$), 129.6 (1C, d, $^{3}J_{C\text{-}P}$ = 17.9 Hz, $PCH_2CH_2\mathbf{C}H$), 131.0 (1C, d, $^{4}J_{C\text{-}P}$ = 0.7 Hz, $\mathbf{C}HC(OCH_2)_2CH_3$).

^{31}P NMR (161.9 MHz) δ 32.3 (1P, s, $(EtO)_2\mathbf{P}(O)CH_2CH_2CHCHC(OCH_2)_2CH_3$).

IR: 2984, 2933, 2904, 1671, 1443, 1392, 1372, 1242, 1213, 1163, 1097, 1053, 1032, 966, 863.

m/z (EI): 279 ($[M+H]^+$ 0.6 %), 278 ($[M]^+$ 0.8 %), 264 ($[M\text{-}CH_2]^+$ 6.4 %), 263 ($[M\text{-}CH_3]^+$ 54.5 %), 235 ($[M\text{-}C_2H_5O]^+$ 9.2 %), 191 ($[M\text{-}C(OCH_2)_2CH_3]^+$ 9.0 %), 125 ($[M\text{-}CH_3\text{-}(EtO)_2POH]^+$ 87.8 %), 87 ($[C(OCH_2)_2CH_3]^+$ 100 %), 43 ($[C_2H_5O]^+$ 50.2 %).

HRMS: (CI) Calcd. for (M+1) $C_{12}H_{24}O_5P$: 279.1361, found: 279.1357.

4.2.1.22 *Threo*-2-(1(*S*),2(*R*)-4-Diethoxyphosphonyl-1,2-dihydroxybutyl)-2-methyl-1,3-dioxolane 90

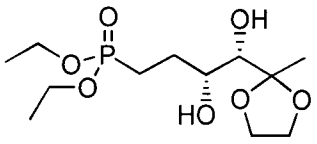

(*E*)-2-Methyl-2-(4-diethoxyphosphonylbut-3-enyl)-1,3-dioxolane **84** (297 mg, 1.07 mmol) was added to a biphasic mixture of AD mix-β (1.51 g) and methanesulphonamide (102 mg, 1.08 mmol) in *tert*-butanol (5.4 ml) and H_2O (5.4 ml). After vigorous stirring for 22 h, the reaction was quenched with Na_2SO_3 (1.62 g, 11.4 mmol in H_2O (10 ml)) and extracted into CH_2Cl_2 (3 × 30 ml). The organic extracts were combined, washed with 1M KOH (10 ml), dried over $MgSO_4$ and then solvent was removed under reduced pressure. Purification of the residue over silica gel (MeOH / Et_2O, 1:6, $KMnO_4$ stain as visualiser) afforded **90** (61.5 mg, 0.20 mmol, 18.5 %) as a clear colourless oil ($[\alpha]_D^{20}$ +10.5 ° (c. 1.0, $CHCl_3$)). ^{31}P NMR analysis indicated > 95 % purity.

^{1}H NMR (299.9 MHz) δ 1.32 (6H, t, $^{3}J_{H\text{-}H}$ = 7.0 Hz, $POCH_2C\mathbf{H}_3$), 1.36 (3H, s, $CO(OCH_2)_2C\mathbf{H}_3$), 1.71-2.07 (4H, m, $PC\mathbf{H}_2C\mathbf{H}_2$), 2.77 (1H, d, $^{2}J_{H\text{-}H}$ = 6.9 Hz, $CH(O\mathbf{H})COCH_3$) 3.22 (1H, d, $^{2}J_{H\text{-}H}$ = 3.0 Hz, $PCH_2CH_2CH(O\mathbf{H})$), 3.40 (1H, dd, $^{2}J_{H\text{-}H}$ =

6.9 Hz, $^{3}J_{H\text{-}H}$ = 1.5 Hz, C**H**(OH)$COCH_3$), 3.87-3.94 (1H, m, PCH_2CH_2C**H**(OH)), 3.99-4.05 (4H, m, OC**H**$_2C$**H**$_2O$), 4.05-4.17 (4H, m, POC**H**$_2$).

^{13}C NMR (75.4 MHz) δ 16.4 (2C, d, $^{3}J_{C\text{-}P}$ = 6.1 Hz, $POCH_2$**C**H_3), 20.8 (1C, s, $C(OCH_2)_2$**C**H_3), 21.9 (1C, d, $^{1}J_{C\text{-}P}$ = 142.1 Hz, P**C**H_2), 27.2 (1C, d, $^{2}J_{C\text{-}P}$ = 4.5 Hz, PCH_2**C**H_2), 61.6 (2C, d, $^{2}J_{C\text{-}P}$ = 6.4 Hz, PO**C**H_2), 65.06, 65.13 (2C, s, OCH_2**C**H_2O), 69.5 (1C, d, $^{3}J_{C\text{-}P}$ = 15.0 Hz, PCH_2CH_2**C**H(OH)), 75.4 (1C, s, **C**H(OH)$C(OCH_2)_2CH_3$), 110.7 (1C, s, **C**$(OCH_2)_2CH_3$),

^{31}P NMR (161.9 MHz) δ 33.8 (s, $(EtO)_2$**P**$(O)CH_2CH_2CH(OH)CH(OH)C(OCH_2)_2CH_3$).

IR: 3385, 2983, 2935, 2905, 1654, 1478, 1444, 1393, 1225, 1166, 1097, 1031, 965, 871, 827, 793.

m/z (FAB): 314 ($[M+2H]^+$ 16.1 %), 313 ($[M+H]^+$ 100 %), 295 ($[M\text{-}OH]^+$ 5.3 %), 280 ($[M\text{-}OH\text{-}CH_3]^+$ 4.5 %), 279 ($[M\text{-}H_2O\text{-}CH_3]^+$ 30.1 %), 278 ($[M\text{-}OH\text{-}OH]^+$ 5.7 %), 277 ($[M\text{-}H_2O\text{-}OH]^+$ 37.9 %), 251 ($[M\text{-}HOCH_2CH_2O]^+$ 13.2 %), 249 ($[M\text{-}H_2O\text{-}Et]^+$ 6.1 %), 239 ($[M\text{-}EtO\text{-}C_2H_4]^+$ 17.2 %), 235 ($[M\text{-}HOCH_2CH_2OH\text{-}CH_3]^+$ 21.0 %), 233 ($[M\text{-}HOCH_2CH_2OH\text{-}OH]^+$ 4.7 %).

HRMS: (FAB) Calcd. for (M+1) $C_{12}H_{26}O_7P$: 313.1416, found: 313.1437.

4.2.1.23 Diethyl *threo*-3,4-dihydroxy-5-oxohexylphosphonate 82

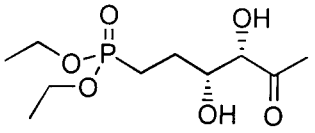

4.2.1.23.1 RuO_4 dihydroxylation

$RuO_4.xH_2O$ (85 mg, 0.64 mmol) and $NaIO_4$ (1.37 g, 6.41 mmol) were added simultaneously to a vigorously stirred solution of diethyl (*E*)-5-oxohex-3-enylphosphonate **76** (1.00 g, 4.27 mmol) in EtOAc / CH_3CN / H_2O (26 ml / 26 ml / 8.5 ml) at 0 °C. After 3 min the reaction was quenched with sat. $Na_2S_2O_{3(aq)}$ (45 ml), the aqueous layer separated and extracted into EtOAc (3 × 65 ml). The organic extracts were combined, dried over $MgSO_4$ and solvent removed under reduced pressure. Purification of the residue over silica gel (CH_2Cl_2 / EtOAc / IPA, 3:1:0.5, $KMnO_4$ stain as visualiser)

afforded **82** (153 mg, 0.57 mmol, 13.4 %) as a clear colourless oil. GCMS analysis indicated > 99 % purity.

^{1}H NMR (400.0 MHz) δ 1.33 (6H, t, $^{3}J_{H\text{-}H}$ = 7.0 Hz, $POCH_2\mathbf{C}H_3$), 2.00-2.18 (4H, m, $PC\mathbf{H}_2C\mathbf{H}_2$), 2.29 (3H, s, $COC\mathbf{H}_3$), 3.23 (1H, d, $^{2}J_{H\text{-}H}$ = 8.4 Hz, CH(O**H**)), 3.87 (1H, d, $^{2}J_{H\text{-}H}$ = 4.8 Hz, CH(O**H**)), 4.02-4.16 (6H, m, $POC\mathbf{H}_2$, C**H**(OH)C**H**(OH)).

^{13}C NMR (100.6 MHz) δ 16.4 (2C, d, $^{3}J_{C\text{-}P}$ = 6.0 Hz, $POCH_2\mathbf{C}H_3$), 22.3 (1C, d, $^{1}J_{C\text{-}P}$ = 141.9 Hz, $P\mathbf{C}H_2$), 25.6 (1C, s, $COCH_3$), 27.0 (1C, d, $^{2}J_{C\text{-}P}$ = 4.5 Hz, $PCH_2\mathbf{C}H_2$), 61.85, 61.92 (2C, d, $^{2}J_{C\text{-}P}$ = 6.9 Hz, $PO\mathbf{C}H_2$), 71.6 (1C, d, $^{3}J_{C\text{-}P}$ = 11.9 Hz, $PCH_2CH_2\mathbf{C}H(OH)$), 79.4 (1C, s, **C**H(OH)$COCH_3$), 208.3 (1C, s, **C**OCH_3).

^{31}P NMR (161.9 MHz) δ 33.8 (1P, s, $(EtO)_2\mathbf{P}(O)CH_2CH_2CH(OH)CH(OH)COCH_3$).

IR: 3373, 2984, 2934, 2912, 1715 (C=O), 1654, 1443, 1392, 1225, 1163, 1098, 1054, 1026, 967, 795.

m/z (FAB): 269 ($[M+H]^+$ 100 %), 252 ($[M-O]^+$ 10.7 %), 251 ($[M-OH]^+$ 74.4 %), 249 ($[M-H_3O]^+$ 11.7 %), 239 ($[M-Et]^+$ 100 %), 235 ($[M-H_2O-CH_3]^+$ 32.5 %), 225 ($[M-COCH_3]^+$ 24.3 %), 223 ($[M-EtO]^+$ 10.2 %), 209 ($[M-O_2CCH_3]^+$ 15.2 %), 207 ($[M-CH_3-C_2H_4-H_2O]^+$ 14.2 %).

HRMS: (FAB) Calcd. for (M+1) $C_{10}H_{22}O_6P$: 269.1154, found: 269.1177.

4.2.1.23.2 OsO_4 dihydroxylation

Diethyl (*E*)-5-oxohex-3-enylphosphonate **76** (1.01 g, 4.30 mmol) was added to a solution of tetraethylammonium acetate tetrahydrate (273 mg, 1.04 mmol) in acetone (8.6 ml) and *tert*-butyl hydroperoxide (70 % w/w in water, 1.0 ml, 8.26 mmol). After cooling the solution to 0 °C, OsO_4 (~ 0.2 ml, of a 0.39 M solution in PhMe, ~ 0.08 mmol) was added and after 1 h the solution was allowed to warm to ambient temperature, the reaction was then quenched 17 h later at 0 °C with sat. $Na_2S_2O_{3(aq)}$ (3 ml). H_2O (20 ml) was added, the aqueous layer separated and washed with EtOAc (3 × 200 ml), the organic fractions were then combined, dried over $MgSO_4$ and solvent removed under reduced pressure. Purification of the residue over silica gel (CH_2Cl_2 / EtOAc / IPA, 3:1:0.5, $KMnO_4$ stain as

visualiser) afforded **82** (574 mg, 2.14 mmol, 49.7 %) as a clear colourless oil. ^{31}P NMR analysis indicated > 99 % purity.

Analytical data was identical to that described in **4.2.1.23.2**.

4.2.1.24 Tribenzyl phosphite[122] 96

Et_3N (12.4 ml, 89.0 mmol) was added dropwise to a mechanically stirred solution of PCl_3 (2.5 ml, 28.7 mmol) in Et_2O (150 ml) at -78 °C, then a solution of benzyl alcohol (8.9 ml, 86.0 mmol) in Et_2O (30 ml) was added over 5 min at this temperature. After 2 h the reaction was allowed to warm up to ambient temperature and after a further 8 h it was filtered, the residue washed with Et_2O (0.5 l), and solvent removed under reduced pressure to give a crude product **96** (1.22 g, ~ 80 % pure by ^{31}P NMR). After leaving for ~ 12 h at -20 °C the sample decomposed (to ~ 50 % purity by ^{31}P NMR). Dry column chromatography over silica gel (solvent gradient of petrol / Et_3N, < 1 %, to petrol / Et_2O / Et_3N, 1:2:< 1 %, $KMnO_4$ stain as visualiser, R_f = 0.75 for **96** using petrol / Et_2O / Et_3N, 2:5:0.05) afforded **96** as a clear colourless oil (1.95 g, 5.54 mmol, 19.3 %) which was stable under nitrogen on storage. ^{31}P NMR analysis indicated > 95 % purity.

^1H NMR (200.0 MHz) δ 4.89 (6H, d, $^3J_{H\text{-}P}$ = 8.0 Hz, OC**H**$_2$Ph), 7.20-7.60 (15H, m, **Ph**).
^{13}C NMR (75.4 MHz) δ 64.4 (3C, d, $^2J_{C\text{-}P}$ = 11.2 Hz, O**C**H$_2$Ph), 127.5 (6C, s, γPh), 127.7 (3C, s, δPh), 128.4 (6C, s, βPh), 138.1 (3C, d, $^3J_{C\text{-}P}$ = 4.8 Hz, αPh).
^{31}P NMR (81.0 MHz) δ 140.7 (1P, s, (BnO)$_3$**P**), Lit.[180] 140.5.
IR: 3064, 3033, 2953, 2927, 2891, 1497, 1455, 1415, 1379, 1312, 1241, 1215, 1081, 1035, 998, 922, 828, 733, 697.
m/z (EI): 352 ($[M]^+$ 0.2 %), 262 ($[M\text{-}C_7H_6]^+$ 3.9 %), 261 ($[M\text{-}Bn]^+$ 25.7 %), 182 (19.9 %), 171 ($[M\text{-}Bn\text{-}C_7H_6]^+$ 10.6 %), 107 ($[BnO]^+$ 19.6 %), 92 ($[BnH]^+$ 23.4 %), 91 ($[Bn]^+$ 100 %), 77 ($[Ph]^+$ 8.2 %), 65 ($[C_5H_5]^+$ 35.7 %), 51 ($[C_4H_3]^+$ 9.8 %), 39 ($[C_3H_3]^+$ 9.3 %).

4.2.1.25 2-(2-Dibenzoxyphosphonylethyl)-1,3-dioxolane 95 and dibenzyl benzylphosphonate[122] 98

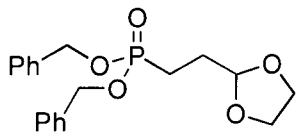

2-(2-Bromoethyl)-1,3-dioxolane (1.54 g, 8.51 mmol) was added to tribenzyl phosphite (305 mg, 0.87 mmol) and heated at 120 °C for 5 h. After cooling, purification over silica gel (Et_2O / CH_2Cl_2, 1:10, $KMnO_4$ stain as visualiser) afforded first tribenzyl phosphate (18.1 mg, 0.05 mmol, 5.7 %), then dibenzyl benzylphosphonate **98** (93.4 mg, 0.27 mmol, 30.6 %) both as clear colourless oils. Increasing the polarity of the solvent system (EtOAc / petrol / CH_2Cl_2, 4:1:1, $KMnO_4$ stain as visualiser) afforded **95** (55.6 mg, 0.15 mmol, 17.7 %) also as a clear colourless oil. ^{31}P NMR analysis indicated > 95 % purity.

^1H NMR (400.0 MHz) δ 1.83-1.98 (4H, m, PC**H**$_2$C**H**$_2$), 3.79-3.96 (4H, m, OC**H**$_2$C**H**$_2$O), 4.88 (1H, t, $^3J_{H\text{-}H}$ = 3.8 Hz, C**H**), 4.96 (2H, dd, $^3J_{H\text{-}P}$ = 8.3 Hz, $^2J_{H\text{-}H}$ = 11.9 Hz, C**H**$_A$H$_B$Ph), 5.04 (2H, dd, $^3J_{H\text{-}P}$ = 8.3 Hz, $^2J_{H\text{-}H}$ = 11.9 Hz, CH$_A$**H**$_B$Ph), 7.28-7.37 (10H, m, **Ph**).

^{13}C NMR (100.6 MHz) δ 19.8 (1C, d, $^1J_{C\text{-}P}$ = 144.2 Hz, P**C**H$_2$), 26.7 (1C, d, $^2J_{C\text{-}P}$ = 4.5 Hz, PCH$_2$**C**H$_2$), 65.0 (2C, s, OCH$_2$**C**H$_2$O), 67.1 (2C, d, $^2J_{C\text{-}P}$ = 6.1 Hz, PO**C**H$_2$), 103.1 (1C, d, $^3J_{C\text{-}P}$ = 19.8 Hz, **C**H), 127.8 (4C, s, γPh), 128.3 (2C, s, δPh), 128.5 (4C, s, βPh), 136.3 (2C, d, $^3J_{C\text{-}P}$ = 6.1 Hz, αPh).

^{31}P NMR (161.9 MHz) δ 35.7 (1P, s, (BnO)$_2$**P**(O)CH$_2$CH$_2$CH(CH$_2$O)$_2$).

IR: 3089, 3063, 3032, 2955, 2886, 1497, 1455, 1441, 1410, 1381, 1248, 1215, 1139, 1081, 1036, 1023, 996, 920, 879, 737, 698.

m/z (EI): 363 ([M+H]$^+$ 0.3 %), 362 ([M]$^+$ 0.1 %), 361 ([M-H]$^+$ 0.3 %), 271 ([M-Bn]$^+$ 2.7 %), 261 ([(BnO)$_2$PO]$^+$ 1.0 %), 211 ([M-Bn-C$_2$H$_4$O$_2$]$^+$ 4.1 %), 199 ([M-C$_7$H$_6$-CH(OCH$_2$)$_2$]$^+$ 11.6 %), 165 ([M-BnO-C$_7$H$_6$]$^+$ 85.3 %), 121 ([M-Bn-C$_7$H$_6$-C$_2$H$_4$O$_2$]$^+$ 27.7 %), 92 ([BnH]$^+$ 8.7 %), 91 ([Bn]$^+$ 100 %), 73 ([CH(OCH$_2$)$_2$]$^+$ 66.0 %), 65 ([C$_5$H$_5$]$^+$ 18.3 %).

HRMS: (CI) Calcd. for (M+1) $C_{19}H_{24}O_5P$: 363.1361, found: 316.1362.

Data for dibenzyl benzylphosphonate[122] 98

^{1}H NMR (400.0 MHz) δ 3.09 (2H, d, $^2J_{H\text{-}P}$ = 21.6 Hz, PC**H**$_2$Ph), 4.82 (4H, d, $^3J_{H\text{-}P}$ = 8.4 Hz, PhC**H**$_2$O), 7.24-7.38 (15H, m, **Ph**).

^{13}C NMR (100.6 MHz) δ 33.9 (1C, d, $^1J_{C\text{-}P}$ = 137.7 Hz, P**C**H$_2$Ph), 67.5 (2C, d, $^2J_{C\text{-}P}$ = 6.8 Hz, O**C**H$_2$Ph), 126.9 (1C, d, $^5J_{C\text{-}P}$ = 3.4 Hz, δPhCH$_2$P), 127.8 (4C, s, γPhCH$_2$OP), 128.2 (2C, s, δPhCH$_2$OP), 128.4 (4C, s, βPhCH$_2$OP), 128.5 (2C, d, $^4J_{C\text{-}P}$ = 3.0 Hz, γPhCH$_2$P), 129.8 (2C, d, $^3J_{C\text{-}P}$ = 6.4 Hz, βPhCH$_2$P), 131.0 (1C, d, $^2J_{C\text{-}P}$ = 9.6 Hz, αPhCH$_2$P), 136.2 (2C, d, $^3J_{C\text{-}P}$ = 6.1 Hz, αPhCH$_2$OP).

^{31}P NMR (161.9 MHz) δ 30.7 (1P, s, (BnO)$_2$**P**(O)Bn), Lit.[122] 28.1.

IR: 3087, 3062, 3031, 2953, 2889, 1496, 1454, 1379, 1251, 1215, 1080, 1035, 1021, 996, 917, 872, 737, 697.

m/z (EI): 353 ([M+H]$^+$ 0.2 %), 262 ([M-C$_7$H$_6$]$^+$ 16.7 %), 261 ([M-Bn]$^+$ 83.7 %), 180 (11.7 %), 107 ([BnO]$^+$ 45.4 %), 92 ([BnH]$^+$ 11.1 %), 91 ([Bn]$^+$ 100 %), 77 ([Ph]$^+$ 5.4 %), 65 ([C$_5$H$_5$]$^+$ 34.7 %), 51 ([C$_4$H$_3$]$^+$ 4.3 %), 39 ([C$_3$H$_3$]$^+$ 6.2 %).

4.2.1.26 2-(2-Iodoethyl)-1,3-dioxane[181] 99

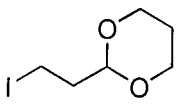

2-(2-Bromoethyl)-1,3-dioxane (2.00 g, 10.3 mmol) and pyridine (2 drops) were added to a solution of NaI (6.15 g, 41.0 mmol) in freshly distilled acetone (40 ml) and the mixture heated under reflux for 16 h. The solvent was removed under reduced pressure and then Et$_2$O (250 ml) was added to the residue. The mixture was washed with 50 % NaCl$_{(aq)}$ (50 ml) followed by sat. NaCl$_{(aq)}$ (25 ml), then dried over MgSO$_4$. Solvent was removed under reduced pressure and distillation (33-36 °C / 0.07 mbar) afforded **99** (2.01 g, 8.3 mmol, 81.0 %) as a dark red oil. ^{1}H NMR analysis indicated > 95 % purity, with the main impurity being 2-(2-bromoethyl)-1,3-dioxane , < 5 %.

^{1}H NMR (400.0 MHz) δ 1.30-1.35 (1H, m, OCH$_2$C**H**$_A$H$_B$), 1.97-2.08 (1H, m, OCH$_2$CH$_A$**H**$_B$), 2.09 (2H, dt, $^3J_{H\text{-}H}$ = 7.2 Hz, $^3J_{H\text{-}H}$ = 5.2 Hz, ICH$_2$C**H**$_2$CH), 3.18 (2H, t,

$^3J_{H\text{-}H}$ = 7.2 Hz, IC**H**$_2$), 3.72-3.79 (1H, m, OC**H**$_A$H$_B$CH$_2$), 4.05-4.10 (1H, m, OCH$_A$**H**$_B$CH$_2$), 4.60 (1H, t, $^3J_{H\text{-}H}$ = 5.2 Hz, C**H**).

^{13}C NMR (100.6 MHz) δ -0.7 (1C, s, I**C**H$_2$), 25.7 (1C, s, OCH$_2$**C**H$_2$CH$_2$O), 38.6 (1C, s, ICH$_2$**C**H$_2$), 66.8 (1C, s, O**C**H$_2$CH$_2$**C**H$_2$O), 101.5 (1C, s, **C**H).

IR: 2965, 2926, 2852, 2736, 1430, 1377, 1239, 1143, 1127, 1088, 1072, 1006, 870.

m/z (EI): 243 ([M+H]$^+$ 5.5 %), 242 ([M]$^+$ 5.1 %), 241 ([M-H]$^+$ 5.5 %), 199 ([M-CH$_3$CH$_2$CH$_2$]$^+$ 3.7 %), 183 ([M-HOCH$_2$CH$_2$CH$_2$]$^+$ 4.2 %), 169 ([ICH$_2$CH$_2$CH$_2$]$^+$ 3.5 %), 155 ([ICH$_2$CH$_2$]$^+$ 11.0 %), 128 ([HI]$^+$ 7.5 %), 127 ([I]$^+$ 12.4 %), 115 ([M-I]$^+$ 13.5 %), 114 ([M-HI]$^+$ 5.4 %), 88 ([M-ICH$_2$CH]$^+$ 5.1 %), 87 ([M-ICH$_2$CH$_2$]$^+$ 100 %), 41 ([CH$_2$CHCH$_2$]$^+$ 28.3 %).

4.2.1.27 Dibenzyl methylphosphonate[124] 105

A solution of dibenzyl phosphite (7.00 g, 26.7 mmol) in THF (15 ml) was added dropwise over 10 min to a solution of NaH (60 % mineral oil dispersion, 1.175 g, 29.4 mmol, mineral oil removed with petrol (2 × 5 ml)) in THF (15 ml) at -15 to -20 °C. Iodomethane (4.55 g, 32.1 mmol) was then added dropwise over 5 min and the solution allowed to warm up to 0 °C over 2 h, and then to ambient temperature. After 20 h, H_2O (10 ml) was added and the THF removed under reduced pressure. The residue was then washed with CH_2Cl_2 (3 × 100 ml), the organic washings were combined, dried over $MgSO_4$ and the solvent removed under reduced pressure. Dry column chromatography of the residue over silica gel (solvent gradient of petrol / EtOAc, 4:1, to neat EtOAc, $KMnO_4$ stain as visualiser, R_f= 0.15 for **105** using petrol / EtOAc, 2:3) afforded **105** as a clear yellow oil (5.02 g, 18.2 mmol, 68.1 %). GC analysis indicated > 99 % purity.

^{1}H NMR (400.0 MHz) δ 1.47 (3H, d, $^2J_{H\text{-}P}$ = 17.6 Hz, C**H**$_3$), 4.96 (2H, dd, $^3J_{H\text{-}P}$ = 8.6 Hz, $^2J_{H\text{-}H}$ = 12.0 Hz, C**H**$_A$H$_B$Ph), 5.06 (2H, dd, $^3J_{H\text{-}P}$ = 8.6 Hz, $^2J_{H\text{-}H}$ = 12.0 Hz, CH$_A$**H**$_B$Ph), 7.31-7.36 (10H, m, **Ph**).

^{13}C NMR (100.6 MHz) δ 11.6 (1C, d, $^1J_{C\text{-}P}$ = 144.2 Hz, P**C**H$_3$), 66.9 (2C, d, $^2J_{C\text{-}P}$ = 6.0 Hz, O**C**H$_2$Ph), 127.8 (4C, s, γPh), 128.3 (2C, s, δPh), 128.5 (4C, s, βPh), 136.2 (2C, d, $^3J_{C\text{-}P}$ = 6.1 Hz, αPh).

^{31}P NMR (161.9 MHz) δ 32.8 (1P, s, $(BnO)_2$**P**(O)CH_3), Lit.[183] 32.2.

IR: 3064, 3033, 2953, 2927, 2891, 1497, 1455, 1415, 1379, 1312, 1241, 1215, 1081, 1035, 998, 922, 828, 733, 697.

m/z (CI): 294 ($[M+NH_4]^+$ 13.5 %), 277 ($[M+H]^+$ 26.5 %), 108 ($[BnOH]^+$ 100 %), 107 ($[BnO]^+$ 18.6 %), 106 ($[PhCHO]^+$ 41.3 %), 91 ($[PhCH_2]^+$ 25.0 %), 78 ($[PhH]^+$ 9.5 %).

4.2.1.28 Dibenzyl but-3-enylphosphonate 106

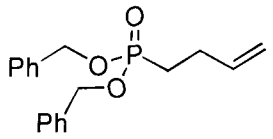

Dibenzyl methylphosphonate (4.80 g, 17.4 mmol) in THF (10 ml) was added dropwise to a solution of 1.6 M butyl lithium in n-hexane (12.5 ml, 20.0 mmol) in THF (25 ml) at -60 °C, and after 10 min at this temperature copper (I) iodide (3.54 g, 19.1 mmol) was added. The solution was allowed to warm to -35 °C over 5 min, then after 1 h allyl bromide (2.31 g, 19.1 mmol) in THF (7.5 ml) was added dropwise and the reaction allowed to warm slowly to ambient temperature after 4 h at -35 °C. The reaction was quenched with H_2O (30 ml), the solution filtered through Hyflo, and the cake washed with CH_2Cl_2 (3 × 50 ml). The eluent was filtered through the cake again and was washed with CH_2Cl_2 (50 ml) and the washings were combined. The aqueous layer was separated, washed with CH_2Cl_2 (50 ml) then the organic fractions were combined, dried over $MgSO_4$ and solvent removed under reduced pressure. Dry column chromatography over silica gel of the residue (solvent gradient of neat petrol to petrol / EtOAc, 1:1, $KMnO_4$ stain as visualiser, R_f = 0.43 for **106** using petrol / EtOAc, 2:3) afforded **106** (3.73 g, 11.8 mmol, 68.0 %) as a clear yellow oil. GCMS analysis indicated > 99 % purity.

^{1}H NMR (499.8 MHz) δ 1.80-1.88 (2H, m, P**CH**$_2$), 2.27-2.35 (2H, m, PCH$_2$**CH**$_2$), 4.94-5.08 (6H, m, CH**CH**$_2$, **CH**$_2$Ph), 5.74-5.82 (1H, m, **CH**CH$_2$), 7.30-7.37 (10H, m, **Ph**).

^{13}C NMR (125.7 MHz) δ 25.3 (1C, d, $^1J_{C\text{-}P}$ = 140.1 Hz, P**C**H$_2$), 26.3 (1C, d, $^2J_{C\text{-}P}$ = 4.4 Hz, PCH$_2$**C**H$_2$), 67.0 (2C, d, $^2J_{C\text{-}P}$ = 6.5 Hz, O**C**H$_2$Ph), 115.1 (1C, s, CH**C**H$_2$), 127.8 (4C, s, γPh), 128.3 (2C, s, δPh), 128.5 (4C, s, βPh), 136.3 (2C, d, $^3J_{C\text{-}P}$ = 5.9 Hz, αPh), 136.9 (1C, d, $^3J_{C\text{-}P}$ = 18.0 Hz, **C**H).

^{31}P NMR (161.9 MHz) δ 33.8 (1P, s, $(BnO)_2$**P**(O)$CH_2CH_2CHCH_2$).

IR: 3065, 3033, 2979, 2952, 2893, 1702, 1641, 1497, 1455, 1379, 1283, 1247, 1215, 1081, 1037, 997, 919, 861, 735, 697.

m/z (EI): 317 ($[M+H]^+$ 0.4 %), 225 ($[M-Bn]^+$ 29.9 %), 180 (7.0 %), 144 (5.1 %), 143 (37.9 %), 108 ($[BnOH]^+$ 5.7 %), 107 ($[BnO]^+$ 54.2 %), 92 ($[PhMe]^+$ 11.3 %), 91 ($[Bn]^+$ 100 %), 79 ($[C_6H_7]^+$ 12.7 %), 65 ($[C_5H_5]^+$ 19.5 %), 55 ($[C_4H_7]^+$ 8.0 %), 39 ($[C_3H_3]^+$ 8.1 %).

HRMS: (CI) Calcd. for (M+1) $C_{18}H_{22}O_3P$: 317.1306, found: 317.1292.

4.2.1.29 Dibenzyl 3,4-dihydroxybutylphosphonate 107

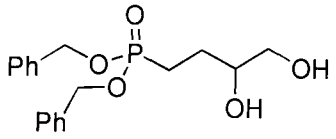

Dibenzyl but-3-enylphosphonate **106** (3.57 g, 11.31 mmol) was added to a solution of tetraethylammonium acetate tetrahydrate (715 mg, 2.74 mmol) in acetone (23 ml) and *tert*-butyl hydroperoxide (70 % w/w in water, 2.65 ml, 21.90 mmol). After cooling the solution to 0 °C, OsO_4 (~ 0.1 ml, of a 0.39 M solution in PhMe, ~ 0.04 mmol) was added and after 1 h the solution was allowed to warm to ambient temperature. The reaction was followed by tlc (IPA / CH_2Cl_2, 1:6, R_f = 0.8 for **106** and 0.37 for **107**, $KMnO_4$ stain as visualiser). After 48 h the solution was cooled to 0 °C and OsO_4 (~ 0.1 ml, of a 0.39 M solution in PhMe, ~ 0.04 mmol) was added. After 1 h the solution was allowed to warm to ambient temperature and 24 h later CH_2Cl_2 (50 ml) was added, then the reaction quenched at 0 °C with 10 % $Na_2S_2O_{3(aq)}$ (6 ml). H_2O (10 ml) was then added, the aqueous layer separated and washed with CH_2Cl_2 (3 × 200 ml). The organic extracts were combined, dried over $MgSO_4$ and solvent removed under reduced pressure. Dry column chromatography over silica gel of the residue (solvent gradient of neat CH_2Cl_2 to IPA / CH_2Cl_2, 1:2) afforded **107** (3.36 g, 9.60 mmol, 85.0 %) as a clear colourless oil. ^{31}P NMR analysis indicated > 99 % purity.

^{1}H NMR (499.8 MHz) δ 1.64-1.73 (2H, m, PC**H**$_2$), 1.80-2.01 (2H, m, PCH$_2$C**H**$_2$), 3.40 (1H, dd, $^3J_{H\text{-}H}$ = 6.7 Hz, $^2J_{H\text{-}H}$ = 11.2 Hz, C**H**$_A$H$_B$OH), 3.55 (1H, dd, $^3J_{H\text{-}H}$ = 3.2 Hz, $^2J_{H\text{-}H}$ = 11.2 Hz, CH$_A$**H**$_B$OH), 4.91-5.05 (4H, m, OC**H**$_2$Ph), 7.29-7.37 (10H, m, **Ph**).

^{13}C NMR (125.7 MHz) δ 22.1 (1C, d, $^1J_{C\text{-}P}$ = 141.1 Hz, P**C**H$_2$), 25.8 (1C, d, $^2J_{C\text{-}P}$ = 4.4 Hz, PCH$_2$**C**H$_2$), 66.3 (1C, s, **C**H$_2$OH), 67.4 (2C, d, $^2J_{C\text{-}P}$ = 6.4 Hz, O**C**H$_2$Ph), 71.6 (1C, d, $^3J_{C\text{-}P}$ = 13.0 Hz, **C**H(OH)), 127.9 (4C, s, γPh), 128.5 (2C, s, δPh), 128.6 (4C, s, βPh), 136.1 (2C, d, $^3J_{C\text{-}P}$ = 5.9 Hz, αPh).

^{31}P NMR (161.9 MHz) δ 35.4 (1P, s, (BnO)$_2$**P**(O)CH$_2$CH$_2$CH(OH)CH$_2$OH).

IR: 3379, 3090, 3064, 3033, 2936, 2891, 1958, 1887, 1816, 1712, 1497, 1455, 1407, 1380, 1215, 1081, 1035, 996, 921, 873, 735, 697.

m/z (CI): 351 ([M+H]$^+$ 24.8 %), 350 ([M]$^+$ 100 %), 260 ([M-C$_7$H$_6$]$^+$ 14.2 %), 243 ([M-BnO]$^+$ 7.1 %).

HRMS: (CI) Calcd. for C$_{18}$H$_{24}$O$_5$P: 351.1361, found: 351.1370.

4.2.1.30 Dibenzyl 3-oxopropylphosphonate 94

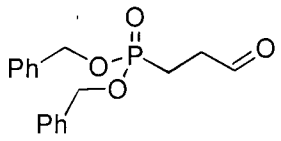

NaIO$_4$ (2.06 g, 9.63 mmol) was added to a solution of dibenzyl 3,4-dihydroxybutylphosphonate **107** (3.06 g, 8.73 mmol) in THF (30 ml) and H$_2$O (30 ml). After 1 h, THF was removed under reduced pressure and the organics were extracted into CH$_2$Cl$_2$ (3 × 200 ml). The organic extracts were combined, dried over MgSO$_4$ and the solvent was removed under reduced pressure to afford **107** as a clear colourless oil (2.76 g, 8.66 mmol, 99.2 %). ^{31}P NMR analysis indicated > 99 % purity.

^{1}H NMR (499.8 MHz) δ 2.00-2.08 (2H, m, PC**H**$_2$), 2.66-2.73 (2H, m, PCH$_2$C**H**$_2$), 4.96 (2H, dd, $^3J_{H\text{-}P}$ = 8.5 Hz, $^2J_{H\text{-}H}$ = 11.7 Hz, C**H**$_A$H$_B$Ph), 5.05 (2H, dd, $^3J_{H\text{-}P}$ = 8.5 Hz, $^2J_{H\text{-}H}$ = 11.7 Hz, CH$_A$**H**$_B$Ph), 7.30-7.38 (10H, m, **Ph**), 9.68 (1H, d, $^4J_{H\text{-}P}$ = 2.0 Hz, C**H**O).

^{13}C NMR (125.7 MHz) δ 18.3 (1C, d, $^1J_{C\text{-}P}$ = 145.7 Hz, P**C**H$_2$), 36.7 (1C, s, PCH$_2$**C**H$_2$), 67.4 (2C, d, $^2J_{C\text{-}P}$ = 5.9 Hz, O**C**H$_2$Ph), 128.0 (4C, s, γPh), 128.5 (2C, s, δPh), 128.6 (4C, s, βPh), 136.1 (2C, d, $^3J_{C\text{-}P}$ = 5.9 Hz, αPh), 198.9 (1C, s, **C**HO).

^{31}P NMR (161.9 MHz) δ 33.2 (1P, s, $(BnO)_2$**P**(O)CH_2CH_2CHO).

IR: 3064, 3033, 2953, 2894, 2833, 2732, 1959, 1888, 1723, 1497, 1455, 1410, 1383, 1243, 1215, 1081, 996, 869, 736, 698.

m/z (EI): 317 ($[M+H]^+$ 0.4 %), 225 ($[M-Bn]^+$ 29.9 %), 180 (7.0 %), 143 (37.9 %), 108 ($[BnOH]^+$ 5.7 %), 107 ($[BnO]^+$ 54.2 %), 92 ($[PhMe]^+$ 11.3 %), 91 ($[Bn]^+$ 100 %), 79 ($[C_6H_7]^+$ 12.7 %), 65 ($[C_5H_5]^+$ 19.5 %), 55 ($[C_4H_7]^+$ 8.0 %), 39 ($[C_3H_3]^+$ 8.1 %).

4.2.1.31 Dibenzyl (*E*)-5-oxohex-3-enylphosphonate 108

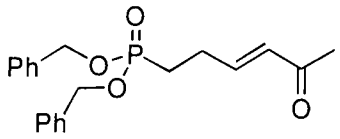

Dibenzyl 3-oxopropylphosphonate **94** (2.72 g, 8.55 mmol) was added to a solution of 1-triphenylphosphoranylidene-2-propanone (2.73 g, 8.56 mmol) in THF (50 ml) and the mixture heated under reflux for 18 h. The solvent was removed under reduced pressure and the residue purified over silica gel (acetonitrile / CH_2Cl_2, 1:2.5, UV lamp as visualiser, R_f = 0.23 for triphenylphosphine oxide and 0.33 for **108**) affording **108** (2.88 g, 8.03 mmol, 94.0 %) as a clear pale yellow oil. ^{31}P NMR analysis indicated > 93 % purity, with the main impurity being triphenylphosphine oxide, ~ 5 %.

^{1}H NMR (400.0 MHz) δ 1.81-1.90 (2H, m, PC**H**$_2$), 2.15 (3H, s, COC**H**$_3$), 2.40-2.49 (2H, m, PCH$_2$C**H**$_2$), 4.95 (2H, dd, $^3J_{H\text{-}P}$ = 8.8 Hz, $^2J_{H\text{-}H}$ = 11.7 Hz, C**H**$_A$H$_B$Ph), 5.06 (2H, dd, $^3J_{H\text{-}P}$ = 8.8 Hz, $^2J_{H\text{-}H}$ = 11.7 Hz, CH$_A$**H**$_B$Ph), 5.98 (1H, dt, $^3J_{H\text{-}H}$ = 16.0 Hz, $^4J_{H\text{-}H}$ = 1.6 Hz, C**H**COCH$_3$), 6.69 (1H, dt, $^3J_{H\text{-}H}$ = 16.0 Hz, $^3J_{H\text{-}H}$ = 6.6 Hz, PCH$_2$CH$_2$C**H**), 7.31-7.37 (10H, m, **Ph**).

^{13}C NMR (100.6 MHz) δ 24.6 (1C, d, $^1J_{C\text{-}P}$ = 141.8 Hz, P**C**H$_2$), 25.2 (1C, d, $^2J_{C\text{-}P}$ = 4.5 Hz, PCH$_2$**C**H$_2$), 26.8 (1C, s, CO**C**H$_3$), 67.3 (2C, d, $^2J_{C\text{-}P}$ = 6.4 Hz, O**C**H$_2$Ph), 128.0 (4C, s, γPh), 128.5 (2C, s, δPh), 128.6 (4C, s, βPh), 131.5 (1C, s, **C**HCOCH$_3$), 136.1 (2C, d, $^3J_{C\text{-}P}$ = 5.7 Hz, αPh), 145.6 (1C, d, $^3J_{C\text{-}P}$ = 16.4 Hz, PCH$_2$CH$_2$**C**H), 198.2 (1C, s, CH**C**OCH$_3$).

^{31}P NMR (161.9 MHz) δ 34.1 (1P, s, $(BnO)_2$**P**(O)$CH_2CH_2CHCHCOCH_3$).

IR: 3064, 3033, 2953, 2894, 1696, 1673, 1628, 1497, 1455, 1426, 1361, 1252, 1214, 1081, 1035, 995, 866, 737, 697.

m/z (EI): 358 ($[M]^+$ 1.0 %), 267 ($[M\text{-}Bn]^+$ 9.6 %), 225 ($[M\text{-}Bn\text{-}C_2H_2O]^+$ 2.5 %), 161 ($[M\text{-}PhCHO\text{-}Bn]^+$ 35.5 %), 122 (9.2 %), 108 ($[BnOH]^+$ 5.7 %), 107 ($[BnO]^+$ 17.2 %), 106 ($[PhCHO]^+$ 7.3 %), 105 ($[PhCO]^+$ 18.6 %), 92 ($[PhCH_3]^+$ 8.4 %), 91 ($[Bn]^+$ 100 %), 83 ($[C_5H_7O]^+$ 56.2 %), 85 (41.1 %), 79 ($[C_6H_7]^+$ 10.2 %), 65 ($[C_5H_5]^+$ 10.3 %).

HRMS: (EI) Calcd. for $C_{20}H_{23}O_4P$: 358.1334, found: 358.1331.

4.2.1.32 Dibenzyl *threo*-3,4-dihydroxy-5-oxohexylphosphonate 109

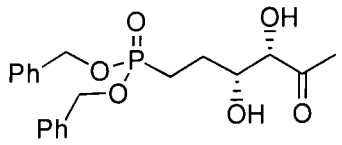

Dibenzyl (*E*)-5-oxohex-3-enylphosphonate **108** (2.55 g, 7.10 mmol) was added to a solution of tetraethylammonium acetate tetrahydrate (450 mg, 1.72 mmol) in acetone (14 ml) and *tert*-butyl hydroperoxide (70 % w/w in water, 1.66 ml, 13.72 mmol). After cooling the solution to 0 °C, OsO_4 (~ 0.2 ml, of a 0.39 M solution in PhMe, ~ 0.08 mmol) was added and after 1 h the solution was allowed to warm to ambient temperature. The reaction was followed by tlc (MeOH / Et_2O, 0.2:5, R_f = 0.55 for **109**, $KMnO_4$ stain as visualiser) and after 26 h, CH_2Cl_2 (30 ml) was added then the reaction was quenched at 0 °C with 10 % $Na_2S_2O_{3(aq)}$ (10 ml). H_2O (15 ml) was then added, the aqueous layer separated and washed with CH_2Cl_2 (3 × 200 ml). The organic fractions were combined, dried over $MgSO_4$ and the solvent was removed under reduced pressure. Purification of the residue over silica gel (MeOH / Et_2O, 1:15, R_f = 0.35 for **109**, $KMnO_4$ stain as visualiser) afforded **109** (1.85 g, 4.71 mmol, 66.4 %) as a creamy coloured solid (mp 60.5-61.5 °C). ^{31}P NMR analysis indicated > 99 % purity.

^1H NMR (400.0 MHz) δ 1.79-2.04 (4H, m, PCH_2CH_2), 2.18 (3H, s, $COCH_3$), 3.29 (1H, s, **OH**), 3.92-4.01 (3H, m, **CH**(OH)**CH**(**OH**)), 4.91-5.07 (4H, m, CH_2Ph), 7.29-7.37 (10H, m, **Ph**).

^{13}C NMR (100.6 MHz) δ 22.4 (1C, d, $^1J_{C\text{-}P}$ = 141.5 Hz, PCH_2), 25.5 (1C, s, $COCH_3$), 26.7 (1C, d, $^2J_{C\text{-}P}$ = 4.5 Hz, PCH_2CH_2), 67.3, 67.4 (2C, d, $^2J_{C\text{-}P}$ = 6.5 Hz, OCH_2Ph), 71.3 (1C, d, $^3J_{C\text{-}P}$ = 13.3 Hz, $CH_2CH(OH)$), 79.3 (1C, s, $CH(OH)COCH_3$), 127.91 (2C, s, γPh),

127.94 (2C, s, γPh), 128.4 (2C, s, δPh), 128.5 (4C, s, βPh), 136.0 (2C, d, $^3J_{C\text{-}P}$ = 6.1 Hz, αPh), 208.3 (1C, s, CH(OH)**C**OCH$_3$).

^{31}P NMR (161.9 MHz) δ 34.9 (1P, s, (BnO)$_2$**P**(O)CH$_2$CH$_2$CH(OH)CH(OH)COCH$_3$).

IR: (KBr) 3473, 3249, 3063, 3029, 2950, 2921, 1713, 1455, 1393, 1351, 1209, 1143, 1117, 1080, 1038, 1023, 996, 971, 924, 869, 847, 741, 696, 589.

m/z (CI): 411 ([M+NH$_4$+H]$^+$ 3.7 %), 410 ([M+NH$_4$]$^+$ 14.4 %), 394 ([M+2H]$^+$ 23.6 %), 393 ([M+H]$^+$ 100 %), 392 ([M]$^+$ 9.4 %), 376 ([M-O]$^+$ 3.8 %), 375 ([M-OH]$^+$ 8.7 %), 374 ([M-H$_2$O]$^+$ 1.6 %), 336 (19.2 %), 319 (16.0 %), 303 ([M-PhCO]$^+$ 5.5 %), 302 ([M-PhCHO]$^+$ 26.0 %), 285 ([M-BnO]$^+$ 5.8 %).

HRMS: (CI) Calcd. for (M+1) $C_{20}H_{26}O_6P$: 393.1467, found: 393.1465.

4.2.1.33 Disodium *threo*-3,4-dihydroxy-5-oxohexylphosphonate 110

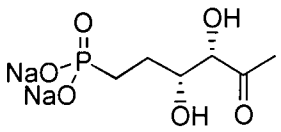

10 % Pd on carbon (59 mg, 55.4 mmol) was added to a solution of dibenzyl 3,4-dihydroxy-5-oxohexylphosphonate **109** (206 mg, 0.52 mmol) in THF (10 ml) and H$_2$O (10 ml) and the suspension stirred under hydrogen (2-3 atm) on a Parr shaker for 45 min. After filtering through Hyflo the reaction was neutralised with 1M NaOH$_{(aq)}$ and centrifuged (14000 rpm for 30 min) to remove residual particulate catalyst. The H$_2$O / THF supernatant was separated and the solvent was removed under reduced pressure followed by freeze drying to afford **110** (103 mg, 0.40 mmol, 76.6 %) as a hygroscopic creamy coloured solid. This compound was unstable to storage and was found to have decomposed within two weeks at ambient temperature.

^{1}H NMR (400.0 MHz) (D$_2$O) δ 1.29-1.60 (4H, m, PC**H$_2$**C**H$_2$**), 1.98 (3H, s, COC**H$_3$**), 3.85-3.91 (1H, m, CH$_2$C**H**(OH)), 4.07-4.10 (1H, m, C**H**(OH)COCH$_3$).

^{13}C NMR (100.6 MHz) (D$_2$O) δ 25-28 (br, P**C**H$_2$), 25.9 (s, CO**C**H$_3$), 27.5 (s, PCH$_2$**C**H$_2$), 72.0 (d, $^3J_{C\text{-}P}$ = 16.8 Hz, CH$_2$**C**H(OH)), 79.1 (s, **C**H(OH)COCH$_3$), 213.3 (s, CH(OH)**C**OCH$_3$).

^{31}P NMR (161.9 MHz) D$_2$O δ 20-33 (br, (NaO)$_2$**P**(O)CH$_2$CH$_2$CH(OH)CH(OH)COCH$_3$).

4.2.1.34 Dibenzyl difluoromethylphosphonate[134] 113

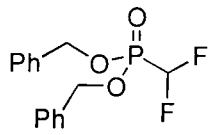

Dibenzyl phosphite (6 ml, 27.2 mmol) was added dropwise to a solution of NaH (1.30 g, 32.5 mmol) in THF (60 ml) at -15 to -10 °C over 20 min. After 5 min chorodifluoromethane (23.0 g, 0.27 mol) was steadily bubbled through the reaction, and the solution allowed to warm to ambient temperature over 15 min. Chlorodifluoromethane was bubbled through for a further 30 min, then the mixture was left to stir for 12 h. THF was removed under reduced pressure then H_2O (70 ml) added and washed with CH_2Cl_2 (3 × 200 ml). The organic washings were combined, dried over $MgSO_4$ then the solvent was removed under reduced pressure. Dry column chromatography over silica gel of the residue with solvent gradient of neat petrol to petrol / EtOAc, 6:1, (impurity at R_f = 0.65, **113** at R_f = 0.20, petrol / EtOAc, 6:1, $KMnO_4$ stain as visualiser) followed by dry column chromatography over silica gel with neat CH_2Cl_2 to CH_2Cl_2 / EtOAc, 12:1, (impurity at R_f = 0.45, **113** at R_f = 0.68 for CH_2Cl_2 / EtOAc, 6:1, $KMnO_4$ stain as visualiser) afforded **113** (5.44 g, 16.4 mmol, 60.5 %) as a clear colourless oil. ^{31}P NMR analysis indicated > 99 % purity.

^1H NMR (400.0 MHz) δ 5.16 (4H, d, $^3J_{H\text{-}P}$ = 8.4 Hz, C**H**$_2$Ph), 5.84 (1H, dt, $^2J_{H\text{-}P}$ = 27.9 Hz, $^2J_{H\text{-}F}$ = 48.7 Hz, PCF$_2$**H**), 7.33-7.39 (10H, m, **Ph**).

^{13}C NMR (100.6 MHz) δ 69.6 (2C, d, $^2J_{C\text{-}P}$ = 6.4 Hz, **C**H$_2$OP), 111.3 (1C, dt, $^2J_{C\text{-}F}$ = 258.5 Hz, $^2J_{C\text{-}P}$ = 213.7 Hz, P**C**H$_2$F), 128.2 (4C, s, γPh), 128.7 (4C, s, βPh), 128.9 (2C, s, δPh), 135.0 (2C, d, $^3J_{C\text{-}P}$ = 5.7 Hz, αPh).

^{19}F NMR (376.3 MHz) δ -135.2 (2F, dd, $^2J_{F\text{-}P}$ = 92.4 Hz, $^2J_{F\text{-}P}$ = 48.7 Hz, CH$_2$**F**).

^{31}P NMR (161.9 MHz) δ 6.8 (1P, t, $^2J_{F\text{-}P}$ = 92.3 Hz, (BnO)$_2$**P**(O)CF$_2$H), Lit.[134] 6.4.

IR: 3090, 3065, 3034, 2961, 2897, 1958, 1884, 1814, 1498, 1456, 1380, 1341, 1271, 1215, 1114, 1061, 1009, 997, 967, 738, 696.

m/z (CI): 330 ($[M+NH_4]^+$ 20.3 %), 108 ($[BnOH]^+$ 57.2 %), 107 ($[BnO]^+$ 83.4 %), 106 ($[PhCHO]^+$ 47.1 %), 105 ($[PhCO]^+$ 64.7 %), 92 ($[PhCH_3]^+$ 34.2 %), 91 ($[Bn]^+$ 100 %), 90 ($[PhCH]^+$ 82.4 %), 77 ($[C_6H_5]^+$ 7.6 %), 65 ($[C_5H_5]^+$ 13.2 %).

4.2.1.35 2,2-Diethoxyethyl trifluoromethanesulphonate[136] 116

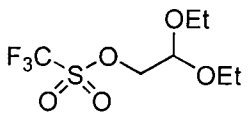

2,6-Di-*tert*-butylpyridine (0.17 ml, 0.76 mmol) was added to a solution of 2,2-diethoxyethanol (99 mg, 0.74 mmol) in CH_2Cl_2 (3 ml), the mixture was cooled to -25 °C and trifluoromethanesulphonic anhydride (0.15 ml, 0.89 mmol) was added dropwise. After 25 min at -25 to -20 °C, H_2O (5 ml) was added and the mixture allowed to warm to ambient temperature. The mixture was washed with CH_2Cl_2 (3 × 40 ml), the organic washings combined, dried over $MgSO_4$ and the solvent removed under reduced pressure. Purification over silica gel (acetonitrile / CH_2Cl_2, 0.1:5, R_f = 0.57 for **116**, PMA stain as visualiser) afforded **116** (136 mg) as a clear colourless oil. NMR analysis indicated **116** was ~ 80 % pure, with the main impurity being 2,6-di-*tert*-butylpyridine, ~ 20 %, therefore **116** was afforded in ~ 65 % yield.

^{1}H NMR (400.0 MHz) δ 1.67 (6H, t, $^3J_{H\text{-}H}$ = 7.0 Hz, C**H**$_3$), 3.55-3.64 (2H, m, OC**H**$_A$H$_B$), 3.71-3.79 (2H, m, OCH$_A$**H**$_B$), 4.31 (2H, d, $^3J_{H\text{-}H}$ = 5.2 Hz, C**H**$_2$CH), 4.67 (1H, t, $^3J_{H\text{-}H}$ = 5.2 Hz, CH$_2$C**H**).

^{13}C NMR (100.6 MHz) δ 15.1 (2C, s, **C**H$_3$), 63.6 (2C, s, O**C**H$_2$), 73.9 (1C, s, **C**H$_2$CH), 98.7 (1C, s, **C**H(OEt)$_2$), 118.5 (1C, q, $^1J_{C\text{-}F}$ = 319.5 Hz, **C**F$_3$).

^{19}F NMR (376.3 MHz) δ -75.1 (3F, s, C**F**$_3$SO$_3$CH$_2$CH(OEt)$_2$).

IR: 2981, 2936, 2903, 1616, 1577, 1481, 1448, 1417, 1377, 1360, 1348, 1247, 1209, 1145, 1075, 1031, 973, 895, 840, 816, 762, 752, 617.

4.2.1.36 Diethyl 3-hydroxy-4-methylpent-4-enylphosphonate 121

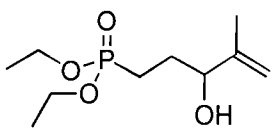

A solution of diethyl 3-oxopropylphosphonate **52** (1.60 g, 8.24 mmol) in THF (20 ml) was added dropwise over 15 min to a -78 °C solution of isopropenylmagnesium bromide in THF (23.5 ml) (prepared from dropwise addition of 2-bromopropene (1.20 g,

9.92 mmol) in THF (20 ml) to I_2 (5 mg) activated magnesium (0.24 g, 9.88 mmol) in THF (3.5 ml)). After 40 min, H_2O (30 ml) was added, and the mixture was extracted into CH_2Cl_2 (3 × 100 ml). The organic extracts were combined, dried over $MgSO_4$ and the solvent removed under reduced pressure. Purification of the residue over silica gel (R_f= 0.36 for **121**, and 0.25 for **52**, petrol / Et_2O / IPA, 1.5:1.5:0.5, $KMnO_4$ stain as visualiser) afforded **121** (0.85 g, 3.61 mmol, 43.8 %) as a clear colourless oil. ^{31}P NMR analysis indicated > 99 % purity.

^1H NMR (400.0 MHz) δ 1.27 (6H, t, $^3J_{H-H}$ = 7.0 Hz, $POCH_2C\mathbf{H}_3$), 1.67 (3H, s, $\mathbf{C}H_3$), 1.68-1.88 (4H, m, $PC\mathbf{H}_2C\mathbf{H}_2$), 3.13 (1H, s, CH(O**H**)), 3.99-4.10 (5H, m, $POC\mathbf{H}_2CH_3$, C**H**(OH)), 4.82 (1H, s, $C(CH_3)C\mathbf{H}_AH_B$), 4.93 (1H, s, $C(CH_3)CH_A\mathbf{H}_B$).

^{13}C NMR (100.6 MHz) δ 16.3 (2C, d, $^3J_{C-P}$ = 6.1 Hz, $POCH_2\mathbf{C}H_3$), 17.8 (1C, s, $\mathbf{C}H_3$), 21.4 (1C, d, $^1J_{C-P}$ = 142.3 Hz, $P\mathbf{C}H_2$), 27.5 (1C, d, $^2J_{C-P}$ = 4.1 Hz, $PCH_2\mathbf{C}H_2$), 61.52, 61.53 (2C, d, $^2J_{C-P}$ = 6.4 Hz, $PO\mathbf{C}H_2$), 74.7 (1C, d, $^3J_{C-P}$ = 16.0 Hz, **C**H(OH)), 111.2 (1C, s, $C(CH_3)\mathbf{C}H_2$), 146.5 (1C, s, $\mathbf{C}(CH_3)CH_2$).

^{31}P NMR (161.9 MHz) δ 34.2 (1P, s, $(EtO)_2\mathbf{P}(O)CH_2CH_2CH(OH)C(CH_3)CH_2$).

IR: 3379, 3073, 2982, 2935, 2911, 2871, 1731, 1651, 1444, 1393, 1370, 1230, 1163, 1097, 1059, 1029, 965, 899, 792, 732.

m/z (CI): 236 ($[M]^+$ 17.0 %), 195 ($[M-C(CH_3)CH_2]^+$ 13.1 %), 191 ($[M-EtO]^+$ 8.3 %), 166 ($[M-C(OH)C(CH_3)CH_2]^+$ 100 %), 165 ($[M-CH(OH)C(CH_3)CH_2]^+$ 33.9 %), 139 ($[(EtO)_2P(O)H_2]^+$ 33.7 %), 138 ($[M-C(OH)C(CH_3)CH_2-C_2H_4]^+$ 63.4 %), 137 ($[(EtO)_2PO]^+$ 13.1 %), 122 ($[M-C(CH_3)CH_2-EtO-C_2H_4]^+$ 17.0 %), 121 ($[M-C(CH_3)CH_2-EtO-Et]^+$ 15.9 %), 111 ($[(EtO)(HO)POH_2]^+$ 45.9 %), 110 ($[(EtO)(HO)POH]^+$ 17.9 %), 109 ($[(EtO)(HO)PO]^+$ 20.8 %), 82 ($[(HO)_2POH]^+$ 25.3 %).

HRMS: (EI) Calcd. for $C_{10}H_{21}O_4P$: 236.1177, found: 236.1177.

4.2.1.37 2-(3-Diethoxyphosphonyl-1-isopropenylpropoxy)-tetrahydropyran 125

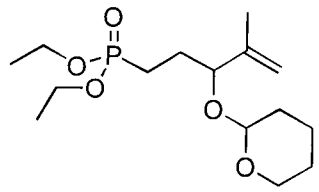

Dihydropyran (0.1 ml, 1.10 mmol) was added to a solution of PTSA.H_2O (1 mg, 0.01 mmol) and diethyl 3-hydroxy-4-methylpent-4-enylphosphonate **124** (56 mg, 0.24 mmol) in CH_2Cl_2 (2 ml). After 25 min, tlc indicated that **124** had been consumed (petrol / Et_2O / IPA, 1.5:1.5:0.5, R_f = 0.36 for **124** and 0.53 for **125**, $KMnO_4$ stain as visualiser), sat. $NaHCO_{3(aq)}$ (5 ml) was then added and the mixture extracted into CH_2Cl_2 (3 × 30 ml). The organic extracts were combined, dried over $MgSO_4$ and solvent removed under reduced pressure. Purification of the residue over silica gel (neat EtOAc, $KMnO_4$ stain as visualiser, R_f= 0.3 for **125**) afforded **125** (50 mg, 0.16 mmol, 65.9 %) as a clear colourless oil. ^{31}P NMR analysis indicated > 99 % purity. NMR resolved two diastereoisomers in the approximate ratio 45 : 55.

^1H NMR (400.0 MHz) δ 1.30 (6H, t, $^3J_{H\text{-}H}$ = 7.2 Hz, $POCH_2C\mathbf{H}_3$), 1.45-2.03 (13H, m, $PC\mathbf{H}_2C\mathbf{H}_2$, $C\mathbf{H}_3$, $O_2CHC\mathbf{H}_2C\mathbf{H}_2C\mathbf{H}_2$), 3.39-3.50 (1H, m, $OC\mathbf{H}_AH_BCH_2$), 3.78-3.86 (1H, m, $OCH_A\mathbf{H}_BCH_2$), 3.98-4.12 (5H, m, $POC\mathbf{H}_2CH_3$, C**H**(OTHP)), 4.52_{maj}, 4.65_{min} (1H, t, $^3J_{H\text{-}H} = 6.8_{maj}$, 7.2_{min} Hz, $O_2C\mathbf{H}$), 4.85-4.97 (2H, m, $C(CH_3)C\mathbf{H}_2$).

^{13}C NMR (100.6 MHz) δ 16.4 (2C, d, $^3J_{C\text{-}P}$ = 6.0 Hz, $POCH_2\mathbf{C}H_3$), 16.8_{maj}, 17.9_{min} (1C, s, $\mathbf{C}H_3$), 19.4 (1C, s, $OCH_2CH_2\mathbf{C}H_2$), 21.1_{min}, 22.1_{maj} (1C, d, $^1J_{C\text{-}P}$ = 142.7 Hz, $P\mathbf{C}H_2$), 25.1_{min}, 26.4_{maj} (1C, d, $^2J_{C\text{-}P} = 4.6_{min}$, 4.1_{maj} Hz, $PCH_2\mathbf{C}H_2$), 25.36_{min}, 25.43_{maj} (1C, s, $OCH_2\mathbf{C}H_2$), 30.66_{maj}, 30.72_{min} (1C, s, $O_2CH\mathbf{C}H_2$), 61.42_{maj}, 61.45_{min} (2C, d, $^2J_{C\text{-}P}$ = 6.4 Hz, $PO\mathbf{C}H_2$), 62.3_{maj}, 62.6_{min} (1C, s, $O\mathbf{C}H_2CH_2$), 78.6_{maj}, 79.6_{min} (1C, d, $^3J_{C\text{-}P} = 19.8_{maj}$, 18.7_{min} Hz, **C**H(OTHP)), 94.9_{maj}, 97.5_{min} (1C, s, $O_2\mathbf{C}H$), 112.5_{min}, 114.5_{maj} (1C, s, $C(CH_3)\mathbf{C}H_2$), 143.2_{maj}, 144.3_{min} (1C, s, $\mathbf{C}(CH_3)CH_2$).

^{31}P NMR (161.9 MHz) δ 33.8_{min}, 33.6_{maj} (s, $(EtO)_2\mathbf{P}(O)CH_2CH_2CH(OTHP)C(CH_3)CH_2$).

IR: 3073, 2977, 2941, 2869, 1649, 1442, 1391, 1375, 1351, 1285, 1245, 1202, 1184, 1163, 1130, 1116, 1097, 1058, 1024, 963, 907, 869, 813, 788, 710.

m/z (CI): 320 ($[M]^+$ 2.2 %), 236 ($[M\text{-}DHP]^+$ 31.0 %), 235 ($[M\text{-}DHP\text{-}H]^+$ 24.8 %), 220 ($[M\text{-}DHP\text{-}O]^+$ 33.6 %), 219 ($[M\text{-}OTHP]^+$ 96.5 %), 195 ($[M\text{-}DHP\text{-}C(CH_3)CH_2]^+$ 13.2 %),

191 ([M-DHP-EtO]$^+$ 21.3 %), 166 ([M-C(OTHP)C(CH_3)CH_2]$^+$ 100 %), 165 ([M-CH(OTHP)C(CH_3)CH_2]$^+$ 17.4 %), 163 ([M-OTHP-C(CH_3)CH_2-CH_3]$^+$ 39.1 %), 139 ([$(EtO)_2P(O)H_2$]$^+$ 17.5 %), 138 ([M-C(OH)C(CH_3)CH_2-C_2H_4]$^+$ 35.6 %), 137 ([$(EtO)_2PO$]$^+$ 4.7 %), 111 ([(EtO)(HO)POH_2]$^+$ 14.5 %), 110 ([(EtO)(HO)POH]$^+$ 5.1 %), 109 ([(EtO)(HO)PO]$^+$ 12.3 %), 85 ([DHP+H]$^+$ 96.3 %), 81 ([$(HO)_2PO$]$^+$ 38.7 %).

HRMS: (CI) Calcd. for (M+1) $C_{15}H_{30}O_5P$: 321.1831, found: 321.1825.

4.2.1.38 Diethyl 3,4,5-trihydroxy-4-methylpentylphosphonate 122 and diethyl 4,5-dihydroxy-4-methyl-3-oxopentylphosphonate 123

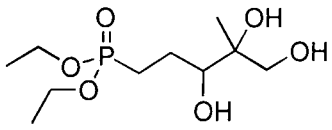

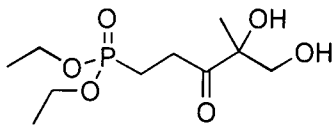

Diethyl 3-hydroxy-4-methylpent-4-enylphosphonate **121** (0.3 g, 1.27 mmol) was added to a solution of tetraethylammonium acetate tetrahydrate (81 mg, 0.31 mmol) in acetone (2.55 ml) and *tert*-butyl hydroperoxide (70 % w/w in water, 0.3 ml, 2.17 mmol). After cooling the solution to 0 °C, OsO_4 (~ 0.05 ml, of a 0.39 M solution in PhMe, ~ 0.02 mmol) was added and after 3 h the solution was allowed to warm to ambient temperature. The reaction was monitored by ^{31}P NMR, and after 2 h was quenched at 0 °C with 10 % $Na_2S_2O_{3(aq)}$ (0.63 ml). H_2O (5 ml) was then added, the mixture washed with CH_2Cl_2 (3 × 30 ml), and the organic washings combined, dried over $MgSO_4$ and the solvent removed under reduced pressure to afford a crude product **123** (0.108 g, ^{31}P NMR analysis indicated > 60 % purity). Purification of **123** over silica gel (IPA / CH_2Cl_2, 1:8, R_f = 0.30 for **123**, $KMnO_4$ stain as visualiser) afforded **123** as a clear colourless oil, > 99 % pure by ^{31}P NMR analysis. Isolation of **122** was achieved by freeze drying the aqueous residue from the extraction, followed by purification of the residue over silica gel (IPA / CH_2Cl_2, 1:4, R_f = 0.27 for **122**, $KMnO_4$ stain as visualiser) to afford **122** (62.2 mg, 0.23 mmol, 18.1 %) as a clear colourless oil. ^{31}P NMR analysis indicated > 99 % purity.

^1H NMR (400.0 MHz) δ 1.06 (3H, s, $\mathbf{C}H_3$), 1.33 (6H, t, $^3J_{H\text{-}H}$ = 7.0 Hz, $POCH_2\mathbf{C}H_3$), 1.55-2.09 (4H, m, $PC\mathbf{H}_2C\mathbf{H}_2$), 3.40 (1H, d, $^1J_{H\text{-}H}$ = 11.4 Hz, $C\mathbf{H}_A\mathbf{H}_B$OH), 3.64 (1H, d, $^3J_{H\text{-}}$

$_H$ = 10.8 Hz, C**H**(OH)), 3.80 (1H, d, $^1J_{H-H}$ = 11.4 Hz, $CH_A\mathbf{H_B}OH$), 3.99-4.10 (4H, m, $POC\mathbf{H}_2CH_3$).

^{13}C NMR (100.6 MHz) δ 16.4 (2C, d, $^3J_{C-P}$ = 6.1 Hz, $POCH_2\mathbf{C}H_3$), 19.1 (1C, s, $\mathbf{C}H_3$), 22.5 (1C, d, $^1J_{C-P}$ = 141.1 Hz, $P\mathbf{C}H_2$), 24.1 (1C, d, $^2J_{C-P}$ = 4.6 Hz, $PCH_2\mathbf{C}H_2$), 61.9, 62.1 (2C, d, $^2J_{C-P}$ = 6.8, 6.4 Hz, $PO\mathbf{C}H_2$), 67.8 (1C, s, $\mathbf{C}H_2OH$), 74.0 (1C, s, $\mathbf{C}(OH)(CH_3)$), 75.4 (1C, d, $^3J_{C-P}$ = 9.9 Hz, **C**H(OH)).

^{31}P NMR (161.9 MHz) δ 35.0 (1P, s, $(EtO)_2\mathbf{P}(O)CH_2CH_2CH(OH)C(OH)(CH_3)CH_2OH$).

IR: 3379, 3073, 2982, 2935, 2911, 2871, 1731, 1651, 1444, 1393, 1370, 1230, 1163, 1097, 1059, 1029, 965, 899, 792, 732.

m/z (EI): 271 ($[M+H]^+$ 22.9 %), 239 ($[M-CH_2OH]^+$ 25.1 %), 195 ($[M-C(OH)(CH_3)CH_2OH]^+$ 100 %), 152 ($[(EtO)_2P(O)CH_3]^+$ 37.0 %), 139 ($[(EtO)_2P(O)H_2]^+$ 14.4 %), 125 ($[(HO)(EtO)P(O)CH_3+H]^+$ 17.5 %), 121 ($[(EtO)_2P]^+$ 28.6 %).

HRMS: (CI) Calcd. for (M+1) $C_{10}H_{24}O_6P$: 271.1311, found: 271.1314.

Data for diethyl 4,5-dihydroxy-4-methyl-3-oxopentylphosphonate 123

^1H NMR (400.0 MHz) δ 1.210, 1.214 (3H, s, $\mathbf{C}H_3$), 1.26 (6H, t, $^3J_{H-H}$ = 7.0 Hz, $POCH_2C\mathbf{H}_3$), 1.96-2.06 (2H, m, $P\mathbf{C}H_2$), 2.83-2.93 (2H, m, $C\mathbf{H}_2CO$), 3.47 (1H, d, $^1J_{H-H}$ = 11.6 Hz, $C\mathbf{H_A}H_BOH$), 3.79 (1H, d, $^1J_{H-H}$ = 11.6 Hz, $CH_A\mathbf{H_B}OH$), 3.97-4.08 (4H, m, $POC\mathbf{H}_2CH_3$).

^{13}C NMR (100.6 MHz) δ 16.2 (2C, d, $^3J_{C-P}$ = 6.1 Hz, $POCH_2\mathbf{C}H_3$), 19.1 (1C, d, $^1J_{C-P}$ = 143.8 Hz, $P\mathbf{C}H_2$), 21.1 (1C, s, $\mathbf{C}H_3$), 30.5 (1C, d, $^2J_{C-P}$ = 3.4 Hz, $PCH_2\mathbf{C}H_2$), 62.0, 61.9 (2C, d, $^2J_{C-P}$ = 6.4 Hz, $PO\mathbf{C}H_2$), 68.4 (1C, s, $\mathbf{C}H_2OH$), 80.2 (1C, s, $\mathbf{C}(OH)(CH_3)$), 212.4 (1C, d, $^3J_{C-P}$ = 12.3 Hz, $CH_2\mathbf{C}O$).

^{31}P NMR (161.9 MHz) δ 33.3 (1P, s, $(EtO)_2\mathbf{P}(O)CH_2CH_2COC(OH)(CH_3)CH_2OH$).

IR: 3373, 2983, 2932, 2912, 2873, 1716, 1655, 1477, 1445, 1409, 1394, 1369, 1221, 1163, 1097, 1054, 1027, 970, 849, 794, 731.

m/z (EI): 269 ($[M+H]^+$ 4.1 %), 238 ($[M-CH_2O]^+$ 36.1 %), 195 ($[(EtO)_2P(O)CH_2CH_2CHOH]^+$ 26.9 %), 193 ($[(EtO)_2P(O)CH_2CH_2CO]^+$ 44.4 %), 166 ($[(EtO)_2P(O)Et]^+$ 100 %), 165 ($[(EtO)_2P(O)CH_2CH_2]^+$ 29.6 %), 152 ($[(EtO)_2P(O)CH_3]^+$ 28.1 %), 139 ($[(EtO)_2POH_2]^+$ 45.9 %), 138 ($[(EtO)_2POH]^+$ 80.9 %), 137 ($[(EtO)_2PO]^+$ 75.7 %), 125 ($[(HO)(EtO)P(O)CH_3+H]^+$ 24.7 %), 122 ($[(EtO)_2PH]^+$ 24.4 %), 121

($[(EtO)_2P]^+$ 29.9 %), 111 ($[(EtO)(HO)POH_2]^+$ 53.9 %), 110 ($[(EtO)(HO)POH]^+$ 21.5 %), 109 ($[(EtO)(HO)PO]^+$ 29.9 %), 82 ($[(HO)_2POH]^+$ 38.5 %).

HRMS: (CI) Calcd. for (M+1) $C_{10}H_{22}O_6P$: 269.1154, found: 269.1152.

4.2.1.39 Disodium 3,4,5-trihydroxy-4-methylpentylphosphonate 128 and sodium, ethyl 3,4,5-trihydroxy-4-methylpentylphosphonate 127

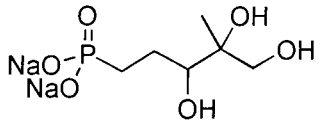

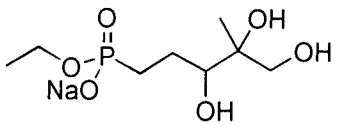

Diethyl 3,4,5-trihydroxy-4-methylpentylphosphonate **122** (33.3 mg, 0.123 mmol) in 0.1 M $NaOH_{(aq)}$ (6.16 ml, 0.616 mmol of NaOH) was heated under reflux for 1 h. After cooling, 0.1 M $HCl_{(aq)}$ was added until the solution became neutral. Freeze drying afforded a sample of NaCl and the monosodium salt **127**, > 99 % pure by ^{31}P NMR. After addition of **127** to 2 M $NaOH_{(aq)}$ (7.5 ml, 15 mmol of NaOH) followed by heating under reflux for 5 h, the solution was neutralised with 1 M $HCl_{(aq)}$ followed by freeze drying to afford NaCl and the disodium salt **128**, > 99 % by ^{31}P NMR analysis.

^1H NMR (400.0 MHz) (D_2O) δ 1.30 (3H, s, $\mathbf{C}H_3$), 1.67-1.80 (2H, m, $PC\mathbf{H}_2$), 1.91-2.10 (2H, m, $PCH_2C\mathbf{H}_2$), 3.67-3.82 (3H, m, $C\mathbf{H}(OH)$, $C\mathbf{H}_2OH$).

^{31}P NMR (161.9 MHz) (D_2O) δ 27.7 $(NaO)_2\mathbf{P}(O)CH_2CH_2CH(OH)C(OH)(CH_3)CH_2OH$.

Data for sodium, ethyl 3,4,5-trihydroxy-4-methylpentylphosphonate 127

^1H NMR (250.1 MHz) (D_2O) δ 0.99 (3H, s, $\mathbf{C}H_3$), 1.11 (3H, t, $^3J_{H\text{-}H}$ = 7.0 Hz, $POCH_2C\mathbf{H}_3$), 1.30-1.54 (2H, m, $PC\mathbf{H}_2$), 1.60-1.80 (2H, m, $PCH_2C\mathbf{H}_2$), 3.35-3.49 (3H, m, $C\mathbf{H}(OH)$, $C\mathbf{H}_2OH$), 3.71-3.63 (2H, m, $POC\mathbf{H}_2CH_3$).

^{13}C NMR (62.9 MHz) δ 18.4 (2C, d, $^3J_{C\text{-}P}$ = 5.7 Hz, $POCH_2\mathbf{C}H_3$), 20.2 (1C, s, $\mathbf{C}H_3$), 25.9 (1C, d, $^1J_{C\text{-}P}$ = 135.9 Hz, $P\mathbf{C}H_2$), 26.7 (1C, d, $^2J_{C\text{-}P}$ = 4.0 Hz, $PCH_2\mathbf{C}H_2$), 63.0 (1C, d, $^2J_{C\text{-}P}$ = 5.7 Hz, $PO\mathbf{C}H_2$), 68.9 (1C, s, $\mathbf{C}H_2OH$), 77.3 (1C, d, $^4J_{C\text{-}P}$ = 1.5 Hz, $\mathbf{C}(OH)(CH_3)$), 77.6 (1C, d, $^3J_{C\text{-}P}$ = 15.7 Hz, $\mathbf{C}H(OH)$).

^{31}P NMR (81.0 MHz) (D_2O) δ 29.4 $(NaO)_2\mathbf{P}(O)CH_2CH_2CH(OH)C(OH)(CH_3)CH_2OH$.

4.2.1.40 Diethyl (*E*)-5-hydroxyhex-3-enylphosphonate 130 and diethyl 5-hydroxyhexylphosphonate 131

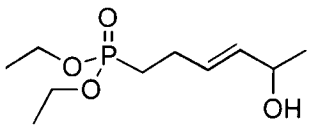
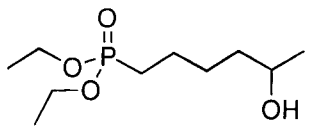

$NaBH_4$ (10 mg, 0.26 mmol) was added to a solution of diethyl *threo*-3,4-dihydroxy-5-oxohexylphosphonate **82** (50 mg, 0.19 mmol) in MeOH (2 ml) at 0 °C. After 1 h tlc indicated that **82** had been consumed (CH_2Cl_2 / EtOAc / IPA, 3:1:1, R_f = 0.53 for **130** and **131**, $KMnO_4$ stain as visualiser). H_2O (2 ml) was added, MeOH removed under reduced pressure then the mixture was washed with EtOAc (3 × 25 ml). The organic washings were combined, dried over $MgSO_4$ and the solvent was removed under reduced pressure, affording a crude mixture of **130** and **131** (60.5 mg). ^{31}P NMR analysis indicated > 95 % purity of a mixture of **130** and **131** in the ratio of 3:1.

^1H NMR (200.0 MHz) δ 1.26 (3H, d, $^3J_{H\text{-}H}$ = 6.6 Hz, CH(OH)C**H**$_3$), 1.28 (6H, t, $^3J_{H\text{-}H}$ = 7.1 Hz, POCH$_2$C**H**$_3$), 1.60-1.85 (2H, m, PC**H**$_2$CH$_2$), 2.19-2.50 (2H, m, PCH$_2$C**H**$_2$), 3.95-4.12 (4H, m, POC**H**$_2$), 4.13-4.29 (1H, m, C**H**(OH)CH$_3$), 5.45-5.70 (1H, m, C**H**C**H**).

^{13}C NMR (50.3 MHz) δ 16.4 (2C, d, $^3J_{C\text{-}P}$ = 5.9 Hz, POCH$_2$**C**H$_3$), 23.3 (1C, s, CH(OH)**C**H$_3$), 25.0 (1C, d, $^2J_{C\text{-}P}$ = 4.4 Hz, PCH$_2$**C**H$_2$), 25.3 (1C, d, $^1J_{C\text{-}P}$ = 140.6 Hz, P**C**H$_2$), 61.5 (2C, d, $^2J_{C\text{-}P}$ = 6.2 Hz, PO**C**H$_2$), 68.2 (1C, s, **C**H(OH)), 128.6 (1C, d, $^3J_{C\text{-}P}$ = 16.4 Hz, CH$_2$**C**H), 135.2 (1C, s, **C**HCH(OH)).

^{31}P NMR (81.0 MHz) δ 32.4 (1P, s, (EtO)$_2$**P**(O)CH$_2$CH$_2$CHCHCH(OH)CH$_3$).

Data for diethyl 5-hydroxyhexylphosphonate 131

^1H NMR (200.0 MHz) δ 1.14 (3H, d, $^3J_{H\text{-}H}$ = 6.6 Hz, CH(OH)C**H**$_3$), 1.28 (6H, t, $^3J_{H\text{-}H}$ = 7.1 Hz, POCH$_2$C**H**$_3$), 1.60-1.85 (2H, m, PC**H**$_2$), 2.19-2.50 (6H, m, C**H**$_2$C**H**$_2$C**H**$_2$CH(OH)), 3.60-3.80 (1H, m, C**H**(OH)CH$_3$), 3.95-4.12 (4H, m, POC**H**$_2$).

^{13}C NMR (50.3 MHz) δ 16.4 (2C, d, $^3J_{C\text{-}P}$ = 5.9 Hz, POCH$_2$**C**H$_3$), 22.4 (1C, d, $^2J_{C\text{-}P}$ = 5.1 Hz, PCH$_2$**C**H$_2$), 23.5 (1C, s, CH(OH)**C**H$_3$), 25.6 (1C, d, $^1J_{C\text{-}P}$ = 140.6 Hz, P**C**H$_2$), 26.6 (1C, d, $^3J_{C\text{-}P}$ = 14.3 Hz, CH$_2$**C**H), 38.6 (1C, s, **C**HCH(OH)), 61.4 (2C, d, $^2J_{C\text{-}P}$ = 5.5 Hz, PO**C**H$_2$), 67.4 (1C, s, **C**H(OH)).

^{31}P NMR (81.0 MHz) δ 33.5 (1P, s, (EtO)$_2$**P**(O)CH$_2$CH$_2$CH$_2$CH$_2$CH(OH)CH$_3$).

4.2.1.41 *Threo*-5-Acetyl-4-(2-diethoxyphosphonylethyl)-2,2-dimethyl-1,3-dioxolane 132

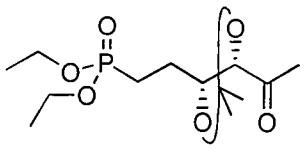

Diethyl 3,4-dihydroxy-5-oxohexylphosphonate **76** (182 mg, 68 mmol) was added to a solution of PTSA.H_2O (50 mg, 0.26 mmol) in 2,2-dimethoxypropane (15 ml, 0.12 mol). After 14 h, tlc indicated that **76** had been consumed (CH_2Cl_2 / EtOAc / IPA, 3:1:0.5, R_f = 0.65 for **132** and 0.2 for **76**, $KMnO_4$ stain as visualiser). The solvent was removed under reduced pressure then H_2O (15 ml) added and the mixture washed with CH_2Cl_2 (3 × 65 ml). The organic washings were combined, dried over $MgSO_4$ and solvent again removed under reduced pressure. Purification of the residue over silica gel (Et_2O / IPA, 25:1, R_f = 0.35 for **132**, $KMnO_4$ stain as visualiser) afforded **132** (166 mg, 54 mmol, 79.4 %) as a clear colourless oil. ^{31}P NMR analysis indicated > 99 % purity and the ^{1}H NMR displayed two rotational isomers in an approximate ratio of 3 : 4.

^{1}H NMR (400.0 MHz) δ 1.28_{maj}, 1.29_{min} (6H, t, $^{3}J_{H\text{-}H}$ = 7.0 Hz, $POCH_2C\mathbf{H}_3$), 1.37_{maj}, 1.38_{min}, 1.40_{maj}, 1.41_{min} (6H, s, $C(C\mathbf{H}_3)_2$), 1.73-2.09 (4H, m, $PC\mathbf{H}_2C\mathbf{H}_2$), 2.23_{maj}, 2.24_{min} (3H, s, $COC\mathbf{H}_3$), 3.91_{maj}, 3.92_{min} (1H, d, $^{3}J_{H\text{-}H}$ = 7.6 Hz, $C\mathbf{H}(OC(CH_3)_2)COCH_3$), 3.94-4.00 (1H, m, $CH_2C\mathbf{H}(OC(CH_3)_2)$), 4.00-4.11 (4H, m, $POC\mathbf{H}_2$).

^{13}C NMR (100.6 MHz) δ 16.4 (2C, d, $^{3}J_{C\text{-}P}$ = 5.7 Hz, $POCH_2\mathbf{C}H_3$), 21.7 (1C, d, $^{1}J_{C\text{-}P}$ = 143.1 Hz, $P\mathbf{C}H_2$), 26.1, 26.4 (2C, s, $C(\mathbf{C}H_3)_2$), 26.7 (1C, d, $^{2}J_{C\text{-}P}$ = 4.2 Hz, $PCH_2\mathbf{C}H_2$), 27.0 (1C, s, $CO\mathbf{C}H_3$), 61.59, 61.53 (2C, d, $^{2}J_{C\text{-}P}$ = 5.9 Hz, $PO\mathbf{C}H_2$), 77.3 (1C, d, $^{3}J_{C\text{-}P}$ = 17.6 Hz, $CH_2\mathbf{C}H(OC(CH_3)_2)$), 84.9 (1C, s, $\mathbf{C}H(OC(CH_3)_2)COCH_3$), 110.4 (1C, s, $\mathbf{C}(CH_3)_2$), 208.4 (1C, s, $\mathbf{C}OCH_3$).

^{31}P NMR (161.9 MHz) δ 32.3 (1P, s, $(EtO)_2\mathbf{P}(O)CH_2CH_2CH(OC(CH_3)_2O)CHCOCH_3$).

IR: 2985, 2934, 2909, 2874, 1717 (C=O), 1457, 1442, 1418, 1382, 1372, 1358, 1241, 1165, 1081, 1056, 1027, 963, 907, 863, 836, 787.

m/z (EI): 309 ($[M+H]^+$ 0.4 %), 293 ($[M\text{-}CH_3]^+$ 12.5 %), 265 ($[M\text{-}COCH_3]^+$ 10.3 %), 250 ($[M\text{-}(CH_3)_2CO]^+$ 20.4 %), 247 ($[M\text{-}O\text{-}EtO]^+$ 27.4 %), 235 ($[M\text{-}(CH_3)_2CO\text{-}CH_3]^+$ 7.2 %), 207 ($[M\text{-}(CH_3)_2CO\text{-}COCH_3]^+$ 100 %), 195 ($[(EtO)_2P(O)CH_2CH_2CHO]^+$ 11.9 %), 179 ($[M\text{-}(CH_3)_2CO\text{-}COCH_3\text{-}C_2H_4]^+$ 32.9 %), 151 ($[M\text{-}(CH_3)_2CO\text{-}COCH_3\text{-}2(C_2H_4)]^+$ 83.4 %).

HRMS: (CI) Calcd. for (M+1) $C_{13}H_{26}O_6P$: 309.1467, found: 309.1470.

4.2.1.42 *Threo*-4-(2-Diethoxyphosphonylethyl)-5-(1(*R*,*S*)-hydroxyethyl)-2,2-dimethyl-1,3-dioxolane 133

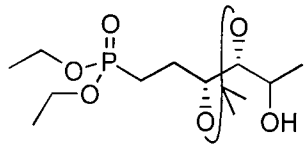

$NaBH_4$ (16.5 mg, 0.44 mmol) was added to a solution of *threo*-5-acetyl-4-(2-diethoxyphosphonylethyl)-2,2-dimethyl-1,3-dioxolane **132** (134 mg, 0.43 mmol) in MeOH (5 ml) at -20 °C. After 15 min tlc indicated that **132** had been consumed (CH_2Cl_2 / EtOAc / IPA, 3:1:0.5, R_f = 0.4 for **133** and 0.65 for **132**, $KMnO_4$ stain as visualiser). H_2O (15 ml) was added, then the mixture was washed with CH_2Cl_2 (3 × 80 ml). The organic washings were combined, dried over $MgSO_4$ and the solvent was removed under reduced pressure, affording **133** (123 mg, 0.40 mmol, 91.2 %) as a clear colourless oil. ^{31}P NMR analysis indicated > 99 % purity of a diastereomeric mixture in the ratio of 3:7.

^1H NMR (400.0 MHz) δ 1.16-1.20 (3H, m, CH(OH)C**H**$_3$), 1.27 (6H, t, $^3J_{H-H}$ = 7.0 Hz, POCH$_2$C**H**$_3$), 1.32-1.36 (6H, m, C(C**H**$_3$)$_2$), 1.69-2.03 (4H, m, PC**H**$_2$C**H**$_2$), 3.45-3.51 (1H, m, C**H**(OC(CH$_3$)$_2$)CH(OH)), 3.64-3.74 (1H, m, C**H**(OH)CH$_3$), 3.76-3.90 (1H, m, CH$_2$C**H**(OC(CH$_3$)$_2$)), 3.96-4.11 (4H, m, POC**H**$_2$).

^{13}C NMR (100.6 MHz) δ 16.3 (2C, d, $^3J_{C-P}$ = 6.1 Hz, POCH$_2$**C**H$_3$), 19.3$_{min}$, 19.7$_{maj}$ (1C, s, C(OH)**C**H$_3$), 21.9$_{min}$, 22.0$_{maj}$ (1C, d, $^1J_{C-P}$ = 142.3 Hz, P**C**H$_2$), 26.5$_{maj}$, 27.4$_{min}$ (1C, d, $^2J_{C-P}$ = 4.5 Hz, PCH$_2$**C**H$_2$), 27.0$_{maj+min}$, 27.2$_{min}$, 27.3$_{maj}$ (2C, s, C(**C**H$_3$)$_2$), 61.5-61.6 (2C, m, PO**C**H$_2$), 67.1$_{maj}$, 67.8$_{min}$ (1C, s, **C**H(OH)), 76.9$_{maj}$, 77.7$_{min}$ (1C, d, $^3J_{C-P}$ = 16.4$_{maj}$, 14.6$_{min}$ Hz, CH$_2$**C**H(OC(CH$_3$)$_2$)), 84.0$_{min}$, 84.5$_{maj}$ (1C, s, **C**H(OC(CH$_3$)$_2$)CH(OH)), 108.5$_{min}$, 108.9$_{maj}$ (1C, s, **C**(CH$_3$)$_2$).

^{31}P NMR (161.9 MHz) δ 32.8$_{maj}$, 33.4$_{min}$ (1P, s, (EtO)$_2$**P**(O)CH$_2$CH$_2$CH(OC(CH$_3$)$_2$O)CHCH(OH)CH$_3$).

IR: 3390, 2984, 2934, 2908, 2875, 1654, 1443, 1379, 1370, 1236, 1178, 1163, 1096, 1058, 1029, 964, 906, 871, 827, 806, 789.

m/z (CI CH$_4$): 351 ([M+C$_3$H$_5$]$^+$ 10.4 %), 339 ([M+Et]$^+$ 25.5 %), 312 ([M+2H]$^+$ 32.8 %), 311 ([M+H]$^+$ 100 %), 295 ([M-CH$_3$]$^+$ 18.1 %), 281 ([M-Et]$^+$ 8.9 %), 265 ([M-CH(OH)CH$_3$]$^+$ 9.2 %), 253 ([M-(CH$_3$)$_2$CO+H]$^+$ 74.0 %), 235 ([M-(CH$_3$)$_2$CO-OH]$^+$ 54.3 %), 209 ([M-(CH$_3$)$_2$CO-COCH$_3$]$^+$ 21.1 %), 207 ([M-(CH$_3$)$_2$CO-CH(OH)CH$_3$]$^+$ 19.7 %),

195 ($[(EtO)_2P(O)CH_2CH_2CHO]^+$ 17.8 %), 179 ($[M-(CH_3)_2CO-CH(OH)CH_3-C_2H_4]^+$ 5.9 %), 139 ($[(EtO)_2POH_2)]^+$ 16.1 %).

HRMS: (CI) Calcd. for (M+1) $C_{13}H_{27}O_6P$: 311.1624, found: 311.1625.

4.2.1.43 Disodium *threo*-5(*R,S*)-3,4,5-trihydroxyhexylphosphonate 134

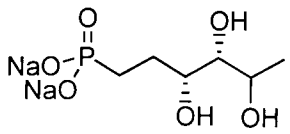

TMSBr (0.3 ml, 2.32 mmol) was added to *threo*-4-(2-diethoxyphosphonylethyl)-5-(1(*R,S*)-hydroxyethyl)-2,2-dimethyl-1,3-dioxolane **133** (56 mg, 0.18 mmol) and after 4 h, H_2O (10 ml) was added. After 14 h 1M $NaOH_{(aq)}$ was added until the solution was neutral. Freeze drying afforded (59 mg) of **134** and NaBr as a white amorphous solid (mp dec. ~ 250 °C). ^{31}P NMR analysis indicated ~ 85 % purity, with the main impurity being sodium, ethyl *threo*-5(*R,S*)-3,4,5-trihydroxyhexylphosphonate **135**, ~ 12 %. ^1H and ^{13}C NMR analysis of **134** indicated a diastereomeric mixture in the ratio of 3:7.

^1H NMR (400.0 MHz) (D_2O) δ 1.04_{maj}, 1.06_{min} (3H, d, $^3J_{H-H}$ = 6.4_{maj}, 7.6_{min} Hz, CH(OH)C**H**$_3$), 1.33-1.66 (4H, m, PC**H**$_2$C**H**$_2$), 3.45-3.51 (1H, m, C**H**(OH)CH_3), 3.15_{maj}, 3.19_{min} (1H, dd, $^3J_{H-H}$ = 5.6_{maj}, 6.8_{min} Hz, $^3J_{H-H}$ = 3.6_{maj}, 3.2_{min} Hz, CH(OH)C**H**(OH)CH(OH)), $3.52\text{-}3.58_{maj}$, $3.58\text{-}3.63_{min}$ (1H, m, CH_2C**H**(OH)), 3.67-3.79 (1H, m, C**H**(OH)CH_3).

^{13}C NMR (100.6 MHz) (D_2O) δ 18.1_{min}, 18.5_{maj} (1C, s, C(OH)**C**H_3), 24.6 (1C, d, $^1J_{C-P}$ = 133.9 Hz, P**C**H_2), 27.6_{min}, 27.5_{maj} (1C, d, $^2J_{C-P}$ = 3.7 Hz, PCH_2**C**H_2), 67.4_{min}, 68.5_{maj} (1C, s, **C**H(OH)CH_3), 71.2_{min}, 72.3_{maj} (1C, d, $^3J_{C-P}$ = 16.8 Hz, CH_2**C**H(OH)), 76.6_{min}, 77.0_{maj} (1C, s, CH(OH)**C**H(OH)CH(OH)).

^{31}P NMR (161.9MHz) (D_2O) δ 26.3 $(NaO)_2$**P**(O)CH_2CH_2CH(OH)CH(OH)CH(OH)CH_3), 29.2 (NaO)(EtO)**P**(O)CH_2CH_2CH(OH)CH(OH)CH(OH)CH_3).

4.2.2 Experimental section for Chapter 2

Work carried out by Hannah F. Sore (4th year MSci student).

4.2.2.1 2-(Diethoxyphosphonyl)propanamide[145] 137

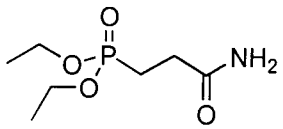

Acrylamide (3.55 g, 0.05 mol) was added to triethyl phosphite (10.72 ml, 0.06 mmol) and phenol (12.5 g, 0.13 mol) and the mixture heated at 100 °C for 1 d. After cooling, the residue was purified over silica gel (EtOAc / IPA, 3:1, $KMnO_4$ stain as visualiser) affording **137** (6.03 g, 0.03 mol, 57.8 %) as a pale yellow solid (mp 76.0-76.5 °C, Lit.[145] 74-76 °C). ^{31}P NMR analysis indicated > 99 % purity.

^{1}H NMR (400.0 MHz) δ 1.33 (6H, t, $^{3}J_{H-H}$ = 7.0 Hz, C**H**$_3$), 2.04-2.13 (2H, m, PC**H**$_2$), 2.49-2.58 (2H, m, PCH$_2$C**H**$_2$), 4.04-4.15 (4H, m, OC**H**$_2$), 5.83 (2H, s, N**H**$_2$).

^{13}C NMR (100.6 MHz) δ 16.4 (2C, d, $^{3}J_{C-P}$ = 5.7 Hz, **C**H$_3$), 20.9 (1C, d, $^{1}J_{C-P}$ = 143.8 Hz, P**C**H$_2$), 28.5 (1C, d, $^{2}J_{C-P}$ = 4.2 Hz, PCH$_2$**C**H$_2$), 61.9 (2C, d, $^{2}J_{C-P}$ = 6.5 Hz, O**C**H$_2$), 173.2 (1C, d, $^{3}J_{C-P}$ = 14.9 Hz, **C**ONH$_2$).

^{31}P NMR (161.9 MHz) δ 36.2 (1P, s, (EtO)$_2$**P**(O)CH$_2$CH$_2$CONH$_2$).

IR: 3375, 3200, 2983, 2931, 1672, 1629, 1437, 1418, 1397, 1313, 1282, 1231, 1159, 1024, 979, 885, 830, 803, 760, 669.

m/z (EI): 209 ([M]$^+$ 4.5 %), 166 ([M-CONH]$^+$ 100 %), 165 ([M-CONH$_2$]$^+$ 37.8 %), 164 ([M-HCONH$_2$]$^+$ 22.9 %), 139 ([(EtO)$_2$POH$_2$]$^+$ 21.9 %), 138 ([(EtO)$_2$POH]$^+$ 62.1 %), 137 ([(EtO)$_2$PO]$^+$ 31.1 %), 136 ([M-Et,CONH$_2$]$^+$ 47.9 %), 122 ([M-Et,-CH$_2$CONH$_2$]$^+$ 12.4 %), 111 ([(EtO)P(OH)(OH$_2$)]$^+$ 48.3 %), 110 ([(EtO)P(OH)$_2$]$^+$ 20.5 %), 109 ([(EtO)PO(OH)]$^+$ 34.0 %), 83 ([(HO)$_3$PH]$^+$ 14.0 %), 82 ([(HO)$_3$P]$^+$ 35.8 %), 81 ([(HO)$_2$PO]$^+$ 21.9 %), 73 ([CH$_2$CH$_2$CONH$_2$]$^+$ 17.5 %), 72 ([M-PO(OEt)$_2$)]$^+$ 16.1 %), 65 ([(HO)$_2$P]$^+$ 20.3 %), 55 ([(CH$_2$CHCO]$^+$ 25.9 %), 44 ([(CONH$_2$]$^+$ 22.0 %).

4.2.2.2 *N*-(3-Diethoxyphosphonyl)propionyl-acetamide 54

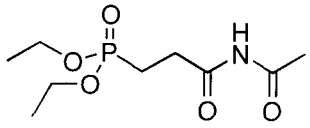

2-(Diethoxyphosphonyl)propanamide (0.50 g, 2.39 mmol) **137** was added to acetic anhydride (1.13 ml, 12.0 mmol) and conc. H_2SO_4 (1 drop) and heated at 84 °C for 2 h. The mixture was then added to H_2O (10 ml) at 0 °C and was washed with CH_2Cl_2 (3 × 20 ml). The organic washings were combined, washed with 5 % $NaHCO_{3(aq)}$ until neutral, and then washed with brine (10 ml). The organic washings were then dried over $MgSO_4$ and solvent was removed under reduced pressure. Purification of the residue by kugelrohr bulb to bulb distillation (~ 30 °C / 0.1 mbar) afforded **54** (0.29 g, 1.12 mmol, 46.9 %) as a viscous colourless oil which solidified on standing to afford white crystals (mp 48-52 °C). ^{31}P NMR analysis indicated > 93 % purity.

^1H NMR (400.0 MHz) δ 1.32 (6H, t, $^3J_{H\text{-}H}$ = 7.0 Hz, C**H**$_3$), 2.04-2.14 (2H, m, PC**H**$_2$), 2.33 (3H, s, COC**H**$_3$), 2.78-2.87 (2H, m, PCH$_2$C**H**$_2$), 4.05-4.17 (4H, m, OC**H**$_2$), 9.25 (1H, s, N**H**).

^{13}C NMR (100.6 MHz) δ 16.4 (2C, d, $^3J_{C\text{-}P}$ = 6.1 Hz, **C**H$_3$), 20.1 (1C, d, $^1J_{C\text{-}P}$ = 144.5 Hz, P**C**H$_2$), 25.1 (1C, s, CO**C**H$_3$), 30.3 (1C, d, $^2J_{C\text{-}P}$ = 3.0 Hz, PCH$_2$**C**H$_2$), 62.0 (2C, d, $^2J_{C\text{-}P}$ = 6.5 Hz, O**C**H$_2$), 171.6 (1C, s, NH**C**OCH$_3$) 171.8 (1C, d, $^3J_{C\text{-}P}$ = 16.8 Hz, PCH$_2$CH$_2$**C**O).

^{31}P NMR (161.9 MHz) δ 31.8 (1P, s, (EtO)$_2$**P**(O)CH$_2$CH$_2$CONHCOCH$_3$).

IR: 3161, 2985, 2934, 1755, 1705, 1514, 1443, 1393, 1375, 1229, 1098, 1026, 975, 797, 708, 610.

m/z (EI): 252 ([M+H]$^+$ 2.2 %), 236 ([M-CH$_3$]$^+$ 12.6 %), 166 ([M-CONCOCH$_3$]$^+$ 70.7 %), 165 ([M-CONHCOCH$_3$]$^+$ 55.5 %), 164 ([M-HCONHCOCH$_3$]$^+$ 38.4 %), 138 ([(EtO)$_2$POH]$^+$ 57.5 %), 137 ([(EtO)$_2$PO]$^+$ 93.4 %), 136 ([M-Et,CONHCOCH$_3$]$^+$ 54.6 %), 111 ([(EtO)P(OH)(OH$_2$)]$^+$ 35.9 %), 109 ([(EtO)PO(OH)]$^+$ 38.5 %), 86 ([CONHCOCH$_3$]$^+$ 36.6 %), 84 ([(HO)$_3$PH]$^+$ 57.7 %), 65 ([(HO)$_2$P]$^+$ 19.7 %), 55 ([(CH$_2$CHCO]$^+$ 34.5 %).

Elemental Analysis: Calcd. for $C_9H_{18}NO_5P$: C: 43.0, H: 7.2, N: 5.6 %, found: C: 42.3, H: 7.2, N: 5.5 %.

4.2.2.3 *N*-(3-Disodiumphosphonyl)propionyl-acetamide 138

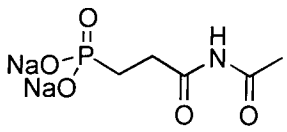

TMSBr (3 equivalents) was added to *N*-(3-Disodiumphosphonyl)propionyl-acetamide **54** (1 equivalent) and 2 h later volatiles were removed under reduced presseure. H_2O (4 ml) was then added and the reaction immediately neutralised with $NaOH_{(aq)}$. Freeze drying afforded impure **138** as a white solid. ^{31}P NMR analysis indicated ~ 80 % purity.

^{1}H NMR (400.0 MHz) δ 1.62-1.73 (2H, m, PC**H**$_2$), 2.09 (3H, s, COC**H**$_3$), 2.48-2.56 (2H, m, PCH$_2$C**H**$_2$).

^{13}C NMR (100.6 MHz) δ 23.3 (1C, d, $^{1}J_{C\text{-}P}$ = 133.5 Hz, P**C**H$_2$), 24.4 (1C, s, CO**C**H$_3$), 32.3 (1C, d, $^{2}J_{C\text{-}P}$ = 2.0 Hz, PCH$_2$**C**H$_2$), 174.5 (1C, s, NH**C**OCH$_3$) 175.9 (1C, d, $^{3}J_{C\text{-}P}$ = 17.5 Hz, PCH$_2$CH$_2$**C**O).

^{31}P NMR (161.9 MHz) δ 23.0 (1P, s, (NaO)$_2$**P**(O)CH$_2$CH$_2$CONHCOCH$_3$).

IR: 3451, 1755, 1639, 1618, 1547, 1505, 1410, 1377, 1279, 1235, 1155, 1135, 1061, 977, 918.

m/z : Positive or negative FAB did not afford any molecular ion information.

4.2.3 Experimental section for Chapter 3

4.2.3.1 2-(Fluoromethyl)pyridine[156] 141

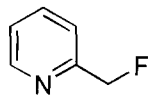

K_2CO_3 (2.51 g, 18.2 mmol) was added to a solution of 2-(chloromethyl)pyridine hydrochloride (5.03 g, 30.7 mmol) in Et_2O (50 ml) and H_2O (20 ml). After 10 min the mixture was extracted into Et_2O (3 × 50 ml), the extracts combined, dried over $MgSO_4$ and solvent removed under reduced pressure. The organic residue was added to a solution of 18-crown-6 (0.52 g, 2.0 mmol) and KF (4.84 g, 83.3 mmol) in CH_3CN (40 ml) then heated under reflux for 8 d (reaction progress monitored by ^1H NMR). After cooling, the reaction was quenched with sat. $NaHCO_{3(aq)}$ (70 ml), the aqueous layer separated, and then extracted into Et_2O (3 × 80 ml). The organic extracts were combined, washed with H_2O (3 × 100 ml), then dried over $MgSO_4$. The solvent was removed under reduced pressure and distillation (64-66 °C / 15 mmHg, Lit.[156] 80 °C / 12 mmHg) afforded **141** (0.47 g, 4.2 mmol, 13.8 %), as a clear colourless oil. GCMS analysis indicated > 99 % purity.

^1H NMR (400.0 MHz) δ 5.44 (2H, d, $^2J_{H\text{-}F}$ = 47.1 Hz, C**H**$_2$F), 7.19 (1H, dd, $^3J_{H4\text{-}H5}$ = 7.4 Hz, $^3J_{H5\text{-}H6}$ = 5.1 Hz, **H5**), 7.40 (1H, d, $^3J_{H3\text{-}H4}$ = 7.9 Hz, **H3**), 7.69 (1H, dt, $^3J_{H3\text{-}H4}$ = 7.9 Hz, $^3J_{H4\text{-}H5}$ = 7.4 Hz, $^4J_{H4\text{-}H6}$ = 1.5 Hz, **H4**), 8.53 (1H, d, $^3J_{H5\text{-}H6}$ = 5.1 Hz, **H6**).

^{13}C NMR (100.6 MHz) δ 84.3 (1C, d, $^1J_{C\text{-}F}$ = 169.7 Hz, **C**α), 120.4 (1C, d, $^3J_{C\text{-}F}$ = 5.7 Hz, **C3**), 122.9 (1C, d, $^5J_{C\text{-}F}$ = 1.1 Hz, **C5**), 136.7 (1C, s, **C4**), 149.1 (1C, s, **C6**), 156.2 (1C, d, $^2J_{C\text{-}F}$ = 21.4 Hz, **C2**).

^{19}F NMR (376.3 MHz) δ -220.8 (1F, t, $^2J_{H\text{-}F}$ = 47.1 Hz, CH_2**F**, Lit.[156] δ -203.4, $^2J_{H\text{-}F}$ = 47.1 Hz).

IR: (GG) 2961(m), 2360(m), 2340(m), 1259(s), 1072(s), 1014(s), 796(s).

m/z (EI): 111 ($[M]^+$ 100 %).

4.2.3.2 Bis-2,6-(fluoromethyl)pyridine 143

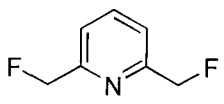

Bis-2,6-(chloromethyl)pyridine (3.88 g, 22.1 mmol) in CH_3CN (20 ml) was added to a solution of 18-crown-6 (0.30 g, 1.1 mmol) and KF (5.60 g, 96.4 mmol) in CH_3CN (40 ml) and heated under reflux for 10 d (reaction progress monitored by ^1H NMR). After cooling, the reaction was quenched with sat. $NaHCO_{3(aq)}$ (100 ml), the aqueous layer separated, and then extracted into Et_2O (3 × 100 ml). The organic extracts were combined, washed with H_2O (3 × 150 ml), then dried over $MgSO_4$. The solvent was removed under reduced pressure and distillation (54-57 °C / 15 mmHg) afforded **143** (1.58 g, 11.0 mmol, 50.0 %), as clear colourless crystals (mp 34.5-35.5 °C). GCMS analysis indicated > 99 % purity. Recrystallisation from acetone / petrol at -20 °C afforded crystals suitable for X-ray analysis.

^1H NMR (400.0 MHz) δ 5.46 (2H, d, $^2J_{H\text{-}F}$ = 46.7 Hz, C**H**$_2$F), 7.41 (2H, d, $^3J_{H\text{-}H}$ = 7.7 Hz, **H3**), 7.81 (1H, t, $^3J_{H\text{-}H}$ = 7.7 Hz, **H4**).

^{13}C NMR (100.6 MHz) δ 84.1 (2C, d, $^1J_{C\text{-}F}$ = 169.7 Hz, **C**α), 119.8 (2C, d, $^3J_{C\text{-}F}$ = 5.7 Hz, **C3**), 137.8 (1C, s, **C4**), 156.0 (2C, d, $^2J_{C\text{-}F}$ = 20.3 Hz, **C2**).

^{19}F NMR (376.3 MHz) δ -221.4 (1F, t, $^2J_{H\text{-}F}$ = 46.7 Hz, CH_2**F**).

IR: (GG) 2953(w), 1597(s), 1582(s), 1460(s), 1449(s), 1368(s), 1026(s), 994(s), 898(s), 786(s), 610(s).

m/z (EI): 142.75 ($[M]^+$ 100%).

HRMS: (EI) Calcd. for $C_7H_7F_2N$: 143.0546, found: 143.0546.

4.2.3.3 2-(Fluoromethyl)quinoline[183] 144

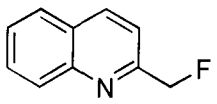

K_2CO_3 (1.69 g, 12.2 mmol) was added to a solution of 2-(chloromethyl)quinoline hydrochloride (5.08 g, 23.7 mmol) in Et_2O (50 ml) and H_2O (10 ml). After 10 min the mixture was extracted into Et_2O (3 × 50 ml), the extracts combined, dried over $MgSO_4$

and solvent removed under reduced pressure. The organic residue (3.84 g) was added to a solution of 18-crown-6 (0.31 g, 1.2 mmol) and KF (2.58 g, 44.4 mmol) in CH_3CN (45 ml) then heated under reflux for 14 d (reaction progress monitored by ^1H NMR). After cooling the reaction was quenched with sat. $NaHCO_{3(aq)}$ (70 ml), the aqueous layer separated and extracted into Et_2O (3 × 80 ml). The organic extracts were combined, washed with H_2O (3 × 90 ml), then dried over $MgSO_4$. The solvent was removed under reduced pressure followed by fractional distillation using a Vigreux column. The first fraction (118-120 °C / 15 mmHg, Lit.[183] 126 °C / 14 mmHg) afforded **144** (1.65 g, 47.3 %), GCMS analysis indicated ≥ 97 % purity, main impurity 2-(chloromethyl)quinoline. The second fraction (45-50 °C / 0.01 mbar) afforded **143** (0.93 g, 26.7 %), GCMS analysis indicated approximately a 1 : 4 ratio of 2-(chloromethyl)quinoline : **144**, to afford **144** in total yield of about 70 %. On standing both fractions slowly decomposed to give dark red oils. Crystallisation from MeOH / H_2O in a sealed system at -10 °C afforded clear colourless needle shaped crystals (mp 39-40 °C) of monohydrated **147** suitable for X-ray analysis.

^1H NMR (400.0 MHz) δ 5.63 (2H, d, $^2J_{H\text{-}F}$ = 47.0 Hz, C**H**$_2$F), 7.50 (1H, t, $^3J_{H8\text{-}H9}$ = 8.2 Hz, $^3J_{H7\text{-}H8}$ = 7.0 Hz, **H8**), 7.54 (1H, d, $^3J_{H3\text{-}H4}$ = 8.6 Hz, **H3**), 7.67 (1H, t, $^3J_{H6\text{-}H7}$ = 8.2 Hz, $^3J_{H7\text{-}H8}$ = 7.0 Hz, **H7**), 7.77 (1H, d, $^3J_{H8\text{-}H9}$ = 8.2 Hz, **H9**), 8.03 (1H, d, $^3J_{H6\text{-}H7}$ = 8.2 Hz, **H6**), 8.15 (1H, d, $^3J_{H3\text{-}H4}$ = 8.6 Hz, **H4**).

^{13}C NMR (100.6 MHz) δ 84.8 (1C, d, $^1J_{C\text{-}F}$ = 170.1 Hz, **C**α), 118.0 (1C, d, $^3J_{C\text{-}F}$ = 4.9 Hz, **C3**), 127.5 (1C, s, **C5**), 126.6 (1C, s, **C7**), 127.6 (1C, s, **C8**), 128.9 (1C, s, **C6**), 129.8 (1C, s, **C9**), 136.9 (1C, s, **C4**), 147.2 (1C, s, **C10**), 156.6 (1C, d, $^2J_{C\text{-}F}$ = 21.7 Hz, **C2**).

^{19}F NMR (376.3 MHz) δ –221.3 (1F, t, $^2J_{H\text{-}F}$ = 47.0 Hz, CH_2**F**).

IR: (GG) 1600(m), 1506(s), 1428(m), 1375(m), 1032(s), 986(s), 821(s), 782(s), 750(s), 726(s), 616(s).

m/z (EI): 161 ($[M]^+$ 100%).

4.2.3.4 2-(Fluoromethyl)pyridine-*N*-oxide 145

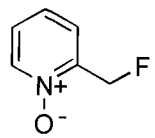

2-(Fluoromethyl)pyridine (153 mg, 1.38 mmol) was added to a mixture of glacial acetic acid (1 ml) and H_2O_2 (27.5 % w/w in water, 0.5 ml) and the mixture then heated for 2 h at 70 °C. After cooling, H_2O (15 ml) was added and the volume reduced to half under reduced pressure. More H_2O (15 ml) was added and the volume reduced to half again under reduced pressure. The residue was taken up in $CHCl_3$ (5 ml), and then shaken with sat. $K_2CO_{3(aq)}$ until effervescence ceased. The organic layer was then separated, dried over $MgSO_4$ and the solvent was removed under reduced pressure followed by kugelrohr bulb to bulb distillation (~ 100 °C / 0.01 mbar) to afford **145** (81 mg, 0.64 mmol, 46.3 %) as a clear yellow oil. GCMS analysis indicated ≥ 99 % purity.

^{1}H NMR (400.0 MHz) δ 5.65 (2H, d, $^2J_{H\text{-}F}$ = 47.0 Hz, C**H**$_2$F), 7.28 (1H, t, $^3J_{H4\text{-}H5}$ = 7.3 Hz, $^3J_{H5\text{-}H6}$ = 6.6 Hz, **H5**), 7.37 (1H, t, $^3J_{H3\text{-}H4}$ = 8.0 Hz, $^3J_{H4\text{-}H5}$ = 7.3 Hz, **H4**), 7.49 (1H, d, $^3J_{H3\text{-}H4}$ = 8.0 Hz, **H3**), 8.22 (1H, d, $^3J_{H5\text{-}H6}$ = 6.6 Hz, **H6**).

^{13}C NMR (100.6 MHz) δ 78.8 (1C, d, $^1J_{C\text{-}F}$ = 170.9 Hz, **C**α), 122.4 (1C, d, $^3J_{C\text{-}F}$ = 8.3 Hz, **C3**), 124.6 (1C, s, **C5**), 126.0 (1C, s, **C4**), 139.0 (1C, s, **C6**), 147.9 (1C, d, $^2J_{C\text{-}F}$ = 26.7 Hz, **C2**).

^{19}F NMR (376.3 MHz) δ -234.3 (1F, t, $^2J_{H\text{-}F}$ = 47.1 Hz, CH$_2$**F**).

IR: (GG) 3088(m), 1494(s), 1434(s), 1368(s), 1222(s), 1028(s), 846(s), 767(s).

m/z (EI): 110 ([M–OH]$^+$ 100 %), 127 ([M]$^+$ 49.6 %).

HRMS: (EI) Calcd. for C_6H_6FNO: 127.0433, found: 127.0433.

Elemental Analysis: Calcd. for C_6H_6FNO: C: 56.7, H: 4.8, N: 11.0 %, found: C: 56.6, H: 4.7, N: 10.9 %.

4.2.3.5 Bis-2,6-(fluoromethyl)pyridine-*N*-oxide 146

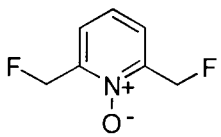

Bis-2,6-(fluoromethyl)pyridine (230 mg, 1.61 mmol) was added to a mixture of glacial acetic acid (2 ml) and H_2O_2 (27.5 % w/w in water, 1 ml) and the mixture then heated for 3 h at 70 °C. After cooling, H_2O (30 ml) was added and the volume reduced to half under reduced pressure. More H_2O (30 ml) was added and the volume reduced to half again under reduced pressure. The residue was taken up in CH_2Cl_2 (20ml), then shaken with sat. $K_2CO_{3(aq)}$ until effervescence ceased. The organic layer was then separated, dried over $MgSO_4$ and the solvent was removed under reduced pressure to yield **146** (156 mg, 61.0 %) as a white amorphous solid (pure by GCMS). Recrystallisation from Et_2O afforded clear colourless crystals (mp 80.5-81.5 °C) suitable for X-ray analysis.

^{1}H NMR (400.0 MHz) δ 5.66 (2H, d, $^2J_{H\text{-}F}$ = 46.4 Hz, C**H**$_2$F), 7.41-7.50 (3H, m, **H3**, **4**, **5**).
^{13}C NMR (100.6 MHz) δ 78.6 (2C, d, $^1J_{C\text{-}F}$ = 171.4 Hz, **C**α), 121.1 (2C, d, $^3J_{C\text{-}F}$ = 8.0 Hz, **C3**), 125.9 (1C, s, **C4**), 147.0 (2C, d, $^2J_{C\text{-}F}$ = 26.4 Hz, **C2**).
^{19}F NMR (376.3 MHz) δ -234.3 (2F, t, $^2J_{H\text{-}F}$ = 46.8 Hz, CH$_2$**F**).
IR: (KBr) 3092, 3049, 2972, 2938, 2455, 1993, 1504, 1456, 1420, 1367, 1266, 1257, 1233, 1221, 1056, 1018, 903, 848, 801, 631, 550.
m/z (EI): 142 ([M–OH]$^+$ 100 %), 159 ([M]$^+$ 40.7 %).
HRMS: (EI) Calcd. for $C_7H_7F_2NO$: 159.0495, found: 159.0495.

4.2.3.6 Benzyl fluoride[167] 148

Tetrabutylammonium bromide (5.42 g, 16.8 mmol) and CsF (25.54g, 168 mmol) were mixed intimately with a pestal and morter then added to benzyl bromide (10 ml, 84.1 mmol) and heated for 3 h and 15 min at 85 °C. After cooling, the mixture was filtered and washed with Et_2O (3 × 100 ml). The filtrate and washings were then combined, and the solvent was removed under reduced pressure. Distillation (25-30 °C / 15 mmHg, Lit.[184] 41 °C / 17 mmHg) afforded **148** (5.94 g, 53.9 mmol, 64.2 %) as a clear

colourless oil. Redistillation (collecting the middle fraction (34 °C / 15 mmHg), gave a sample of **148** which was > 99.9 % pure by GCMS analysis) provided a sample suitable for low temperature X-ray analysis.

^{1}H NMR (400.0 MHz) δ 5.40 (2H, d, $^{2}J_{H\text{-}F}$ = 47.8 Hz, C**H**$_2$F), 7.34-7.46 (5H, m, **Ph**).
^{13}C NMR (100.6 MHz) δ 84.6 (1C, d, $^{1}J_{C\text{-}F}$ = 165.9 Hz, **C**H$_2$F), 127.5 (2C, d, $^{3}J_{C\text{-}F}$ = 5.7 Hz, **C2**), 128.6 (2C, d, $^{4}J_{C\text{-}F}$ = 1.1 Hz, **C3**), 128.7 (1C, d, $^{5}J_{C\text{-}F}$ = 3.1 Hz, **C4**), 136.2 (1C, d, $^{2}J_{C\text{-}F}$ = 16.8 Hz, **C1**).
^{19}F NMR (376.3 MHz) δ -203.8 (1F, t, $^{2}J_{H\text{-}F}$ = 47.8 Hz, PhCH$_2$**F**).
IR: 3090, 3067, 3035, 2959, 2897, 1955, 1879, 1813, 1589, 1498, 1455, 1379, 1313, 1216, 1080, 983, 913, 820, 745, 697.
m/z (EI): 111 ([M+H]$^+$ 3.1 %), 110 ([M]$^+$ 48.6 %), 109 ([M-H]$^+$ 100 %), 91 ([M-F]$^+$ 3.9 %), 83 (8.9 %), 63 (5.9 %), 51 (5.3 %).

4.2.3.7 4-Bromobenzyl fluoride[185] 149

Diethylaminosulphur trifluoride (1.20 g, 7.44 mmol) was added dropwise to a solution of 4-bromobenzyl alcohol **151** (1.00 g, 5.35 mmol) in CH_2Cl_2 (15 ml) at -78 °C. After 30 min H_2O (30 ml) was added, the organic phase separated then washed with CH_2Cl_2 (2 × 30 ml). The organic phase was then dried over $MgSO_4$ and the solvent removed under reduced pressure. Purification of the residue over silica gel (petrol / EtOAc, 10 : 1, R_f = 0.1 for **151**, and 0.6 for **149**, UV lamp or $KMnO_4$ stain as visualiser) afforded **149** (0.30 g, 1.60 mmol, 30 % yield) as a white waxy solid (mp 33 °C, Lit.[185] 33 °C). Slow cooling of a neat liquid sample afforded crystals suitable for X-ray analysis.

^{1}H NMR (299.9 MHz) δ 5.33 (2H, d, $^{2}J_{H\text{-}F}$ = 47.6 Hz, C**H**$_2$F), 7.23-7.27 (2H, m, **Ph**), 7.51-7.54 (2H, m, **Ph**).
^{13}C NMR (75.4 MHz) δ 83.7 (1C, d, $^{1}J_{C\text{-}F}$ = 167.4 Hz, **C**H$_2$F), 122.7 (1C, d, $^{5}J_{C\text{-}F}$ = 3.7 Hz, **C4**), 129.0 (2C, d, $^{3}J_{C\text{-}F}$ = 6.2 Hz, **C2**), 131.7 (2C, d, $^{4}J_{C\text{-}F}$ = 1.1 Hz, **C3**), 135.1 (1C, d, $^{2}J_{C\text{-}F}$ = 17.3 Hz, **C1**).
^{19}F NMR (188.2 MHz) δ -208.0 (1F, t, $^{2}J_{H\text{-}F}$ = 47.6 Hz, CH$_2$**F**).

IR: 3047, 3032, 2960, 2897, 1901, 1785, 1595, 1489, 1467, 1408, 1374, 1305, 1213, 1106, 1071, 1011, 987, 944, 837, 799, 630.

4.2.3.8 *Trans*-4-fluoromethylstilbene 150

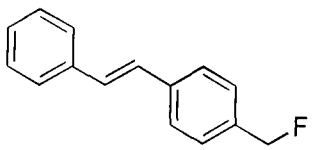

Diethylaminosulphur trifluoride (142 mg, 0.88 mmol) was added dropwise to a solution of *trans*-4-hydroxymethylstilbene **152** (169 mg, 0.80 mmol) in THF (5 ml) at -78 °C. After 30 min H_2O (10 ml) was added, the mixture washed with CH_2Cl_2 (3 × 30 ml), the organic washings combined, dried over $MgSO_4$ and then solvent removed under reduced pressure. Purification over silica gel (neat CH_2Cl_2, R_f = 0.2 for **152**, and 0.85 for **150**, UV lamp or $KMnO_4$ stain as visualiser) gave **150** (41 mg, 24 % yield for **150**). Recrystallisation from $CHCl_3$ afforded a sample > 99 % pure by NMR. Mp 131-132 °C from CH_3CN / H_2O.

^{1}H NMR (400.0 MHz) δ 5.31 (2H, d, $^2J_{H\text{-}F}$ = 47.6 Hz, C**H**$_2$F), 7.06 (2H, d, $^3J_{H\text{-}H}$ = 2.0 Hz, PhC**H**C**H**PhCH$_2$F), 7.18-7.50 (9H, m, **Ph**).

^{13}C NMR (100.6 MHz) δ 84.4 (1C, d, $^1J_{C\text{-}F}$ = 165.9 Hz, **C**α), 126.6 (2C, s, **C8**), 126.7 (2C, d, $^3J_{C\text{-}F}$ = 1.5 Hz, **C2**), 127.8 (1C, s, **C10**), 128.0 (1C, s, **C5**), 128.1 (1C, s, **C6**), 128.7 (2C, s, **C9**), 129.4 (2C, d, $^4J_{C\text{-}F}$ = 1.5 Hz, **C3**), 135.3 (1C, d, $^2J_{C\text{-}F}$ = 16.8 Hz, **C1**), 137.1 (1C, s, **C7**), 137.9 (1C, d, $^5J_{C\text{-}F}$ = 3.4 Hz, **C4**).

^{19}F NMR (376.3 MHz) δ -206.3 (1F, t, $^2J_{H\text{-}F}$ = 47.6 Hz, PhCHCHPhCH$_2$**F**).

IR: 3027, 2957, 2895, 1607, 1510, 1492, 1450, 1419, 1372, 1215, 1179, 973, 948, 839, 824, 785, 759, 694, 625, 567, 522.

4.2.3.9 *N*-(2-Fluoroethyl)-3,5-dinitrobenzamide 155

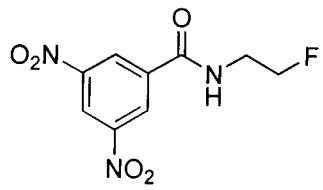

K_2CO_3 (282 mg, 2.04 mmol) in H_2O (1 ml) was added to 2-fluoroethylamine hydrochloride (101 mg, 1.01 mmol) and 3,5-dinitrobenzoyl chloride (219 mg, 1.01 mmol) in benzene (3 ml) and CH_2Cl_2 (3 ml). The reaction was followed by tlc (EtOAc / petrol, 1:1, R_f = 0.44 for **155**, $KMnO_4$ stain as visualiser). After 90 min CH_2Cl_2 (10 ml), 10 % $K_2CO_{3(aq)}$ (5 ml) and MeOH (1 ml) were added, the organic layer separated, CH_2Cl_2 (10 ml) and 10 % $K_2CO_{3(aq)}$ (15 ml) added. The organic layer was separated again, then washed with H_2O (10 ml), dried over $MgSO_4$ and the solvent removed under reduced pressure to afford crude **155** as a white solid (43 mg). Recrystallisation twice from CH_2Cl_2 / $CHCl_3$ afforded **155** as clear colourless needle shaped crystals (10 mg, 0.04 mmol, 3.8 %) suitable for X-ray analysis (mp 139-149 °C, from CH_2Cl_2 / $CHCl_3$).

^{1}H NMR (400.0 MHz) δ 3.76 (2H, dq, $^3J_{H\text{-}F}$ = 27.9 Hz, $^3J_{H\text{-}H}$ = 5.1 Hz, NC**H**$_2$), 4.60 (2H, dt, $^2J_{H\text{-}F}$ = 47.3 Hz, $^3J_{H\text{-}H}$ = 4.7 Hz, C**H**$_2$F), 8.37 (1H, s, N**H**), 9.05 (2H, d, $^4J_{H\text{-}H}$ = 2.0 Hz, **H2**), 9.12 (1H, t, $^4J_{H\text{-}H}$ = 2.0 Hz, **H4**).

^{13}C NMR (100.6 MHz) δ 40.9 (1C, d, $^2J_{C\text{-}F}$ = 19.8 Hz, N**C**H$_2$), 82.1 (1C, d, $^1J_{C\text{-}F}$ = 167.9 Hz, **C**H$_2$F), 121.0 (1C, s, **C4**), 127.6 (2C, s, **C2**), 137.5 (1C, s, **C1**), 148.5 (2C, s, **C3**), 163.3 (1C, s, **C**O).

^{19}F NMR (376.3 MHz) δ -224.0 (1F, tt, $^2J_{H\text{-}F}$ = 47.2 Hz, $^2J_{H\text{-}F}$ = 27.8 Hz, CH$_2$CH$_2$**F**).

IR: (KBr) 3312, 3086, 3010, 2982, 2950, 2920, 2880, 1864, 1646, 1627, 1539, 1474, 1452, 1432, 1347, 1325, 1297, 1191, 1083, 1039, 936, 923, 863, 732, 724.

m/z (EI): 257 ([M]$^+$ 18.5 %), 237 ([M-HF]$^+$ 11.8 %), 224 ([M-CH_2F]$^+$ 30.7 %), 220 ([M-HF-OH]$^+$ 10.7 %), 207 ([M-NO-HF]$^+$ 29.8 %), 195 ([M-$HNCH_2CH_2F$]$^+$ 100 %), 149 ([M-$HNCH_2CH_2F$-NO_2]$^+$ 39.0 %), 103 ([M-$HNCH_2CH_2F$-2(NO_2)]$^+$ 11.3 %), 75 ([C_6H_3)]$^+$ 44.7 %).

Elemental Analysis: Calcd. for $C_9H_8FN_3O_5$: C: 42.0, H: 3.1, N: 16.3 %, found: C: 42.0, H: 3.1, N: 16.0 %.

4.2.3.10 *N*-(2-Fluoroethyl)-4-nitrobenzamide 156

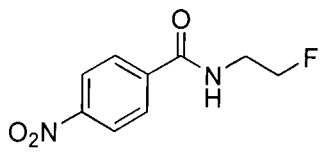

K_2CO_3 (290 mg, 2.10 mmol) in H_2O (2.5 ml) was added to 2-fluoroethylamine hydrochloride (10 mg, 1.00 mmol) and 4-nitrobenzoyl chloride (200 mg, 1.08 mmol) in benzene (3 ml) and CH_2Cl_2 (0.5 ml). After 2 h the mixture was filtered, washed with H_2O (30 ml), 10 % $K_2CO_{3(aq)}$ (15 ml), then additional H_2O (20 ml), to afford crude **156** (43 mg). Crystallisation from CH_2Cl_2 afforded **156** as clear colourless needle shaped crystals (13.6 mg, 0.06 mmol, 6.4 %). Recrystallisation from THF afforded crystals suitable for X-ray analysis (mp 123-124 °C, from THF).

^{1}H NMR (400.0 MHz) δ 3.82 (2H, dq, $^3J_{H\text{-}F}$ = 28.4 Hz, $^3J_{H\text{-}H}$ = 5.1 Hz, NC**H**$_2$), 4.63 (2H, dt, $^2J_{H\text{-}F}$ = 47.3 Hz, $^3J_{H\text{-}H}$ = 4.7 Hz, C**H**$_2$F), 6.59 (1H, s, N**H**), 7.94-7.98 (2H, m, **H2**), 8.28-8.33 (2H, m, **H3**).

^{13}C NMR (100.6 MHz) δ 40.7 (1C, d, $^2J_{C\text{-}F}$ = 19.4 Hz, N**C**H$_2$), 82.5 (1C, d, $^1J_{C\text{-}F}$ = 167.1 Hz, **C**H$_2$F), 123.9 (2C, s, **C3**), 128.2 (2C, s, **C2**), 139.6 (1C, s, **C1**), 149.7 (1C, s, **C4**), 165.6 (1C, s, **C**O).

^{19}F NMR (376.3 MHz) δ -224.7 (1F, tt, $^2J_{H\text{-}F}$ = 47.2 Hz, $^2J_{H\text{-}F}$ = 28.2 Hz, CH$_2$CH$_2$**F**).

IR: (KBr) 3334, 3109, 3085, 2960, 2934, 1941, 1807, 1643, 1601, 1551, 1523, 1490, 1420, 1345, 1297, 1119, 1055, 1044, 1027, 1014, 871, 855, 812, 717, 684, 639, 624.

m/z (EI): 212 ([M]$^+$ 12.7 %), 193 ([M-F]$^+$ 5.8 %), 192 ([M-HF]$^+$ 42.3 %), 179 ([M-CH$_2$F]$^+$ 9.2 %), 163 ([M-NO-F]$^+$ 8.6 %), 162 ([M-NO-HF]$^+$ 60.4 %), 151 ([M-NCH$_2$CH$_2$F]$^+$ 6.6 %), 150 ([M-HNCH$_2$CH$_2$F]$^+$ 60.9 %), 120 ([M-HNCH$_2$CH$_2$F-NO]$^+$ 5.5 %), 104 ([M-HNCH$_2$CH$_2$F-NO$_2$]$^+$ 23.9 %), 76 ([C$_6$H$_4$]$^+$ 32.2 %), 46 ([NO$_2$]$^+$ 43.9 %), 30 ([NO]$^+$ 100 %).

Elemental Analysis: Calcd. for $C_9H_9FN_2O_3$: C: 51.0, H: 4.3, N: 13.2 %, found: C: 50.7, H: 4.3, N: 12.8 %.

4.2.3.11 *N*-(2-Fluoroethyl)acetamide 157

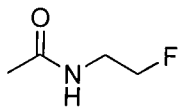

Acetyl chloride (0.29 ml, 4.08 mmol) was added to an ice cold solution of 2-fluoroethylamine hydrochloride (0.3 g, 3.01 mmol) in CH_2Cl_2 (10 ml), followed by pyridine (0.49 ml, 6.06 mmol). After 20 min, H_2O (5 ml) was added and the mixture was washed with CH_2Cl_2 (4 × 20 ml). The organic extracts were combined, dried over $MgSO_4$ and then solvent was removed under reduced pressure. Purification of the residue over silica gel (CH_2Cl_2 / IPA, 7:1, R_f = 0.35 for **157**, Iodine as visualiser), followed by lyophilisation to remove acetic acid afforded **157** (59.6 mg, 0.57 mmol, 18.8 %) as a clear pale yellow oil. ^{19}F NMR analysis indicated > 92 % purity.

^1H NMR (400.0 MHz) δ 1.97 (3H, s, C**H**$_3$), 3.49 (2H, dq, $^3J_{H\text{-}F}$ = 28.4 Hz, $^3J_{H\text{-}H}$ = 5.2 Hz, NC**H**$_2$), 4.43 (2H, dt, $^2J_{H\text{-}F}$ = 47.2 Hz, $^3J_{H\text{-}H}$ = 4.8 Hz, C**H**$_2$F), 6.52 (1H, s, N**H**).

^{13}C NMR (100.6 MHz) δ 22.9 (1C, s, **C**H$_3$), 39.9 (1C, d, $^2J_{C\text{-}F}$ = 19.4 Hz, N**C**H$_2$), 82.6 (1C, d, $^1J_{C\text{-}F}$ = 166.3 Hz, **C**H$_2$F), 170.8 (1C, s, **C**O).

^{19}F NMR (376.3 MHz) δ -224.4 (1F, tt, $^2J_{H\text{-}F}$ = 47.8 Hz, $^2J_{H\text{-}F}$ = 27.7 Hz, CH$_2$CH$_2$**F**).

IR: 3439, 3296, 3095, 2967, 2934, 2852, 1713, 1659, 1650, 1643, 1633, 1564, 1555, 1468, 1428, 1377, 1298, 1241, 1126, 1107, 1046, 951, 884, 823.

m/z (EI): 106 ($[M+1]^+$ 53.1 %), 105 ($[M]^+$ 100 %), 90 ($[M\text{-}CH_3]^+$ 10.1 %), 86 ($[M\text{-}F]^+$ 2.7 %), 85 ($[M\text{-}HF]^+$ 27.3 %), 72 ($[M\text{-}CH_2F]^+$ 72.9 %), 62 ($[M\text{-}CH_3CO]^+$ 8.6 %), 60 ($[CH_3CONH_3]^+$ 16.4 %), 48 ($[CH_3CH_2F]^+$ 27.5 %), 47 ($[CH_2CH_2F]^+$ 28.2 %), 44 ($[CH_3CHO]^+$ 72.9 %), 43 ($[CH_3CO]^+$ 82.3 %).

HRMS: (EI) Calcd. for C_4H_8FNO: 105.0590, found: 105.0591.

References

1 J. W. Cornforth, R. H. Cornforth, A. Pelter, M. G. Horning, G. Popják; *Tetrahedron;* 1959, **5**, 311-339.

2 G. Flesch, M. Rohmer; *Eur.J. Biochem;* 1988, **175**, 405-411.

3 H. K. Lichtenthaler, M. Rohmer, J. Schwender; *Physiologia Plantarum;* 1997, **101**, 643-652.

4 M. Rohmer, B. Sutter, H. Sahm; *J. Chem. Soc. Chem. Commun;* 1989, 1471-1472.

5 M. Rohmer, M. Knani, P. Simonin, B. Sutter, H. Sahm; *Biochem. J;* 1993, **295**, 517-524.

6 M. Rohmer, M. Seemann, S. Horbach. S. Bringer-Meyer, H. Sahm; *J. Am. Chem. Soc;* 1996, **118**, 2564-2566.

7 S.T.J. Broers; *PhD Thesis;* ETH Zürich, Switzerland; 1994, No. 10978.

8 G. A. Sprenger, U. Schörken, T. Wiegert, S. Grolle, A. A. De Graaf, S. V. Taylor, T. P. Begley, S. Bringer-Meyer, H. Sahm; *Proc. Natl. Acad. Sci. USA;* 1997, **94**, 12857-12862.

9 L. M. Lois, N. Campos, S. R. Putra, K. Danielsen, M. Rohmer, A. Boronat; *Proc. Natl. Acad. Sci. USA;* 1998, **95**, 2105-2110.

10 T. Kuzuyama, S. Takahashi, H. Watanabe, H. Seto; *Tetrahedron Lett;* 1998, **39**, 4509-4512.

11 S. Takahashi, T. Kuzuyama, H. Watanabe, H. Seto; *Proc. Natl. Acad. Sci. USA;* 1998, **95**, 9879-9884.

12 T. Duvold, P. Calf, J-M Bravo, M. Rohmer; *Tetrahedron Lett;* 1997, **35**, 6181-6184.

13 J-L. Giner, B. Jaun, D. Arigoni; *J. Chem. Soc; Chem. Commun;* 1998, 1857-1858.

14 J-L. Giner, B. Jaun; *Tetrahedron Lett;* 1998, **39**, 8021-8022.

15 J. Schwender, M. Seeman, H. K. Lichtenthaler, M. Rohmer; *Biochem. J;* 1996, **316**, 73-80.

16 W. Eisenreich, B. Menhard, P. J. Hylands, M. H. Zenk, A. Bacher; *Proc. Natl. Acad. Sci. USA;* 1996, **93**, 6431-6436.

17 H. K. Lichtenthaler, J. Schwender, A. Disch, M. Rohmer; *FEBS Letters;* 1997, **400**, 271-274.

18 W. Eisenreich, S. Sagner, M. H. Zenk, A. Bacher; *Tetrahedron Lett;* 1997, **38**, 3889-3892.

19 D. Arigoni, W. Eisenreich, C. Latzel, S. Sagner, T. Radykewicz, M. H. Zenk, A. Bacher; *Proc. Natl. Acad. Sci. USA;* 1999, **96**, 1309-1314.

20 M. Fellermeier, K. Kis, S. Sagner, U. Maier, A. Bacher, M. H. Zenk; *Tetrahedron Lett;* 1999, **40**, 2743-2746.

21 D. J. Fowler, J. T. G. Hamilton, A. J. Humphrey, D. O'Hagan; *Tetrahedron Lett;* 1999, **40**, 3803-3806.

22 D. Arigoni, J-L. Giner, S. Sagner, J. Wungsintaweekul, M. H. Zenk, K. Kis, A. Bacher, W. Eisenreich; *J. Chem. Soc; Chem. Commun;* 1999, 1127-1128.

23 B. M. Lange, R. Croteau; *Arch. Biochem. Biophys;* 1999, **365**, 170-174.

24 I. D. Spenser, R. L. White; *Angew. Chem. Int. Ed. Engl;* 1997, **36**, 1032-1046.

25 T. Bugg; *An Introduction to Enzyme and Coenzyme Chemistry;* 1997, 155-157, Blackwell Science, Oxford.

26 H. Kumaoka, G. M. Brown; *Arch. Biochem. Biophys. Acta;* 1967, **122**, 378-384.

27 S. David, B. Estramareix, H. Hirshfeld; *Biochem. Biophys. Acta;* 1967, **148**, 11-21.

28 P. C. Newell, R. G. Tucker; *Biochem. J;* 1968, **106**, 271-277.

29 P. C. Newell, R. G. Tucker; *Biochem. J;* 1968, **106**, 279-287.

30 B. Estramareix, S. David; *Biochem. Biophys. Acta;* 1990, **1035**, 154-160.

31 B. Estramareix, M. Thérisod; *J. Am. Chem. Soc;* 1984, **106**, 3857-3860.

32 K. Tazuya, K. Yamada, H. Kumaoka; *Biochem. Biophys. Acta;* 1989, **990**, 73-79.

33 K. Tazuya, C. Azumi, K. Yamada, H. Kumaoka; *Biochem. Mol. Biol. Int;* 1995, **36**, 883-888.

34 B. Estramareix, M. Thérisod; *Biochem. Biophys. Acta;* 1972, **273**, 275-282.

35 R. H. White, F. B. Rudolph; *Biochem. Biophys. Acta;* 1978, **542**, 340-347.

36 J-H. Julliard, R. Douce; *Proc. Natl. Acad. Sci. USA;* 1991, **88**, 2042-2045.

37 K. Himmeldirk, I. D. Spenser, *J. Am. Chem. Soc;* 1998, **120**, 3581-3589.

38 K. Himmeldirk, I. A. Kennedy, R. E. Hill, B. G. Sayer, I. D. Spenser; *J. Chem. Soc; Chem. Commun;* 1996, 1187-1188.

39 I. D. Spenser, R. E. Hill; *Nat. Prod. Rep;* 1995, **12**, 555-565.

40 J.-H. Julliard, *C. R. Seances Acad. Sci. Paris (Ser. III);* 1992, **314**, 285-290.

41 R. E. Hill, P. Horsewood, I. D. Spenser, Y. Tani; *J. Chem. Soc; Perkin Trans. 1;* 1975, 1622-1627.

42 G. J. Vella, R. E. Hill, B. S. Mootoo, I. D. Spenser; *J. Biol. Chem;* 1980, **255**, 3042-3048.

43 A. Iwanow, R. E. Hill, B. G, Sayer, I. D. Spenser; *J. Am. Chem. Soc;* 1984, **106**, 1840-1841.

44 G. Zhao, M. E. Winkler; *J. Bacteriol;* 1994, **176**, 6134-6138.

45 Y. Yang, G. Zhao, T.-K. Man, M. E. Winkler; *J. Bacteriol;* 1998, **180**, 4294-4299.

46 C. Drewke, M. Klein, D. Clade, A. Arenz, R. Müller, E. Leistner; *FEBS Lett;* 1996, **390**, 179-181.

47 E. Wolf, R. E. Hill, B. G, Sayer, I. D. Spenser; *J. Chem. Soc; Chem. Commun;* 1995, 1339-1340.

48 I. A. Kennedy, R. E. Hill, R. M. Pauloski, B. G, Sayer, I. D. Spenser; *J. Am. Chem. Soc;* 1995, **117**, 1661-1662.

49 G. Zhao, M. E; *FEMS Microbiol. Lett;* 1996, **135**, 275-280.

50 B. Laber, W. Maurer, S. Scharf, K. Stepusin, F. S. Schimdt; *FEBS Lett;* 1999, **449**, 45-48.

51 D. E. Cane, S. Du, J. K. Robinson, Y. Hsiung, I. D. Spenser; *J. Am. Chem. Soc;* 1999, **121**, 7722-7723.

52 D. E. Cane, Y. Hsiung, J. A. Cornish, J. K. Robinson, I. D. Spenser; *J. Am. Chem. Soc;* 1998, **120**, 1936-1937.

53 T. Kuzuyama, T. Shimizu, S. Takahashi, H. Seto; *Tetrahedron Lett;* 1998, **39**, 7913-7916.

54 T. Bugg; *An Introduction to Enzyme and Coenzyme Chemistry;* 1997, 90-91, Blackwell Science, Oxford.

55 D. F. Wiemer; *Tetrahedron;* 1997, **53**, 16609-16644.

56 D. O'Hagan, H. S. Rzepa; *J. Chem. Soc; Chem. Commun;* 1997, 645-652.

57 K. E. Stremler, C. D. Poulter; *J. Am. Chem. Soc;* 1987, **109**, 5542-5544.

58 T. R. Burke, M. S. Smyth, A. Otaka, M. Nomizu, P. P. Roller, G. Wolf, R. Case, S. E. Shoelson; *Biochemistry*; 1994, **33**, 6490-6494.

59 J. Nieschalk, A. S. Batsanov, D. O'Hagan, J. A. K. Howard; *Tetrahedron;* 1996, **52**, 165-176.

60 S. C. Fields; *Tetrahedron;* 1999, **55**, 12237-12273.

61 T. Kamiya, K. Hemmi, H. Takeno, M. Hashimoto; *Tetrahedron Lett;* 1980, **21**, 95-98.

62 E. Takahashi, T. Kimura, K. Nakamura, M. Arahira, M. Iida; *J. Antibiotics;* 1995, **48**, 1124-1129.

63 K. Nakamura, S. Yamamura; *Tetrahedron Lett;* 1997, **38**, 437-438.

64 T. Bugg; *An Introduction to Enzyme and Coenzyme Chemistry;* 1997, 113-115, Blackwell Science, Oxford.

65 A. Bacher, *et al*; *Biochem. Soc. Trans;* 1996, **24**, 89-94.

66 D. B. Jordan, K. O. Bacot, T. J. Carlson, M. Kessel, P. V. Viitanen; *J. Biol. Chem;* 1999, **274**, 22114-22121.

67 E. Gotze, K. Kis, W. Eisenreich, N. Yamauchi, K. Kakinuma, A. Bacher; *J. Org. Chem;* 1998, **63**, 6456-6457.

68 R. Volk, A. Bacher; *J. Biol. Chem;* 1991, **266**, 20610-20618.

69 M. H. Gelb, J. P. Saven, R. H. Abeles; *Biochemistry;* 1985, **24**, 1813-1817.

70 R. J. Linderman, D. M. Graves, S. Garg, K. Venkatesh, D. D. Anspaugh, R. M. Roe; *Tetrahedron Lett;* 1993, **34**, 3227-3230.

71 D. Schirlin, S. Baltzer, J. M. Altenburger, C. Tarnus, J. M. Renny; *Tetrahedron;* 1996, **52**, 305-318.

72 K. N. Allen, R. H. Abeles; *Biochemistry;* 1989, **28**, 8466-8473.

73 D. Bouvet, D. O'Hagan; *Tetrahedron;* 1999, **55**, 10481-10486.

74 C. E. McKenna, M. T. Higa, N. H. Cheung, M.-C. McKenna; *Tetrahedron Lett;* 1977, **2**, 155-158.

75 H. C. Kolb, M. S. VanNieuwenhze, K. B. Sharpless; *Chem. Rev;* 1994, **94**, 2483-2547.

76 P. J. Walsh, K. B. Sharpless; *Synlett;* 1993, 605-606.

77 T. Yokomatsu, T. Yamagishi, K. Suemune, Y. Yoshida, S. Shibuya; *Tetrahedron;* 1998, **54**, 767-780.

78 R. D. Chambers, R. Jaouhari, D. O'Hagan; *J. Fluorine Chem;* 1989, **44**, 275-284.

79 D. J. Burton, R. Takei, S. Shin-Ya; *J. Fluorine Chem;* 1981, **18**, 197-202.

80 D. J. Burton, R. M. Flynn; *J. Fluorine Chem;* 1977, **10**, 329-332.

81 S. A. Matlin, P. G. Sammes; *J. Chem. Soc; Chem. Commun;* 1972, 1222-1223.

82 M. Tiecco, L. Testaferri, M. Tingoli, D. Bartoli, R. Balducci; *J. Org. Chem;* 1990, **55**, 429-434.

83 T. Janecki, R. Bodalski; *Synthesis*; 1989, 506-510.

84 D. J. Burton, L. G. Sprague; *J. Org. Chem;* 1989, **54**, 613-617.

85 C. Patois, P. Savignac; *J. Chem. Soc; Chem. Commun;* 1993, 1711-1712.

86 R. Waschbüsch, J. Carren, P. Savignac; *Tetrahedron;* 1996, **52**, 14199-14216.

87 G. Sturtz, A. Pondaven-Raphalen; *J. Chem. Res. Miniprint;* 1980, 2512-2523.

88 G. Lavielle, G. Sturtz, H. Normant; *Bull. Soc. Chim. Fr;* 1967, 4186-4194.

89 J.-M. Varlet, N. Colligon; *Syn. Commun;* 1978, 335-343.

90 Z. H. Kudzin, A. Kotyński, G. Andrijewske; *J. Organomet. Chem;* 1994, **479**, 199-205.

91 J. M. Varlet, G. Fabre, F. Sauveur, N. Collignon; *Tetrahedron;* 1981, **37**, 1377-1384.

92 A. I. Razumov, V. V. Moskva; *J. Gen. Chem. USSR;* 1964, **34**, 2612-2616.

93 P. Savignac, A. Brèque, F. Mathey; *Syn. Commun;* 1979, 487-496.

94 S. F. Martin, Y. L. Wong, A. S. Wagman; *J. Org. Chem.;* 1994, **59**, 4821-4831.

95 J.-M. Varlet, N. Colligon; *Syn. Commun;* 1978, 335-343.

96 Z. H. Kudzin, A. Kotyński, G. Andrijewske; *J. Organomet. Chem;* 1994, **479**, 199-205.

97 J. M. Varlet, G. Fabre, F. Sauveur, N. Collignon; *Tetrahedron;* 1981, **37**, 1377-1384.

98 A. I. Razumov, V. V. Moskva; *J. Gen. Chem. USSR;* 1964, **34**, 2612-2616.

99 B. Iorga, F. Eymery, V. Mouriès, P. Savignac; *Tetrahedron;* 1998, **54**, 14637-14677.

100 J. Leroy, C. Wakselman; *Synthesis;* 1982, 496-497.

101 M. M. Chaabouni, A. Baklouti; *Bull. Soc. Chim. Fr;* 1989, 549-553.

102 E. D. Bergmann, S. Cohen; *J. Chem. Soc;* 1958, 2259-2262.

103 E. Cherbuliez, A. Yazgi, J. Rabinowitz; *Helv. Chim, Acta;* 1960, **43**, 1135-1145.

104 J. B. Silverman, P. S. Babiarz, K. P. Mahajan, J. Buschek, T. P. Fondy; *Biochemistry;* 1975, **14**, 2252-2258.

105 M. M. Chaabouni, A. Baklouti; *J. Fluorine Chem;* 1990, **47**, 227-233.

106 R. F. Hudson, P. A. Chopard; *J. Org. Chem;* 1963, **28**, 2446-2447.

107 G. H. Posner, G. L. Loomis; *Tetrahedron Lett;* 1978, 4213-4216.

108 T. Tsunoda, M. Susuki, R. Noyori; *Tetrahedron Lett;* 1980, **21**, 1357-1358.

109 J. R. Hwu, L.-C. Leu, J. A. Robl, D. A. Anderson, J. M. Wetzel; *J. Org. Chem;* 1987, **52**, 188-191.

110 W. G. Dauben, J. M. Gerdes, G. C. Look; *J. Org. Chem;* 1986, **51**, 4964-4970.

111 E. A. Mash, S. B. Hemperly; *J. Org. Chem;* 1990, **55**, 2055-2060.

112 J. March; *Advanced Oragnic Synthesis, 4th Ed;* Wiley; 1992, p.823.

113 R. B. Woodward, F. V. Brutcher; *J. Am. Chem. Soc;* 1958, **80**, 209-211.

114 L. Mangoni, M. Adinolfi, G. Barone, M. Parrilli; *Tetrahedron Lett;* 1973, 1357-1358.

115 T. K. M. Shing, E. K. W. Tam, V. W.-F. Tai, I. H. F. Chung, Q. Jiang; *Chem. Eur. J;* 1996, **2**, 50-57.

116 K. Nakamura, T. Kimura, H. Kanno, E. Takahashi; *J. Antibiotics;* 1995, 1134-1137.

117 A. Pondaven-Raphalen, G. Sturtz; *Phosphorus and Sulfur;* 1987, **29**, 329-339.

118 K. Akashi, R. E. Palermo, K. B. Sharpless; *J. Org. Chem;* 1978, **43**, 2063-2066.

119 P. A. Bartlett, L. J. Vanmaele, W. B. Kezer; *Bull. Soc. Chim. Fr;* 1986, 776-779.

120 P. Page, C. Blonski, J. Périé; *Tetrahedron Lett;* 1995, **36**, 8027-8030.

121 C.-P. Mak, C. Mayerl, H. Fliri; *Tetrahedron Lett;* 1983, **24**, 347-350.

122 M. Saady, L. Lebeau, C. Mioskowski; *Helvetica Chimica Acta;* 1995, **78**, 670-678.

123 K. W. Jung, K. D. Janda, P. J. Sanfilippo, M. Wachter; *Bioorganic & Medicinal Chemistry Lett;* 1996, **6**, 2281-2282.

124 R. Wu, N. H. Saab, H. Huang, L. Wiest, A. E. Pegg, R. A. Casero, P. M. Woster; *Bioorganic & Medicinal Chemistry;* 1996, **4**, 825-836.

125 M. M. Cambell, N. I. Carruthers, S. J. Mickel; *Tetrahedron;* 1982, **38**, 2513-2524.

126 J. Baddiley, V. M. Clark, J. J. Michalski, A. R. Todd; *J. Chem. Soc;* 1949, 815-821.

127 T. Kofoed, M. H. Caruthers; *Tetrahedron Lett;* 1996, **37**, 6457-6460.

128 W. F. Bailey, E. R. Punzalan; *J. Org. Chem;* 1990, **55**, 5404-5406.

129 I. Mori, Y. Kimura, T. Nakano, S.-I. Matsunaga, G. Iwasaki, A. Ogawa, K. Hayakawa; *Tetrahedron Lett;* 1997, **38**, 3543-3546.

130 K. S. Colle, E. S. Lewis; *J. Org. Chem;* 1978, **43**, 571-574.

131 L. Z. Avila, P. A. Bishop, J. W. Frost; *J. Am. Chem. Soc;* 1991, **113**, 2242-2246.

132 T. Mahmood, J. M. Shreeve; *Syn. Commun;* 1987, 71-75.

133 A. Holy; *Tetrahedron Lett;* 1967, 881-884.

134 S. R. Piettre, P. Raboisson; *Tetrahedron Lett;* 1996, **37**, 2229-2232.

135 D. B. Berkowitz, D. Bhuniya, G. Peris; *Tetrahedron Lett;* 1999, **40**, 1869-1872.

136 M. Reuman *et al; J. Med. Chem;* 1995, **38**, 2531-2540.

137 R. W. Binkley, M. G. Ambrose; *J. Org. Chem;* 1983, **48**, 674-677.

138 D. B. Berkowitz, M. Eggen, Q. Shen, R. K. Shoemaker; *J. Org. Chem;* 1996, **61**, 4666-4675.

139 J.K. Cha, W. J. Christ, Y. Kishi; *Tetrahedron;* 1984, **40**, 2247-2255.

140 G. Stork, M. Kahn; *Tetrahedron Lett;* 1983, **24**, 3951-3954.

141 D. A. Mootoo, B. Fraser-Reid; *J. Org. Chem;* 1987, **52**, 4511-4517.

142 R. E. Dunbar, G. C. White; *J. Org. Chem;* 1958, **23**, 915-916.

143 Q. E. Thompson; *J. Am. Chem. Soc;* 1951, **55**, 5841-5846.

144 K. Baburao, A. M. Costello, R. C. Petterson, G. E. Sander; *J. Chem. Soc. C;* 1968, 2779-2781.

145 R. G. Harvey; *Tetrahedron;* 1966, **22**, 2561-2573.

146 S. A. Matlin, P. G. Sammes; *J. Chem. Soc; Chem. Commun;* 1972, 1222-1223.

147 A. Bondi; *J. Phys. Chem;* 1964, **64**, 441-451.

148 L. Pauling; *The Nature of the Chemical Bond;* Cornell University Press; Ithaca, New York, 1960, p.82.

149 J. A. K. Howard, V. J. Hoy, D. O' Hagan, G. T. Smith; *Tetrahedron*; 1996, **52**, 12613-12622.

150 E. L. Eliel, S. H. Wilen; *Stereochemistry of organic compounds;* Wiley; 1994, pp. 875-887.

151 N . T. Anh, O. Eisenstein; *Nouv. J. Chim;* 1977, **1**, 61-70.

152 S. S. Wong, M. N. Paddon-Row; *J. Chem. Soc. Chem. Commun;* 1990, 456-458.

153 P. Kalaritis, R. W. Regenye, J. J. Partridge, D. L. Coffin; *J. Org. Chem;* 1990, **55**, 812.

154 T. Kitazume, K. Murata, T. Ikeya; *J. Fluorine Chem;* 1986, **31**, 143-150.

155 D. O'Hagan, H. S. Rzepa; *J. Chem. Soc. Perkin Trans. 2;* 1994, 3-4.

156 C. Moberg, H. Adolfsson, K. Wärnmark, P.-O. Norrby, K.-M. Marstokk, H. Mollendal; *Chem. Eur. J;* 1996, **2**, 516-522.

157 C. L. Liotta, H. P. Harris; *J. Am. Chem. Soc;* 1973, **96**, 2250-2252.

158 E. Ochiai; *J. Org. Chem;* 1953, **18**, 534-551.

159 R. T. C. Brownlee, D. J. Craik; *Tetrahedron Lett;* 1980, **21**, 1681-1684.

160 H.-S. Im, E. R. Berstein, H. V. Secor, J. I. Seeman; *J. Am. Chem. Soc;* 1991, **113**, 4422-4431.

161 R. K. Bohn, S. A. Sorenson, N. S. True, T. Brupbacher, M. C. L. Gerry, W. Jäger; *J. Mol. Spectrosc;* 1997, **184**, 167-171.

162 C. Beaulieu, G. H Penner, T. Schaefer; *Can. J. Chem;* 1990, **68**, 581-590.

163 F. E. Hruska, T. Schaefer, R. Sebastian, R. W. Schurko; *Can. J. Chem;* 1995, **73**, 816-825.

164 D. J. Tozer; *Chem. Phys. Lett;* 1999, **308**, 160-164.

165 G. Bram, A. Loupy, P. Pigeon; *Syn. Commun;* 1988, 1661-1667.

166 W. J. Middleton; *J. Org. Chem;* 1975, **40**, 574-578.

167 E. L. Eliel, S. H. Wilen; *Stereochemistry of Organic Compounds;* Wiley; 1994, p 1199.

168 S. Wolfe; *Acc. Chem. Res;* 1972, **5**, 102-111.

169 R. D. Amos, N. C. Handy, R. G. Jones, A. J. Kirby, J. K. Parker, J. M. Percy, M. D. Su; *J. Chem. Soc. Perkin Trans. 2;* 1992, 549-558.

170 N. C. Craig, A. Chen, K. H. Suh, S. Klee, G. C. Mellau, B. P. Winnewisser, M. Winnewisser; *J. Am. Chem. Soc;* 1997, **119**, 4789-4790.

171 K. B. Wiberg; *Acc. Chem. Res;* 1996, **29**, 229-234.

172 A. J. Kirby; *Stereoelectronic Effects;* Oxford University Press, 1994, p. 21.

173 S. K. Holmgren, L. E. Bretscher, K. M. Taylor, R. T. Raines; *Chemistry & Biology;* 1999, **6**, 63-70.

174 B. A. Philips, G. Fodor, J. Gal, F. Letourneau, J. J. Ryan; *Tetrahedron;* 1973, **29**, 3309-3327.

175 Dr. D. J. Tozer; Personal communication.

176 P. Coutrot, M. Youssefi-Tabrizi, C. Grison; *J. Organomet. Chem;* 1986, **316**, 13-18.

177 T. Yokomatsu, Y. Shioya, H. Iwasawa, S. Shibuya; *Heterocycles;* 1997, **46**, 463-472.

178 B. A. Arbuzov, V. S. Vinogradova, O. D. Zolova; *Bull. Acad. Sci. USSR Div. Chem. Sci. (Engl. Transl.);* 1968, 2164-2166.

179 J. J. Perie, P. de M. Puyau; Phosphorus, *Sulfur, Silicon Relat. Elements;* 1997, **129**, 13-46.

180 T. Kofoed, M. H. Caruthers; *Tetrahedron Lett;* 1996, **36**, 6457-6460.

181 W. F. Bailey, E. R. Punzalan; *J. Org. Chem;* 1990, **55**, 5404-5406.

182 K. L. Mlodnosky, H. M. Holmer; *Tetrahedron Lett;* 1997, **38**, 8803-8806.

183 A. V. Bogolyubskii, A. Y. Il'chesako, V. L. Popov, A. A. Skrynnikova, L. M. Yagupol'skii; *J. Org. Chem. USSR (Engl. Transl.);* 1988, **24**, 977-981.

184 C. G. Swain, R. E. T. Spalding; *J. Am. Chem. Soc;* 1960, **82**, 6104-6106.

185 J. Bernstein, J. S. Roth, W. T. Miller Jr; *J. Am. Chem. Soc;* 1948, **70**, 2310-2314.

Appendices

Appendix 1

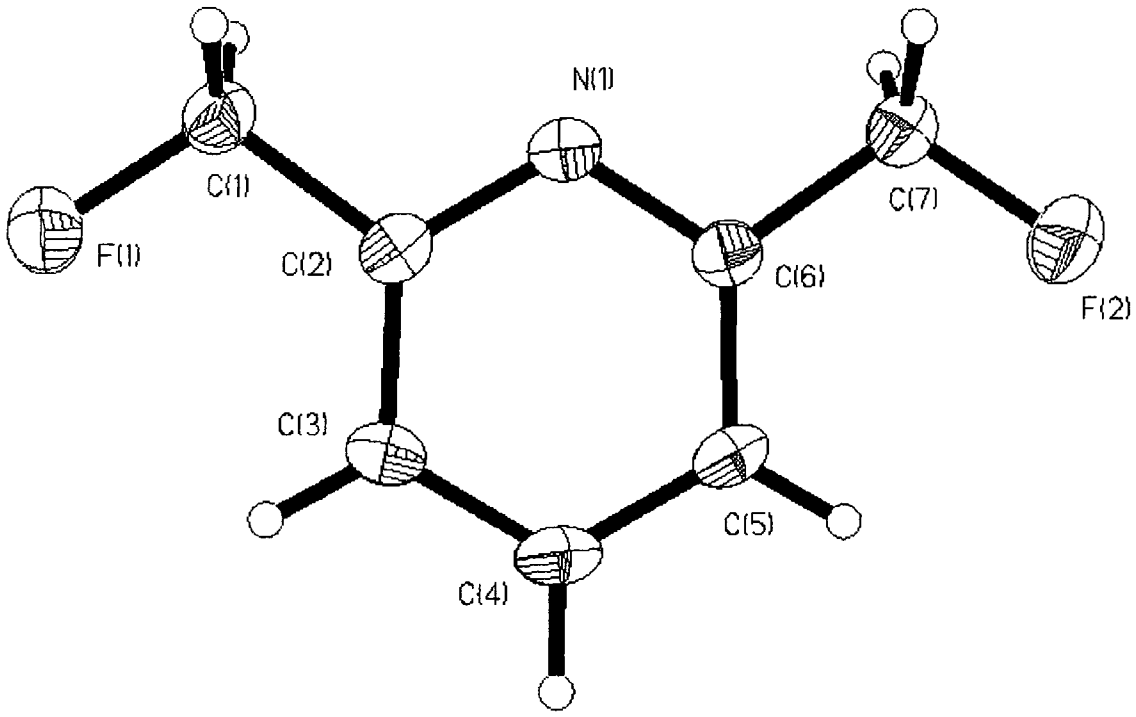

Bis-2,6-(fluoromethyl)pyridine 143

Table 1 Crystal data and structure refinement for bis-2,6-(fluoromethyl)pyridine **143**.

Identification code	76	
Empirical formula	C7 H7 F2 N	
Formula weight	143.14	
Temperature	150 K	
Wavelength	0.71073 Å	
Crystal system	Triclinic	
Space group	P-1	
Unit cell dimensions	a = 6.3493(4) Å	α= 114.651(3)°.
	b = 7.6080(4) Å	β= 107.054(2)°.
	c = 8.1979(5) Å	γ = 97.189(3)°.
Volume	329.84(3) Å3	
Z	2	
Density (calculated)	1.441 Mg/m3	
Absorption coefficient	0.126 mm-1	
F(000)	148	
Crystal size	0.6 x 0.14 x 0.12 mm3	
Theta range for data collection	2.96 to 30.30°.	
Index ranges	-8<=h<=9, -10<=k<=10, -11<=l<=9	
Reflections collected	2605	
Independent reflections	1736 [R(int) = 0.0647]	
Absorption correction	None	
Refinement method	Full-matrix least-squares on F2	
Data / restraints / parameters	1725 / 0 / 91	
Goodness-of-fit on F2	1.106	
Final R indices [I>2sigma(I)]	R1 = 0.0629, wR2 = 0.1317	
R indices (all data)	R1 = 0.1139, wR2 = 0.1788	
Largest diff. peak and hole	0.321 and -0.249 e.Å-3	

Table 2 Atomic coordinates (x 10^4) and equivalent isotropic displacement parameters (Å2x 10^3) for bis-2,6-(fluoromethyl)pyridine **143**. U(eq) is defined as one third of the trace of the orthogonalized Uij tensor.

	x	y	z	U(eq)
N(1)	15825(3)	25000(3)	17660(3)	23(1)
C(7)	17046(5)	27990(4)	20703(4)	30(1)
C(5)	19856(4)	26758(4)	19126(4)	25(1)
C(6)	17639(4)	26537(4)	19110(4)	23(1)
C(3)	18347(4)	23720(4)	16066(4)	26(1)
C(4)	20189(4)	25317(4)	17572(4)	29(1)
C(2)	16176(4)	23626(4)	16164(3)	22(1)
F(2)	18985(3)	29440(3)	22250(3)	51(1)
F(1)	14496(3)	20690(2)	13043(2)	39(1)
C(1)	14039(4)	21995(4)	14622(4)	27(1)

Table 3 Bond lengths [Å] for bis-2,6-(fluoromethyl)pyridine **143**.

N(1)-C(2)	1.340(3)
N(1)-C(6)	1.345(3)
C(7)-F(2)	1.385(3)
C(7)-C(6)	1.503(4)
C(7)-H(7B)	0.97
C(7)-H(7A)	0.97
C(5)-C(4)	1.386(4)
C(5)-C(6)	1.392(3)
C(5)-H(5)	0.93
C(3)-C(4)	1.384(4)
C(3)-C(2)	1.399(3)
C(3)-H(3)	0.93
C(4)-H(4)	0.93
C(2)-C(1)	1.497(3)

F(1)-C(1)	1.401(3)
C(1)-H(1A)	0.97
C(1)-H(1B)	0.97
C(2)-N(1)-C(6)	118.2(2)
F(2)-C(7)-C(6)	111.9(2)
F(2)-C(7)-H(7B)	109.23(15)
C(6)-C(7)-H(7B)	109.23(14)
F(2)-C(7)-H(7A)	109.23(15)
C(6)-C(7)-H(7A)	109.23(14)
H(7B)-C(7)-H(7A)	107.9
C(4)-C(5)-C(6)	118.0(2)
C(4)-C(5)-H(5)	120.99(15)
C(6)-C(5)-H(5)	120.99(15)
N(1)-C(6)-C(5)	123.0(2)
N(1)-C(6)-C(7)	113.7(2)
C(5)-C(6)-C(7)	123.3(2)
C(4)-C(3)-C(2)	118.1(2)
C(4)-C(3)-H(3)	120.9(2)
C(2)-C(3)-H(3)	120.93(14)
C(3)-C(4)-C(5)	120.0(2)
C(3)-C(4)-H(4)	120.0(2)
C(5)-C(4)-H(4)	120.01(14)
N(1)-C(2)-C(3)	122.7(2)
N(1)-C(2)-C(1)	113.9(2)
C(3)-C(2)-C(1)	123.5(2)
F(1)-C(1)-C(2)	111.0(2)
F(1)-C(1)-H(1A)	109.45(13)
C(2)-C(1)-H(1A)	109.45(14)
F(1)-C(1)-H(1B)	109.45(13)
C(2)-C(1)-H(1B)	109.45(13)
H(1A)-C(1)-H(1B)	108.0

Table 4 Anisotropic displacement parameters (Å2x 10^3) for bis-2,6-(fluoromethyl)pyridine **143**. The anisotropic displacement factor exponent takes the form: $-2\pi^2[h^2 a^{*2} U_{11} + ... + 2 h k a^* b^* U_{12}]$.

	U11	U22	U33	U23	U13	U12
N(1)	20(1)	24(1)	27(1)	14(1)	10(1)	7(1)
C(7)	26(1)	28(1)	29(1)	9(1)	9(1)	4(1)
C(5)	17(1)	30(1)	28(1)	16(1)	5(1)	3(1)
C(6)	22(1)	23(1)	25(1)	13(1)	9(1)	8(1)
C(3)	23(1)	30(1)	32(1)	16(1)	14(1)	13(1)
C(4)	18(1)	40(2)	35(2)	22(1)	11(1)	10(1)
C(2)	21(1)	24(1)	23(1)	15(1)	5(1)	6(1)
F(2)	33(1)	42(1)	41(1)	-4(1)	9(1)	-1(1)
F(1)	33(1)	35(1)	33(1)	6(1)	10(1)	9(1)
C(1)	22(1)	27(1)	26(1)	11(1)	6(1)	6(1)

Table 5 Hydrogen coordinates (x 10^4) and isotropic displacement parameters (Å2x 10^3) for bis-2,6-(fluoromethyl)pyridine **143**.

	x	y	z	U(eq)
H(7B)	16031(5)	28648(4)	20189(4)	36
H(7A)	16231(5)	27251(4)	21160(4)	36
H(5)	21076(4)	27840(4)	20149(4)	30
H(3)	18547(4)	22737(4)	15018(4)	31
H(4)	21651(4)	25424(4)	17541(4)	34
H(1A)	13426(4)	21234(4)	15161(4)	32
H(1B)	12890(4)	22597(4)	14179(4)	32

Appendix 2

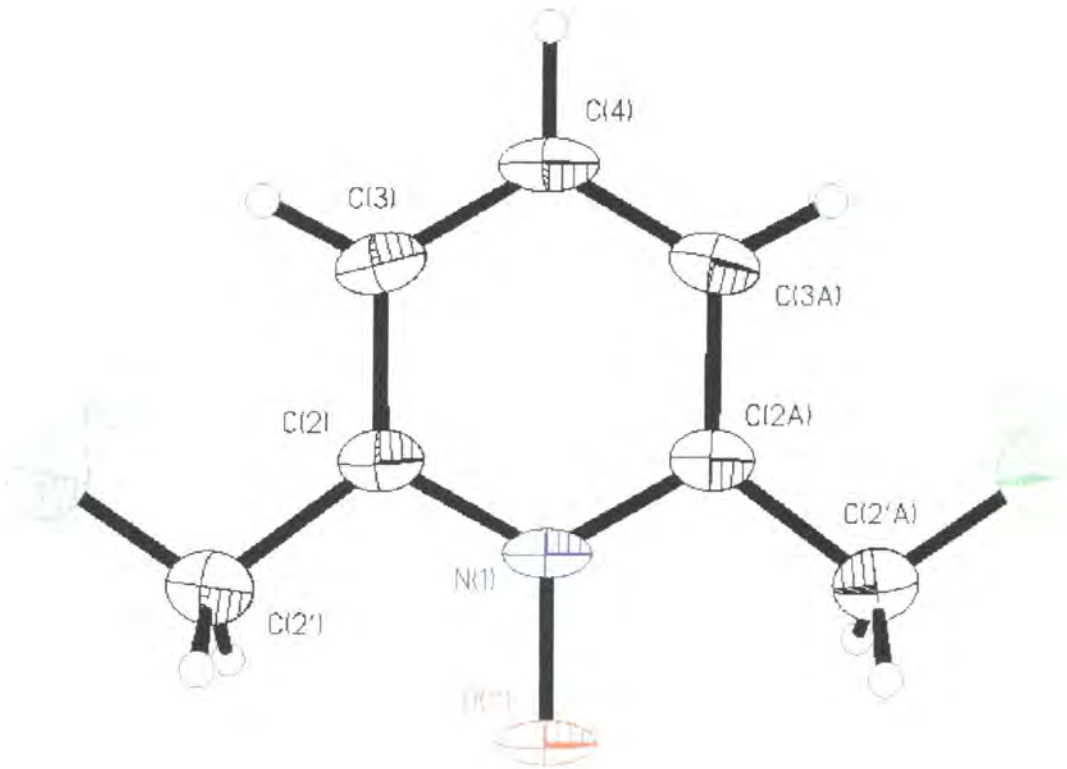

Bis-2,6-(fluoromethyl)pyridine-*N*-oxide 146

Table 1 Crystal data and structure refinement for bis-2,6-(fluoromethyl)pyridine-*N*-oxide **146**.

Identification code	fluom	
Empirical formula	C7 H7 F2 N O	
Formula weight	159.14	
Temperature	150(2) K	
Wavelength	0.71073 Å	
Crystal system	Monoclinic	
Space group	C2/c	
Unit cell dimensions	a = 14.2949(14) Å	α= 90°.
	b = 7.2427(6) Å	β= 121.2660(10)°.
	c = 8.1325(8) Å	γ = 90°.
Volume	719.70(12) Å3	
Z	4	
Density (calculated)	1.469 Mg/m3	
Absorption coefficient	0.133 mm-1	
F(000)	328	
Crystal size	.08mm x .38mm x .4mm mm3	
Theta range for data collection	3.27 to 27.50°.	
Index ranges	-16<=h<=18, -9<=k<=9, -10<=l<=10	
Reflections collected	2552	
Independent reflections	829 [R(int) = 0.0734]	
Absorption correction	None	
Refinement method	Full-matrix least-squares on F2	
Data / restraints / parameters	822 / 0 / 66	
Goodness-of-fit on F2	1.105	
Final R indices [I>2sigma(I)]	R1 = 0.0431, wR2 = 0.1217	
R indices (all data)	R1 = 0.0558, wR2 = 0.1490	
Largest diff. peak and hole	0.251 and -0.292 e.Å-3	

Table 2 Atomic coordinates (x 10^4) and equivalent isotropic displacement parameters (Å2x 10^3) for bis-2,6-(fluoromethyl)pyridine-*N*-oxide **146**. U(eq) is defined as one third of the trace of the orthogonalized Uij tensor.

	x	y	z	U(eq)
C(2)	782(1)	7176(2)	9083(2)	28(1)
O(1')	0	9917(2)	7500	35(1)
N(1)	0	8087(2)	7500	27(1)
F(2')	2367(1)	7308(2)	12201(2)	49(1)
C(4)	0	4292(3)	7500	34(1)
C(3)	795(1)	5258(2)	9091(2)	31(1)
C(2')	1556(1)	8406(2)	10704(2)	36(1)

Table 3 Bond lengths [Å] for bis-2,6-(fluoromethyl)pyridine-*N*-oxide **146**.

C(2)-N(1)	1.359(2)
C(2)-C(3)	1.389(2)
C(2)-C(2')	1.497(2)
O(1')-N(1)	1.326(2)
N(1)-C(2)#1	1.359(2)
F(2')-C(2')	1.412(2)
C(4)-C(3)#1	1.389(2)
C(4)-C(3)	1.389(2)
C(4)-H(4)	0.98(3)
C(3)-H(3)	0.95(2)
C(2')-H(2A)	0.98(2)
C(2')-H(2B)	0.96(2)
N(1)-C(2)-C(3)	119.5(2)
N(1)-C(2)-C(2')	114.46(13)
C(3)-C(2)-C(2')	126.1(2)

O(1')-N(1)-C(2)#1	119.02(9)
O(1')-N(1)-C(2)	119.02(9)
C(2)#1-N(1)-C(2)	122.0(2)
C(3)#1-C(4)-C(3)	119.5(2)
C(3)#1-C(4)-H(4)	120.25(10)
C(3)-C(4)-H(4)	120.25(10)
C(2)-C(3)-C(4)	119.8(2)
C(2)-C(3)-H(3)	118.2(14)
C(4)-C(3)-H(3)	122.0(13)
F(2')-C(2')-C(2)	108.99(13)
F(2')-C(2')-H(2A)	109.4(11)
C(2)-C(2')-H(2A)	107.8(11)
F(2')-C(2')-H(2B)	109.6(12)
C(2)-C(2')-H(2B)	107.1(12)
H(2A)-C(2')-H(2B)	113.9(17)

Symmetry transformations used to generate equivalent atoms: #1 -x,y,-z+3/2

Table 4 Anisotropic displacement parameters (Å2x 10_3) for bis-2,6-(fluoromethyl)pyridine-*N*-oxide **146**. The anisotropic displacement factor exponent takes the form: $-2\pi 2[\ h_2\ a^*2U_{11} + \ldots + 2\ h\ k\ a^*\ b^*\ U_{12}\ ]$.

	U11	U22	U33	U23	U13	U12
C(2)	36(1)	20(1)	36(1)	1(1)	24(1)	1(1)
O(1')	50(1)	10(1)	51(1)	0	31(1)	0
N(1)	39(1)	13(1)	39(1)	0	27(1)	0
F(2')	46(1)	44(1)	41(1)	1(1)	12(1)	2(1)
C(4)	53(1)	16(1)	47(1)	0	36(1)	0
C(3)	43(1)	20(1)	40(1)	6(1)	28(1)	5(1)
C(2')	41(1)	28(1)	41(1)	-2(1)	22(1)	-1(1)

Table 5 Hydrogen coordinates (x 10^4) and isotropic displacement parameters (Å2x 10^3) for bis-2,6-(fluoromethyl)pyridine-*N*-oxide **146**.

	x	y	z	U(eq)
H(3)	1357(18)	4647(31)	10202(32)	44(6)
H(2A)	1137(15)	9054(26)	11168(26)	32(4)
H(2B)	1891(17)	9211(29)	10212(29)	39(5)
H(4)	0	2943(46)	7500	51(8)

Appendix 3

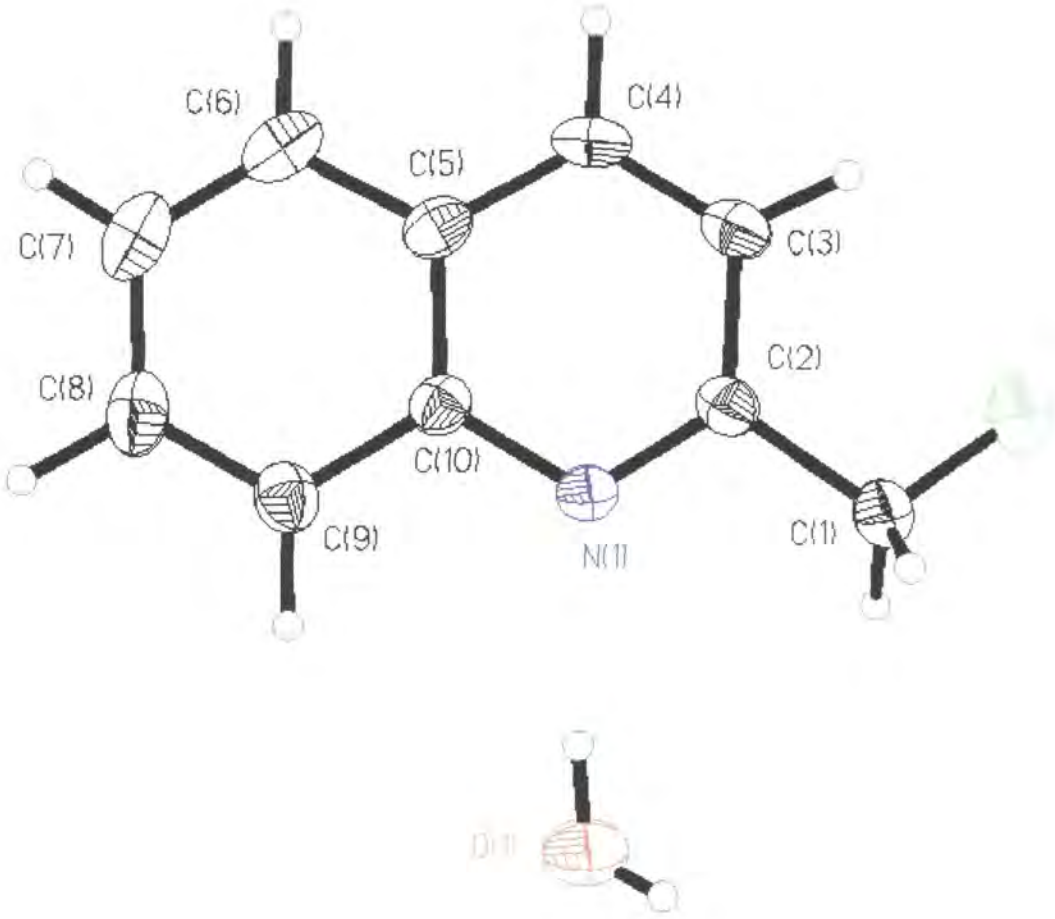

2-(Fluoromethyl)quinoline monohydrate 147

Table 1 Crystal data and structure refinement for 2-(fluoromethyl)quinoline monohydrate **147**.

Identification code	152	
Empirical formula	C10 H10 F N O	
Formula weight	179.19	
Temperature	150 K	
Wavelength	0.71073 Å	
Crystal system	monoclinic	
Space group	P2(1)/c	
Unit cell dimensions	a = 4.4905(5) Å	α= 90°.
	b = 11.6238(12) Å	β= 95.302(4)°.
	c = 17.1041(19) Å	γ = 90°.
Volume	888.96(17) Å3	
Z	4	
Density (calculated)	1.339 Mg/m3	
Absorption coefficient	0.101 mm-1	
F(000)	376	
Crystal size	0.4 x 0.2 x 0.05 mm3	
Theta range for data collection	2.12 to 27.49°.	
Index ranges	-5<=h<=5, -11<=k<=13, -9<=l<=22	
Reflections collected	2700	
Independent reflections	1877 [R(int) = 0.0659]	
Completeness to theta = 27.49°	92.4 %	
Refinement method	Full-matrix least-squares on F2	
Data / restraints / parameters	1877 / 0 / 162	
Goodness-of-fit on F2	1.163	
Final R indices [I>2sigma(I)]	R1 = 0.0656, wR2 = 0.1317	
R indices (all data)	R1 = 0.0885, wR2 = 0.1474	
Largest diff. peak and hole	0.218 and -0.261 e.Å-3	

Table 2 Atomic coordinates (x 10^4) and equivalent isotropic displacement parameters (Å2x 10^3) for 2-(fluoromethyl)quinoline monohydrate **147**. U(eq) is defined as one third of the trace of the orthogonalized Uij tensor.

	x	y	z	U(eq)
N(1)	1101(4)	2420(2)	4051(1)	24(1)
C(2)	-692(5)	1748(2)	4416(1)	25(1)
F(1)	-3711(4)	1541(2)	5493(1)	44(1)
C(5)	949(5)	995(2)	2995(1)	27(1)
C(4)	-960(6)	314(2)	3414(2)	31(1)
C(9)	3887(6)	2770(2)	2943(2)	30(1)
C(10)	1947(5)	2059(2)	3339(1)	24(1)
C(7)	3763(6)	1387(3)	1880(2)	39(1)
C(3)	-1785(6)	674(2)	4124(2)	29(1)
C(1)	-1517(7)	2214(3)	5195(2)	35(1)
C(6)	1878(6)	690(3)	2250(2)	35(1)
C(8)	4774(6)	2438(3)	2230(2)	36(1)
O(1)	2354(6)	4732(2)	4582(2)	49(1)

Table 3 Bond lengths [Å] for 2-(fluoromethyl)quinoline monohydrate **147**.

N(1)-C(2)	1.320(3)
N(1)-C(10)	1.375(3)
C(2)-C(3)	1.415(4)
C(2)-C(1)	1.516(3)
F(1)-C(1)	1.392(3)
C(5)-C(4)	1.410(4)
C(5)-C(6)	1.423(4)
C(5)-C(10)	1.424(4)
C(4)-C(3)	1.368(4)
C(4)-H(4)	0.98(3)

C(9)-C(8)	1.373(4)
C(9)-C(10)	1.417(3)
C(9)-H(9)	1.01(3)
C(7)-C(6)	1.369(4)
C(7)-C(8)	1.416(4)
C(7)-H(7)	0.95(3)
C(3)-H(3)	0.99(3)
C(1)-H(1B)	1.02(3)
C(1)-H(1A)	1.07(4)
C(6)-H(6)	0.97(4)
C(8)-H(8)	0.99(3)
O(1)-HB	0.86(5)
O(1)-HAA	0.95(8)
O(1)-HAB	0.87(7)

C(2)-N(1)-C(10)	118.0(2)
N(1)-C(2)-C(3)	124.2(2)
N(1)-C(2)-C(1)	114.4(2)
C(3)-C(2)-C(1)	121.4(2)
C(4)-C(5)-C(6)	123.9(3)
C(4)-C(5)-C(10)	117.5(2)
C(6)-C(5)-C(10)	118.6(2)
C(3)-C(4)-C(5)	120.4(2)
C(3)-C(4)-H(4)	121.0(15)
C(5)-C(4)-H(4)	118.6(15)
C(8)-C(9)-C(10)	120.2(3)
C(8)-C(9)-H(9)	121.3(17)
C(10)-C(9)-H(9)	118.5(17)
N(1)-C(10)-C(9)	118.6(2)
N(1)-C(10)-C(5)	121.9(2)
C(9)-C(10)-C(5)	119.5(2)
C(6)-C(7)-C(8)	120.2(3)
C(6)-C(7)-H(7)	116(2)

C(8)-C(7)-H(7)	123(2)
C(4)-C(3)-C(2)	118.1(2)
C(4)-C(3)-H(3)	122.0(18)
C(2)-C(3)-H(3)	119.8(18)
F(1)-C(1)-C(2)	111.1(2)
F(1)-C(1)-H(1B)	107.8(19)
C(2)-C(1)-H(1B)	109.7(18)
F(1)-C(1)-H(1A)	103.7(18)
C(2)-C(1)-H(1A)	110.4(19)
H(1B)-C(1)-H(1A)	114(3)
C(7)-C(6)-C(5)	120.8(3)
C(7)-C(6)-H(6)	123(2)
C(5)-C(6)-H(6)	116(2)
C(9)-C(8)-C(7)	120.6(3)
C(9)-C(8)-H(8)	121.4(18)
C(7)-C(8)-H(8)	117.9(18)
HB-O(1)-HAA	100(5)
HB-O(1)-HAB	103(6)
HAA-O(1)-HAB	109(7)

Table 4 Anisotropic displacement parameters (Å2x 103) for 2-(fluoromethyl)quinoline monohydrate **147**. The anisotropic displacement factor exponent takes the form: -2π2[h2 a*2U11 + ... + 2 h k a* b* U12].

	U11	U22	U33	U23	U13	U12
N(1)	28(1)	18(1)	28(1)	-3(1)	4(1)	0(1)
C(2)	26(1)	20(1)	30(1)	0(1)	4(1)	0(1)
F(1)	47(1)	46(1)	43(1)	0(1)	22(1)	-10(1)
C(5)	26(1)	24(1)	29(1)	-4(1)	-1(1)	6(1)
C(4)	31(1)	18(1)	42(2)	-6(1)	-4(1)	-1(1)
C(9)	30(1)	27(2)	32(1)	4(1)	5(1)	2(1)

C(10)	25(1)	20(1)	26(1)	0(1)	2(1)	5(1)
C(7)	38(2)	51(2)	27(1)	-4(1)	4(1)	15(1)
C(3)	28(1)	22(1)	37(1)	-1(1)	3(1)	-4(1)
C(1)	42(2)	30(2)	37(2)	-4(1)	17(1)	-7(1)
C(6)	37(1)	34(2)	33(1)	-10(1)	-3(1)	9(1)
C(8)	38(2)	41(2)	32(1)	8(1)	11(1)	8(1)
O(1)	62(2)	27(1)	59(2)	-12(1)	15(1)	-6(1)

Table 5 Hydrogen coordinates (x 10^4) and isotropic displacement parameters (Å2x 10^3) for 2-(fluoromethyl)quinoline monohydrate **147**.

	x	y	z	U(eq)
H(4)	-1640(60)	-430(20)	3190(15)	24(7)
H(9)	4640(60)	3500(30)	3205(18)	39(8)
H(8)	6210(70)	2900(30)	1956(18)	40(8)
H(3)	-3220(60)	240(30)	4413(17)	38(8)
H(1B)	310(70)	2210(30)	5593(19)	51(10)
HB	2160(80)	4040(40)	4420(20)	66(12)
H(6)	1140(70)	-30(30)	2030(20)	53(10)
H(1A)	-2560(80)	3040(30)	5120(20)	59(10)
H(7)	4320(70)	1130(30)	1390(20)	56(10)
HAA	4130(170)	4660(70)	4920(50)	60(30)
HAB	830(170)	4820(70)	4860(50)	60(30)

Appendix 4

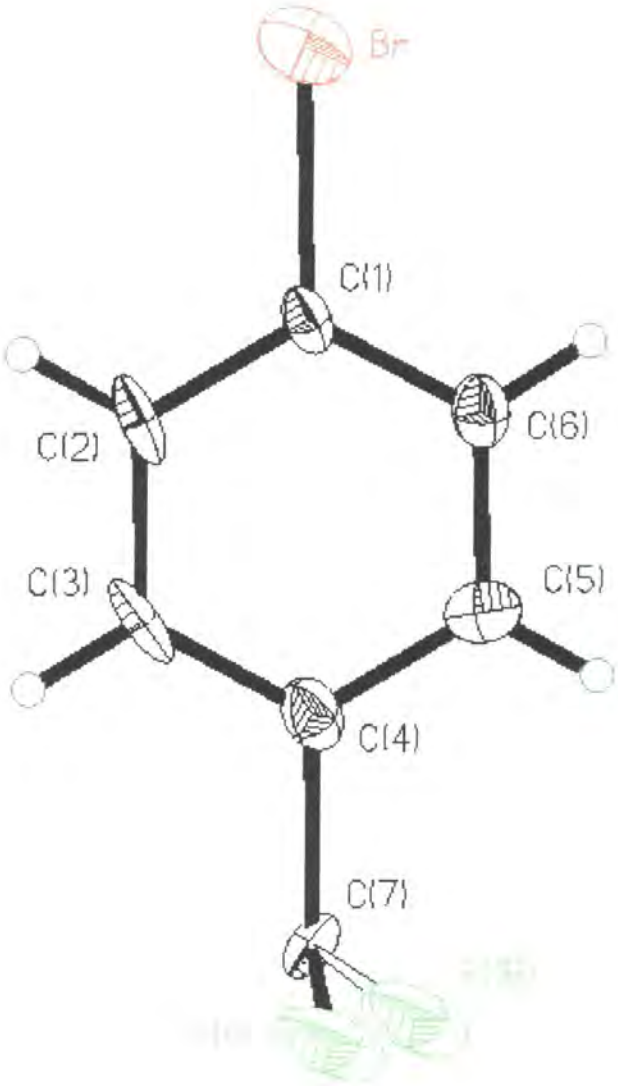

4-Bromobenzyl fluoride 149

Table 1 Crystal data and structure refinement for 4-bromobenzyl fluoride **149**.

Identification code	asb	
Empirical formula	C7 H6 Br F	
Formula weight	189.03	
Temperature	150 K	
Wavelength	0.71073 Å	
Crystal system	Monoclinic	
Space group	P2(1)	
Unit cell dimensions	a = 5.9266(2) Å	α= 90°.
	b = 7.3604(3) Å	β= 90.753(2)°.
	c = 7.9376(3) Å	γ = 90°.
Volume	346.23(2) Å3	
Z	2	
Density (calculated)	1.813 Mg/m3	
Absorption coefficient	5.855 mm-1	
F(000)	184	
Crystal size	0.6 x 0.16 x 0.10 mm3	
Theta range for data collection	2.57 to 27.43°.	
Index ranges	-7<=h<=7, -9<=k<=9, -10<=l<=10	
Reflections collected	3129	
Independent reflections	1432 [R(int) = 0.0919]	
Absorption correction	None	
Refinement method	Full-matrix least-squares on F2	
Data / restraints / parameters	1427 / 1 / 86	
Goodness-of-fit on F2	1.725	
Final R indices [I>2sigma(I)]	R1 = 0.0940, wR2 = 0.2266	
R indices (all data)	R1 = 0.1100, wR2 = 0.2464	
Absolute structure parameter	0.27(5)	
Largest diff. peak and hole	2.573 and -1.351 e.Å-3	

Table 2 Atomic coordinates (x 10^4) and equivalent isotropic displacement parameters ($Å^2$x 10^3) for 4-bromobenzyl fluoride **149**. U(eq) is defined as one third of the trace of the orthogonalized Uij tensor.

	x	y	z	U(eq)
Br	5351(2)	2502(2)	8418(1)	39(1)
C(1)	3656(15)	2798(14)	6403(12)	18(3)
C(2)	1578(16)	3601(14)	6459(15)	23(2)
C(3)	374(16)	3939(13)	4945(16)	24(2)
C(4)	1276(18)	3392(16)	3428(15)	26(2)
C(5)	3401(14)	2519(29)	3379(10)	24(2)
C(6)	4627(16)	2256(23)	4896(13)	23(3)
C(7)	-229(17)	3676(14)	1685(12)	15(2)
F(1A)	-1330(29)	2307(40)	1346(39)	52(5)
F(1B)	-452(33)	2007(38)	1109(44)	52(5)

Table 3 Bond lengths [Å] for 4-bromobenzyl fluoride **149**.

Br-C(1)	1.890(9)
C(1)-C(2)	1.367(13)
C(1)-C(6)	1.393(14)
C(2)-C(3)	1.41(2)
C(2)-H(2)	0.93
C(3)-C(4)	1.38(2)
C(3)-H(3)	0.93
C(4)-C(5)	1.42(2)
C(4)-C(7)	1.649(15)
C(5)-C(6)	1.411(14)
C(5)-H(5)	0.93
C(6)-H(6)	0.93
C(7)-F(1A)	1.23(3)

C(7)-F(1B)	1.32(3)
C(2)-C(1)-C(6)	122.3(10)
C(2)-C(1)-Br	119.4(8)
C(6)-C(1)-Br	118.2(7)
C(1)-C(2)-C(3)	119.6(10)
C(1)-C(2)-H(2)	120.2(7)
C(3)-C(2)-H(2)	120.2(6)
C(4)-C(3)-C(2)	119.5(9)
C(4)-C(3)-H(3)	119.9(6)
C(2)-C(3)-H(3)	120.6(6)
C(3)-C(4)-C(5)	120.7(10)
C(3)-C(4)-C(7)	118.9(9)
C(5)-C(4)-C(7)	120.4(9)
C(6)-C(5)-C(4)	119.2(11)
C(6)-C(5)-H(5)	120.0(8)
C(4)-C(5)-H(5)	120.7(6)
C(1)-C(6)-C(5)	118.7(10)
C(1)-C(6)-H(6)	120.5(6)
C(5)-C(6)-H(6)	120.7(7)
F(1A)-C(7)-C(4)	111.1(16)
F(1B)-C(7)-C(4)	102.9(16)

Table 4 Anisotropic displacement parameters (Å2x 10_3) for 4-bromobenzyl fluoride **149**. The anisotropic displacement factor exponent takes the form: $-2\pi 2[h2 a^{*2} U11 + ... + 2 h k a^* b^* U12]$.

	U11	U22	U33	U23	U13	U12
Br	32(1)	43(1)	43(1)	2(1)	-9(1)	0(1)
C(1)	11(4)	16(8)	27(4)	-4(4)	0(3)	1(3)
C(2)	8(4)	14(5)	49(7)	-5(5)	5(4)	1(4)
C(3)	7(4)	12(5)	54(7)	0(5)	-2(4)	2(4)
C(4)	19(5)	23(6)	37(6)	-11(5)	-3(4)	2(4)
C(5)	24(4)	26(4)	21(4)	4(8)	-2(3)	-7(9)
C(6)	17(4)	25(9)	27(4)	-2(5)	4(3)	0(5)
C(7)	28(5)	7(4)	9(4)	3(3)	6(4)	-2(4)
F(1A)	37(12)	38(12)	80(11)	-23(7)	-36(12)	10(11)
F(1B)	37(12)	38(12)	80(11)	-23(7)	-36(12)	10(11)

Table 5 Hydrogen coordinates (x 10_4) and isotropic displacement parameters (Å2x 10_3) for 4-bromobenzyl fluoride **149**.

	x	y	z	U(eq)
H(2)	962(16)	3925(14)	7488(15)	28
H(3)	-1024(16)	4511(13)	4962(16)	29
H(5)	3960(14)	2073(29)	2371(10)	28
H(6)	6087(16)	1794(23)	4885(13)	28

Appendix 5

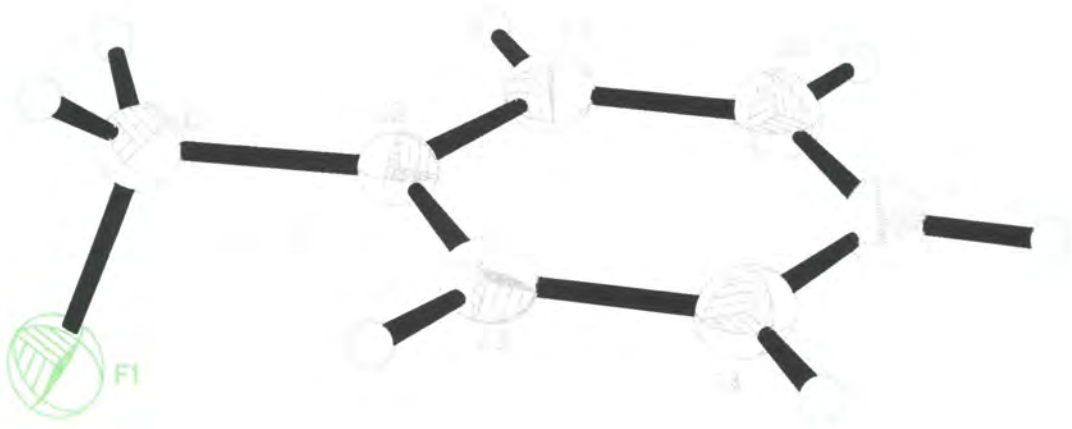

Benzyl fluoride 148

Table 1 Crystal data and structure refinement for benzyl fluoride **148**.

Identification code	99srv154	
Empirical formula	C7 H7 F	
Formula weight	110.13	
Temperature	120 K	
Wavelength	0.71073 Å	
Crystal system	Orthorhombic	
Space group	Pbcn	
Unit cell dimensions	a = 7.3453(15) Å	α = 90°.
	b = 12.048(2) Å	β = 90°.
	c = 13.586(3) Å	γ = 90°.
Volume	1202.3(4) Å3	
Z	9	
Density (calculated)	1.369 Mg/m3	
Absorption coefficient	0.102 mm-1	
F(000)	522	
Crystal size	diameter 0.3mm, length 0.7mm	
Theta range for data collection	3.00 to 30.45°.	
Index ranges	-9<=h<=10, -16<=k<=15, -18<=l<=18	
Reflections collected	13119	
Independent reflections	1710 [R(int) = 0.0367]	
Completeness to theta = 30.45°	93.4 %	
Absorption correction	None	
Refinement method	Full-matrix least-squares on F2	
Data / restraints / parameters	1710 / 0 / 101	
Goodness-of-fit on F2	1.054	
Final R indices [I>2sigma(I)]	R1 = 0.0421, wR2 = 0.1077	
R indices (all data)	R1 = 0.0561, wR2 = 0.1180	
Largest diff. peak and hole	0.345 and -0.183 e.Å-3	

Table 2 Atomic coordinates (x 10^4) and equivalent isotropic displacement parameters (Å2x 10^3) for benzyl fluoride **148**. U(eq) is defined as one third of the trace of the orthogonalized Uij tensor.

	x	y	z	U(eq)
F(1)	2423(1)	8857(1)	3132(1)	44(1)
C(2)	3439(1)	8929(1)	4796(1)	23(1)
C(3)	2241(2)	9626(1)	5312(1)	26(1)
C(5)	2492(2)	8451(1)	6750(1)	31(1)
C(7)	4172(2)	7995(1)	5272(1)	27(1)
C(6)	3704(2)	7760(1)	6247(1)	30(1)
C(4)	1753(2)	9384(1)	6282(1)	30(1)
C(1)	3904(2)	9178(1)	3739(1)	31(1)

Table 3 Bond lengths [Å] for benzyl fluoride **148**.

F(1)-C(1)	1.4194(13)
C(2)-C(3)	1.4040(15)
C(2)-C(7)	1.4054(15)
C(2)-C(1)	1.5057(15)
C(3)-C(4)	1.3959(16)
C(3)-H(3)	0.998(15)
C(5)-C(6)	1.3967(17)
C(5)-C(4)	1.4003(17)
C(5)-H(5)	0.952(17)
C(7)-C(6)	1.3980(16)
C(7)-H(7)	0.983(15)
C(6)-H(6)	0.950(16)
C(4)-H(4)	0.961(16)
C(1)-H(1B)	0.989(17)
C(1)-H(1A)	0.994(17)
C(3)-C(2)-C(7)	119.30(10)

C(3)-C(2)-C(1)	119.96(10)
C(7)-C(2)-C(1)	120.74(10)
C(4)-C(3)-C(2)	120.46(10)
C(4)-C(3)-H(3)	118.4(9)
C(2)-C(3)-H(3)	121.2(9)
C(6)-C(5)-C(4)	120.21(10)
C(6)-C(5)-H(5)	120.9(10)
C(4)-C(5)-H(5)	118.9(10)
C(6)-C(7)-C(2)	120.25(10)
C(6)-C(7)-H(7)	119.8(8)
C(2)-C(7)-H(7)	119.9(8)
C(5)-C(6)-C(7)	119.96(10)
C(5)-C(6)-H(6)	121.6(9)
C(7)-C(6)-H(6)	118.4(9)
C(3)-C(4)-C(5)	119.80(10)
C(3)-C(4)-H(4)	118.5(9)
C(5)-C(4)-H(4)	121.7(9)
F(1)-C(1)-C(2)	109.06(9)
F(1)-C(1)-H(1B)	106.5(9)
C(2)-C(1)-H(1B)	111.8(9)
F(1)-C(1)-H(1A)	107.4(10)
C(2)-C(1)-H(1A)	112.5(10)
H(1B)-C(1)-H(1A)	109.4(14)

Table 4 Anisotropic displacement parameters (Å2x 10_3) for benzyl fluoride **148**. The anisotropic displacement factor exponent takes the form: $-2\pi^2[h^2 a^{*2}U_{11} + ... + 2 h k a^* b^* U_{12}]$.

	U11	U22	U33	U23	U13	U12
F(1)	45(1)	60(1)	27(1)	0(1)	-9(1)	-19(1)
C(2)	20(1)	27(1)	23(1)	-1(1)	-2(1)	-4(1)
C(3)	23(1)	26(1)	30(1)	0(1)	-3(1)	1(1)
C(5)	31(1)	37(1)	24(1)	0(1)	0(1)	-7(1)
C(7)	23(1)	27(1)	31(1)	-2(1)	0(1)	2(1)
C(6)	30(1)	29(1)	32(1)	6(1)	-5(1)	0(1)
C(4)	26(1)	33(1)	30(1)	-7(1)	3(1)	0(1)
C(1)	29(1)	39(1)	24(1)	0(1)	-1(1)	-7(1)

Table 5 Hydrogen coordinates (x 104) and isotropic displacement parameters (Å2x 10_3) for benzyl fluoride **148**.

	x	y	z	U(eq)
H(7)	5000(20)	7498(12)	4915(10)	38(4)
H(3)	1750(20)	10316(12)	5006(11)	35(4)
H(4)	940(20)	9882(13)	6618(11)	38(4)
H(6)	4220(20)	7125(13)	6551(11)	39(4)
H(5)	2150(20)	8298(13)	7412(12)	40(4)
H(1B)	4090(20)	9981(14)	3629(11)	41(4)
H(1A)	4990(20)	8764(14)	3509(12)	48(4)

Table 6 Torsion angles [°] for benzyl fluoride **148**.

C(7)-C(2)-C(3)-C(4)	-1.27(16)
C(1)-C(2)-C(3)-C(4)	177.85(10)
C(3)-C(2)-C(7)-C(6)	0.33(16)
C(1)-C(2)-C(7)-C(6)	-178.79(10)
C(4)-C(5)-C(6)-C(7)	-0.45(18)
C(2)-C(7)-C(6)-C(5)	0.53(17)
C(2)-C(3)-C(4)-C(5)	1.35(17)
C(6)-C(5)-C(4)-C(3)	-0.49(18)
C(3)-C(2)-C(1)-F(1)	-76.61(13)
C(7)-C(2)-C(1)-F(1)	102.50(12)

Appendix 6

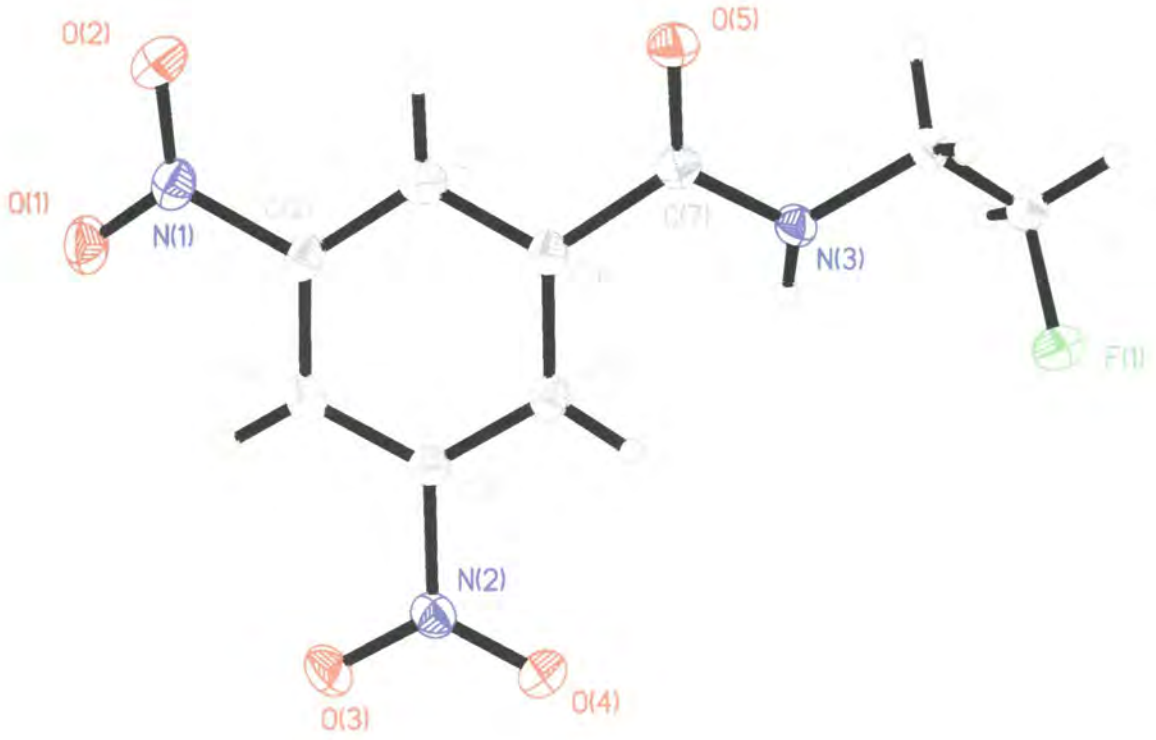

N-(2-Fluoroethyl)-3,5-dinitrobenzamide 154

Table 1 Crystal data and structure refinement for *N*-(2-fluoroethyl)-3,5-dinitrobenzamide **154**.

Identification code	99srv092	
Empirical formula	C9 H8 F N3 O5	
Formula weight	257.18	
Temperature	150 K	
Wavelength	0.71073 Å	
Crystal system	Monoclinic	
Space group	P2(1)/n	
Unit cell dimensions	a = 10.1176(6) Å	α= 90°.
	b = 4.8253(3) Å	β= 93.610(4)°.
	c = 21.0006(14) Å	γ = 90°.
Volume	1023.22(11) Å3	
Z	3	
Density (calculated)	1.252 Mg/m3	
Absorption coefficient	0.112 mm-1	
F(000)	396	
Crystal size	0.6 x 0.15 x 0.12 mm3	
Theta range for data collection	1.94 to 23.25°.	
Index ranges	-11<=h<=11, -5<=k<=5, -23<=l<=19	
Reflections collected	4851	
Independent reflections	1475 [R(int) = 0.0572]	
Completeness to theta = 23.25°	100.0 %	
Absorption correction	None	
Refinement method	Full-matrix least-squares on F2	
Data / restraints / parameters	1475 / 0 / 195	
Goodness-of-fit on F2	1.056	
Final R indices [I>2sigma(I)]	R1 = 0.0310, wR2 = 0.0764	
R indices (all data)	R1 = 0.0373, wR2 = 0.0803	
Largest diff. peak and hole	0.132 and -0.216 e.Å-3	

Table 2 Atomic coordinates (x 10^4) and equivalent isotropic displacement parameters ($Å^2$x 10^3) for *N*-(2-fluoroethyl)-3,5-dinitrobenzamide **154**. U(eq) is defined as one third of the trace of the orthogonalized Uij tensor.

	x	y	z	U(eq)
F(1)	8660(1)	1239(2)	5067(1)	30(1)
O(1)	16687(1)	3667(3)	7806(1)	29(1)
O(2)	15449(1)	7359(3)	7805(1)	29(1)
O(5)	11287(1)	7781(3)	6440(1)	23(1)
N(3)	10588(1)	3766(3)	5963(1)	19(1)
C(6)	12842(2)	4055(4)	6419(1)	17(1)
O(3)	16188(1)	-2296(3)	5939(1)	30(1)
N(1)	15733(2)	5066(3)	7600(1)	22(1)
C(4)	14578(2)	883(4)	6194(1)	17(1)
N(2)	15077(2)	-1367(3)	5795(1)	21(1)
O(4)	14353(1)	-2205(3)	5346(1)	30(1)
C(5)	13325(2)	1945(4)	6040(1)	18(1)
C(2)	14882(2)	3926(4)	7068(1)	19(1)
C(1)	13635(2)	5076(4)	6934(1)	20(1)
C(3)	15386(2)	1802(4)	6709(1)	19(1)
C(8)	9245(2)	4827(4)	5813(1)	20(1)
C(9)	8298(2)	2535(4)	5635(1)	22(1)
C(7)	11498(2)	5359(4)	6277(1)	18(1)

Table 3 Bond lengths [Å] for *N*-(2-fluoroethyl)-3,5-dinitrobenzamide **154**.

F(1)-C(9)	1.415(2)
O(1)-N(1)	1.234(2)
O(2)-N(1)	1.228(2)
O(5)-C(7)	1.240(2)
N(3)-C(7)	1.341(2)
N(3)-C(8)	1.467(2)

N(3)-H(8)	0.86(2)
C(6)-C(1)	1.394(3)
C(6)-C(5)	1.399(3)
C(6)-C(7)	1.512(2)
O(3)-N(2)	1.2291(19)
N(1)-C(2)	1.473(2)
C(4)-C(5)	1.387(3)
C(4)-C(3)	1.386(3)
C(4)-N(2)	1.480(2)
N(2)-O(4)	1.2268(19)
C(5)-H(5)	0.94(2)
C(2)-C(3)	1.388(3)
C(2)-C(1)	1.391(3)
C(1)-H(1)	0.93(2)
C(3)-H(3)	0.93(2)
C(8)-C(9)	1.496(3)
C(8)-H(8B)	0.99(2)
C(8)-H(8A)	0.97(2)
C(9)-H(9B)	0.99(2)
C(9)-H(9A)	1.01(2)
C(7)-N(3)-C(8)	120.21(16)
C(7)-N(3)-H(8)	117.7(14)
C(8)-N(3)-H(8)	120.1(14)
C(1)-C(6)-C(5)	119.57(16)
C(1)-C(6)-C(7)	118.25(16)
C(5)-C(6)-C(7)	122.15(15)
O(2)-N(1)-O(1)	124.38(15)
O(2)-N(1)-C(2)	117.70(15)
O(1)-N(1)-C(2)	117.92(16)
C(5)-C(4)-C(3)	123.32(17)
C(5)-C(4)-N(2)	118.62(15)
C(3)-C(4)-N(2)	118.06(16)
O(4)-N(2)-O(3)	124.14(15)

O(4)-N(2)-C(4)	117.94(14)
O(3)-N(2)-C(4)	117.92(15)
C(4)-C(5)-C(6)	118.87(16)
C(4)-C(5)-H(5)	119.0(12)
C(6)-C(5)-H(5)	122.2(12)
C(3)-C(2)-C(1)	122.95(17)
C(3)-C(2)-N(1)	118.06(16)
C(1)-C(2)-N(1)	118.95(17)
C(2)-C(1)-C(6)	119.12(18)
C(2)-C(1)-H(1)	119.9(12)
C(6)-C(1)-H(1)	121.0(12)
C(4)-C(3)-C(2)	116.16(17)
C(4)-C(3)-H(3)	123.6(12)
C(2)-C(3)-H(3)	120.2(12)
N(3)-C(8)-C(9)	111.45(16)
N(3)-C(8)-H(8B)	109.3(11)
C(9)-C(8)-H(8B)	109.2(11)
N(3)-C(8)-H(8A)	108.1(11)
C(9)-C(8)-H(8A)	111.6(11)
H(8B)-C(8)-H(8A)	107.0(16)
F(1)-C(9)-C(8)	110.01(15)
F(1)-C(9)-H(9B)	105.6(11)
C(8)-C(9)-H(9B)	112.1(11)
F(1)-C(9)-H(9A)	106.7(11)
C(8)-C(9)-H(9A)	111.5(11)
H(9B)-C(9)-H(9A)	110.6(15)
O(5)-C(7)-N(3)	123.46(17)
O(5)-C(7)-C(6)	120.39(16)
N(3)-C(7)-C(6)	116.14(16)

Table 4 Anisotropic displacement parameters (Å2x 10_3) for *N*-(2-fluoroethyl)-3,5-dinitrobenzamide **154**. The anisotropic displacement factor exponent takes the form: $-2\pi 2[\ h_2\ a^{*2}U_{11} + \ldots + 2\ h\ k\ a^*\ b^*\ U_{12}\ ]$.

	U11	U22	U33	U23	U13	U12
F(1)	27(1)	34(1)	29(1)	-12(1)	1(1)	1(1)
O(1)	22(1)	36(1)	27(1)	1(1)	-6(1)	0(1)
O(2)	34(1)	28(1)	25(1)	-7(1)	0(1)	-3(1)
O(5)	23(1)	18(1)	29(1)	-4(1)	2(1)	1(1)
N(3)	17(1)	15(1)	23(1)	-2(1)	0(1)	2(1)
C(6)	17(1)	17(1)	18(1)	2(1)	1(1)	-3(1)
O(3)	20(1)	30(1)	41(1)	-7(1)	-1(1)	8(1)
N(1)	22(1)	26(1)	18(1)	1(1)	2(1)	-5(1)
C(4)	18(1)	16(1)	18(1)	0(1)	3(1)	-1(1)
N(2)	19(1)	20(1)	24(1)	0(1)	3(1)	0(1)
O(4)	27(1)	34(1)	30(1)	-13(1)	-2(1)	1(1)
C(5)	19(1)	18(1)	16(1)	1(1)	1(1)	-3(1)
C(2)	19(1)	21(1)	15(1)	1(1)	0(1)	-5(1)
C(1)	22(1)	17(1)	20(1)	1(1)	6(1)	-2(1)
C(3)	17(1)	20(1)	22(1)	6(1)	1(1)	-2(1)
C(8)	18(1)	21(1)	20(1)	-1(1)	0(1)	4(1)
C(9)	19(1)	27(1)	20(1)	-3(1)	2(1)	2(1)
C(7)	19(1)	19(1)	15(1)	1(1)	4(1)	-1(1)

Table 5 Hydrogen coordinates (x 10^4) and isotropic displacement parameters (Å2x 10^3) for *N*-(2-fluoroethyl)-3,5-dinitrobenzamide **154**.

	x	y	z	U(eq)
H(3)	16220(20)	1090(40)	6814(9)	24(5)
H(9B)	8318(18)	1060(40)	5960(9)	23(5)
H(5)	12835(19)	1260(40)	5676(10)	24(5)
H(8B)	8938(18)	5820(40)	6188(9)	23(5)
H(8A)	9286(18)	6180(40)	5472(10)	23(5)
H(1)	13335(19)	6490(50)	7190(10)	28(6)
H(9A)	7370(20)	3250(40)	5548(9)	23(5)
H(8)	10740(20)	2020(50)	5941(10)	31(6)

Appendix 7

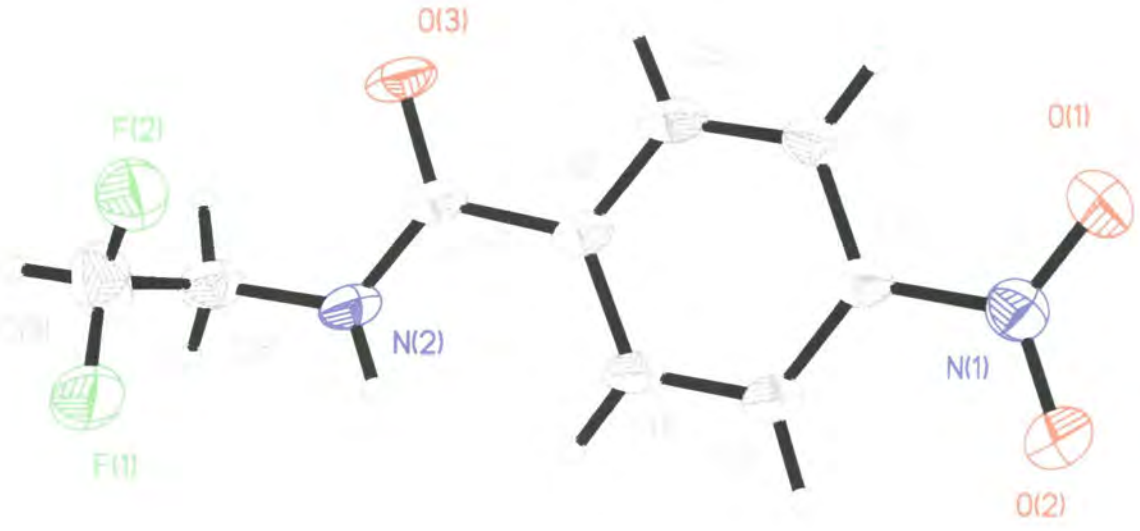

N-(2-Fluoroethyl)-4-nitrobenzamide 155

Table 1 Crystal data and structure refinement for *N*-(2-fluoroethyl)-4-nitrobenzamide **155**.

Identification code	pna21	
Empirical formula	C9 H9 F N2 O3	
Formula weight	212.18	
Temperature	150 K	
Wavelength	0.71073 Å	
Crystal system	Orthorhombic	
Space group	Pna2(1)	
Unit cell dimensions	a = 9.955(2) Å	α = 90°.
	b = 20.411(4) Å	β = 90°.
	c = 4.6400(9) Å	γ = 90°.
Volume	942.8(3) Å3	
Z	4	
Density (calculated)	1.495 Mg/m3	
Absorption coefficient	0.126 mm-1	
F(000)	440	
Crystal size	0.5 x 0.2 x 0.05 mm3	
Theta range for data collection	2.00 to 30.13°.	
Index ranges	-13<=h<=13, -27<=k<=28, -6<=l<=6	
Reflections collected	11454	
Independent reflections	2644 [R(int) = 0.0455]	
Completeness to theta = 30.13°	96.3 %	
Refinement method	Full-matrix least-squares on F2	
Data / restraints / parameters	2644 / 1 / 177	
Goodness-of-fit on F2	1.039	
Final R indices [I>2sigma(I)]	R1 = 0.0473, wR2 = 0.1034	
R indices (all data)	R1 = 0.0795, wR2 = 0.1146	
Absolute structure parameter	-0.6(12)	
Largest diff. peak and hole	0.221 and -0.244 e.Å-3	

Table 2 Atomic coordinates (x 10^4) and equivalent isotropic displacement parameters ($Å^2$x 10^3) for *N*-(2-fluoroethyl)-4-nitrobenzamide **155**. U(eq) is defined as one third of the trace of the orthogonalized Uij tensor.

	x	y	z	U(eq)
N(2)	7122(2)	7427(1)	1551(4)	33(1)
C(3)	7313(2)	9314(1)	8624(4)	30(1)
O(3)	4955(1)	7675(1)	2497(4)	42(1)
C(6)	6621(2)	8322(1)	4864(4)	27(1)
C(8)	6789(2)	6880(1)	-330(5)	38(1)
C(2)	8321(2)	8997(1)	7110(5)	35(1)
N(1)	7687(2)	9830(1)	10666(4)	37(1)
C(7)	6175(2)	7780(1)	2874(4)	30(1)
C(1)	7974(2)	8496(1)	5242(5)	34(1)
C(4)	5967(2)	9156(1)	8287(5)	35(1)
C(5)	5635(2)	8657(1)	6386(5)	35(1)
O(2)	8867(2)	9944(1)	11066(4)	54(1)
O(1)	6792(2)	10113(1)	11973(6)	80(1)
C(9)	6755(3)	6237(1)	1248(6)	51(1)
F(2)	6043(3)	6248(1)	3519(7)	50(1)
F(1)	7832(2)	6052(1)	2630(8)	52(1)

Table 3 Bond lengths [Å] for *N*-(2-fluoroethyl)-4-nitrobenzamide **155**.

N(2)-C(7)	1.337(3)
N(2)-C(8)	1.455(3)
C(3)-C(2)	1.386(3)
C(3)-C(4)	1.387(3)
C(3)-N(1)	1.465(3)
O(3)-C(7)	1.245(2)
C(6)-C(5)	1.390(3)

C(6)-C(1)	1.403(2)
C(6)-C(7)	1.508(3)
C(8)-C(9)	1.503(3)
C(2)-C(1)	1.384(3)
N(1)-O(2)	1.211(2)
N(1)-O(1)	1.222(3)
C(4)-C(5)	1.387(3)
C(9)-F(2)	1.270(4)
C(9)-F(1)	1.305(3)
C(7)-N(2)-C(8)	121.90(17)
C(2)-C(3)-C(4)	122.21(19)
C(2)-C(3)-N(1)	118.73(17)
C(4)-C(3)-N(1)	119.06(17)
C(5)-C(6)-C(1)	119.29(19)
C(5)-C(6)-C(7)	117.65(16)
C(1)-C(6)-C(7)	123.05(17)
N(2)-C(8)-C(9)	112.48(18)
C(1)-C(2)-C(3)	118.80(18)
O(2)-N(1)-O(1)	122.7(2)
O(2)-N(1)-C(3)	118.84(17)
O(1)-N(1)-C(3)	118.38(18)
O(3)-C(7)-N(2)	122.1(2)
O(3)-C(7)-C(6)	119.99(18)
N(2)-C(7)-C(6)	117.95(15)
C(2)-C(1)-C(6)	120.35(19)
C(5)-C(4)-C(3)	118.23(18)
C(4)-C(5)-C(6)	121.09(18)
F(2)-C(9)-F(1)	93.2(3)
F(2)-C(9)-C(8)	113.7(2)
F(1)-C(9)-C(8)	118.3(2)

Table 4 Anisotropic displacement parameters (Å2x 103) for *N*-(2-fluoroethyl)-4-nitrobenzamide **155**. The anisotropic displacement factor exponent takes the form: $-2\pi^2[h^2 a^{*2} U_{11} + ... + 2 h k a^* b^* U_{12}]$.

	U11	U22	U33	U23	U13	U12
N(2)	19(1)	43(1)	36(1)	-1(1)	-4(1)	-4(1)
C(3)	24(1)	31(1)	34(1)	5(1)	0(1)	2(1)
O(3)	17(1)	54(1)	54(1)	-3(1)	-5(1)	-6(1)
C(6)	19(1)	34(1)	30(1)	6(1)	-3(1)	-2(1)
C(8)	25(1)	54(1)	34(1)	-8(1)	-2(1)	-1(1)
C(2)	20(1)	39(1)	45(1)	-2(1)	0(1)	-2(1)
N(1)	34(1)	35(1)	42(1)	0(1)	-1(1)	4(1)
C(7)	20(1)	37(1)	34(1)	7(1)	-2(1)	-3(1)
C(1)	17(1)	41(1)	46(1)	0(1)	3(1)	0(1)
C(4)	22(1)	44(1)	39(1)	0(1)	1(1)	7(1)
C(5)	18(1)	44(1)	43(1)	6(1)	-2(1)	2(1)
O(2)	31(1)	63(1)	68(1)	-21(1)	-2(1)	-7(1)
O(1)	40(1)	84(1)	114(2)	-58(2)	1(1)	12(1)
C(9)	60(2)	45(1)	48(1)	-16(1)	-13(1)	10(1)
F(2)	47(2)	44(1)	58(2)	0(1)	12(1)	-1(1)
F(1)	34(1)	46(1)	76(2)	-1(1)	-24(1)	3(1)

Table 5 Hydrogen coordinates (x 10^4) and isotropic displacement parameters (Å2x 10^3) for *N*-(2-fluoroethyl)-4-nitrobenzamide **155**.

	x	y	z	U(eq)
H(1)	8670(20)	8282(12)	4070(60)	44(7)
H(8B)	7470(20)	6864(10)	-1890(50)	34(6)
H(4)	5300(20)	9354(12)	9410(60)	44(6)
H(9)	6540(20)	5903(11)	-110(60)	38(6)
H(5)	4720(20)	8521(10)	6120(60)	45(6)
H(8A)	5890(20)	6940(10)	-1330(50)	35(6)
H(2)	9270(20)	9103(11)	7320(70)	47(7)
H(6)	7930(30)	7488(13)	2000(60)	48(7)

Conferences

RSC 30th Stereochemistry at Sheffield, Dec 17th, 1996.

RSC Perkin Division – BioOrganic Group, Cardiff, University of Wales, Dec 17th, 1997.

RSC National Congress & Young Researchers' Meeting, University of Durham, April 6-9th, 1998.

12th European Symposium on Fluorine Chemistry, Freie Universität Berlin, July 8-12th, 1998. Presented poster, 'Conformational preferences of 2-(fluoromethyl)pyridines and related compounds'.

RSC 32th Stereochemistry at Sheffield, Dec 7th, 1998.

RSC Perkin Division – BioOrganic Group, University of Leicester, Dec 17th, 1999. Presented poster, 'Synthesis of 1-deoxy-D-xyulose-5-phosphates analogues as putative antibiotics'.

Heterocycles as Synthetic Reagents: a Review Symposium, University of Sunderland, May 5th 1999.

RSC National Congress & Young Researchers' Meeting, Heriot-Watt University, September 6-10th, 1999. Presented poster 'Synthesis of 1-deoxy-D-xyulose-5-phosphates analogues as putative antibiotics'.